ornl

ORNL-6854

OAK RIDGE NATIONAL LABORATORY

LOCKHEED MARTIN

Extraction of Nitric Acid, Uranyl Nitrate, and Bismuth Nitrate from Aqueous Nitric Acid Solutions with CMPO

Barry B. Spencer

MANAGED BY
LOCKHEED MARTIN ENERGY SYSTEMS, INC.
FOR THE UNITED STATES
DEPARTMENT OF ENERGY

UCN-13873 (3& 6-95)

ORNL-6854

Chemical Technology Division

EXTRACTION OF NITRIC ACID, URANYL NITRATE, AND BISMUTH NITRATE FROM AQUEOUS NITRIC ACID SOLUTIONS WITH CMPO

Barry B. Spencer*

* Robotics and Process Systems Division, ORNL.

Date Published–August 1995

Prepared for the
U.S. Department of Energy, Office of Technology Development
Underground Storage Tank Integrated Demonstration Program

Prepared by the
OAK RIDGE NATIONAL LABORATORY
Oak Ridge, Tennessee 37831-6285
managed by
LOCKHEED MARTIN ENERGY SYSTEMS, INC.
for the
U.S. DEPARTMENT OF ENERGY
under contract DE-AC05-84OR21400

CONTENTS

LIST OF TABLES

LIST OF FIGURES

LIST OF ACRONYMS

AMV	apparent molal volume
ASTM	American Society for Testing and Materials
CMPO	octyl(phenyl)-N,N-diisobutylcarbamoylmethyl phosphine oxide
DOE	Department of Energy
EPA	Environmental Protection Agency
e.s.u.	electrostatic units
HEDL	Hanford Engineering Development Laboratory
HPLC	high-performance liquid chromatograph
ICP	inductively coupled plasma
INEL	Idaho National Engineering Laboratory
LANL	Los Alamos National Laboratory
MS	mass spectrometry
MVST	Melton Valley Storage Tanks
NIST	National Institute of Science and Technology
NPH	normal paraffin hydrocarbon
ORNL	Oak Ridge National Laboratory
PMT	photomultiplier tube
RCRA	Resource Conservation and Recovery Act
RFP	Rocky Flats Plant
RSD	relative standard deviation
RTD	resistance-temperature device
TBP	tri-*n*-butyl phosphate
TCE	tetrachloroethylene
TRU	transuranium
TRUEX	transuranium extraction

ACKNOWLEDGMENTS

This work was sponsored by the U.S. Department of Energy's Office of Technology Development—Underground Storage Tank Integrated Demonstration under U.S. Government contract DE-AC05-84OR21400 with Lockheed Martin Energy Systems, Inc. The work was performed at the Oak Ridge National Laboratory under the auspices of the Chemical Technology Division. The assistance of the Analytical Services Division in performing wet-chemical titrations and ICP-MS analyses is also acknowledged.

Parts of this report, in another form, were prepared as a dissertation and submitted to the Faculty of the Graduate School of The University of Tennessee, Knoxville, in partial fulfillment of the degree of Doctor of Philosophy with a major in Chemical Engineering.

ABSTRACT

Production operations at many Department of Energy (DOE) sites throughout the United States have resulted in large inventories of stored radioactive wastes. Because disposal costs for transuranium-bearing wastes are exorbitant, it seemed prudent to examine final disposal options involving actinide removal so that the bulk of the waste could be disposed of by less expensive methods. The DOE sponsors development of the transuranium extraction (TRUEX) process for removing actinides from such wastes. The solvent is a mixture of octyl(phenyl)-N,N-diisobutylcarbamoylmethyl phosphine oxide (CMPO) and tri-*n*-butyl phosphate (TBP). The extraction characteristics of CMPO are not as well understood as those of TBP.

The extraction characteristics of nitric acid, uranyl nitrate, and bismuth nitrate with CMPO were studied in an experimental program where CMPO was dissolved in *n*-dodecane to produce the organic-extracting medium. Three different aqueous systems were used in the tests: (1) nitric acid, (2) uranyl nitrate in nitric acid, and (3) bismuth nitrate in nitric acid. In each experiment, aqueous solution was equilibrated with the organic extractant and the concentration of the solute was measured in each phase to obtain distribution data. The objectives of the project were to estimate extraction stoichiometry and equilibrium constants for the extraction of nitric acid, uranyl nitrate, and bismuth nitrate with CMPO.

Experiments were performed over a limited range of concentrations to avoid conditions favoring formation of a third phase. Aqueous nitric acid concentrations were limited to 0.30 *M* at 25°C, 1.0 *M* at 40°C, and 3.0 *M* at 50°C. These limits were decreased by the addition of other nitrates to the system. Uranyl nitrate and bismuth nitrate concentrations were limited to tracer levels.

The data indicate that CMPO extracts nitric acid with a 1:1 stoichiometry. The value of the equilibrium constant was calculated to be 2.660 ± 0.092 at 25°C. The enthalpy of the extraction was estimated to be –5.46 ± 0.46 kcal/mol.

Slope analysis indicates that uranyl nitrate extracts with a mixed equilibria of 1:1 and 2:1 stoichiometries occurring in nearly equal proportion. Over the range of the data, the extraction was well modeled by a 2:1 stoichiometry. Effects of nitric acid concentration were well modeled by an aqueous nitrate complexation equilibrium. The equilibrium constant of the 2:1 extraction was calculated to be $1.213 \times 10^6 \pm 3.56 \times 10^4$ at 25°C. The enthalpy of the reaction was estimated to be –9.610 ± 0.594 kcal/mol. The nitrate complexation constant was calculated to be 8.412 ± 0.579 at 25°C. The enthalpy of the complexation was estimated to be –10.72 ± 1.87 kcal/mol.

Slope-analysis studies show that bismuth nitrate also extracts with a mixed equilibria of, perhaps, 1:1 and 2:1 stoichiometries. Over the range of the data, a 2:1 extraction equilibrium and a nitrate complexation were found to adequately model the data. The equilibrium constant for the extraction equilibrium was estimated to be $7.847 \times 10^7 \pm 4.27 \times 10^6$ at 25°C. The corresponding enthalpy of the extraction was estimated to be –18.99 ± 0.82 kcal/mol. The nitrate complexation constant was estimated to be 76.47 ± 12.03 at 25°C, while the corresponding enthalpy of the complexation reaction was estimated at –21.75 ± 5.07 kcal/mol.

1. INTRODUCTION

1.1 Background

Production operations at many Department of Energy (DOE) sites throughout the United States have resulted in massive quantities of stored radioactive and hazardous wastes. These wastes have accumulated since the early 1940s (about 50 years) during the production of weapons materials and, to a lesser extent, products for the civilian marketplace, such as isotopes for research and medical purposes. Processing of irradiated nuclear fuel to recover uranium and plutonium, for example, results in a high-level radioactive waste containing fission products, some of which are highly radioactive, and transuranium elements produced by neutron capture, which are also radioactive. Typically, these wastes are stored in large tanks and await final disposal. Storage sites for such waste include, but are not limited to, the Hanford Engineering Development Laboratory (HEDL), Idaho National Engineering Laboratory (INEL), Oak Ridge National Laboratory (ORNL), Los Alamos National Laboratory (LANL), and Rocky Flats Plant (RFP). The DOE is responsible for these wastes and their ultimate disposition.

Wastes containing transuranium (TRU) elements that contribute ionizing radiation of more than 100 nCi/g must be considered TRU wastes and must be disposed of accordingly, in deep geologic repositories (Moghissi, 1986). The stored wastes contain TRU components as a minor constituent. Studies conducted by Sears et al. (1990, 1991) have shown that the stored wastes at ORNL are composed of two major "phases": (1) a high-pH supernatant containing sodium and nitrate ions in large concentration with essentially no TRU content, and (2) a sludge consisting of precipitated solids that contain the bulk of the TRU materials.

Options to dispose of the waste have been considered by McGinnis (1992). One option is to dry the waste and, without any additional pretreatment, vitrify it in glass. Preliminary

evaluations of the vitrification of the Hanford wastes alone are estimated to produce 200,000 canisters of waste requiring repository disposal. Each canister would have an estimated life cycle cost of $750,000, for a total disposal cost of $150 billion. Separation of the waste prior to vitrification promises to reduce the number of canisters to, conservatively, one-tenth or, at best, one-hundredth of the above figure. A potential cost savings of around $100 billion is sufficient incentive to pursue separations technology as a precursor to waste disposal.

A substantial program is under way at ORNL to demonstrate waste processing technologies. Wastes in the Melton Valley Storage Tanks (MVST) are representative of the materials throughout the DOE complex that must be processed and are being used in these demonstrations. Table 1.1 summarizes the preliminary characterization data on wastes in tank W-25, from which the test materials are taken. Although there are discrepancies between the chemical and radiological analyses in these preliminary data, the data do show the large number of components in the waste and their relative concentrations. The waste contains small (essentially trace) concentrations of TRU elements. Because of the advantages of disposing of non-TRU waste using near-surface disposal techniques, separation of the TRU components is an important part of the predisposal treatment. The general processing scheme is to treat the supernatant and the sludge separately. Sludge can be separated from the supernatant by either gravity or centrifugation. The sludge contains the TRU materials, but still at small concentrations. Treatment of the sludge is thought to be best accomplished in several steps (McGinnis, 1992). First, it is washed with mild caustic solutions to remove as much of the highly soluble materials as possible, particularly cesium and strontium, while keeping the TRU materials in the solid phase. Second, the insoluble residue containing the TRU elements is dissolved in nitric acid. Third, the dissolved material is processed using the transuranium extraction (TRUEX) process to remove the TRU materials from

Table 1.1. Analytical data for supernatant and sludge samples from tank W-25

Measured attribute	Supernatant		Sludge	
	(Bq/mL)	(mg/L)	(Bq/g)	(mg/kg)
Physical properties and miscellaneous data				
Total solids		3.48×10^5		5.31×10^5
Density (g/mL)		1.2018		1.32
pH		12.5		
H^+ (*M*)				
OH^- (*M*)		0.06		
CO_3^{2-} (*M*)		<0.01		
HCO_3^- (*M*)		<0.01		
Chloride (*M*)		0.071		
Fluoride (*M*)		<0.026		
Nitrate (*M*)		4.19		
Phosphate (*M*)		<0.053		
Sulfate (*M*)		<0.052		
Resource Conservation and Recovery Act (RCRA) metals				
Ag		<0.69		<7.6
As		<3.7		<41
Ba		3.2		59
Cd		<0.12		11
Cr		1.9		59
Hg		0.054		37
Ni		0.45		34
Pb		<2.1		220
Se		<4.7		<51
Tl		<1.4		<16
Process metals				
Al		<4.2		2800
B		0.60		<1.5
Ca		280		3.80×10^4
Co		<0.57		
Cs				<1.3
Fe		<2.6		940
K		1.70×10^4		9200
Mg		<1.3		5900
Na		7.80×10^4		6.60×10^4
Si		<1		
Sr		23		150
Th		<2.2		3860
U		<0.10		4800

Table 1.1 (continued)

Measured attribute	Supernatant		Sludge	
	(Bq/mL)	(mg/L)	(Bq/g)	(mg/kg)
Beta/gamma emitters				
^{14}C	3.29×10^{2}	1.91×10^{-3}	1.71×10^{2}	9.92×10^{-4}
^{144}Ce	$<1.3 \times 10^{3}$	$<1.13 \times 10^{-5}$	$<4.2 \times 10^{3}$	$<3.64 \times 10^{-5}$
^{60}Co	1.88×10^{3}	4.46×10^{-5}	4.03×10^{4}	9.55×10^{-4}
^{134}Cs	3.77×10^{3}	8.86×10^{-5}	7.07×10^{2}	1.66×10^{-5}
^{137}Cs	3.27×10^{5}	1.02×10^{-1}	2.21×10^{5}	6.91×10^{-2}
^{152}Eu	$<1.6 \times 10^{2}$	$<2.36 \times 10^{-5}$	8.14×10^{4}	1.20×10^{-2}
^{154}Eu	$<1.2 \times 10^{2}$	$<2.22 \times 10^{-5}$	5.06×10^{4}	9.37×10^{-3}
^{155}Eu	$<6.9 \times 10^{2}$	$<1.37 \times 10^{-5}$	1.63×10^{4}	3.24×10^{-4}
^{3}H	3.45×10^{2}	9.64×10^{-7}		
^{95}Nb	$<6.3 \times 10^{1}$	$<4.34 \times 10^{-8}$	$<5.9 \times 10^{2}$	$<4.07 \times 10^{-7}$
^{106}Ru	$<1.9 \times 10^{3}$	$<1.52 \times 10^{-5}$	$<5.9 \times 10^{3}$	$<4.73 \times 10^{-5}$
^{90}Sr	1.95×10^{4}	3.63×10^{-3}	1.65×10^{6}	3.08×10^{-1}
^{95}Zr	$<1.2 \times 10^{2}$	$<1.49 \times 10^{-7}$	$<4.6 \times 10^{3}$	$<5.73 \times 10^{-6}$
Alpha emitters				
^{232}U				
^{233}U			8.37×10^{2}	2.37
^{235}U			$<4.2 \times 10^{3}$	$<5.30 \times 10^{1}$
$^{239}Pu/^{240}Pu$			2.93×10^{3}	<1.29
$^{238}Pu/^{241}Am$			7.35×10^{3}	$<6.25 \times 10^{-2}$
^{243}Cm			$<3.9 \times 10^{3}$	$<2.55 \times 10^{-3}$
^{244}Cm			3.32×10^{4}	1.12×10^{-2}

Source: M. B. Sears et al., *Sampling and Analysis of Radioactive Liquid Wastes and Sludges in the Melton Valley and Evaporator Facility Storage Tanks at ORNL*, ORNL/TM-11652, Martin Marietta Energy Systems, Oak Ridge National Laboratory, September 1990.

the aqueous phase and concentrate them into a relatively small volume. Fourth, the TRU concentrates are disposed of following a vitrification process or even used as a resource from which valuable elements such as americium and curium may be obtained.

The TRUEX process has been under development for nearly a decade as a means of removing actinides from high-level radioactive waste. Development of the process and technical data for it are described by Horwitz et al. (1982, 1985), Vandegrift et al. (1984), Leonard et al. (1985, 1987), Schulz and Horwitz (1988), and Horwitz and Schulz (1990). Recent tests of the process to demonstrate removal of actinides from waste streams have been reported by Ozawa et al. (1992), Mathur et al. (1993), and Koma et al. (1993).

In the TRUEX process, metal nitrates are extracted from an aqueous nitric acid phase with an organic extractant. The organic extractant is a mixture of octyl(phenyl)-N,N-diisobutylcarbamoylmethyl phosphine oxide (CMPO) and tri-*n*-butyl phosphate (TBP) in an organic diluent. Figure 1.1 shows the chemical and structural formulas for these two extractants. Pure CMPO is a solid at room temperature but is readily dissolved in many common organic solvents. Solvents that have densities significantly different from water are usually selected to enhance phase separation. To be an effective separation medium, the extractant should not distribute appreciably into the aqueous phase. From measurements on a normal paraffin hydrocarbon (NPH) containing 0.2 *M* CMPO and 1.2 *M* TBP equilibrated with a 1.0 *M* aqueous nitric acid solution, Horwitz et al. (1985) report the distribution ratios (organic-phase concentration divided by aqueous-phase concentration) for CMPO and TBP to be 6100 and 1600, respectively. Other properties such as fire resistance are also considered (Tse and Vandegrift, 1989). Because CMPO can form a third, heavy, organic phase upon extraction of metal nitrate complexes, TBP is added as a phase modifier to increase the capacity of the organic phase for nitrate without forming a third phase (Horwitz et al., 1985). The formation of a third phase is problematic for extraction processes that typically operate with only two liquid phases. Third-phase formation can also be suppressed by higher operating temperatures, and Ozawa et al. (1992) have shown that the third phase vanishes over a very narrow temperature band once a critical temperature is reached. Two types of diluent are typically used for the TRUEX solvent: (1) an NPH such as *n*-dodecane, in which case the concentrations of CMPO and TBP are typically 0.2 and 1.4 *M*, respectively; and (2) tetrachloroethylene (TCE) in which the concentrations of CMPO and TBP are typically 0.25 and 0.75 *M*, respectively.

TBP has long been known as an extractant for the recovery of uranium and plutonium (Alcock et al., 1958; Sato, 1958). In their summaries of the TRUEX process, Horwitz et al. (1985)

CMPO

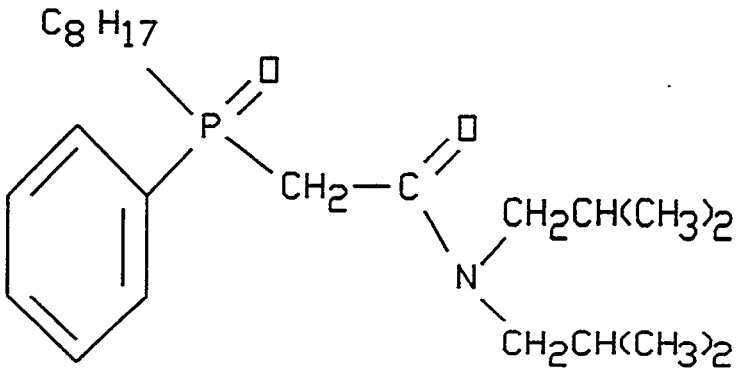

octyl(phenyl)-N,N-diisobutylcarbamoylmethylphosphine oxide (CMPO)

Simple formula: $C_{24}NH_{42}PO_2$

Formula weight: 407.58

TBP

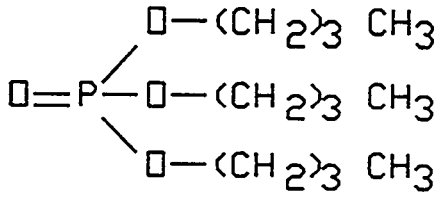

tri-n-butylphosphate (TBP)

Simple formula: $C_{12}H_{27}PO_4$

Formula weight: 266.32

Figure 1.1. Structural formulas of CMPO and TBP.

and Horwitz and Schulz (1990) provide data showing that the mixed TBP-CMPO solvent is a strong extractant for uranium, plutonium, americium, and neptunium, and is a moderate extractant for yttrium, lanthanum, and other elements in the lanthanide series. Because of its similarity to americium, curium is also expected to be strongly extracted by CMPO. The waste materials to be processed contain additional species that may be extracted as well. Concern arises that there may be competition for the extractants by such species or exhaustion of the extractants before the sought materials are removed. If the equilibria in multicomponent systems are unfavorable, other methods may be used to enhance selectivity. For example, studies of the extraction of zirconium from nitric acid solutions with TBP by Siczek and Meisenhelder (1980), Meisenhelder and Siczek (1980), Mailen et al. (1980), and DeMuth (1989) indicate that even though the distribution coefficient can be large, slow kinetics permit selection of process conditions to reduce its extraction. Bismuth, which is a large constituent in the HEDL waste, is reported by Yukhin (1988) to be mildly extracted by TBP. In a recent study, Lumetta et al. (1993) measured the distribution of bismuth between an aqueous nitric acid solution and TRUEX-NPH solvent. The large distribution coefficient suggests strong extraction by the CMPO component.

Even though much work has been done to develop the TRUEX process and measure important distribution coefficients, additional experimental data are needed to model the process so that optimum flowsheets may be developed. Several experimental studies have been made of the extraction of metal nitrates using the TRUEX solvent (i.e., the mixed CMPO-TBP solvent). Development of a detailed thermodynamic model of the extraction process requires information on the extraction characteristics of the individual organic extractants. The literature contains data on the distribution of many of the species of interest between an acidic aqueous nitrate solution and solutions of TBP in NPH diluents. No data are available on the extraction of uranium or bismuth into a CMPO-based NPH solvent in the absence of TBP. Because of the known salting-

out effect of nitric acid, some measurements have been made on the extraction of nitric acid by CMPO in a TCE diluent, and smaller amounts of information have been obtained for the extraction of nitric acid by CMPO in an NPH diluent. There is a need for data that describe the distribution of uranyl nitrate, bismuth nitrate, and nitric acid between an aqueous phase and a CMPO-NPH organic phase.

1.2 Objectives

The overall objective of this work was to develop a thermodynamically consistent model of the extraction equilibria of uranyl nitrate and bismuth nitrate (separately) describing the distribution of these species between an aqueous-phase nitric acid solution and a CMPO-NPH organic phase. Experimental data describing the distribution of the extractable species were used in conjunction with the model to (1) infer the stoichiometry of the extraction reaction (equilibria), (2) estimate values for the thermodynamic equilibrium constants of these equilibria, and (3) estimate the enthalpy of extraction. Activity coefficients of the aqueous species were obtained from the literature and were calculated using existing correlations, such as those developed by Pitzer (1973). The organic phase was typically assumed to be ideal (all activity coefficients equal unity) because of (1) a lack of data and (2) the supposed electrical neutrality of species in the organic phase. However, the organic-phase activity coefficients, for which values are not known, affect the values of the equilibrium constants as though they were lumped together with the equilibrium constant. The effect of the organic-phase activity coefficients on the equilibrium constants was also estimated.

1.3 Primary Areas of Investigation

The work necessary to meet the objectives may be subdivided into four primary areas of investigation.

Measurement of Distribution Coefficients. The distribution coefficients of uranyl nitrate and bismuth nitrate, separately, need to be measured between an acidic aqueous solution and a CMPO-NPH solvent since data for these systems are currently nonexistent. Experimental data needs cover a range of concentrations for various actinide-bearing waste applications. Therefore, it is likely that insufficient data on the distribution characteristics of nitric acid with this solvent will require laboratory measurements. Measurements on the distribution of uranium and bismuth between the aqueous and organic phases will be made at a constant temperature around 25°C because most extraction processes operate near room temperature. Measurements will also be made at an elevated temperature (40°C) in an attempt to estimate the enthalpy of the extraction reactions. Concentrations of solutes (e.g., nitric acid, uranyl nitrate, and bismuth nitrate) in the aqueous phase will be varied throughout an applicable range. Because of the danger of third-phase formation, the concentration of metal nitrates may be limited to a low level; however, increasing the process temperature will increase the concentration required to form a third phase.

Estimation of Extraction Stoichiometry. Experiments performed at various organic-phase CMPO concentrations and fixed aqueous-phase compositions are used to infer the stoichiometry of extraction by the slope-analysis method described by Hesford and McKay (1958). Under conditions where both phases are nearly ideal, a plot of the logarithm of the distribution ratio vs the logarithm of the extractant concentration gives a straight line whose slope is equal to the extraction stoichiometry (sometimes called solvation number). The extraction stoichiometries for nitric acid, uranyl nitrate, and bismuth nitrate are estimated by this method. The results are

compared with those reported in the literature for similar systems, for example, the extraction of uranyl nitrate from nitric acid media by CMPO in a TCE diluent.

Development of a Model. A thermodynamically consistent model is developed of the equilibrium distribution of uranyl nitrate between an aqueous nitric acid phase and a CMPO-NPH organic phase that are in intimate contact. The model is based on chemical mass action equations and relates the aqueous- and organic-phase concentrations of the extracting species. Thermodynamic equilibrium constants are the parameters of the model. Similar models are developed for the partitioning of bismuth nitrate between an aqueous nitric acid phase and a CMPO-NPH organic phase. Because nitric acid is present in both cases and competes for the extractant, similar models for the extraction of nitric acid are also developed.

Determination of Equilibrium Constants and Enthalpy of Extraction. Because the equilibrium constants are the parameters of the model, fitting the experimental data to the models results in values of the equilibrium constants. With equilibrium constants determined at different temperatures, the enthalpy of the associated reaction is estimated.

2. LITERATURE REVIEW

Solvent extraction processes are based on the preferential solubility of the species of interest in one phase of a two-phase system. For example, in the recovery of uranium, uranyl nitrate salt dissolved in an aqueous phase is brought into contact with an organic solvent containing a species (extractant) that complexes with the salt. The uranyl nitrate transfers into the organic phase in the form of a uranyl nitrate salt–extractant complex. Contaminants in the aqueous phase are not complexed by the extractant (ideally) and do not transfer to the organic phase with the uranium. Often the reaction at the interface between aqueous and organic phases is rapid; and, if the mixing is sufficiently vigorous in both phases, the phases rapidly approach an equilibrium concentration of the extractable salt (Olander and Benedict, 1963). Extraction of uranyl nitrate into the organic phase is enhanced by the presence of additional nitrate ions, for example, from nitric acid or a nitrate salt. Typically, uranyl nitrate is extracted from a strong nitric acid solution (Sato, 1958) or ammonium nitrate solution (Blanco, 1961) into the organic and recovered from the organic into an aqueous phase having a very low nitrate concentration by a reverse extraction. The equilibrium established in such a procedure can be modeled as chemical reactions depicting the formation and destruction of uranyl nitrate–organic complexes. Other ions in solution affect the equilibrium, and their presence must also be included in any useful model. The aqueous phase is highly nonideal because of the dissociation of the salts and acids into ionic species. A thermodynamic model of the equilibrium must consider the activities of these strong electrolytes.

2.1 Thermodynamic Treatment of Extraction Equilibria

Extraction equilibria are often modeled as chemical equilibria. In many books (e.g., Denbigh, 1971) a general chemical equilibrium is written in the compact form

$$0 = \sum_i \nu_i r_i \quad , \tag{2-1}$$

where ν = the stoichiometric coefficient (positive for products and negative for reactants),

r = a reactant or a product, and

i = the counter or identifier for reactant or product species.

The thermodynamic equilibrium constant based on such a mass action equation may then be written as

$$K = \exp\left(-\frac{\sum_i \nu_i \mu_i^0}{RT}\right) = \exp\left(\frac{-\Delta G^0}{RT}\right) = \prod_i (\gamma_i m_i)^{\nu_i} \quad , \tag{2-2}$$

where R = ideal gas law constant, 1.9872 cal/(mol·K);

T = absolute temperature, K;

ΔG^0 = change in Gibbs free energy for the reaction, cal/mol;

μ^0 = the chemical potential at some convenient standard state;

γ = the activity coefficient; and

m = concentration (may be molar, molal, or other appropriate unit).

The product of the activity coefficient and concentration of a species is called the activity,

$$a_i = \gamma_i m_i \quad , \tag{2-3}$$

where a = the activity of a species.

Assignment of values for concentration is straightforward, but the activity coefficients may vary considerably from unity and are concentration dependent.

2.1.1 Effects of Temperature and Pressure on Equilibrium Constant

The temperature and pressure dependence of the equilibrium constant is given in standard textbooks (e.g., Harned and Owen, 1943; Denbigh, 1971; Smith and Van Ness, 1975) as

$$R\ dln\ K = \frac{\Delta H^0}{T^2} dT - \frac{\Delta V^0}{T} dP \quad , \tag{2-4}$$

where P = pressure,

ΔH^0 = either the molar enthalpy change of the pure liquid component or the partial molar enthalpy change at infinite dilution, depending on the limiting behavior of the selected species; and

ΔV^0 = volume change on reaction when each component approaches ideal behavior.

In liquid phases the effect of pressure on the equilibrium constant is very small, so the term in Eq. (2-4) regarding pressure change is small and may be neglected unless very large pressure changes are encountered. In the present work, all experiments were performed at atmospheric pressure. Under constant pressure conditions, the equation may be written as

$$\left(\frac{dln\ K}{dT}\right)_P = \frac{\Delta H^0}{RT^2} \quad , \tag{2-5}$$

which is known as the van't Hoff equation and, upon integration, yields

$$\ln \frac{K_2}{K_1} = \frac{\Delta H^0}{R}\left(\frac{1}{T_1} - \frac{1}{T_2}\right) \tag{2-6}$$

if the enthalpy change is independent of temperature. Equation (2-6) provides the means for correlating the equilibrium constant, at least over a limited range of temperature.

2.2 Activity Coefficients

The concept of activity was introduced by G. N. Lewis in 1907 to account for deviations from ideal solution behavior. Activity coefficients are expressed as a partial derivative of the excess Gibbs free energy with respect to the number of moles of the substance in question (Smith and Van Ness, 1975). That is,

$$\ln \gamma_i = \left[\frac{\partial (nG^{ex}/RT)}{\partial n_i} \right]_{T,P,n_j}, \qquad (2\text{-}7)$$

where n = quantity of material, moles;

i = the component permitted to change;

j = all components except i;

G^{ex} = excess partial molar Gibbs free energy, cal/mol; and

P = pressure, atm.

The excess Gibbs free energy is simply the difference between the actual free energy and the free energy of a corresponding ideal system. Equations that describe the energy potential of a system can be used to develop equations or equation forms for the activity coefficient.

Activity coefficients and osmotic coefficients may be inferred from a variety of physical measurements. Traditional methods described by Guggenheim (1935) include freezing point depression, boiling point elevation, vapor pressure measurements where Henry's Law defines ideality, and electric potential. Mikhailov and Torgov (1964) show that an extraction method may be used. The osmotic coefficient is usually used to describe the nonideality of the solvent. Guggenheim (1935) describes this as a numerical convenience because, even in solutions considered quite nonideal, the activity coefficient of the solvent may be only slightly different

from unity, thereby requiring several significant digits. The osmotic coefficient is a more sensitive indicator of deviations from ideality and is defined by

$$\mu_i = \mu_i^0 + \phi^{(x)} RT \ln x_i \quad , \tag{2-8}$$

where μ = the chemical potential,

$\phi^{(x)}$ = the rational osmotic coefficient, and

x_i = mole fraction.

Equation (2-8) defines what is often called the rational osmotic coefficient. Another often-used osmotic coefficient is the practical osmotic coefficient defined by Harned and Owen (1943) as

$$\mu_0 = \mu_0^0 - \phi RT \sum_i \frac{\nu_i m_i M_0}{1000} \quad , \tag{2-9}$$

where ϕ = the practical osmotic coefficient;

m = concentration, mol/kg of solvent (molal); and

M_0 = molecular weight of the solvent.

Solute properties are often correlated in terms of the activity coefficient and solvent properties by the osmotic coefficient. Pitzer (1973) makes extensive use of the practical osmotic coefficient, which is also related to the excess Gibbs free energy by the equation

$$\phi - 1 = - \frac{1}{RT \sum_i m_i} \left[\frac{\partial (n G^{ex})}{\partial n_0} \right]_{T,P,n_j} \quad , \tag{2-10}$$

where n_0 = amount of solvent, moles.

When the osmotic coefficient of the solvent is known, its activity may be readily calculated from

$$\ln a_0 = - \frac{M_0 \sum_i \nu_i m_i}{1000.} \phi \quad . \tag{2-11}$$

2.2.1 Conventions and Relationships Among Different Concentration Scales

Classic thermodynamics texts usually develop activities in terms of mole fraction. In addition, other concentration scales such as molar and molal are often used. Activity coefficients can be translated into the different scales when the conversions among the concentration scales are known. Starting with the definitions of mole fraction, molar, and molal, the following concentration conversions can be derived:

from mole fraction to molal,

$$m_i = \frac{1000 x_i}{M_0 x_0} \quad ; \tag{2-12}$$

from mole fraction to molar,

$$c_i = \frac{1000 \rho x_i}{M_0 x_0 + \sum M_i x_i} \quad ; \tag{2-13}$$

from molar to molal,

$$m_i = \frac{c_i}{\rho - 0.001 \sum c_i M_i} \quad ; \tag{2-14}$$

and

from molal to molar,

$$c_i = \frac{m_i \rho}{1 + 0.001 \sum m_i M_i} \quad ; \tag{2-15}$$

where i = subscript referring to solutes,

0 = subscript referring to solvent,

x = mole fraction,

c = concentration, mol/L (i.e., molar),

m = concentration, mol/kg of solvent,

M = molecular weight of the indicated species, and

ρ = density of the solution, g/mL.

Denbigh (1971) derives the conversion between activity coefficients on the mole fraction scale and molal scales:

$$\gamma_i^{(x)} = \frac{\gamma_i m_i M_0}{x_i} \quad , \tag{2-16}$$

where $\gamma^{(x)}$ = activity coefficient on the mole fraction scale.

[For convenience, the superscript (m) is not used for the molal scale because further identification is not required when the other scales are identified and it simplifies equations in much of the remainder of this paper.] Similar mathematical manipulations can be used to convert between activity coefficients on a molar and a molal scale;

$$\gamma_i^{(c)} = \frac{\gamma_i m_i \rho_0}{c_i} \quad , \tag{2-17}$$

where $\gamma^{(c)}$ = activity coefficient on the concentration scale, and

ρ_0 = density of the pure solvent, g/mL.

Both mole fraction and molal concentrations are independent of temperature, but the molar concentration changes with temperature because the solution density changes with temperature. For these reasons, the activity coefficients found in the literature are usually correlated on a molal basis.

2.2.2 Effects of Temperature and Pressure

The temperature dependence of the activity coefficient is developed in thermodynamics texts, for example, the book by Denbigh (1971). Dependence of the activity coefficient on temperature is

$$\frac{\partial \ln \gamma_i}{\partial T} = - \frac{H_i - H_i^0}{RT^2} \quad , \tag{2-18}$$

where H_i = the partial molar enthalpy of component i, and

H_i^0 = the molar enthalpy of pure substance ($m_i \rightarrow$ pure material), or

H_i^0 = the partial molar enthalpy of solute at infinite dilution ($m_i \rightarrow 0$).

Two meanings for H_i^0 result, as indicated, from selecting either the pure substance or its infinite dilution condition as the standard state at which the activity coefficient approaches unity. The effect of pressure may be written as

$$\frac{\partial \ln \gamma_i}{\partial P} = \frac{V_i - V_i^0}{RT} \quad , \tag{2-19}$$

where V_i = the partial molar volume of component i, and

V_i^0 = the molar volume of pure substance ($m_i \rightarrow$ pure material), or

V_i^0 = the partial molar volume of solute at infinite dilution ($m_i \rightarrow 0$).

In liquid solutions the volume changes caused by pressure changes are quite small so that pressure effects on the activity coefficient may be safely ignored.

Because the activity coefficient is expressed in terms of the excess Gibbs free energy, as illustrated in Eq. (2-7), it is convenient to express the temperature effect in terms of that same function. The Gibbs-Helmholtz equation may be written in terms of excess quantities as

$$\frac{\partial(G^{ex}/RT)_{P,m}}{\partial T} = -\frac{H^{ex}}{RT^2} \quad , \tag{2-20}$$

where H^{ex} = the excess enthalpy (enthalpy of the solution minus the enthalpy of the components in their standard states).

Silvester and Pitzer (1977, 1978), and Phutela and Pitzer (1986) identify terms in Eq. (2-20) having the form H^{ex} [or, equivalently, the term $H_i - H_i^0$ in Eq. (2-18)] as related to the enthalpy of dilution and the enthalpy of solution. Now consider the coefficients in the function for G^{ex} used to compute the values of the activity coefficient [see Eq. (2-7)]. Together, these ideas imply that the temperature derivatives of the coefficients used in the excess Gibbs free energy function describe the temperature effect on the activity coefficient. The enthalpy of solution permits assignment of values to those temperature derivatives.

2.2.3 Additional Definitions for Electrolytes

Dissociation of an electrolyte in solution is usually represented as a chemical equilibrium having the form of Eq. (2-1). At equilibrium the chemical potential of the electrolyte, as a whole, is shown by Denbigh (1971) to be equal to that of the undissociated portion of the electrolyte, which is also equal to the linear combination of the chemical potential of the separate ions:

$$\mu = \nu_+\mu_+ + \nu_-\mu_- \quad , \tag{2-21}$$

where ν_+ = number of cations produced per dissociated molecule, and

ν_- = number of anions produced per dissociated molecule.

Because individual ionic chemical potentials are not measurable, due to electroneutrality constraints, the ionic activity coefficients have no physical significance even though the ionic concentrations can be quantified for totally ionized electrolytes. The combination of individual ionic chemical potentials does have physical significance, as indicated above, so it is convenient to define a mean ionic activity coefficient as

$$\gamma_{\pm}^{\nu} = \gamma_+^{\nu_+}\gamma_-^{\nu_-} \quad , \tag{2-22}$$

where $\nu = \nu_+ + \nu_-$.

Mean ionic molalities may be similarly defined:

$$m_{\pm} = \left(m_+^{\nu_+} m_-^{\nu_-}\right)^{1/\nu} = m\left(\nu_+^{\nu_+}\nu_-^{\nu_-}\right)^{1/\nu} \quad . \tag{2-23}$$

In cases where the electrolyte is not completely dissociated, the usual convention is to make the calculations as though it were. Then $\gamma_{\pm}$ is referred to as the mean stoichiometric activity coefficient. Mean stoichiometric activity coefficients contain information on the degree of dissociation of the electrolyte. Clegg and Brimblecombe (1990) show that it is unnecessary to include association in predicting the vapor pressure of nitric acid.

2.2.4 Pitzer Method of Correlating Activity Coefficients

Calculations of aqueous-phase activity coefficients are required for thermodynamic models of extraction in this report. The Pitzer model is generally considered the most reliable, is most used, and is best documented. Therefore, the Pitzer treatment will be used in this report because of its more mature stage of development and availability of parameters.

Activity coefficients can be correlated to ionic strengths of about 6 *m*, using the Pitzer method, to yield results having standard deviations within 0.001. The greatest practical advantage of the Pitzer equations is that the Pitzer parameters obtained from data on binary mixtures and tertiary mixtures can be used to calculate the activity coefficient of the subject species in multicomponent mixtures. Pitzer and Kim (1974) estimated that activity coefficients for binary mixtures with a common ion could be calculated to within standard deviations of 0.02 using only pure-component parameters. Often the tertiary terms are exceedingly small and make only minor corrections to the activity coefficients.

Development of the Pitzer model is detailed in a series of papers by Pitzer and coworkers (Pitzer, 1973; Pitzer and Mayorga, 1973, 1974; Pitzer and Kim, 1974; Pitzer, 1975; Pitzer and Silvester, 1976; Pitzer et al., 1977). The resulting equations for mixed electrolytes, as shown by Pitzer (1991), are given here for the reader's convenience.

Mixed Electrolytes. The osmotic coefficient for a solution containing more than one salt is given by

$$
\begin{aligned}
(\phi - 1)\frac{1}{2}\sum_i m_i = & -\frac{A_\phi I^{3/2}}{1 + bI^{1/2}} + \sum_c \sum_a m_c m_a (B^\phi_{ca} + ZC_{ca}) \\
& + \sum_c \sum_{<c'} m_c m_{c'} (\Phi^\phi_{cc'} + \sum_a m_a \Psi_{cc'a}) \\
& + \sum_a \sum_{<a'} m_a m_{a'} (\Phi^\phi_{aa'} + \sum_c m_c \Psi_{caa'}) \\
& + \sum_n \sum_c m_n m_c \lambda_{nc} + \sum_n \sum_a m_n m_a \lambda_{na} \\
& + \sum_n \sum_{<n'} m_n m_{n'} \lambda_{nn'} + \frac{1}{2}\sum_n m_n^2 \lambda_{nn} \ldots .
\end{aligned}
\qquad (2\text{-}24)
$$

The individual activity coefficients of an ionized electrolyte in a mixed solution are given by the following equations:

$$\ln \gamma_M = z_M^2 F + \sum_a m_a\left[2B_{Ma} + ZC_{Ma}\right] + \sum_c m_c\left[2\Phi_{Mc} + \sum_a m_a \Psi_{Mca}\right] + z_M \sum_c \sum_a m_c m_a C_{ca} + \sum_a \sum_{<a'} m_a m_{a'} \Psi_{Maa'} + 2\sum_n m_n \lambda_{nM} + \ldots , \tag{2-25}$$

and

$$\ln \gamma_X = z_X^2 F + \sum_c m_c\left[2B_{cX} + ZC_{cX}\right] + \sum_a m_a\left[2\Phi_{Xa} + \sum_c m_c \Psi_{cXa}\right] + |z_X| \sum_c \sum_a m_c m_a C_{ca} + \sum_c \sum_{<c'} m_c m_{c'} \Psi_{cc'X} + 2\sum_n m_n \lambda_{nX} + \ldots , \tag{2-26}$$

where M = a cation of a specific species,

X = an anion of a specific species,

a = an anion in a mixture, and

c = a cation in a mixture.

These individual ion activity coefficients are combined by a logarithmic form of Eq. (2-22) to give the mean stoichiometric activity coefficient:

$$\ln \gamma_{MX} = \left(\nu_M \ln \gamma_M + \nu_X \ln \gamma_X\right)/\nu. \tag{2-27}$$

The activity of the solvent is calculated from the osmotic coefficient by use of Eq. (2-11). The remaining terms in the equations are defined by

$$F = f^{\gamma} + \sum_c \sum_a m_c m_a B'_{ca} + \sum_c \sum_{<c'} m_c m_{c'} \Phi'_{cc'} + \sum_a \sum_{<a'} m_a m_{a'} \Phi'_{aa'} , \tag{2-28}$$

$$f^{\gamma} = -A_{\phi}\left[\frac{I^{1/2}}{\left(1 + bI^{1/2}\right)} + \frac{2}{b}\ln\left(1 + bI^{1/2}\right)\right] , \tag{2-29}$$

$$B^{\gamma}_{MX} = B_{MX} + B^{\phi}_{MX} \quad , \tag{2-30}$$

$$C^{\gamma}_{MX} = \frac{3}{2} C^{\phi}_{MX} \quad , \tag{2-31}$$

$$C_{MX} = \frac{C^{\phi}}{2|z_M z_X|^{1/2}} \quad , \tag{2-32}$$

$$Z = \sum_i m_i |z_i| \quad , \tag{2-33}$$

where A_ϕ = Debye-Hückel constant for osmotic pressure, and

b = a constant (equal to about 1.2 for most electrolytes).

For all except 2-2 salts, values for B_{MX} and B^{ϕ}_{MX} are given by

$$B_{MX} = \beta^{(0)}_{MX} + \beta^{(1)}_{MX} g(\alpha I^{1/2}) \quad , \tag{2-34}$$

$$B^{\phi}_{MX} = \beta^{(0)}_{MX} + \beta^{(1)}_{MX} \exp(-\alpha I^{1/2}) \quad , \tag{2-35}$$

and g is an empirical function defined by

$$g(x) = \frac{2[1 - (1 + x)\exp(-x)]}{x^2} \quad . \tag{2-36}$$

Parameter b is a universal parameter having a value of 1.2 $kg^{1/2}/mol^{1/2}$, and α has a value of 2.0 $kg^{1/2}/mol^{1/2}$. The parameters $\beta^{(0)}_{MX}$, $\beta^{(1)}_{MX}$, and C^{ϕ} are specific for each salt and have been tabulated for a large number of systems. For 2-2 salts Pitzer and Mayorga (1974) show that an additional term is required for the functions describing B_{MX} and B^{ϕ}_{MX}; thus,

$$B_{MX} = \beta^{(0)}_{MX} + \beta^{(1)}_{MX} g(\alpha_1 I^{1/2}) + \beta^{(2)}_{MX} g(\alpha_2 I^{1/2}) \tag{2-37}$$

and

$$B^{\phi}_{MX} = \beta^{(0)}_{MX} + \beta^{(1)}_{MX}\exp(-\alpha_1 I^{1/2}) + \beta^{(2)}_{MX}\exp(-\alpha_2 I^{1/2}) \quad . \tag{2-38}$$

Here α_1 and α_2 are 1.4 $kg^{1/2}/mol^{1/2}$ and 12 $kg^{1/2}/mol^{1/2}$, respectively. Parameter $\beta^{(2)}_{MX}$ is an additional salt specific parameter, which is tabulated. The remaining functions are:

$$B'_{MX} = \left[\beta^{(1)}_{MX} g'(\alpha_1 I^{1/2}) + \beta^{(2)}_{MX} g'(\alpha_2 I^{1/2})\right] / I \tag{2-39}$$

and

$$g'(x) = -\frac{2}{x^2}\left[1 - (1 + x + x^2/2)\exp(-x)\right] \quad . \tag{2-40}$$

The difference parameters Φ and ψ are correlated to the difference between measured activity coefficients in binary mixtures with a common ion and those estimated from single electrolyte parameters. Usually the difference parameters are very small; and, when no data are available, satisfactory values of activity coefficients for components of a mixed system may be calculated by assuming that the difference parameters are zero. These equations reduce to the pure electrolyte form when only one electrolyte is present.

Temperature Effect. Silvester and Pitzer (1977, 1978) and Phutela and Pitzer (1986) describe how the Pitzer method may be extended to temperatures other than 25°C. The basic idea was briefly described in Sect. 2.2.2. The equations presented in the foregoing correlate the activity coefficient at a given temperature. Because the functional form is independent of the temperature, temperature effects are necessarily included in the adjustable parameters; that is, the values of the Debye-Hückel coefficient and the parameters $\beta^{(i)}$ and C^{ϕ} vary with temperature. Values of the Debye-Hückel coefficient for the osmotic function A_{ϕ}, according to Silvester and Pitzer (1977), "depend only on the thermodynamic and electrostatic properties of water" and vary appreciably. The molal-based Debye-Hückel coefficient for aqueous solution is given by Bradley and Pitzer (1979, 1983) as

$$A_\phi = \frac{1}{3}A_\gamma = \frac{1}{3}\left(\frac{2\pi N_A \rho_0}{1000}\right)^{1/2}\left(\frac{\varepsilon^2}{D_0 kT}\right)^{3/2} \quad . \tag{2-41}$$

Here the density and dielectric constant of water vary with temperature and pressure, so it is necessary to know those functionalities. Bradley and Pitzer (1979, 1983) give the following empirical equation for the dielectric constant of water as

$$D_0 = D_{1000} + C \ln\left(\frac{B + P}{B + 1000}\right), \tag{2-42}$$

where

$$D_{1000} = u_1 \exp(u_2 T + u_3 T^2) \quad , \tag{2-43}$$

$$C = u_4 + \frac{u_5}{u_6 + T} \quad , \tag{2-44}$$

$$B = u_7 + \frac{u_8}{T} + u_9 T \quad , \tag{2-45}$$

P = pressure, in bars, and

T = temperature, in K.

The values of the u's are:

$u_1 = 3.4279 \times 10^2$, $u_6 = -1.8289 \times 10^2$,

$u_2 = -5.0866 \times 10^{-3}$, $u_7 = -8.0325 \times 10^3$,

$u_3 = 9.4690 \times 10^{-7}$, $u_8 = 4.2142 \times 10^6$,

$u_4 = -2.0525$, $u_9 = 2.1417$.

$u_5 = 3.1159 \times 10^3$,

The notation D_{1000} is used as a reminder that the reference pressure is 1000 bars. These equations are valid from 0 to 350°C and 0 to 1 kbar. Equations for the density of water are given in Sect. 2.3.1.

When using Eq. (2-41) to compute the Debye-Hückel coefficient, it is convenient to use ε in electrostatic units (4.8029×10^{-10} e.s.u.), which makes substitution of the values straightforward. However, if the unit electric charge is given in SI units (i.e., 1.60206×10^{-19} C), it is necessary to multiply the dielectric constant of water by $4\pi D_{vac}$, where D_{vac} is the dielectric (or permittivity) of free space (Pitzer, 1991). The permittivity of a vacuum is given by Sears and Zemansky (1964) as 8.85×10^{-12} $C^2/(\mathrm{N \cdot m^2})$.

Silvester and Pitzer (1978) fit the temperature derivatives of $\beta^{(i)}$ and C^{ϕ} (e.g., $\partial\beta^{(i)}/\partial T$, etc.) to the enthalpy of solution data given in the literature. These temperature derivatives were found to be very small, and the authors expected that they would not vary appreciably for temperature changes of perhaps 20°C. Second derivatives, which are related to the heat capacity of the solution, would need to be evaluated for larger temperature changes.

The parameters ordinarily tabulated for use in the Pitzer model include the Debye-Hückel coefficient at various temperatures [calculated from Eq. (2-41)], the Pitzer parameters at a given temperature (usually 25°C), and the temperature derivatives of the Pitzer parameters. Over a narrow range of temperature, it is permissible to write

$$\beta^{(0)} = \beta^{(0)}_{Tref} + \frac{\partial\beta^{(0)}}{\partial T}(T - T_{ref}) , \qquad (2\text{-}46)$$

where tabulated values at the reference temperature are simply inserted for $\beta_{\mathrm{Tref}}{}^{(0)}$ and $\partial\beta^{(0)}/\partial T$. Similar expressions may be written for the other Pitzer parameters.

2.2.5 Data for Systems of Interest

Activity and osmotic coefficients are derived from various physical and thermochemical data as already described in Sect. 2.2. Over time, data have been accumulated by many workers using several methods. Other researchers have already gathered these data, checked them for consistency, compared the data with one another, and smoothed the data by regression methods to produce what are considered accepted values. Table 2.1 summarizes the sources of data for compounds used in this research.

Table 2.1. Sources of accepted values for activity and osmotic coefficients for selected nitrates in aqueous solution at 25°C

Salt	Source	Data range (*m*)
HNO_3	*a*	0.001 to 28.000
NH_4NO_3	*a*	0.001 to 25.954
$CsNO_3$	*a*	0.001 to 1.500
$UO_2(NO_3)_2$	*b*	0.001 to 5.511
$Sm(NO_3)_3$	*c*	0.1 to 4.2774

[a]W. J. Hamer and Y. C. Wu, "Osmotic Coefficients and Mean Activity Coefficients of Uni-univalent Electrolytes in Water at 25°C," *J. Phys. Chem. Ref. Data* **1**(4), 1047–99 (1972).

[b]R. N. Goldberg, "Evaluated Activity and Osmotic Coefficients for Aqueous Solutions: Bi-Univalent Compounds of Lead, Copper, Manganese, and Uranium," *J. Phys. Chem. Ref. Data* **8**(4), 1005–50 (1979).

[c]J. A. Rard et al., "Isopiestic Determination of the Activity Coefficients of Some Aqueous Rare Earth Electrolyte Solutions at 25°C. 3. The Rare Earth Nitrates," *J. Chem. Eng. Data* **22**(3), 337–47 (1977).

Pitzer parameters are developed by fitting the Pitzer equations to the accepted values of activity coefficients. Table 2.2 lists the Pitzer parameters for pure salts of interest. As noted in the table, values for bismuth nitrate are estimated as shown in Appendix A. Two sets of parameters are given for nitric acid to illustrate that differences may occur due to differences in computational techniques used to obtain those parameters, for example, using as the basis either smoothed data (Clegg and Brimblecombe, 1986; reproduced in Pitzer, 1991) or raw data (Clegg and

Table 2.2. Pitzer parameters for selected salts at 25°C

Salt	$\beta^{(0)}$	$\beta^{(1)}$	C^{ϕ}	Maximum conc. (m)	Source
HNO_3	0.1168	0.3546	−0.00539	6.0	*a*
HNO_3	0.12556	0.28778	−0.00559	6.0	*b*
NH_4NO_3	−0.0154	0.1120	0.00003	6.0	*a*
$CsNO_3$	−0.0758	−0.0669	0.0	1.4	*a*
$UO_2(NO_3)_2$	0.4607	1.613	−0.03154	2.0	*a*
$Sm(NO_3)_3$	0.4673	5.133	−0.05042	1.5	*c*
$Bi(NO_3)_3$	0.4693	5.133	−0.04965	1.5	Estimated; see Appendix A

[a]K. S. Pitzer, *Activity Coefficients in Electrolyte Solutions*, 2nd ed., CRC Press, Boca Raton, Fla., 1991, pp. 100–117.

[b]S. L. Clegg and P. Brimblecombe, "Equilibrium Partial Pressures and Mean Activity and Osmotic Coefficients of 0–100% Nitric Acid as a Function of Temperature," *J. Phys. Chem.* **94**(13), 5369–80 (1990).

[c]K. S. Pitzer et al., "Thermodynamics of Electrolytes. IX. Rare Earth Chlorides, Nitrates, and Perchlorates," *J. Solution Chem.* **7**(1), 45–56 (1978).

Brimblecombe, 1990). The parameters from Pitzer (1991) result in calculated activity coefficients that deviate a maximum of 0.002 from the smoothed data of Hamer and Wu (1972); in comparison, the parameters of Clegg and Brimblecombe (1990) result in deviations as large as 0.08. The former parameters are used for nitric acid in this report. Kim and Frederick (1988a) give different values for the salts appearing in Table 2.2 because the parameters were derived for data spanning a greater concentration range. However, parameters derived in this manner have a greater deviation at any particular value. Because concentrations in this work are limited to less than 6 m, the parameters resulting in the more accurate values are used. Calculation of activity (or osmotic) coefficients at temperatures other than 25°C require the temperature derivatives of the Pitzer parameters. Temperature derivatives of the Pitzer parameters for salts listed in Table 2.2 are given in Table 2.3. Again, the parameters for bismuth nitrate are estimated as shown in Appendix A.

Table 2.3. Temperature derivatives of Pitzer parameters for selected salts at 25°C

Salt	$\partial\beta^{(0)}/\partial T$ $\times 10^4$	$\partial\beta^{(1)}/\partial T$ $\times 10^4$	$\partial C^{\phi}/\partial T$ $\times 10^5$	Maximum conc. (m)	Source
HNO_3[a]	2.4401	13.396	–0.9274	6.0	*b*
NH_4NO_3	0.0	0.0	0.0	6.0	*c*
$CsNO_3$	0.0	0.0	0.0	1.4	*c*
$UO_2(NO_3)_2$	0.0	0.0	0.0	2.0	*c*
$Sm(NO_3)_3$	14.347	168.67	–38.61	1.5	*d*
$Bi(NO_3)_3$	14.600	172.00	–38.87	1.5	Estimated; see Appendix A

[a]Second derivative also available.

[b]S. L. Clegg and P. Brimblecombe, "Equilibrium Partial Pressures and Mean Activity and Osmotic Coefficients of 0-100% Nitric Acid as a Function of Temperature," *J. Phys. Chem.* **94**(13), 5369–80 (1990).

[c]Data not available for these salts; assumed values of zero.

[d]K. S. Pitzer et al., "Thermodynamics of Electrolytes. IX. Rare Earth Chlorides, Nitrates, and Perchlorates," *J. Solution Chem.* **7**(1), 45–56 (1978).

Mixture parameters for Pitzer's method are rare because the literature contains few activity data on mixtures. Baes and Moyer (1988) have examined the issue of mixture parameters for systems containing $UO_2(NO_3)_2$, HNO_3, and $NaNO_3$. They found (using earlier, less accurate parameters than those given in Table 2.2) that mixture parameters were not necessary for the aqueous HNO_3-$UO_2(NO_3)_2$ system. For aqueous $NaNO_3$-$UO_2(NO_3)_2$, Baes and Moyer (1988) concluded that only one mixture parameter ($\phi_{Na,\,UO_2^{2+}} = -0.069$) could be justified; and it may easily vary 65%, depending on the data set from which it is derived. In view of the small value of this particular mixture parameter and the general lack of mixture parameters in the literature, no mixture parameters are used in this work.

In this work, the osmotic coefficients are calculated using Eq. (2-24) and the activity coefficients of individual ions are calculated using Eqs. (2-25) and (2-26). Mean stoichiometric

activity coefficients are calculated by combining individual activity coefficients according to Eq. (2-27).

2.3 Densities of Solutions

Solution densities are required in this study primarily to convert between the molar and molal concentration scales. Activity coefficients can be converted using only the density of the solvent. The molar concentration scale will be used most frequently in the analysis of samples; and, because aqueous activity coefficients are correlated by the Pitzer method using the molal scale, information on aqueous density will be required. Generally, the density of a liquid varies with temperature, but only slightly with pressure. In this work, correlations for pressures at or near 1 atm are adequate. Most experiments will be performed at temperatures between 25 and 50°C, so this defines the minimum temperature range.

Density information in the form of correlations is summarized in this section. Highly accurate empirical correlations are used when available. For multicomponent systems where few data are available, apparent molal volumes of species in solution are used to estimate solution density.

2.3.1 Water

An empirical correlation for the density of water is given in the *70th CRC Handbook* (Weast, 1989). The correlation is

$$\rho_0 = \frac{u_1 + u_2 T + u_3 T^2 + u_4 T^3 + u_5 T^4 + u_6 T^5}{1 + u_7 T}, \qquad (2\text{-}47)$$

where ρ_0 = density of water, kg/m^3;

T = temperature, °C;

and the coefficients are

$u_1 = 999.83952;$

$u_2 = 16.945176;$

$u_3 = -7.9870401 \times 10^{-3};$

$u_4 = -46.170461 \times 10^{-6};$

$u_5 = 105.56302 \times 10^{-9};$

$u_6 = -280.54253 \times 10^{-12};$ and

$u_7 = 16.879850 \times 10^{-3}.$

The density may be easily converted to units of g/mL by dividing by 1000. Equation (2-47) is valid from –30 to 150°C at a pressure of 1 atm below 100°C and at the vapor pressure of water above 100°C. The equation is good to within about 1 ppm over the stated range.

2.3.2 Nitric Acid Solution

The density of nitric acid at 1 atm has been tabulated by Perry (1973) for concentrations from 0 to 100 wt % nitric acid and temperatures ranging from 0 to 100°C. A large subset of these data has been correlated by Spencer (1991) using relatively simple linear functions. The density of an aqueous nitric acid solution at 25°C was found to be well represented by

$$\frac{1}{\rho_{25}} = u_0 + u_1 c + u_2 c^2 + u_3 c^3 , \qquad (2\text{-}48)$$

where ρ_{25} = density at 25°C, g/mL;

c = nitric acid concentration at 25°C, M;

and the coefficients are

$u_0 = 1.003124;$

$u_1 = -3.364529 \times 10^{-2};$

$u_2 = 1.219254 \times 10^{-3}$; and

$u_3 = -1.681279 \times 10^{-5}$.

This equation covers the range from 0 to 21.2 *M* (0 to 90 wt %) and deviates a maximum of 0.05% from the data. The densities at other temperatures were correlated by

$$\frac{1}{\rho} = \left(\frac{1}{\rho_{25}}\right)\left[1 + (u_0 + u_1\rho_{25} + u_2 T)(T - 25)\right], \tag{2-49}$$

where ρ = density at the specified temperature, g/mL;

T = temperature, °C;

and the coefficients are

$u_0 = -1.647365 \times 10^{-3}$;

$u_1 = 1.897063 \times 10^{-3}$; and

$u_2 = 2.017796 \times 10^{-6}$.

Again, this covers the range of concentration from 0 to about 21.2 *M* (0 to 90 wt %), a temperature range of 0 to 100°C, and deviates a maximum of 0.6% from the data. When the acid concentration is zero, the correlation closely reproduces the density of pure water. Extrapolations up to 100% nitric acid were found to be good.

Calculation of the density from concentrations measured at temperatures other than 25°C require an iterative solution to Eqs. (2-48) and (2-49). Spencer (1991) describes the necessary algorithm and presents a computer program for performing the calculations.

2.3.3 Nitric Acid–Uranyl Nitrate Solutions

Spencer (1991) has correlated the density of aqueous nitric acid–uranyl nitrate solutions by the simple linear equation

$$\rho = u_0 + (u_1 + u_2 T)c_H + u_3 c_U + u_4 T \,, \tag{2-50}$$

where c_H = nitric acid concentration, M;

c_U = uranium concentration (as elemental uranium), g/L;

and the coefficients are

$u_0 = 1.022811$;

$u_1 = 2.935808 \times 10^{-2}$;

$u_2 = -3.475035 \times 10^{-5}$;

$u_3 = 1.312180 \times 10^{-3}$; and

$u_4 = -4.680629 \times 10^{-4}$.

Concentrations are expected to be given at the specified temperature. Equation (2-50) was developed from data covering a temperature range of 25 to 95°C, an acid concentration range of 2 to 6 M, and a uranium concentration range of 0 to 300 g/L, and correlates the data to within 0.66%. Extrapolations down to about 15°C, down to 0 M acid, up to 7 M acid, and up to 450 g/L uranium are expected to be good.

2.3.4 Multicomponent Solutions by Apparent Molal Volumes

When a solute is added to a solvent, it is a simple matter of addition to compute the mass of the mixture. Calculation of the volume of the resulting mixture, and hence its density, is not simple. The apparent molal volume has long been used as an effective device in correlating and

predicting the density of electrolyte solutions and some of the structural interactions of these solutions (Millero, 1971).

Masson (1929) provides a succinct description of the apparent molal volume. The molecular volume of a solute may be readily deduced from the specific gravity and composition of a solution when it is assumed that the volume of the solvent is unchanged by the addition of solute and that all changes in volume are assigned to the solute. Because the assumption is not generally valid, the molecular volume so calculated is called the apparent molal volume, which may be written as

$$\phi_V = \frac{(V - n_0 V_0')}{n} = \frac{-1000(\rho/\rho_0 - 1)}{c} + \frac{M}{\rho_0}, \qquad (2\text{-}51)$$

where ϕ_V = apparent molal volume of solute, cm^3/mol;

V = volume of the solution, cm^3;

V_0' = molar volume of solvent (water), cm^3/mol;

n_0 = number of moles of water;

n = number of moles of electrolyte (solute);

M = molecular weight of the solute;

c = molar concentration of solute, M;

ρ = density of the solution, g/cm^3; and

ρ_0 = density of the pure solvent (water), g/cm^3.

Based on Masson's (1929) observation that the apparent molal volume, ϕ_V, varied linearly with the square root of the solute concentration and his own observation that apparent molal

volumes are additive, Root (1933) proposed the following equation for correlating the density of electrolyte solutions:

$$\rho = \rho_0 + \frac{1}{1000}\sum_i (M_i - \rho_0 \phi_{V,i}^0) c_i - \frac{1}{1000}\sum_i (s_i^* \rho_0) c_i^{3/2} \quad . \qquad (2\text{-}52)$$

Millero (1971) reports that for dilute solutions the equation can "predict the densities of unknown solutions more precisely than the best experimental measurements."

Millero (1971) and Roux et al. (1978) have examined much of the data in the literature on the density of aqueous electrolyte solutions. Assuming that electrolytes are totally dissociated in solution, the additivity property of apparent molal volume permits values to be assigned to individual ions when a value for any one ion can be established. In ionic systems the proton (H^+) is arbitrarily assigned an apparent molal volume of 0.0; values of other ions can then be calculated from experimental data. Table 2.4 lists the apparent molal volume for ions applicable to the present study. As shown, the volumes are temperature dependent. Söhnel and Novotný (1985) have correlated density data for several single-electrolyte aqueous solutions. They show that the temperature dependence of the constants in Eq. (2-52) were adequately represented by a simple quadratic in temperature. Because no data on the apparent molal volume of Bi^{3+} were found in the literature, the value shown in Table 2.4 was estimated as described in Appendix B.

Values for the apparent molal volumes shown in Table 2.4 were fit by the present author using a least-squares technique to a quadratic function of temperature as suggested by Söhnel and Novotný (1985). The results are shown in Table 2.5. Because data at only three different temperatures are given (except for UO_2^{2+} and Bi^{3+}), the fit is exact. However, extrapolation outside the temperature range may be risky. Interpolation within the data range should be quite good. Since apparent molal volumes for UO_2^{2+} and Bi^{3+} are given at only one temperature, it will be necessary to assume that the values are constant over a narrow range, for example, up to 40°C.

Table 2.4. Apparent molal volumes of ions in water at infinite dilution

Ion	Temp. (°C)	ϕ_V^0 (cm^3/mol)	Source
H^+	All	0.0	*a*
Na^+	0.0	−3.51	*a*
	25.0	−1.21	*a*
	25.0	−1.2[d]	*b*
	50.0	−0.30	*a*
Cs^+	0.0	19.68	*a*
	25.0	21.34	*a*
	50.0	22.22	*a*
NH_4^+	0.0	17.47	*a*
	25.0	17.86	*a*
	25.0	17.9[d]	*b*
	50.0	19.20	*a*
UO_2^{2+}	25.0	15.91	*c*
Bi^{3+}	25.0	−42.03	Estimated; see Appendix B
NO_3^-	0.0	26.6	*a*
	25.0	29.00	*a*
	25.0	29.5[d]	*b*
	50.0	30.3	*a*

[a]F. J. Millero, "The Molal Volumes of Electrolytes," *Chem. Rev.* **71**(2), 147–76 (1971).

[b]A. Roux et al., "Apparent Molal Heat Capacities and Volumes of Aqueous Electrolytes at 25°C: $NaClO_3$, $NaClO_4$, $NaNO_3$, $NaBrO_3$, $KClO_3$, $KBrO_3$, KIO_3, NH_4NO_3, NH_4Cl, and NH_4ClO_4," *Can. J. Chem.* **56**, 24–28 (1978).

[c]G. F. Vandegrift, Argonne National Laboratory, personal communication to Barry Spencer, Oak Ridge National Laboratory, Apr. 15, 1993.

[d]Preferred value at indicated temperature and value used in this work.

Table 2.5 also shows values for apparent molal volumes of the selected ions at 40°C found by using this interpolation technique.

Table 2.5. Correlation of temperature variation of apparent molal volumes for selected ions[a]

Ion	Coefficient			ϕ_V^0 at 40°C (cm^3/mol)[b]
	u_1	u_2	u_3	
H^+	0	0	0	0
Na^+	−3.51	0.1206	-1.128×10^{-3}	−0.491
Cs^+	19.68	0.082	-6.24×10^{-4}	21.96
NH_4^+	17.47	−0.0002	6.96×10^{-4}	18.58
UO_2^{2+}	15.91	0.[c]	0.[c]	15.91
Bi^{3+}	−42.03	0.[c]	0.[c]	−42.03
NO_3^-	26.6	0.1580	-1.68×10^{-3}	30.2

[a]Listed coefficients are for the function $\phi_V^0 = u_1 + u_2T + u_3T^2$, where ϕ_V^0 = apparent molal volume, cm^3/mol; and T = temperature, °C.

[b]Interpolated by use of the above correlation.

[c]Because the apparent molal volume is known at only one temperature, no temperature coefficients are given.

2.4 Extraction Equilibria

Modern models of the solvent extraction process typically include the nonideality of the aqueous solution. Section 2.2 describes some useful techniques for calculating activity coefficients of aqueous species. The organic phase is usually considered ideal because ionic species are absent and the organic complexes formed are considered electronically neutral. However, some measurements have been made by Diamond et al. (1986) of the vapor pressure of toluene over solutions of CMPO in toluene at 25°C. These data show that the activity coefficient of CMPO decreases with increasing CMPO concentration for solutions in which the organic is equilibrated with water or nitric acid solutions, and this decrease partly explains the "negative deviations from third-power extractant dependency exhibited by americium distribution ratios." [Note: In the paper by Diamond et al. (1986), the calculation of the solute activity coefficient from solvent activity coefficient gives reasonable values and the reduction of solute activity coefficient with increasing solute concentration is an expected trend. However, the equations given for the two activity

coefficients do not satisfy the Gibbs-Duhem equation. It is presumed that an unstated approximation for the function describing the solvent activity coefficient is used to permit integration of the Gibbs-Duhem equation.]

Limited data presented by Horwitz et al. (1987a) show that the water concentration in a CMPO-TCE organic solution decreases as neodymium nitrate is extracted from an aqueous lithium nitrate solution. Data are also presented that show a decrease in water concentration in a CMPO-TBP-TCE organic solution when nitric acid is extracted and a further reduction in water concentration when neodymium nitrate is extracted with the nitric acid. These data seem to suggest that water is not coextracted from nitrate media by CMPO, but is replaced upon extraction of an anhydrous nitrate species.

Extraction is normally modeled by starting with mass action equations. Chemical reactions that may be included in a thermodynamic model of the extraction process describe (1) the dissociation of electrolytes in the aqueous phase; (2) the extraction of the species to be recovered; and (3) the extraction of species, such as nitric acid, that compete for the organic extractant.

For the purposes of discussion, consider the general extraction equilibria

$$M^{z+}\cdot(H_2O)_h + zX^- + nE \rightleftharpoons MX_z\cdot nE + hH_2O \ , \tag{2-53}$$

where a hydrated salt is extracted by a general extractant, E, as an anhydrous salt with an accompanying release of the waters of hydration. The equilibrium constant may be written as

$$K = \frac{[MX_z\cdot nE]\gamma_{MX_z\cdot nE}(a_w)^h}{\gamma_{MX_z}^{(1+z)}[M^{z+}][X^-]^z[E]^n\gamma_E^n} \ , \tag{2-54}$$

where the brackets indicate concentrations and the activity coefficients of both aqueous and organic species are included. Separating the organic-phase activity coefficients from the right-hand

side of Eq. (2-54) and lumping them with the equilibrium constant as suggested by Chaiko and Vandegrift (1988) yields

$$K' = \frac{K\gamma_E^n}{\gamma_{MX_z \cdot nE}} = \frac{[MX_z \cdot nE](a_w)^h}{\gamma_{MX_z}^{(1+z)}[M^{z+}][X^-]^z[E]^n} \quad . \tag{2-55}$$

The equilibrium constant K' is the quantity calculated under the assumption that the organic phase is ideal. If the organic phase is ideal, then the activity coefficients of the organic species are unity and K' is equal to the true equilibrium constant, K. Otherwise, K' will vary with organic-phase activities unless the ratio of these coefficients [as shown in Eq. (2-55)] is constant. The equation also shows a strong effect of the waters of hydration. Even in systems where the activity of water deviates little from unity, a large value for the waters of hydration, h, can cause a significant effect on the equilibrium constant.

An important parameter in modeling extraction behavior is the coordination number, which is essentially the stoichiometry indicating the number of extractant molecules associated with the extractable salt in the organic phase [n in Eq. (2-53)]. The following subsections describe general methods of determining the coordination number and present specific information on the extraction of selected salts by CMPO.

2.4.1 Methods to Determine Coordination Number

Several techniques have been developed to determine the coordination number (or solvation number) for solvent extraction. The book by Schulz and Navratil (1984b) summarizes these techniques. Only a few of the simpler methods are described here.

Slope Analysis. The coordination number can be inferred from experiments in which the organic-phase extractant concentration is varied. Extensive use of this method was first reported

by Hesford and McKay (1958) and is developed as follows: Define a distribution ratio as the ratio of salt concentration in the organic phase to the concentration in the aqueous phase,

$$D = \frac{[MX_z \cdot nE]}{[M^{z+}]} \quad . \tag{2-56}$$

Combine this definition with Eq. (2-55) and rearrange to obtain

$$D = \frac{K\gamma_{MX_z}^{(1+z)}[X^-]^z[E]^n\gamma_E^n}{\gamma_{MX_z \cdot nE}(a_w)^h} \quad , \tag{2-57}$$

which may be expressed in logarithmic form as

$$\begin{aligned} \ln D = \ln K + (1 + z) \ln \gamma_{MX_z} + z \ln[X^-] \\ + n \ln[E] + n \ln \gamma_E - \ln \gamma_{MX_z \cdot nE} - h \ln a_w \quad . \end{aligned} \tag{2-58}$$

Because the extractant concentration is to be varied experimentally, with all other variables held constant, the effect of changing extractant concentration is quantified by taking the derivative of both sides of Eq. (2-58) with respect to ln[E] to obtain

$$\frac{\partial \ln D}{\partial \ln [E]} = n \quad . \tag{2-59}$$

Equation (2-59) implies that a log-log plot of the distribution ratio vs the extractant concentration is a straight line whose slope is the coordination number. Noninteger slopes indicate more than one equilibrium or stoichiometry. Changes in the distribution ratio indicate that the concentration of the extractable salt changes in one or both phases. This, together with the assumption that aqueous and organic activities are constant, makes Eq. (2-59) valid only for the limiting case of very dilute solutions where ideality is approached. Moyer et al. (1991) have critically reviewed the slope-analysis technique and point out that the need to restrict concentrations to limiting cases leaves questions regarding behavior at other conditions. They also state that "on the basis of

equilibrium data alone, definitive identification of species and determination of equilibrium constants cannot be made without knowledge of organic-phase activity coefficients."

Saturation. Coordination numbers can be inferred from total saturation of the organic phase with the extracting salt. The organic is repeatedly contacted with an aqueous phase containing the extractable species until further extraction no longer occurs. The ratio of organic extractant concentration to extractable salt concentration then gives the coordination number. Compared with slope analysis, the opposite end of the concentration spectrum is utilized. This approach requires that the organic remain a single phase (i.e., there is no formation of a second organic phase).

Third-Phase Analysis. A third phase (second organic phase) is sometimes formed when the concentration of the solvate exceeds its solubility in the organic matrix. The ratio of extractant to extract in the third phase is determined and is assumed to be equivalent to the coordination number.

Spectroscopic Analysis. Studies on infrared absorption by the functional group (such as P=O) indicate shifts in the absorption peak as solvates are formed. Coordination numbers can be assigned, based on the amount of shift in these absorption peaks. Further information can be obtained by referring to Schulz and Navratil (1984b).

2.4.2 General CMPO Extraction Stoichiometry

Horwitz and Schulz (1990) report that CMPO tends to form a third phase during extraction when used in a paraffinic hydrocarbon diluent (without TBP as a phase modifier) and that little or no third-phase formation occurs in a TCE diluent. This is probably the reason that most of the available information on CMPO has been derived from systems in which TCE was the organic diluent. It is generally assumed that the stoichiometry is unaffected by the choice of

diluent, provided the diluent is electrically neutral. The equilibrium constants themselves cannot be numerically equivalent unless the organic-phase activities (or their ratios) are equivalent. Measurements of the distribution ratios of uranium, reported by Marsh and Yarbro (1988), are slightly higher for TRUEX extractant in a TCE diluent than in an NPH diluent. This suggests a diluent effect. Marcus (1989) has reviewed the concept of diluent parameters that depend only on a universal diluent constant and a parameter characteristic of the specific extraction system. Unfortunately, parameters are not available for the diluents of interest here.

The development of CMPO was motivated by the need for an extractant to remove americium from PUREX process waste streams. Initial development and evaluation of this neutral bifunctional extractant by Horwitz et al. (1982) demonstrated selectivity for Am(III) over Fe(III) and other fission products. In addition, the distribution ratio strongly favored the organic phase at high acid concentration, but low distribution ratios in dilute acid favored back-extraction. Their work also showed that the extraction stoichiometry for americium was three extractant molecules to each extract molecule (i.e., a stoichiometry of 3:1). Horwitz et al. (1985) found that the distribution ratio decreased as the temperature increased. This is assumed to be a general trend for all metal salts.

Schulz and Navratil (1984a) discuss bifunctional organophosphorus extractants. The neutral monofunctional extractant TBP contains the active phosphoryl group (P=O) and extracts both tetravalent and hexavalent actinides. The bifunctional extractant CMPO contains both phosphoryl and carbonyl (C=O) groups and are important because trivalent actinides, as well as tetravalent and hexavalent actinides, are extracted. Navratil (1985) summarizes that, in general, trivalent actinides are extracted by CMPO with a 3:1 stoichiometry and that tetravalent and hexavalent actinides are extracted with a 2:1 stoichiometry. Horwitz and Schulz (1990) report that hexavalent uranium is much more strongly extracted than trivalent americium. For example, in

1 to 3 *M* nitric acid the distribution ratio for americium is between 1 and 20, whereas the ratio is much greater than 20 for uranium. Horwitz et al. (1985) indicate that the distribution ratios for tetravalent actinides (e.g., thorium) are about ten times larger than those for hexavalent actinides. [The above discussion should not be taken to mean that TBP does not extract any trivalent species. Hesford et al. (1959) and Robinson and Topp (1964) show that the trivalent rare-earth nitrates are extracted with moderate distribution ratios with TBP in a 3:1 stoichiometry at high acid concentrations.]

2.4.3 Nitric Acid

Aqueous nitric acid is often the solvent used in processing nuclear fuel or stored nuclear fuel reprocessing wastes. Because it competes with other extractable species for the CMPO, its behavior needs to be quantified in building a good extraction model.

Unless the nitric acid concentration is very high, the dissociation of nitric acid is nearly complete and molecular nitric acid need not be considered in extraction models. In their models of the extraction of nitric acid by TBP, Davis (1962a, 1962b, 1962c), Olander and Benedict (1963), Lietzke et al. (1963), Tedder and Davis (1983), and Chaiko and Vandegrift (1988) do not consider molecular nitric acid. In fact, the association reaction has been found to be unnecessary for the representation of thermodynamic properties of pure aqueous nitric acid (see Pitzer, 1991).

Extraction of nitric acid by 0.5 *M* CMPO in TCE was measured at 25°C and at various acid concentrations by Horwitz et al. (1987b). The data suggested that the stoichiometry was approximately 1:1; thus,

$$H^+_{(aq)} + NO^-_{3(aq)} + CMPO_{(org)} \rightleftharpoons CMPO{\cdot}HNO_{3(org)} \quad . \tag{2-60}$$

Kolarik and Horwitz (1988) assumed that a 1:1 solvation of CMPO with nitric acid predominated to permit calculation of the free CMPO concentration in their studies on the extraction of

neodymium and the solubility of its CMPO solvate in solutions of dodecane-TBP. Later, Chaiko et al. (1988a) made additional measurements on the extraction of nitric acid with 0.25 *M* CMPO–0.75 *M* TBP in TCE. The effects of the TBP on the distribution ratio were removed by separately modeling the extraction of nitric acid by TBP, using data from the literature. It was suggested that the equilibrium

$$2H^{+}_{(aq)} + 2NO^{-}_{3(aq)} + CMPO_{(org)} \rightleftharpoons CMPO{\cdot}2HNO_{3(org)} \qquad (2\text{-}61)$$

should also be used in modeling the extraction when the nitric acid concentration is "moderately high." Further studies by Chaiko et al. (1989) at CMPO concentrations of 1.0 *M* in TCE indicated that the extraction constant for Eq. (2-60), when used as part of the two-parameter model, increased linearly with CMPO concentration, suggesting a dimeric CMPO species. A third equilibrium,

$$H^{+}_{(aq)} + NO^{-}_{3(aq)} + 2CMPO_{(org)} \rightleftharpoons (CMPO)_2{\cdot}HNO_{3(org)} \quad , \qquad (2\text{-}62)$$

was added to the model. Using Bromley's method to calculate aqueous activity coefficients, all three extraction constants, K', were evaluated by a nonlinear least-squares fit to the data. Their results are summarized in Table 2.6. Chaiko et al. (1988b) claim that the extraction constants can be reevaluated for other systems, such as CMPO and TBP in dodecane, if the activity coefficient ratios [see left-hand equality of Eq. (2-55)] for the particular organic systems are known. This is based on the assumption that the true equilibrium constants, K, are independent of solvent type.

2.4.4 Uranyl Nitrate

The available data on the extraction of uranium with CMPO are derived from experiments performed with mixed CMPO-TBP extractants in an inert diluent. Hexavalent uranium and CMPO have been reported by both Navratil (1985) and Horwitz et al. (1987b) to form the disolvate

Table 2.6. Nitric acid extraction constants for CMPO in TCE at 25°C

Species formed	Extraction constant, K'
$CMPO \cdot HNO_3$	1.60 ± 0.04
$CMPO \cdot 2HNO_3$	0.010 ± 0.001
$(CMPO)_2 \cdot HNO_3$	1.66 ± 0.06

Source: D. J. Chaiko et al., "Modeling of Aqueous and Organic Phase Speciation for Solvent Extraction Systems," presented at the Fall Meeting of the Metallurgical Society, Las Vegas, Nev., February 1989.

during extraction. These results were confirmed by Kolarik and Horwitz (1988), using the slope analysis method. Tedder and Davis (1983) used an aqueous-phase hydration number of 6 in thermodynamic models of the extraction of uranium with TBP. The extraction of uranyl nitrate with CMPO, then, might be described by the equilibrium

$$UO_2(H_2O)^{2+}_{6(aq)} + 2NO^-_{3(aq)} + 2CMPO_{(org)} \rightleftharpoons UO_2(NO_3)_2 \cdot 2CMPO_{(org)} + 6H_2O_{(aq)}. \quad (2\text{-}63)$$

Distribution ratios for uranyl nitrate partitioned between a solution of 0.2 *M* CMPO–1.2 *M* TBP in *n*-dodecane and aqueous nitric acid media at 25°C are given in graphical form by Schulz and Horwitz (1988). The distribution ratios are approximately 5, 50, 300, and 500 at nitric acid concentrations of 0.02, 0.08, 0.50, and 1.0 *M*, respectively. Because of these high distribution ratios at low acidities, Horwitz et al. (1985) suggest stripping with aqueous oxalic acid or sodium carbonate solutions rather than dilute acid.

Mincher (1989) presented distribution data collected at 25°C for a similar system where the organic phase was 0.1 *M* CMPO–1.4 *M* TBP in *n*-dodecane. The graphical data indicated that the uranium distribution ratio increased greatly as the nitric acid concentration increased. In this system, for example, the distribution ratio for uranyl nitrate was ~75 at an aqueous nitric acid

concentration of 0.5 *M*. Ignoring the effects of TBP, when this result is compared with the data of Schulz and Horwitz described above, a coordination number of 2 is indicated. Kolarik and Horwitz (1988) report distribution data for uranyl nitrate using a solvent composed of 0.2 *M* CMPO and 1.2 *M* TBP in dodecane. Experiments performed at 25°C and about 1.0 *M* nitric acid give a distribution ratio of ~300 at a low uranium concentration of 0.0001 *M*. The distribution ratio was found to decrease with increasing aqueous uranium concentration, slowly at first and then more rapidly as the solvent loaded. At aqueous uranium concentrations of ~0.01 *M*, the distribution ratio was as low as 10. Kolarik and Horwitz observed that organic loadings high enough to promote a third phase also caused the remaining light organic phase to remain cloudy.

Marsh and Yarbro (1988) also measured distribution ratios for uranium with, primarily, 0.25 *M* CMPO–1.0 *M* TBP in a TCE diluent. They noticed that the addition of TBP decreased the distribution ratio for uranium at low nitric acid concentrations.

2.4.5 Bismuth Nitrate

Extraction equilibria for bismuth nitrate with CMPO are not reported in the literature. Because bismuth is a trivalent metal, it can be assumed, as a first approximation, that it will behave similarly to other trivalent metals. For example, Chaiko et al. (1988a) modeled the extraction of americium at low acid concentrations with the equilibrium

$$Am(H_2O)^{3+}_{9(aq)} + 3NO^{-}_{3(aq)} + 3CMPO_{(org)} \rightleftharpoons Am(NO_3)_3 \cdot 3CMPO_{(org)} + 9H_2O_{(aq)} \quad . \qquad (2\text{-}64)$$

Chaiko et al. also included extraction of americium by the $HNO_3 \cdot$ CMPO solvate to help explain the coextraction of americium and nitric acid reported by Schulz and Horwitz (1988). Bismuth nitrate is often produced by crystallization in the pentahydrate form (Dean, 1973). Assuming a

hydration number of 5 in the aqueous phase and an anhydrous extraction, a proposed equilibrium may be written as follows:

$$Bi(H_2O)^{3+}_{5(aq)} + 3NO^{-}_{3(aq)} + 3CMPO_{(org)} \rightleftharpoons Bi(NO_3)_3 \cdot 3CMPO_{(org)} + 5H_2O_{(aq)} \quad . \qquad (2\text{-}65)$$

Lumetta et al. (1993) measured the distribution of bismuth from nitric acid with 0.2 *M* CMPO–1.4 *M* TBP in an NPH diluent. The temperature at which the tests were performed was not reported. Using an organic:aqueous phase ratio of 1:3, distribution ratios were measured for nitric acid concentrations ranging from 0.1 to 10.0 *M*. From the plot given in the report, the distribution ratio was ~25 at 0.1 *M* nitric acid and peaked at ~110 at 1.0 *M* nitric acid. The addition of oxalic acid to the aqueous phase suppressed the distribution ratio but also caused precipitation when the nitric acid concentration was less than 5 *M*.

3. EXPERIMENTAL METHODS

3.1 Apparatus

3.1.1 Dry Box

A laboratory dry box (LABCONCO) having the dimensions shown schematically in Figure 3.1 was used for two primary purposes: (1) to prepare atmosphere-sensitive reagents, and (2) to maintain a controlled temperature during the extraction tests.

Some reagents used in the experimental program are hygroscopic. Accurate weighing of these materials to prepare solutions of known concentration required that the material be isolated in a dry environment. For example, the CMPO appeared to slowly liquefy on contact with air, presumably due to the absorption of moisture. Bottled, dry nitrogen was fed to the dry box as illustrated in Figure 3.2. Before entering the dry box, the nitrogen passed through a Drierite™ (anhydrous calcium sulfate marketed by W. A. Hammond Drierite Co.) trap to ensure removal of all moisture, then through an ascarite (sodium hydroxide-coated, nonfibrous, silicate granules) trap to remove any carbon dioxide, in case any reagents were to be used that were sensitive to carbon dioxide and, finally, through a rotameter so that a positive indication of gas flow was available. The gas was removed from the dry box through both ascarite and Drierite™ traps to ensure that no unwanted species could accidentally backflow in the event of equipment failure. Exhaust gas could flow into an exhaust hood either of its own accord (i.e., due to the pressure in the dry box) or could be removed from the dry box using a vacuum pump. Use of the vacuum pump and adjustment of a needle valve in the line proved to be the most reliable method for maintaining pressures in the dry box at near atmospheric.

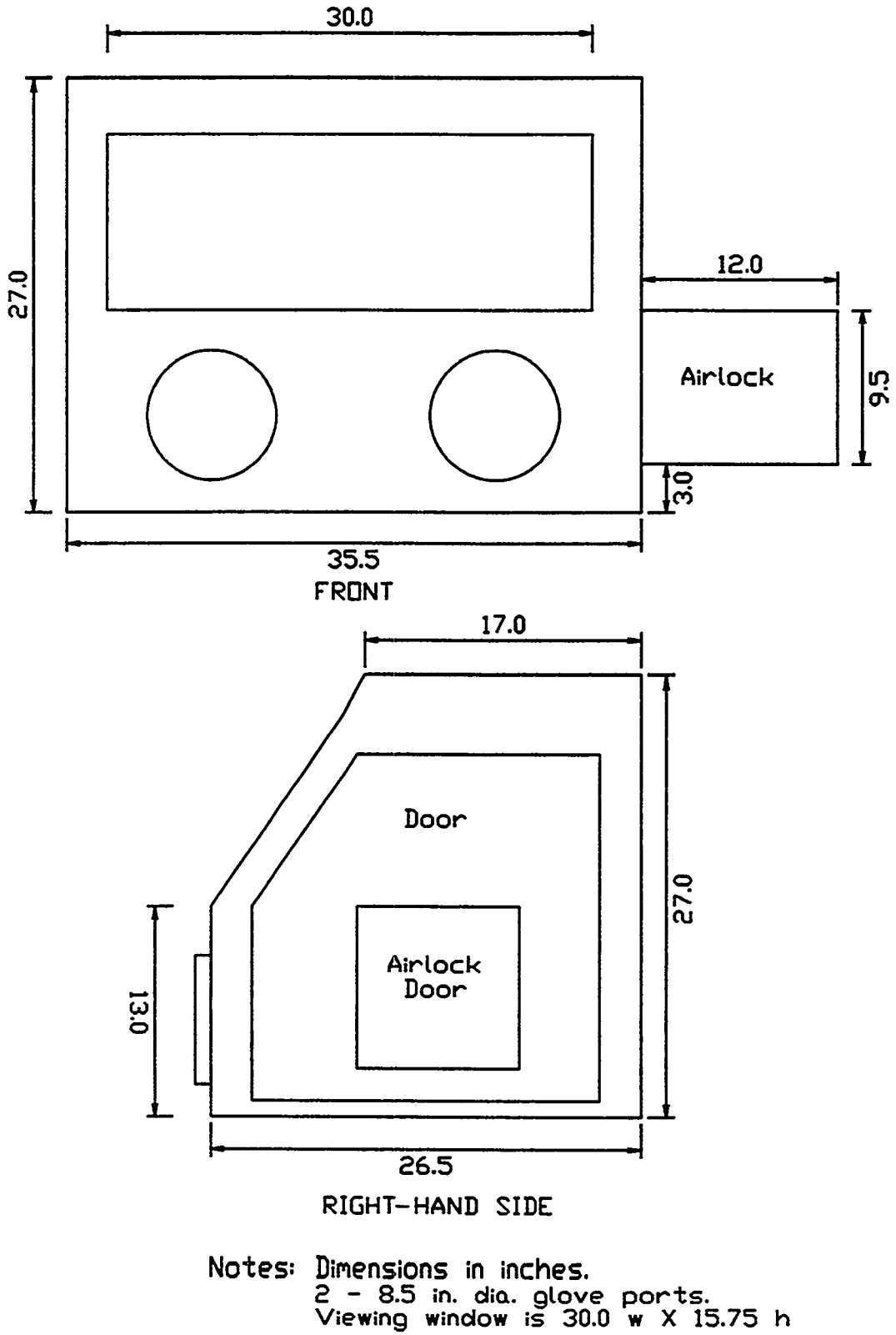

Figure 3.1. Schematic of laboratory dry box, showing approximate dimensions.

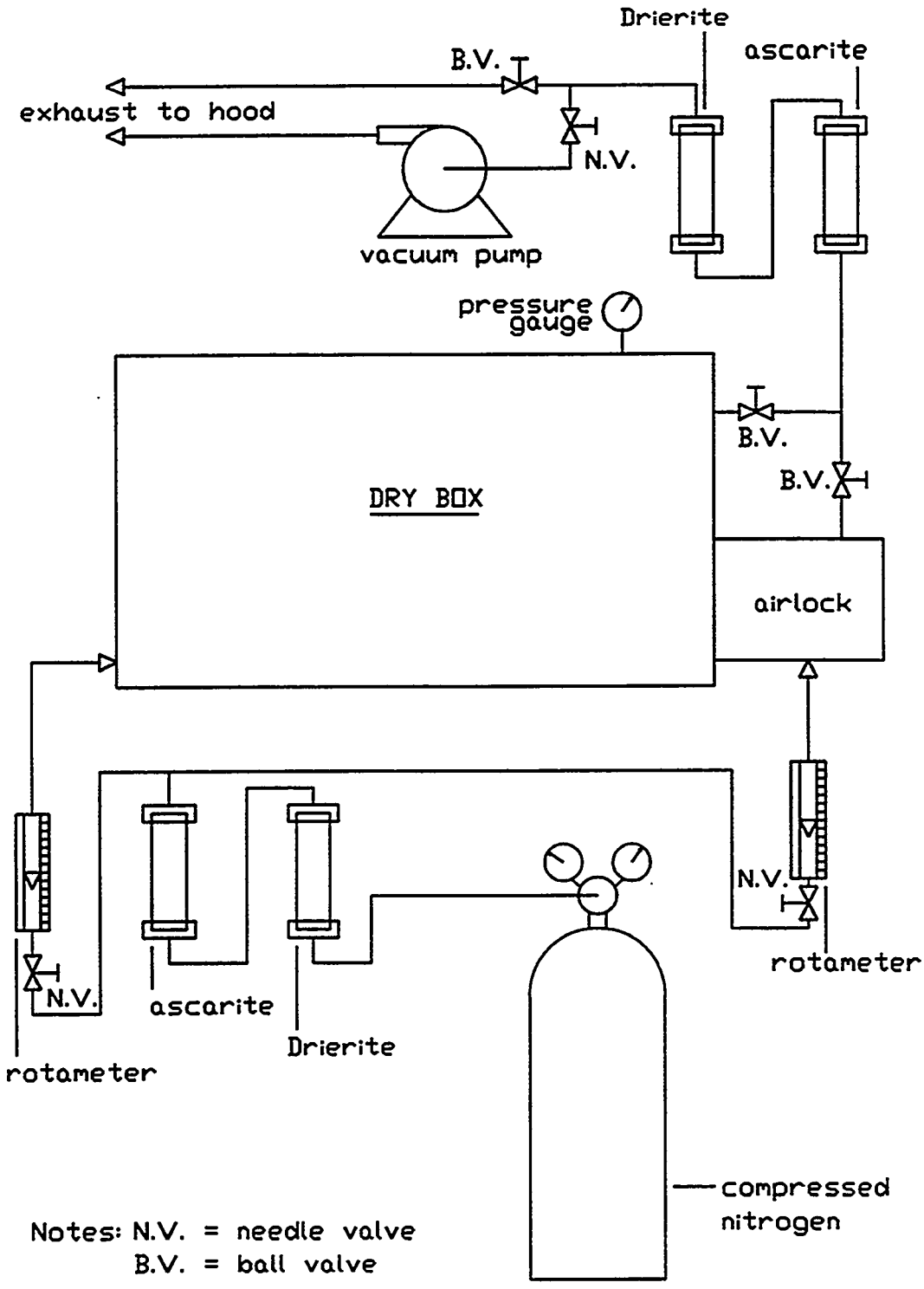

Figure 3.2. Flowsheet for controlling atmospheric composition within dry box.

3.1.2 Temperature Measurement and Control

The extraction tests were to be performed at specified and controlled temperatures; however, there was no requirement to control the atmospheric composition during the tests because, after being placed in solution, the reagents exhibited no adverse reaction to the atmosphere. (For example, the CMPO once dissolved in *n*-dodecane was to be contacted with an aqueous nitric acid solution, so that moisture from the air was no longer significant.) Test temperatures were to be 25°C or higher (above ordinary room temperature), so a small heating unit was built to heat the air inside the dry box. All reagents, sample bottles, pipettors, and separatory funnels required for a test could be placed inside the box.

Control of the temperature in the dry box was implemented as illustrated in Figure 3.3. A small heating unit was built from two 100-W, wire-wound heaters and an instrument cabinet (Muffin) fan enclosed in a metal shroud. The fan was permitted to run at all times, while power to the heaters was controlled by an Omega CN9112A time proportioning temperature controller. This controller could be programmed to use one of several types of thermocouples or a resistance-temperature device (RTD). A wire-wound, air-sensing (baffled-shield) platinum RTD, Omega PRX-AP-100-E-12 (100-Ω resistance at 0°C), was used as the sensing device to measure the temperature within the dry box. Operation at temperatures higher than about 35°C required more than the 200 W of heat provided by the aforementioned heaters. For such instances, another 200-W, wire-wound resistance heater was placed in the dry box downstream of the first heater so that air emanating from the first heater would flow across it. The auxiliary heater was fed power through a Variac to provide an adjustable background heat source.

Calibration of the temperature controller was verified by comparison with a certified thermometer [H-B Instrument Co., –20 to 110°C, 1° divisions, compared with National Institute of Science and Technology (NIST) standards per NIST test 247503]. Although the calibration of

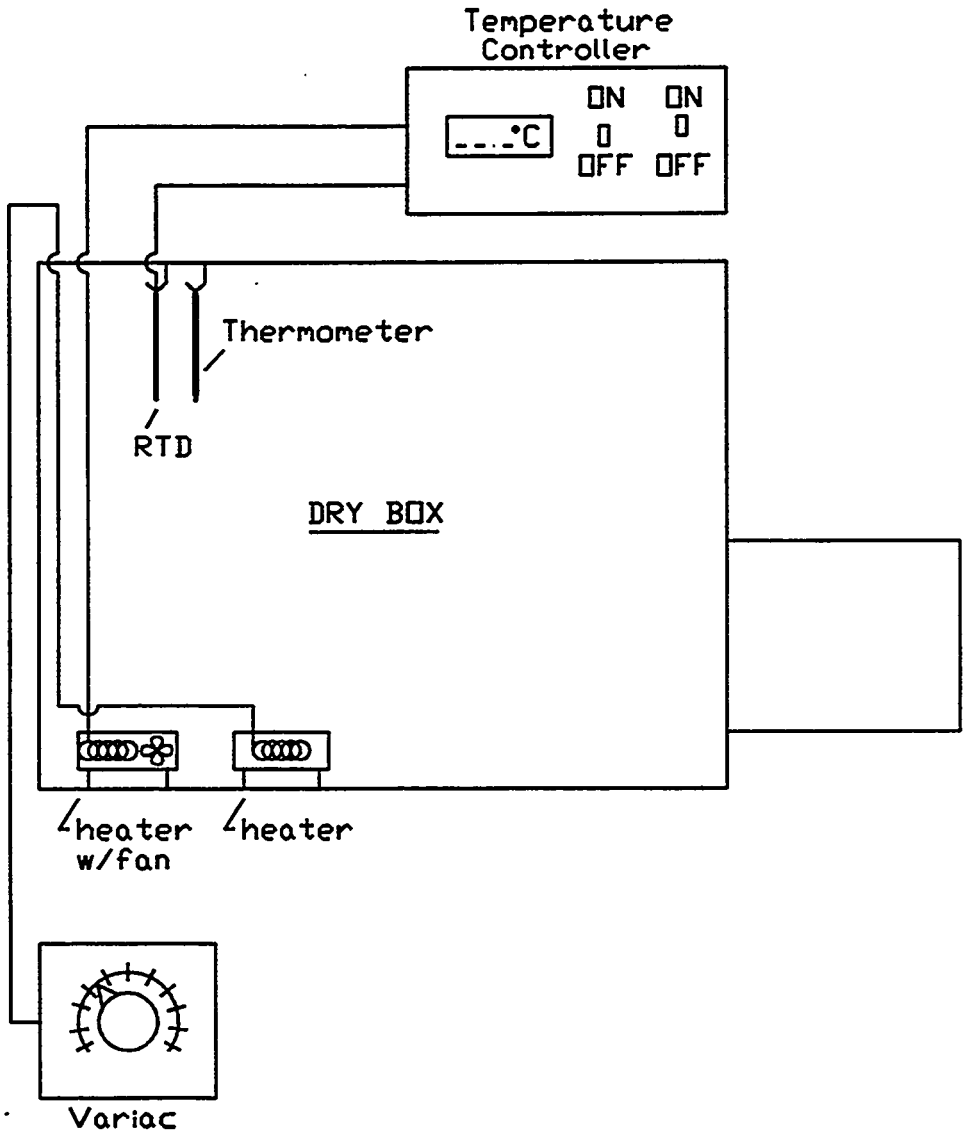

Figure 3.3. Temperature control scheme used for extraction tests.

this thermometer indicates that readings to 0.01°C were possible, readings were made with the unaided eye to an estimated error of 0.1°C. A VWR, Inc., student's thermometer, also calibrated against the certified thermometer, was suspended in the dry box to provide constant verification of the digital readout on the controller during experiments.

3.1.3 Other Laboratory Equipment

A Mettler PM1200 electronic balance (range, 0 to 1200 g; resolution, 0.001 g) was used to weigh reagents. A Büchi model R rotavapor was available to concentrate organic solutions. Ordinary temperature measurements were made using VWR student thermometers (-20 to 110°C, 1° divisions). A variable-speed orbital mixer, Lab-Line Instruments, Inc., Model 4600, was available for contacting the aqueous and organic phases; however, space constraints in the dry box prevented the mixer from being used and, consequently, the samples were shaken by hand.

3.2 Reagents

3.2.1 General Laboratory Reagents

Reagent-grade chemicals were purchased for use in purification of the extractant and for use as the working chemicals in the extraction tests. Table 3.1 lists the chemicals used, their source, and comments concerning their purity. Water used in the experimental program was distilled and demineralized with an ion-exchange resin. The resulting "ultrapure" water had a measured resistance of ≥17.7 MΩ/cm.

Table 3.1. List of reagents used in extraction studies

Chemical	Supplier	Comments
Amberlyst® A-26, anionic resin[a]	Aldrich Chemical Co.	
Bismuth(III) nitrate, anhydrous solid	Aldrich Chemical Co.	99.999%
n-Dodecane, anhydrous	Aldrich Chemical Co.	99%+ (density = 0.750)
Dowex® AG MP-50, cationic resin[b]	Bio-Rad Laboratories	
n-Heptane	J. T. Baker, Inc.	Analyzed reagent, 99.8%
Methanol	J. T. Baker, Inc.	Analyzed reagent, 100.0%
Nitric acid, 0.1006 *M*	J. T. Baker, Inc.	Analyzed reagent, ±1 part per 1000
Nitric acid, 2.030 *M*	J. T. Baker, Inc.	Analyzed reagent, ±1 part per 1000
Nitric acid, 6.0 *M*	EM Science	Standardized within 5.9 to 6.1 *M*
Sodium carbonate, 1 *N*	J. T. Baker, Inc.	Analyzed reagent, ±1 part per 1000
Sodium hydroxide, solid	Fisher Scientific	Certified A.C.S. reagent
Sodium sulfate, anhydrous solid	J. T. Baker, Inc.	Analyzed reagent, 99.9%+
Cesium nitrate	EM Science	Assay, 99%+
Uranyl nitrate	ORNL	High purity in ^{238}U isotope
Uranyl nitrate	ORNL	High purity in ^{233}U isotope

[a]Amberlyst® is a registered trademark of Rohm and Haas Company.
[b]Dowex® is a registered trademark of Dow Chemical Company.

3.2.2 Purification of CMPO

CMPO was purchased from ATOCHEM North America (Philadelphia, PA) having a purity of 95 to 97% (lot No. UDDEV007K). It was desired that the purity of the CMPO be >99% for solvent extraction tests in order to quantify the equilibrium constants for extraction of selected metal species. The CMPO was purified according to a procedure developed by Gatrone et al. (1987) and Tse and Vandegrift (1989), with modifications supplied by Vandegrift (1993). Details of the purification as actually performed are reported here.

Purification of the CMPO requires anionic (Amberlyst® A-26) and cationic (Dowex® AG MP-50) resins to remove any ionic impurities. The Amberlyst® was (1) washed with ultrapure

(distilled and treated with ion-exchange resins) water, (2) treated with 0.902 *M* sodium hydroxide solution to convert the resin from the H^+ to the Na^+ form, (3) rinsed with analytical-grade methanol to remove water, and (4) rinsed with analytical-grade *n*-heptane. Cleaning of the Dowex® resin consisted of (1) rinsing it with ultrapure water, (2) washing with analytical-grade methanol, and (3) rinsing with analytical-grade *n*-heptane. Both resins were stored under *n*-heptane until used.

The first step of the CMPO purification procedure involved dissolving 383.174 g of the purchased material in 1250 mL of *n*-heptane. The resulting solution was then filtered through grade 494 quantitative filter paper in a Büchner funnel fitted with a porous glass frit. Next, 50 g of the cleaned Dowex® AG MP-50 cationic resin was added to the *n*-heptane–CMPO solution, which was then vigorously mixed with a magnetic stirrer for 2 h. Subsequently, ~50 g of the prepared Amberlyst® A-26 anionic resin was added to the solution, and the solution was mixed for an additional 2 h. Finally, the solution was filtered through grade 494 quantitative filter paper supported by a glass-frit Büchner funnel to remove the resin particles.

The CMPO filtrate was washed with a 0.25 *M* sodium carbonate solution. Washing consisted of placing the sodium carbonate solution in a large separatory funnel with the *n*-heptane–CMPO solution in a ratio of 2 mL organic to 1 mL aqueous. The phases were vigorously contacted for 15 s, vented, contacted again for 60 s, and allowed to separate. The aqueous phase was drained, and the washing was repeated with a second aliquot of fresh aqueous solution. The entire washing procedure was then repeated using 0.1 *M* nitric acid solution as the aqueous wash. Subsequently, the washing procedure was repeated using ultrapure water as the aqueous wash. The organic solution was finally collected in an Erlenmeyer flask, and about 200 g of anhydrous sodium sulfate was added to the solution to remove any water.

The dried CMPO solution was filtered through spun glass and collected in a tear-shaped flask. This flask was then attached to a rotavapor, for distilling the *n*-heptane from the solution. Low pressure was maintained during the vacuum distillation using a vacuum pump. A water bath was used to warm the organic solution in the rotavapor, and the condensate collection flask was placed in an ice-water bath. The warm-water bath never exceeded a temperature of 45°C. The organic solution, was reduced to about one-third of its original volume as the *n*-heptane was driven off. At this point, the organic solution, which was oily looking and very viscous, was placed in a large beaker. A small amount of the "as received" CMPO was vacuum desiccated and added to the solution, which was subsequently refrigerated. Four days later, the CMPO had crystallized, leaving about 20% of the volume as a supernatant. The crystals were scraped from the beaker and placed in a crystallization dish for drying in a vacuum desiccator overnight. The dried CMPO was stuck firmly to the crystallization dish but could be removed with a stainless steel spatula. The crystals were crushed using a mortar and pestle, placed back into the crystallization dish, and returned to the vacuum desiccator. The CMPO powder was allowed to dry under vacuum overnight and was then transferred to preweighed amber bottles. The bottles were sealed and weighed, after which they were reopened and placed in the vacuum desiccator for 4 h. The bottles were subsequently removed from the desiccator, sealed, and reweighed. A small decrease in the weight was observed, so another 4.5 h of vacuum desiccation was performed. Since an extremely small decrease in weight was observed following this procedure, the material was considered to be completely dry. The sealed amber bottles containing 273.619 g of purified CMPO were then stored until needed for the extraction tests.

The supernatant from the first crystallization was refrigerated in a beaker for 10 d to allow additional crystallization. At the end of this period, the supernatant was poured off, and the crystals were rinsed with cold *n*-heptane and then placed in a crystallization dish. Vacuum

desiccation of the crystals was allowed to continue overnight. Subsequently, the crystals were crushed using a mortar and pestle, placed in an amber bottle, and subjected to another 4 h of vacuum desiccation. Following this procedure, it was determined that another 27.191 g of purified CMPO had been recovered. Overall, a total of 300.810 g of CMPO was recovered by crystallization. Based on the starting amount of material, recovery was 78.5%.

Four samples of the CMPO were prepared for analysis. Samples included (1) the "as-received" CMPO from the shipping container (raw), (2) desiccated "as-received" CMPO, (3) CMPO from the first crystallization, and (4) CMPO from the second crystallization. The samples of the CMPO were analyzed by a Hewlett-Packard model 1090 high-performance liquid chromatograph (HPLC) under the following conditions:

Column	2.1 mm diam × 15 cm long ZORBAX RX-C18
Mobile phase	80% methanol/20% water (nominally)
Temperature	38°C
Flow rate	0.2 to 0.4 mL/min
Sample size	5 μL

A UV absorbance wavelength of 222 nm is the most sensitive for detection of CMPO and its impurities (Tse and Vandegrift, 1989), but wavelengths both higher and lower than this value were used to ensure that other organic compounds would be detected. The built-in software of the chromatograph integrated the areas under the detection peaks, providing the relative area of the CMPO peak as a percentage of the total. The results are shown in Table 3.2. Simple desiccation of the CMPO appeared to remove a volatile, polar compound. Purification by the crystallization process described above further improved the purity of the CMPO. The purified material was judged to be suitable for solvent extraction studies.

Table 3.2. Results of chromatographic analysis of CMPO

Sample	Description	CMPO peak area (%) at UV absorption wavelength			
		206 nm	222 nm	254 nm	Avg
CMPO-04	Raw	98.29 ± 0.12	98.73 ± 0.05	89.79 ± 0.52	95.60[a]
CMPO-01	Raw, desiccated	98.81 ± 1.12	99.24 ± 0.08	96.93 ± 1.59	98.32[b]
CMPO-02	First crystallization	98.98 ± 0.65	99.47 ± 0.08	97.88 ± 0.92	98.78[b]
CMPO-03	Second crystallization	99.50 ± 0.64	99.76 ± 0.23	98.41 ± 0.86	99.22[b]

[a]Three measurements at each wavelength.
[b]Two measurements at each wavelength.

3.2.3 Uranyl Nitrate

Two high-purity uranium solutions were used to prepare test solutions having count rates adequate for analysis (≥1000 dpm/mL). One solution contained isotopically pure ^{238}U spiked with a small quantity of ^{233}U, while the other contained only ^{233}U. These solutions were well characterized as follows:

^{238}U stock solution: (225.2 ± 0.23) g U/L
(3.72 ± 0.01) *M* HNO_3
$(3.132 \times 10^6 \pm 3.975 \times 10^4)$ dpm/mL

^{233}U stock solution: (0.4720 ± 0.0003) g U/L
(0.1006 ± 0.0001) *M* HNO_3
$(9.908 \times 10^6 \pm 6.547 \times 10^3)$ dpm/mL

These solutions were of analytical quality but, because of aging, were purified by TBP extraction to remove decay daughters. Additionally, the ^{233}U stock was precipitated with sodium hydroxide, recovered by filtration, washed with very mild caustic (~0.01 *M* NaOH), and redissolved in nitric acid. After purification, the solution was characterized with the following results:

^{238}U stock solution: (126.8 ± 1.61) g U/L
(2.11 ± 0.01) *M* HNO_3
$(1.780 \times 10^6 \pm 3.707 \times 10^4)$ dpm/mL

^{233}U stock solution: (0.1165 ± 0.0005) g U/L
(0.1013 ± 0.0001) *M* HNO_3
$(2.447 \times 10^6 \pm 1.070 \times 10^4)$ dpm/mL

Use of either set of stock solutions to prepare test solutions gave the same results.

The ^{238}U stock solution was used to prepare uranium solutions of various strengths for the extraction tests (typically, ~1 g U/L); and the ^{233}U was added in small amounts, as necessary, to increase the counting rate. Since half-lives of ^{238}U and ^{233}U are 4.9×10^9 and 1.6×10^5 years, respectively, the concentrations are (for practical purposes) constant over the time span of the experimental program.

3.3 Experimental Procedures

Aliquots of the organic extractant were measured by a mechanical pipettor and placed in 60-mL, screw-top separatory funnels. The funnels containing the organic solution and stoppered flasks containing the aqueous reagents were then transferred to the dry box and allowed to reach the desired experimental temperature. Organic extractant was then preequilibrated with equal (or greater) volumes of aqueous nitric acid having the same concentration as the final aqueous contact for which distributions were to be measured. Three preequilibrations were completed before the final contact. Each time the aqueous phase was drained from the separatory funnel, taking care to avoid loss of organic material. The mechanical pipettor was used to add a volume of aqueous solution equal to the organic-phase volume to the separatory funnel for the final contact. After separation, a small volume of the aqueous phase was withdrawn from the separatory funnel to clear the spout and was discarded. A sample of the aqueous phase was then decanted directly into a sample vial, which was immediately sealed. A sample of the organic phase was withdrawn from below the surface of the organic with the mechanical pipettor, removed through the top of the funnel, and immediately transferred to a sample vial, which was then sealed.

In the case of the uranium distribution tests, the procedure was modified for small-volume experiments. A 20-mL sample vial was used as the contacting container. Materials were added to

the vial with a high-precision electronic pipettor that utilized disposable tips. Aqueous preequilibration solutions were removed from beneath the organic phase with needle-shaped disposable pipettes. Next, the organic solution was transferred to a clean sample vial with the electronic pipettor for the final contact. Final organic samples were taken with the electronic pipettor; then the remaining organic was skimmed with the pipettor, and the final aqueous samples were taken from below the liquid surface with the electronic pipettor. Because of difficulties with interferences from decay daughters in tests using ^{233}U, a back-extraction method was also used. In the back-extraction, a portion of the loaded organic solution was contacted with an equal volume of clean aqueous phase having the same acid concentration as in the forward extraction. Aqueous and organic samples were then taken as just described. Details concerning the necessity of a back-extraction method have been discussed by Spencer (1994).

Each equilibration included both a mixing time and a settling time. Mixing was achieved by manually shaking the separatory funnels because there was insufficient space for the orbital shaker in the dry box. It was thought that temperature control would be more important than the convenience of a mechanical shaker. A mixing time of 1 min for each equilibration was evidently sufficient because tests conducted with mixing times of 15 s, 2 min, and 4 min gave essentially the same results. Settling, or separation time, was at least 10 min; again, longer separation times appeared to make no difference in the results.

Equal volumes of aqueous and organic phases were used in the final contact to simplify a material balance to check the analytical results.

3.4 Analytical Techniques

The primary data required for studying the extraction equilibria are the concentrations of the species of interest in the aqueous and organic phases. Typically, laboratory analyses provide

volumetric (molar) concentration data. Because most of the activity coefficient correlations in general use employ the molal concentration scale, solution density is required to convert between the different concentration scales. Few data are available for solution density, especially the organic phase; therefore, it was necessary to measure solution density in, at least, a few cases.

In some experiments, where the solvent was heavily loaded, a third phase was noted to form when the temperature of the sample decreased to room temperature (while transporting the sample from the temperature-controlled dry box to the analytical laboratory). To ensure that aliquots withdrawn from the sample for analysis were homogeneous, the samples were routinely reheated to the temperature at which the experiment was performed prior to unsealing the container and taking the aliquot. This procedure also ensured that the density measurements would give the density at the experimental temperature.

3.4.1 Nitric Acid

Aqueous Phase. The aqueous nitric acid concentration was measured using Environmental Protection Agency (EPA) Acidity (Titrimetric) Method 305.2. Titration in this method is accomplished by using a standardized 0.02 *N* sodium hydroxide solution. A Corning model 155 pH meter (resolution of ±0.01 pH unit) was used to determine the endpoint of the titration, which occurs at a pH of 8.3. It is possible "to achieve a precision of less than 10 μeq/L" with this method. However, with the equipment used, measurement of the titrant was within 0.1 mL, and an error of ±5% was estimated from historical results.

Organic Phase. The acid in the organic phase was measured using essentially the same technique and the same equipment. A sample aliquot of 1 mL was dissolved in 50 mL of anhydrous methanol. The resulting solution was then titrated to a pH of 8.3, using a standardized 0.02 *N* sodium hydroxide–methanol solution.

3.4.2 Organic-Phase Water

Water in the organic phase was measured using ASTM Method E-1064, coulometric Karl Fischer titration. This method is based on the reduction of iodine by sulfur dioxide in the presence of water, which is quantitative in the presence of pyridine and methyl alcohol. A current of 10.71 C is generated for each 1 mg of water consumed. The method is applicable for water concentrations ranging from a few parts per million to approximately 2.0 wt %. Greater accuracy is achieved at the lower concentrations.

Using Martin Marietta Energy Systems, Inc., Analytical Services Division procedure 182807, "Addendum to ASTM Method E-1064," the titrations were performed in an Allied Fisher Scientific model 447 automatic coulometric titrator. Precision of the method has been shown to be 5.7% on measurements of 5000 μg of water in alcohol. Tests on extraction samples related to this work gave wildly varying results, possibly caused by an inadequate isolation of the sample from the atmosphere during transfers.

3.4.3 Bismuth Nitrate

Bismuth nitrate concentrations were not measured directly. Since there is one bismuth atom for each $Bi(NO_3)_3$ molecule, it was sufficient to measure only the bismuth without regard to the associated nitrate groups. Measurements were made using inductively coupled plasma–mass spectrometry (ICP-MS), which is a very sensitive system for heavy species such as bismuth. The particular instrument used was a Fisons, Inc., Plasma Quad PQII+, which contains two primary components: a plasma-based ion generator and a quadrapole mass spectrometer. The instrument operates in the following way. The aqueous sample is injected into a radiofrequency-induced plasma, where it is dissolved, atomized, and ionized. The ions are extracted from the plasma through a vacuum interface and separated magnetically. Magnetic separation is selective, based

on the charge/mass ratio. Separated ions deposit their charge on a Faraday detector, and the resulting signal (current) is processed electronically. The magnetic mass spectrometer has a resolution of 1 atomic mass unit. Overall, the instrument has a lower detection limit of ~10 to 300 parts per trillion (depending on the atomic mass of the analyte) and a precision of ≤1% relative standard deviation (determined from at least three data acquisitions). Due to interferences, which include atoms from the materials of construction of the instrument itself, the lower reporting limit is ~1 part per billion (i.e., 0.001 g/L).

Aqueous Phase. Martin Marietta Energy Systems, Inc., Analytical Services Division procedure ACD-TP-070002, which complies with EPA Method 6020, describes the method used to measure bismuth concentration with the instrumentation described above. According to this procedure, the sample is adjusted to a nitric acid concentration of about 10 wt % and then diluted 10:1 with water before introduction to the instrument.

Organic Phase. Bismuth in the organic samples was measured by the same technique as that used for the aqueous samples following a pretreatment process. Since an organic matrix cannot be analyzed by the ICP-MS, the organic material must first be destroyed. Thus, the organic sample was added to a 10% aqueous nitric acid solution and placed in a high-pressure asher operating at 100 atm and 300°C. The organic was completely destroyed, leaving the bismuth in the aqueous acid solution. An aliquot was diluted with water and then injected into the instrument for analysis as before.

3.4.4 Uranyl Nitrate

The uranium concentrations in the aqueous and organic phases were measured using the same radiocounting technique with a Packard Instrument Co. Liquid Scintillation Analyzer. Use of the equipment required a 0.5-mL sample to be added to 5.0 mL of an organic scintillation fluid

and thoroughly mixed. The scintillation fluid contains a fluorescent material that releases a photon when struck by the high-energy particles emitted during atomic decay. These photons strike the photosensitive surface in a photomultiplier tube (PMT), producing an electrical pulse that can be measured. The results obtained by counting the pulses provide quantitative information on the number of decay events, which, in turn, is related to the concentration of radioisotope in the sample. For ^{233}U, an alpha emitter, the machine is nearly 100% efficient, which means that the measured count rate is equal to the disintegration rate of the isotope [counts/min = disintegrations/min (dpm)]. The instrument also discriminates energy levels of the emitted particle. It was found experimentally that an energy range setting between 100 and 350 keV was optimum for measuring ^{233}U concentration.

Interferences in scintillation counting caused by the decay daughters of uranium led to the use of a back-extraction technique to reduce these interferences. To verify that the back-extraction procedure described by Spencer (1994) was adequate, some ^{238}U analyses were made using ICP-MS. The instrument used was a V. G. Elemental, Inc., Plasma Quad 2+ having the same principle of operation as that described in Sect. 3.4.3. Instrument sensitivity for uranium was 0.01 part per billion, and analytical results were within −10%. Forward-extraction samples, which had already been placed in scintillation fluid, were submitted for the ICP-MS analysis. (These samples had been saved from the first group of experiments performed before decay daughters were recognized as a problem. The ICP-MS analyses were done at the same time that a second group of experiments using the back-extraction technique was under way.) Any organic material associated with the samples had to be destroyed prior to analysis, which made the analysis more difficult, and perhaps more error-prone, than if the scintillation fluid had not been present.

3.4.5 Solution Density

Solution density was measured by a gravimetric technique described in Martin Marietta Energy Systems, Inc., Analytical Services Division procedure 182407. This procedure calls for taring a clean volumetric cylinder, adding about 50 mL of solution, and then weighing the solution and cylinder. Masses are measured on an analytical balance to within 1 mg, providing a precision of 2.0% in the calculated density. Because the volume of solution utilized in each of these experiments was much smaller than 50 mL (usually on the order of a total of 20 mL or less in each phase), the procedure was modified to permit use of smaller volumes.

A 10-mL pycnometer was used to measure density. The volume of the pycnometer was measured at the desired temperature using both pure water and pure acetone as references for the aqueous and organic samples, respectively. Using essentially the same procedure, the dry pycnometer is weighed on an analytical balance within 0.1 mg, and then reweighed after being filled with either pure water or pure acetone. (Use of the density of pure water, or acetone, at the measuring temperature permits the volume of the pycnometer to be calculated). The density of the sample solution is calculated by using the measured mass of the solution and the calculated volume of the pycnometer. The precision of density measurements made in this manner is expected to be within about 0.1%.

4. THEORETICAL DEVELOPMENT

The framework for the thermodynamic treatment of extraction equilibria has been well developed in the literature. Specific equilibria are modeled using this general framework.

The present work concentrates on the extraction of a compound from an aqueous nitric acid phase into an organic phase comprised of CMPO dissolved in an inert diluent. Three extractable compounds are investigated: nitric acid, uranyl nitrate, and bismuth(III) nitrate. Because nitric acid is present in each situation, models for its extraction are developed first.

4.1 Extraction of Nitric Acid

As reported in Sect. 2.4.3, the extraction of nitric acid by CMPO dissolved in TCE has been modeled with a combination of three equilibria:

$$H^+_{(aq)} + NO^-_{3(aq)} + CMPO_{(org)} \rightleftharpoons HNO_3 \cdot CMPO_{(org)} \quad , \tag{4-1}$$

$$H^+_{(aq)} + NO^-_{3(aq)} + 2CMPO_{(org)} \rightleftharpoons HNO_3 \cdot 2CMPO_{(org)} \quad , \tag{4-2}$$

and

$$2H^+_{(aq)} + 2NO^-_{3(aq)} + CMPO_{(org)} \rightleftharpoons 2HNO_3 \cdot CMPO_{(org)} \quad , \tag{4-3}$$

representing 1:1, 2:1, and 1:2 stoichiometries, respectively. The third equilibrium is important only when the nitric acid concentration is "moderately high" (Chaiko et al., 1989). Similar equilibria should occur for CMPO in an *n*-dodecane diluent.

4.1.1 Slope Analysis

Experiments can be performed to support slope analysis, which may be used to select an appropriate stoichiometry. By writing the equilibrium in the more general form,

$$H^{+}_{(aq)} + NO^{-}_{3(aq)} + nCMPO_{(org)} \rightleftharpoons HNO_3 \cdot nCMPO_{(org)} \quad , \tag{4-4}$$

the equilibrium constant may be written, according to Eq. (2-54), as

$$K = \frac{[HNO_3 \cdot nCMPO]\gamma^{(c)}_{HNO_3 \cdot nCMPO}}{\left(\gamma^{(c)}_{\pm,HNO_3}\right)^2 [H^+][NO_3^-][CMPO]^n \left(\gamma^{(c)}_{CMPO}\right)^n} \quad , \tag{4-5}$$

where the brackets indicate molar concentrations. Rearranging this equation to give the distribution ratio in terms of the equilibrium constant according to Eq. (2-57) yields

$$D = \frac{[HNO_3 \cdot nCMPO]}{[H^+]} = K\left(\gamma^{(c)}_{\pm,HNO_3}\right)^2 [NO_3^-] \left\{ \frac{\left(\gamma^{(c)}_{CMPO}\right)^n}{\gamma^{(c)}_{HNO_3 \cdot nCMPO}} \right\} [CMPO]^n \quad , \tag{4-6}$$

where the aqueous activity coefficients are the concentration-based mean stoichiometric coefficients. Experimentally, the aqueous nitric acid concentration and, hence, its activity coefficient can be held constant while the CMPO concentration in the organic phase is varied. If the ratio shown in braces [Eq. (4-6)] is constant, then the slope-analysis method given by Eq. (2-59) is applicable. It is known from the work by Diamond et al. (1986) that the activity coefficient of CMPO dissolved in toluene is not unity but decreases slightly with the CMPO concentration. From the same work, the activity coefficient of CMPO is about the same, regardless of whether the organic is equilibrated with pure water or 0.5 *M* nitric acid. The implication is that, if the CMPO behaves similarly in an *n*-dodecane diluent, the term in braces [in Eq. (4-6)] will be very nearly constant at a value around unity when $n = 1$, but will vary directly with the activity of the CMPO when $n = 2$. Based on the work of Diamond et al. (1986), the activity coefficient is expected to vary from 1.0 to about 0.92 as the CMPO concentration ranges from 0 to 0.2 *M*. Slope analysis should give good results even if n is as high as 2. If the activity coefficients were

known for the CMPO–*n*-dodecane system, the slope-analysis equation could be modified to correct for those deviations from ideality.

4.1.2 Extraction Models

The equilibrium constants for reactions (4-1) through (4-3) may be written as

$$K'_{1:1} = \frac{K_{1:1}\gamma^{(c)}_{CMPO}}{\gamma^{(c)}_{HNO_3 \cdot CMPO}} = \frac{[HNO_3 \cdot CMPO]}{\left(\gamma^{(c)}_{\pm,HNO_3}\right)^2 [HNO_3]^2 [CMPO]} \quad , \tag{4-7}$$

$$K'_{2:1} = \frac{K_{2:1}\left(\gamma^{(c)}_{CMPO}\right)^2}{\gamma^{(c)}_{HNO_3 \cdot 2CMPO}} = \frac{[HNO_3 \cdot 2CMPO]}{\left(\gamma^{(c)}_{\pm,HNO_3}\right)^2 [HNO_3]^2 [CMPO]^2} \quad , \tag{4-8}$$

and

$$K'_{1:2} = \frac{K_{1:2}\gamma^{(c)}_{CMPO}}{\gamma^{(c)}_{2HNO_3 \cdot CMPO}} = \frac{[2HNO_3 \cdot CMPO]}{\left(\gamma^{(c)}_{\pm,HNO_3}\right)^4 [HNO_3]^4 [CMPO]} \quad , \tag{4-9}$$

respectively. Because nitric acid is practically the only solute in the aqueous phase, the identity $[H^+] = [NO_3^-] = [HNO_3]$ has been used. The subscripts on the equilibrium constants, K, were chosen as reminders of the stoichiometry, and the primed values represent the equilibrium constant calculated under the assumption that the organic phase is ideal, similar to the convention shown in Eq. (2-55). These relationships include expressions for (1) the aqueous and organic nitric acid concentrations; (2) the aqueous-phase activity coefficients, which may be calculated from the aqueous concentrations using Pitzer's method; and (3) the free CMPO concentration in the organic phase. Based on the literature review, the extraction is assumed to involve the anhydrous form of nitric acid. Extraction of water, by itself, is ignored as a secondary effect.

One-Parameter Models. The initial CMPO concentrations are known from the conditions of the experiment. Equations (4-7) through (4-9) depend on the free CMPO concentrations, that

is, the CMPO not complexed with nitric acid. The equivalents of CMPO complexed with the acid are calculated from the measured organic-phase nitric acid concentration and the stoichiometry. Material balances on the CMPO for each of the three stoichiometries are as follows:

$$[CMPO] = [CMPO]_0 - [HNO_3 \cdot CMPO] \quad , \tag{4-10}$$

$$[CMPO] = [CMPO]_0 - 2[HNO_3 \cdot 2CMPO] \quad , \tag{4-11}$$

and

$$[CMPO] = [CMPO]_0 - \frac{1}{2}[2HNO_3 \cdot CMPO] \quad , \tag{4-12}$$

respectively, where the zero subscript indicates the initial concentration before phase contact. The nitric acid balances require

$$[HNO_3]_{org} = [HNO_3 \cdot CMPO] \quad , \tag{4-13}$$

$$[HNO_3]_{org} = [HNO_3 \cdot 2CMPO] \quad , \tag{4-14}$$

and

$$[HNO_3]_{org} = 2[2HNO_3 \cdot CMPO] \quad , \tag{4-15}$$

respectively. The organic nitric acid concentration for 1:1 stoichiometry is given by combining Eqs. (4-7), (4-10), and (4-13), and rearranging to yield

$$[HNO_3]_{org} = [HNO_3 \cdot CMPO] = \frac{K'_{1:1}\left(\gamma^{(c)}_{\pm,HNO_3}\right)^2 [HNO_3]^2 [CMPO]_0}{1 + K'_{1:1}\left(\gamma^{(c)}_{\pm,HNO_3}\right)^2 [HNO_3]^2} \quad . \tag{4-16}$$

Equations (4-8), (4-11), and (4-14) may be combined to give the corresponding relationship for 2:1 stoichiometry. This operation yields a quadratic equation wherein the negative

of the square-root term must be taken to satisfy the requirement for a zero organic acid concentration at an initial zero CMPO concentration. The result is as follows:

$$[HNO_3]_{org} = [HNO_3 \cdot 2CMPO] = \frac{\Omega - \sqrt{\Omega^2 - [CMPO]_0^2}}{2} \quad , \tag{4-17}$$

where

$$\Omega = \left(\frac{1}{4K'_{2:1}\left(\gamma^{(c)}_{\pm,HNO_3}\right)^2 [HNO_3]^2} + \frac{[CMPO]_0}{2} \right) \quad . \tag{4-18}$$

Combining Eqs. (4-9), (4-12), and (4-15) gives the organic acid concentration as a function of aqueous acid concentration for 1:2 stoichiometry:

$$[HNO_3]_{org} = 2[2HNO_3 \cdot CMPO] = \frac{2K'_{1:2}\left(\gamma^{(c)}_{\pm,HNO_3}\right)^4 [HNO_3]^4 [CMPO]_0}{1 + K'_{1:2}\left(\gamma^{(c)}_{\pm,HNO_3}\right)^4 [HNO_3]^4} \quad . \tag{4-19}$$

Two-Parameter Models. Given the three stoichiometries shown in Eqs. (4-1) through (4-3), only three different models can be developed by combining two stoichiometries at a time. First, consider a model combining 1:1 and 2:1 stoichiometries. A balance on the CMPO gives the free CMPO concentration as

$$[CMPO] = [CMPO]_0 - 2[HNO_3 \cdot 2CMPO] - [HNO_3 \cdot CMPO] \quad , \tag{4-20}$$

and an acid balance is

$$[HNO_3]_{org} = [HNO_3 \cdot 2CMPO] + [HNO_3 \cdot CMPO] \quad . \tag{4-21}$$

Combining Eqs. (4-7), (4-8), and (4-21) gives the organic-phase acid concentration

$$[HNO_3]_{org} = [CMPO]\left(\gamma^{(c)}_{\pm,HNO_3}\right)^2[HNO_3]^2\left(K'_{1:1} + K'_{2:1}[CMPO]\right) \quad . \tag{4-22}$$

However, the free CMPO concentration is found from combining Eqs. (4-7), (4-8), and (4-20) to produce the quadratic form

$$\left\{2K'_{2:1}\left(\gamma^{(c)}_{\pm,HNO_3}\right)^2[HNO_3]^2\right\}[CMPO]^2 + \left\{1 + K'_{1:1}\left(\gamma^{(c)}_{\pm,HNO_3}\right)^2[HNO_3]^2\right\}[CMPO] - [CMPO]_0 = 0 \quad . \tag{4-23}$$

Inspection reveals that the positive square root of the quadratic term is required in order to get a positive value of the free CMPO concentration from this equation. Equations (4-22) and (4-23) represent the model.

Now a model combining 2:1 and 1:2 stoichiometries may be similarly developed. The CMPO and acid balances are

$$[CMPO] = [CMPO]_0 - 2[HNO_3 \cdot 2CMPO] - [2HNO_3 \cdot CMPO] \tag{4-24}$$

and

$$[HNO_3]_{org} = [HNO_3 \cdot 2CMPO] + 2[2HNO_3 \cdot CMPO] \quad . \tag{4-25}$$

Combining these with Eqs. (4-8) and (4-9), the model becomes

$$[HNO_3]_{org} = [CMPO]\left(\gamma^{(c)}_{\pm,HNO_3}\right)^2[HNO_3]^2\left\{K'_{2:1}[CMPO] + 2K'_{1:2}\left(\gamma^{(c)}_{\pm,HNO_3}\right)^2[HNO_3]^2\right\} \tag{4-26}$$

and

$$\left\{2K'_{2:1}\left(\gamma^{(c)}_{\pm,HNO_3}\right)^2[HNO_3]^2\right\}[CMPO]^2 + \left\{1 + K'_{1:2}\left(\gamma^{(c)}_{\pm,HNO_3}\right)^4[HNO_3]^4\right\}[CMPO] - [CMPO]_0 = 0 \quad . \tag{4-27}$$

The positive root of the quadratic is again required for the same reasons as discussed previously.

Finally, a model combining 1:1 and 1:2 stoichiometries begins with the following CMPO and acid balances:

$$[CMPO] = [CMPO]_0 - [HNO_3 \cdot CMPO] - [2HNO_3 \cdot CMPO] \tag{4-28}$$

and

$$[HNO_3]_{org} = [HNO_3 \cdot CMPO] + 2[2HNO_3 \cdot CMPO] \ . \tag{4-29}$$

Combining these with Eqs. (4-7) and (4-9) yields

$$[HNO_3]_{org} = [CMPO]\left(\gamma^{(c)}_{\pm,HNO_3}\right)^2[HNO_3]^2\left\{K'_{1:1} + 2K'_{1:2}\left(\gamma^{(c)}_{\pm,HNO_3}\right)^2[HNO_3]^2\right\} , \tag{4-30}$$

with the free CMPO concentration given by

$$[CMPO] = \frac{[CMPO]_0}{1 + K'_{1:1}\left(\gamma^{(c)}_{\pm,HNO_3}\right)^2[HNO_3]^2 + K'_{1:2}\left(\gamma^{(c)}_{\pm,HNO_3}\right)^4[HNO_3]^4} \ . \tag{4-31}$$

Three-Parameter Model. The CMPO and acid balances for the three-parameter model combining the stoichiometries shown in Eqs. (4-1) through (4-3) are

$$[CMPO] = [CMPO]_0 - [HNO_3 \cdot CMPO] - 2[HNO_3 \cdot 2CMPO] - [2HNO_3 \cdot CMPO] \tag{4-32}$$

and

$$[HNO_3]_{org} = [HNO_3 \cdot CMPO] + [HNO_3 \cdot 2CMPO] + 2[2HNO_3 \cdot CMPO] \ . \tag{4-33}$$

Substituting Eqs. (4-7) through (4-9) into these expressions yields the model equations

$$\begin{aligned}[HNO_3]_{org} &= [CMPO]\left(\gamma^{(c)}_{\pm,HNO_3}\right)^2 \\ &\times [HNO_3]^2\left\{K'_{1:1} + K'_{2:1}[CMPO] + 2K'_{1:2}\left(\gamma^{(c)}_{\pm,HNO_3}\right)^2[HNO_3]^2\right\}\end{aligned} \tag{4-34}$$

and

$$\left\{2K'_{2:1}\left(\gamma^{(c)}_{\pm,HNO_3}\right)^2[HNO_3]^2\right\}[CMPO]^2 + \left\{1 + K'_{1:1}\left(\gamma^{(c)}_{\pm,HNO_3}\right)^2[HNO_3]^2 + 2K'_{1:2}\left(\gamma^{(c)}_{\pm,HNO_3}\right)^4[HNO_3]^4\right\}[CMPO] - [CMPO]_0 = 0 \quad . \tag{4-35}$$

The positive root in the quadratic form of Eq. (4-35) is required to give positive values for the free CMPO concentration.

4.2 Extraction of Uranyl Nitrate

Extraction of uranium, as uranyl nitrate, with CMPO is expected to follow a 2:1 stoichiometry based on the literature. Additionally, the uranyl ion is reported to associate with six waters of hydration, a conclusion indirectly supported by the crystallized form, uranyl nitrate hexahydrate. The expected extraction equilibria may be written as

$$UO_2(H_2O)^{2+}_{6(aq)} + 2NO^-_{3(aq)} + 2CMPO_{(org)} \rightleftharpoons UO_2(NO_3)_2 \cdot 2CMPO_{(org)} + 6H_2O_{(aq)}. \tag{4-36}$$

It is possible that CMPO will also coextract nitric acid in a manner similar to that reported for americium, according to

$$UO_2(H_2O)^{2+}_{6(aq)} + 3NO^-_{3(aq)} + H^+_{(aq)} + 2CMPO_{(org)} \rightleftharpoons UO_2(NO_3)_2 \cdot 2CMPO \cdot HNO_{3(org)} + 6H_2O_{(aq)} \tag{4-37}$$

at high nitric acid concentrations. Models may be developed that include even more acid molecules in the coextraction. A nitrate complexation of the uranyl ion has also been suggested by Tedder and Davis (1983) and may be expressed as

$$UO_2(H_2O)^{2+}_{6(aq)} + NO^-_{3(aq)} \rightleftharpoons UO_2NO_3(H_2O)^+_{5(aq)} + H_2O_{(aq)} \ , \tag{4-38}$$

where the pentahydrate form is assumed to be inextractable. Incomplete ionization effects are included in the mean stoichiometric activity coefficients, such as those calculated by Pitzer's method, but an explicit description of the speciation does affect model predictions.

4.2.1 Slope Analysis

The stoichiometry of the extraction of uranyl nitrate with CMPO may be deduced using slope analysis even when nitric acid is coextracted if near-ideal conditions can be utilized. A general form of the extraction equilibria may be written as

$$UO_2(H_2O)^{2+}_{6(aq)} + 2NO^-_{3(aq)} + nCMPO_{(org)} \rightleftharpoons UO_2(NO_3)_2 \cdot nCMPO_{(org)} + 6H_2O_{(aq)}. \tag{4-39}$$

The equilibrium constant is

$$K = \frac{\left[UO_2(NO_3)_2 \cdot nCMPO\right]\gamma^{(c)}_{UO_2(NO_3)_2 \cdot nCMPO}\, a_w^6}{\left(\gamma^{(c)}_{\pm,UO_2(NO_3)_2}\right)^3\left[UO_2(H_2O)^{2+}_6\right]\left[NO_3^-\right]^2\left[CMPO\right]^n\left(\gamma^{(c)}_{CMPO}\right)^n} \tag{4-40}$$

in molar concentration units according to Eq. (2-54). The distribution ratio, in terms of the equilibrium constant, is found by rearrangement of this equation to yield

$$D = \frac{\left[UO_2(NO_3)_2 \cdot nCMPO\right]}{\left[UO_2(H_2O)^{2+}_6\right]} = \frac{K\left(\gamma^{(c)}_{\pm,UO_2(NO_3)_2}\right)^3\left[NO_3^-\right]^2}{a_w^6}\left\{\frac{\left(\gamma^{(c)}_{CMPO}\right)^n}{\gamma^{(c)}_{UO_2(NO_3)_2 \cdot nCMPO}}\right\}\left[CMPO\right]^n . \tag{4-41}$$

The slope-analysis method of Eq. (2-59) gives the equilibrium stoichiometry under ideal conditions where the activity coefficients in the organic phase, the activity coefficient of aqueous uranyl nitrate, and the activity of water can be held constant. However, even small variations in the activity of water may have a significant effect because it is raised to the sixth power. Similarly, the third power on the activity of the uranyl nitrate accentuates its effect. A modified

distribution ratio can be developed to help correct these nonidealities when the aqueous-phase properties are known. That is,

$$D' = \frac{D a_w^6}{\left(\gamma^{(c)}_{\pm,UO_2(NO_3)_2}\right)^3} = K\left[NO_3^-\right]^2 \left\{ \frac{\left(\gamma^{(c)}_{CMPO}\right)^n}{\gamma^{(c)}_{UO_2(NO_3)_2 \cdot nCMPO}} \right\} [CMPO]^n \quad . \tag{4-42}$$

If the ratio of the organic-phase activity coefficients (shown in braces) is constant, then the plot of ln D' vs ln[$CMPO$] will give a line whose slope is n, the stoichiometric ratio. Further corrections can be made if the nitrate concentration cannot be made constant; for example, the expression for the nitrate concentration can be moved to the left-hand side of Eq. (4-42) with D.

4.2.2 Extraction Models

In the experimental program, the concentrations of nitric acid were limited to obviate the formation of a third phase. Because the acid concentrations were low (≤0.2 M), the coextraction of acid with uranium as shown by Eq. (4-37) was thought to be insignificant. Extraction according to Eq. (4-36) and nitrate complexation of the uranyl ion shown by Eq. (4-39) were thought to be the dominating equilibria. Because slope-analysis data (Sect. 5) did not rule out a 1:1 stoichiometry, a 1:1 stoichiometric equation is also considered.

One-Parameter Models. First, a one-parameter model is developed for a 2:1 complexation of CMPO with uranium. The equilibrium constant for the reaction [i.e., Eq. (4-36)] may be written as

$$K'_{U2} = \frac{K_{U2}\left(\gamma^{(c)}_{CMPO}\right)^2}{\gamma^{(c)}_{UO_2(NO_3)_2 \cdot 2CMPO}} = \frac{\left[UO_2(NO_3)_2 \cdot 2CMPO\right] a_w^6}{\left(\gamma^{(c)}_{\pm,UO_2(NO_3)_2}\right)^3 \left[UO_2(H_2O)_6^{2+}\right] \left[NO_3^-\right]^2 [CMPO]^2} \quad , \tag{4-43}$$

where the subscript $U2$ is a reminder of the stoichiometry. In this one-parameter model, the measured concentrations are identified with model variables; thus,

$$[U]_{org} = [UO_2(NO_3)_2]_{org} = [UO_2(NO_3)_2 \cdot 2CMPO] \quad , \tag{4-44}$$

$$[U]_{aq} = [UO_2(NO_3)_2]_{aq} = [UO_2(H_2O)_6^{2+}] \quad , \tag{4-45}$$

and

$$[NO_3^-] = [HNO_3]_{aq} + 2[UO_2(NO_3)_2]_{aq} \quad . \tag{4-46}$$

A material balance for the free CMPO concentration can be written as follows:

$$[CMPO] = [CMPO]_0 - 2[UO_2(NO_3)_2 \cdot 2CMPO] - [HNO_3 \cdot CMPO] \quad . \tag{4-47}$$

Now Eq. (4-43) can be combined with Eqs. (4-44) and (4-45), and the result can be rearranged to express the organic-phase uranyl nitrate concentration:

$$[U]_{org} = \frac{K'_{U2}\left(\gamma^{(c)}_{\pm,UO_2(NO_3)_2}\right)^3 [U]_{aq}[NO_3^-]^2[CMPO]^2}{a_w^6} \quad . \tag{4-48}$$

Nitric acid is also extracted by a competing reaction since it is present in the aqueous phase with the uranyl nitrate. The experimental data (presented in Sect. 5) on the extraction of nitric acid is adequately represented by a one-parameter model. Because the nitrate in the solution is supplied by both the nitric acid and the uranyl nitrate, the amount of CMPO complexed with acid must be expressed in the more general form

$$K'_{1:1} = \frac{[HNO_3 \cdot CMPO]}{\left(\gamma^{(c)}_{\pm,HNO_3}\right)^2 [H^+][NO_3^-][CMPO]} \quad , \tag{4-49}$$

which can be rearranged to give the organic acid concentration; thus,

$$[HNO_3 \cdot CMPO] = K'_{1:1}\left(\gamma^{(c)}_{\pm,HNO_3}\right)^2[H^+][NO_3^-][CMPO] \quad . \tag{4-50}$$

Equations (4-48) and (4-50) may then be substituted into Eq. (4-47) to give the free CMPO concentration in the implicit form

$$\left\{\frac{2K'_{U2}\left(\gamma^{(c)}_{\pm,UO_2(NO_3)_2}\right)^3[U]_{aq}[NO_3^-]^2}{a_w^6}\right\}[CMPO]^2 + \left\{1 + K'_{1:1}\left(\gamma^{(c)}_{\pm,HNO_3}\right)^2[H^+][NO_3^-]\right\}[CMPO] - [CMPO]_0 = 0 \quad . \tag{4-51}$$

The quadratic form of this equation indicates that the positive square root must be used to obtain positive free CMPO concentrations. Inserting the resulting concentration into Eq. (4-48) completes a model that expresses organic uranium concentration as a function of aqueous uranium concentration. It is customary to express the model in terms of the distribution ratio, which can easily be developed by dividing both sides of Eq. (4-48) by the aqueous uranium concentration:

$$D = \frac{[U]_{org}}{[U]_{aq}} = \frac{K'_{U2}\left(\gamma^{(c)}_{\pm,UO_2(NO_3)_2}\right)^3[NO_3^-]^2[CMPO]^2}{a_w^6} \quad . \tag{4-52}$$

A different one-parameter model can be developed for the 1:1 stoichiometric equilibrium

$$UO_2(H_2O)^{2+}_{6(aq)} + 2NO^-_{3(aq)} + CMPO_{(org)} \rightleftharpoons UO_2(NO_3)_2 \cdot CMPO_{(org)} + 6H_2O_{(aq)} \quad , \tag{4-53}$$

where the equilibrium constant is

$$K'_{U1} = \frac{K_{U1}\left(\gamma^{(c)}_{CMPO}\right)}{\gamma^{(c)}_{UO_2(NO_3)_2 \cdot CMPO}} = \frac{[UO_2(NO_3)_2 \cdot CMPO]a_w^6}{\left(\gamma^{(c)}_{\pm,UO_2(NO_3)_2}\right)^3\left[UO_2(H_2O)_6^{2+}\right][NO_3^-]^2[CMPO]} \quad . \tag{4-54}$$

The measured aqueous- and organic-phase uranium concentrations are identified with model variables by Eqs. (4-44) and (4-45) as before, and the total aqueous nitrate concentration is given by Eq. (4-46). With this different stoichiometry, a material balance on the CMPO now becomes

$$[CMPO] = [CMPO]_0 - [UO_2(NO_3)_2 \cdot CMPO] - [HNO_3 \cdot CMPO] \quad , \tag{4-55}$$

where the amount of CMPO complexed with nitric acid is given by Eq. (4-50). After substitution, the model equations become

$$[CMPO] = \frac{[CMPO]_0}{1 + K'_{1:1}\left(\gamma^{(c)}_{\pm,HNO_3}\right)^2[H^+]\left[NO_3^-\right] + \dfrac{K'_{UI}\left(\gamma^{(c)}_{\pm,UO_2(NO_3)_2}\right)^3[U]_{aq}\left[NO_3^-\right]^2}{a_w^6}} \tag{4-56}$$

and

$$D = \frac{[U]_{org}}{[U]_{aq}} = \frac{K'_{UI}\left(\gamma^{(c)}_{\pm,UO_2(NO_3)_2}\right)^3\left[NO_3^-\right]^2[CMPO]}{a_w^6} \quad . \tag{4-57}$$

In this model the distribution ratio varies linearly with the free CMPO concentration rather than with the square of the free CMPO concentration [see Eq. (4-52)]. The free CMPO concentration has a much different form between models with 2:1 and 1:1 stoichiometries, as shown by comparing Eqs. (4-51) and (4-56).

Two-Parameter Models. Uranyl nitrate may complex with CMPO in both 1:1 and 2:1 ratios. Each equilibrium constant for a combined model has already been defined by Eqs. (4-43) and (4-54). Because this model does not distinguish separate aqueous uranyl species, the variables in the model are related to the measured aqueous uranyl nitrate concentration by Eq. (4-45). The

total aqueous nitrate ion concentration is, again, given by Eq. (4-46). A material balance on the CMPO may be written as

$$[CMPO] = [CMPO]_0 - 2[UO_2(NO_3)_2 \cdot 2CMPO] - [UO_2(NO_3)_2 \cdot CMPO] - [HNO_3 \cdot CMPO] \quad . \tag{4-58}$$

Substituting Eqs. (4-43), (4-50), and (4-54) into Eq. (4-58) and rearranging yields

$$\left\{\frac{2K'_{U2}\left(\gamma^{(c)}_{\pm,UO_2(NO_3)_2}\right)^3[U]_{aq}[NO_3^-]^2}{a_w^6}\right\}[CMPO]^2 + \left\{1 + K'_{1:1}\left(\gamma^{(c)}_{\pm,HNO_3}\right)^2[H^+][NO_3^-] + \frac{K'_{U1}\left(\gamma^{(c)}_{\pm,UO_2(NO_3)_2}\right)^3[U]_{aq}[NO_3^-]^2}{a_w^6}\right\}[CMPO] - [CMPO]_0 = 0 \quad . \tag{4-59}$$

By comparison with Eq. (4-51), this simply adds a parameter to the linear CMPO term. The positive root of the equation is required to obtain positive free CMPO concentrations. An organic uranium balance includes both the solvate and the disolvate,

$$[U]_{org} = [UO_2(NO_3)_2]_{org} = [UO_2(NO_3)_2 \cdot 2CMPO] + [UO_2(NO_3)_2 \cdot CMPO] \quad . \tag{4-60}$$

Substitution of Eqs. (4-43) and (4-54) yields the organic-phase uranium concentration in terms of the aqueous-phase uranium concentration; thus,

$$[U]_{org} = \frac{\left(\gamma^{(c)}_{\pm,UO_2(NO_3)_2}\right)^3[U]_{aq}[NO_3^-]^2}{a_w^6}\left\{K'_{U2}[CMPO]^2 + K'_{U1}[CMPO]\right\} \quad . \tag{4-61}$$

As compared with the one-parameter model given by Eq. (4-48), this equation just adds a linear term in the free CMPO concentration.

Another two-parameter model may be developed from consideration of the equilibria shown by Eqs. (4-36) and (4-38). Basically, this adds an aqueous nitrate complexation to the

one-parameter model describing the 2:1 solvation. The nitrate complexation equilibrium constant may be written as

$$\beta_U = \frac{\left[UO_2NO_3(H_2O)_5^+\right]\left(\gamma^{(c)}_{UO_2NO_3(H_2O)_5^+}\right)a_w}{\left[UO_2(H_2O)_6^{2+}\right]\left(\gamma^{(c)}_{UO_2(H_2O)_6^{2+}}\right)\left[NO_3^-\right]\gamma^{(c)}_{NO_3^-}} \quad . \tag{4-62}$$

Mean stoichiometric activity coefficients, determined by such methods as vapor pressure measurements, include the effects of partial ionization. Such coefficients are calculated by the Pitzer method. Since the mean stoichiometric activity coefficient is defined as though the salt is completely dissociated and no distinction is made between the two ions, it is assumed that the activity coefficient of $UO_2NO_3(H_2O)_5^+$ is equal to that of $UO_2(H_2O)_6^{2+}$. The mean activity coefficient of the nitrate ion is calculated by the Pitzer method. Now, Eq. (4-62) may be written as

$$\beta_U = \frac{\left[UO_2NO_3(H_2O)_5^+\right]a_w}{\left[UO_2(H_2O)_6^{2+}\right]\left[NO_3^-\right]\gamma^{(c)}_{NO_3^-}} \quad . \tag{4-63}$$

A material balance on the aqueous uranyl nitrate concentration is

$$\left[U\right]_{aq} = \left[UO_2(H_2O)_6^{2+}\right]_{aq} + \left[UO_2NO_3(H_2O)_5^+\right]_{aq} \quad . \tag{4-64}$$

Combining Eqs. (4-63) and (4-64) and rearranging to solve explicitly for the hexahydrated uranyl ion concentration yields

$$\left[UO_2(H_2O)_6^{2+}\right]_{aq} = \frac{a_w\left[U\right]_{aq}}{a_w + \beta_U\left[NO_3^-\right]\gamma^{(c)}_{NO_3^-}} \quad . \tag{4-65}$$

Substituting Eq. (4-65) into Eq. (4-64) to obtain the concentration of the pentahydrate ion yields

$$\left[UO_2NO_3(H_2O)_5^+\right]_{aq} = \frac{\beta_U\left[NO_3^-\right]\gamma_{NO_3^-}^{(c)}\left[U\right]_{aq}}{a_w + \beta_U\left[NO_3^-\right]\gamma_{NO_3^-}^{(c)}} \quad . \tag{4-66}$$

The total free nitrate concentration balance is given by

$$\left[NO_3^-\right] = \left[HNO_3\right]_{aq} + 2\left[UO_2(H_2O)_6^{2+}\right] + \left[UO_2NO_3(H_2O)_5^+\right] \quad , \tag{4-67}$$

which, upon substitution of Eqs. (4-65) and (4-66), gives

$$\left[NO_3^-\right]_{aq} = \left[HNO_3\right]_{aq} + \frac{2a_w + \beta_U\left[NO_3^-\right]\gamma_{NO_3^-}^{(c)}}{a_w + \beta_U\left[NO_3^-\right]\gamma_{NO_3^-}^{(c)}}\left[U\right]_{aq} \quad . \tag{4-68}$$

This equation is a quadratic in terms of the nitrate concentration and can be solved; however, when the aqueous uranyl nitrate concentration is small compared with the nitric acid concentration, then the nitrate concentration will be almost entirely due to the nitric acid. Additionally, when β_U approaches zero, two nitrate ions are contributed by each uranyl group; and, when β_U is very large, only one nitrate ion is contributed by each uranyl group. Therefore, under conditions where the uranyl nitrate concentration is small compared with the nitric acid concentration, negligible error will be introduced by setting the total nitrate concentration as defined by Eq. (4-46), and the model will be greatly simplified.

The nitrate complexation equilibrium essentially reduces the aqueous concentration of the extracting species according to Eq. (4-65). Only one complex is formed in the organic phase, the disolvate, so the CMPO material balance is given by Eq. (4-47). With these simplifications, this

two-parameter model has the same form as the one-parameter disolvate model; the difference is that $[U]_{aq}$ is replaced by $[UO_2(H_2O)_6^{2+}]$. The model equations can now be written as

$$[U]_{org} = \frac{K'_{U2}\left(\gamma^{(c)}_{\pm,UO_2(NO_3)_2}\right)^3\left[UO_2(H_2O)_6^{2+}\right]_{aq}\left[NO_3^-\right]^2[CMPO]^2}{a_w^6} \tag{4-69}$$

and

$$\left\{\frac{2K'_{U2}\left(\gamma^{(c)}_{\pm,UO_2(NO_3)_2}\right)^3\left[UO_2(H_2O)_6^{2+}\right]_{aq}\left[NO_3^-\right]^2}{a_w^6}\right\}[CMPO]^2 + \left\{1 + K'_{1:1}\left(\gamma^{(c)}_{\pm,HNO_3}\right)^2[H^+]\left[NO_3^-\right]\right\}[CMPO] - [CMPO]_0 = 0 \quad . \tag{4-70}$$

Because of the definition of distribution ratio, the calculated distribution ratio can be found by dividing both sides of Eq. (4-69) by the **total** aqueous uranyl nitrate concentration,

$$D = \frac{[U]_{org}}{[U]_{aq}} = \frac{K'_{U2}\left(\gamma^{(c)}_{\pm,UO_2(NO_3)_2}\right)^3\left[UO_2(H_2O)_6^{2+}\right]_{aq}\left[NO_3^-\right]^2[CMPO]^2}{a_w^6[U]_{aq}} \quad . \tag{4-71}$$

Comparison of this equation with Eq. (4-52) shows that the right-hand side now contains the ratio of the concentrations of the fully ionized uranyl species to the total uranyl nitrate. The model equations are Eqs. (4-46), (4-65), (4-70), and (4-69) or (4-71).

A third two-parameter model that includes unisolvate formation and the nitrate complexation is now considered. The nitrate complexation equilibrium enters into the model for 1:1 extraction in parallel fashion to the 2:1 extraction model. The model equations are as follows:

$$[CMPO] = \frac{[CMPO]_0}{1 + K'_{1:1}\left(\gamma^{(c)}_{\pm,HNO_3}\right)^2[H^+]\left[NO_3^-\right] + \dfrac{K'_{U1}\left(\gamma^{(c)}_{\pm,UO_2(NO_3)_2}\right)^3\left[UO_2(H_2O)_6^{2+}\right]_{aq}\left[NO_3^-\right]^2}{a_w^6}} \tag{4-72}$$

and

$$D = \frac{[U]_{org}}{[U]_{aq}} = \frac{K'_{UI}\left(\gamma^{(c)}_{\pm,UO_2(NO_3)_2}\right)^3\left[UO_2(H_2O)_6^{2+}\right]_{aq}\left[NO_3^-\right]^2[CMPO]}{a_w^6[U]_{aq}} \quad . \tag{4-73}$$

4.3 Extraction of Bismuth Nitrate

The extraction stoichiometry of bismuth nitrate with CMPO has not been reported in the literature. However, it has been reported that CMPO extracts trivalent metal nitrates with a stoichiometry of 3:1 (e.g., americium and neodymium), so this seems to be a reasonable initial estimate for development of a model. Additionally, the crystallized form of bismuth nitrate contains five waters of hydration; and, in fact, highly purified bismuth nitrate pentahydrate was the source of bismuth for the experiments reported here. With this information in mind, the expected extraction equilibrium is

$$Bi(H_2O)^{3+}_{5(aq)} + 3NO^-_{3(aq)} + 3CMPO_{(org)} \rightleftharpoons Bi(NO_3)_3 \cdot 3CMPO_{(org)} + 5H_2O_{(aq)} \quad . \tag{4-74}$$

4.3.1 Slope Analysis

The stoichiometry of the extraction of bismuth nitrate can be determined by slope analysis. The equilibrium can be written in a form having an indeterminate coordination number as

$$Bi(H_2O)^{3+}_{5(aq)} + 3NO^-_{3(aq)} + nCMPO_{(org)} \rightleftharpoons Bi(NO_3)_3 \cdot nCMPO_{(org)} + 5H_2O_{(aq)} \quad . \tag{4-75}$$

In this case, Eq. (2-54) becomes

$$K = \frac{\left[Bi(NO_3)_3 \cdot nCMPO\right]\gamma^{(c)}_{Bi(NO_3)_3 \cdot nCMPO}a_w^5}{\left(\gamma^{(c)}_{\pm,Bi(NO_3)_3}\right)^4\left[Bi(H_2O)_5^{3+}\right]\left[NO_3^-\right]^3[CMPO]^n\left(\gamma^{(c)}_{CMPO}\right)^n} \quad . \tag{4-76}$$

Following the previous equation developments, the distribution ratio is found by algebraic rearrangement,

$$D = \frac{[Bi(NO_3)_3 \cdot nCMPO]}{[Bi(H_2O)_5^{3+}]} = \frac{K\left(\gamma^{(c)}_{\pm,Bi(NO_3)_3}\right)^4 [NO_3^-]^3}{a_w^5} \left\{ \frac{\left(\gamma^{(c)}_{CMPO}\right)^n}{\gamma^{(c)}_{Bi(NO_3)_3 \cdot nCMPO}} \right\} [CMPO]^n \quad . \tag{4-77}$$

At low concentrations where the activity coefficients are unity (ideal conditions), the slope method of Eq. (2-59) gives the stoichiometry. Because methods to estimate the aqueous deviations from ideality are available, it is possible to produce a modified distribution ratio to correct for these nonidealities. The equation is

$$D' = \frac{Da_w^5}{\left(\gamma^{(c)}_{\pm,Bi(NO_3)_3}\right)^4} = K[NO_3^-]^3 \left\{ \frac{\left(\gamma^{(c)}_{CMPO}\right)^n}{\gamma^{(c)}_{Bi(NO_3)_3 \cdot nCMPO}} \right\} [CMPO]^n \quad . \tag{4-78}$$

If the ratio of the organic-phase activity coefficients (shown in braces) is constant, then a plot of ln D' vs ln[$CMPO$] will be a straight line whose slope is the stoichiometric ratio, n. However, there is no reason to expect the activity coefficients of free CMPO and CMPO complexed with bismuth nitrate to be equal. Based on a value of $n = 3$, and assuming that activity coefficients of free CMPO and CMPO–bismuth nitrate complex are only slightly different, then the ratio of the organic-phase activity coefficients (shown in braces) may vary appreciably and the slope method will give only approximate results.

4.3.2 Extraction Models

Extraction of bismuth nitrate by CMPO is likely to involve complications of acid coextraction and nitrate complexation as in the case of uranyl nitrate. Because low acid concentrations were used to avoid third-phase formation, acid coextraction was probably

negligible. Development of an extraction model can proceed along the same lines as that for uranyl nitrate.

One-Parameter Models. With a 3:1 stoichiometry as shown in Eq. (4-74), the equilibrium constant can be written as

$$K'_{B3} = \frac{K_{B3}\left(\gamma^{(c)}_{CMPO}\right)^3}{\gamma^{(c)}_{Bi(NO_3)_3\cdot 3CMPO}} = \frac{\left[Bi(NO_3)_3\cdot 3CMPO\right]a_w^5}{\left(\gamma^{(c)}_{\pm,Bi(NO_3)_3}\right)^4\left[Bi(H_2O)_5^{3+}\right]\left[NO_3^-\right]^3\left[CMPO\right]^3} \quad , \tag{4-79}$$

where the subscript *B*3 is a reminder of the stoichiometry. The measured aqueous and organic bismuth concentrations can be identified by

$$\left[Bi\right]_{aq} = \left[Bi(NO_3)_3\right]_{aq} = \left[Bi(H_2O)_5^{3+}\right] \tag{4-80}$$

and

$$\left[Bi\right]_{org} = \left[Bi(NO_3)_3\right]_{org} = \left[Bi(NO_3)_3\cdot 3CMPO\right] \quad , \tag{4-81}$$

respectively. The total nitrate concentration is given by

$$\left[NO_3^-\right]_{aq} = \left[HNO_3\right]_{aq} + 3\left[Bi(NO_3)_3\right]_{aq} \quad . \tag{4-82}$$

A material balance for the free CMPO concentration is

$$\left[CMPO\right] = \left[CMPO\right]_0 - 3\left[Bi(NO_3)_3\cdot 3CMPO\right] - \left[HNO_3\cdot CMPO\right] \quad . \tag{4-83}$$

The CMPO associated with nitric acid is given by Eq. (4-50) as discussed previously. The free CMPO concentration is found by substituting Eqs. (4-50) and (4-79) into Eq. (4-83):

$$\left\{\frac{3K'_{B3}\left(\gamma^{(c)}_{\pm,Bi(NO_3)_3}\right)^4\left[Bi(H_2O)_5^{3+}\right]\left[NO_3^-\right]^3}{a_w^5}\right\}[CMPO]^3 + \left\{1 + K'_{1:1}\left(\gamma^{(c)}_{\pm,HNO_3}\right)^2[H^+]\left[NO_3^-\right]\right\}[CMPO] - [CMPO]_0 = 0 \quad . \tag{4-84}$$

This cubic equation can be solved for the free CMPO concentration. Equation (4-79) can be rearranged to express the organic-phase bismuth concentration in terms of the aqueous-phase bismuth concentration:

$$\left[Bi(NO_3)_3 \cdot 3CMPO\right] = \frac{K'_{B3}\left(\gamma^{(c)}_{\pm,Bi(NO_3)_3}\right)^4\left[Bi(H_2O)_5^{3+}\right]\left[NO_3^-\right]^3[CMPO]^3}{a_w^5} \quad . \tag{4-85}$$

Again, the customary distribution ratio can be found by dividing both sides of Eq. (4-85) by the aqueous bismuth nitrate concentration.

Slope-analysis results reported in Sect. 5.3.2 indicate that a 2:1 extraction stoichiometry for bismuth nitrate is likely. The equilibrium may be written as

$$Bi(H_2O)^{3+}_{5(aq)} + 3NO^-_{3(aq)} + 2CMPO_{(org)} \rightleftharpoons Bi(NO_3)_3 \cdot 2CMPO_{(org)} + 5H_2O_{(aq)} \quad . \tag{4-86}$$

Development of the model parallels that for the 3:1 stoichiometry. In this case, the free CMPO concentration is given by

$$\left\{\frac{2K'_{B2}\left(\gamma^{(c)}_{\pm,Bi(NO_3)_3}\right)^4\left[Bi(H_2O)_5^{3+}\right]\left[NO_3^-\right]^3}{a_w^5}\right\}[CMPO]^2 + \left\{1 + K'_{1:1}\left(\gamma^{(c)}_{\pm,HNO_3}\right)^2[H^+]\left[NO_3^-\right]\right\}[CMPO] - [CMPO]_0 = 0 \quad , \tag{4-87}$$

which is now a quadratic, rather than a cubic, in the free CMPO concentration. The positive square root in the quadratic is required to obtain positive values of the free CMPO concentration. The organic-phase bismuth concentration in terms of the aqueous concentration is given by

$$\left[Bi(NO_3)_3 \cdot 2CMPO\right] = \frac{K'_{B2}\left(\gamma^{(c)}_{\pm,Bi(NO_3)_3}\right)^4\left[Bi(H_2O)_5^{3+}\right]\left[NO_3^-\right]^3\left[CMPO\right]^2}{a_w^5} \quad . \tag{4-88}$$

Two-Parameter Models. Suppose there is a nitrate complexation of the bismuth ion. Because an ion of unity charge is more likely to occur than one of higher charges, let it be assumed that the complexation can be represented by

$$Bi(H_2O)^{3+}_{5(aq)} + 2NO^-_{3(aq)} \rightleftharpoons Bi(NO_3)_2(H_2O)^+_{3(aq)} + 2H_2O_{(aq)} \quad . \tag{4-89}$$

Making the same assumptions about the activity coefficients of the individual ions as was made for the case of uranium, the complexation constant is

$$\beta_B = \frac{\left[Bi(NO_3)_2(H_2O)_3^+\right]a_w^2}{\left[Bi(H_2O)_5^{3+}\right]\left[NO_3^-\right]^2\left(\gamma^{(c)}_{NO_3^-}\right)^2} \quad . \tag{4-90}$$

A material balance on the aqueous-phase bismuth concentration yields

$$\left[Bi\right]_{aq} = \left[Bi(H_2O)_5^{3+}\right] + \left[Bi(NO_3)_2(H_2O)_3^+\right] \quad . \tag{4-91}$$

By presumption, the nitrate complex is inextractable and only the pentahydrate form of bismuth extracts. The concentration of the extractable species, in terms of the measured aqueous bismuth nitrate concentration, is found by combining Eqs. (4-90) and (4-91):

$$\left[Bi(H_2O)_5^{3+}\right] = \frac{a_w^2\left[Bi\right]_{aq}}{a_w^2 + \beta_B\left[NO_3^-\right]^2\left(\gamma^{(c)}_{NO_3^-}\right)^2} \quad . \tag{4-92}$$

To modify the 3:1 stoichiometric model to include the nitrate complexation, Eq. (4-92) can be substituted into Eqs. (4-84) and (4-85) to calculate the free CMPO concentration and the organic-phase bismuth nitrate concentration, respectively. As usual, division by the total aqueous bismuth concentration will yield the distribution ratio.

To include the nitrate complexation equilibria in the 2:1 stoichiometric model only requires the substitution of Eq. (4-92) into Eqs. (4-87) and (4-88).

4.4 Estimation of Solvent Activity Coefficients

The slope-analysis method can be used to deduce the extraction stoichiometry when both the organic and aqueous phases approximate ideal conditions, or if the experimental conditions are such that the quantities involved are constant. Suppose that the coordination number, n, is known by other means, but the slope-analysis method gives different results. Further, suppose that all variables except the activity coefficients of the extractant can be quantified and are shown to be constant (i.e., have no effect on the slope-analysis results). Basically, this is the case where it is suspected that the organic-phase is quite nonideal and the activity coefficients of the organic-phase components differ appreciably from unity. A general analysis begins with Eq. (2-57), which may be rewritten as

$$D' = \frac{D a_w^h}{\gamma_{MX_z}^{(1+z)}} = K[X^-]^z \mathbb{R}[E]^n \quad , \tag{4-93}$$

where

$$\mathbb{R} = \left\{ \frac{\gamma_E^n}{\gamma_{MX_z \cdot nE}} \right\} \quad . \tag{4-94}$$

Taking the logarithm of both sides of Eq. (4-93) yields

$$\ln D' = \ln K + z \ln[X^-] + \ln \mathbb{R} + n \ln[E] \, , \tag{4-95}$$

and taking the partial derivative with respect to ln[E] yields

$$\frac{\partial \ln D'}{\partial \ln[E]} = \frac{\partial \ln K}{\partial \ln[E]} + z\frac{\partial \ln[X^-]}{\partial \ln[E]} + \frac{\partial \ln \mathbb{R}}{\partial \ln[E]} + n \quad . \tag{4-96}$$

By definition, K is constant, and the aqueous-phase anion concentration can be made constant experimentally. Therefore, Eq. (4-96) reduces to

$$\frac{\partial \ln D'}{\partial \ln[E]} = n + \frac{\partial \ln \mathbb{R}}{\partial \ln[E]} \quad . \tag{4-97}$$

Now, by supposition, the ordinary slope-analysis method, defined by Eq. (2-59), gives a different coordination number than expected. The data correlate strongly with a straight line, but the slope is not equal to the expected coordination number. This condition means that the right-most term of Eq. (4-97) is a constant; that is,

$$\frac{\partial \ln \mathbb{R}}{\partial \ln[E]} = \omega \ , \tag{4-98}$$

and Eq. (4-97) may be written as

$$\frac{\partial \ln D'}{\partial \ln[E]} = n + \omega = n_s \quad . \tag{4-99}$$

When the slope-analysis method gives a coordination number, n_s, and the true coordination number, n, is known, then the difference, ω, is a measure of the ratio of the organic-phase activity coefficients shown in Eq. (4-94).

Because the slope-analysis method requires the extractant concentration to change, an expression for $\mathbb{R}$ in terms of extractant concentration can be derived by integration of Eq. (4-98):

$$\ln \mathbb{R} = \omega \ln[E] + constant \quad . \tag{4-100}$$

When $[E]$ approaches zero, the activity coefficients approach unity and $\mathbb{R}$ should approach unity. The form of Eq. (4-100) makes use of these boundary conditions difficult. If the extractant concentration is less than unity, the logarithmic term can be approximated by the expansion

$$\ln(1+x) = x - \frac{x^2}{2} + \frac{x^3}{3} - \frac{x^4}{4} + \ldots , \tag{4-101}$$

which applies for absolute values of x less than 1. Truncating the series to only the first term permits Eq. (4-100) to be approximated by

$$\ln \mathbb{R} = \omega([E]-1) + constant, \tag{4-102}$$

which, upon substitution of the boundary conditions and rearrangement, yields

$$\mathbb{R} = e^{\omega[E]} \quad . \tag{4-103}$$

This equation has the proper limiting value at zero extractant concentration but is only an approximation. Performing the differentiation shown on the left-hand side of Eq. (4-98) results in

$$\frac{\partial \ln \mathbb{R}}{\partial \ln[E]} = \omega \frac{\partial[E]}{\partial \ln[E]} = \omega \frac{\partial[E]}{\frac{\partial[E]}{[E]}} = \omega[E] \quad . \tag{4-104}$$

Comparing Eqs. (4-98) and (4-104) demonstrates the error introduced by the approximation. However, the approximation can be improved by selecting a value of ω different from that suggested by Eq. (4-99). Assuming that the exponential function adequately models the behavior of $\mathbb{R}$ when the extractant concentration is low, Eq. (4-103) can be substituted into Eq. (4-93) and rearranged to obtain

$$\frac{D'}{K[X^-]^z[E]^n} = \mathbb{R} = e^{\omega[E]} \quad . \tag{4-105}$$

Taking the logarithm of both sides of the equation and rearranging yields

$$\ln d \equiv \ln\left\{\frac{D'}{[X^-]^z[E]^n}\right\} = \omega[E] + \ln K \quad . \tag{4-106}$$

If we recall that the coordination number, n, is known by other means, then the term in braces can be evaluated. A semilogarithmic plot of the term in braces vs $[E]$ is a straight line with a slope equal to ω and an intercept K. Equation (4-106), together with Eq. (4-103), provides the means for exploring the magnitude of organic-phase activity coefficients and their effect on slope analysis, and also gives an estimate of the true equilibrium constant. This type of analysis does not appear in the literature. Henceforth, it will be convenient to refer to Eq. (4-106) as the solvent slope-analysis method.

5. RESULTS AND DISCUSSION

At the beginning of the experimental program, some simple tests were performed to determine whether there would be a volume change in either the organic or the aqueous phase during extraction. Equal volumes of dry organic (0.20 *M* CMPO in *n*-dodecane) and pure water were placed in a graduated cylinder, mixed, and allowed to separate. No changes in the volume of either phase could be measured. Based on this information and because small quantities of salts were extracted in the partitioning experiments, the phase volumes are considered to be constant for the purposes of making material balances.

The raw data collected during the experimental program are tabulated in three separate appendixes: Appendix C—extraction of nitric acid, Appendix D—extraction of uranyl nitrate from nitric acid, and Appendix E—extraction of bismuth nitrate from nitric acid. Within each appendix, the data are grouped by campaign. In this chapter, they are presented in a more compact form and are arranged in a logical order (e.g., ascending concentration). However, the sample numbers are also included to make the information easier to cross-reference.

5.1 Extraction of Nitric Acid with CMPO

Equilibrium concentrations of nitric acid distributed between a CMPO–*n*-dodecane organic phase and a nitric acid aqueous phase were measured primarily at 25 and 40°C; a few experiments were performed at 50°C. Aqueous concentrations of nitric acid were restricted to low values to prevent formation of a third phase. Higher working temperatures permitted higher concentrations to be used. Most experiments were performed with organic-phase CMPO concentrations of 0.20 *M*, with some experiments performed at lower CMPO concentrations to provide slope-analysis data. Equilibrium constants are inferred by fitting the data to mathematical models.

5.1.1 Approximate Regions of Third-Phase Formation

The solubility of CMPO-extract complexes in *n*-dodecane is limited and leads to a CMPO-rich third phase when the solvent is sufficiently loaded. Equilibrium concentrations of aqueous nitric acid causing a third phase were bracketed experimentally. Table 5.1 gives the nitric acid concentration range in which a third phase forms as a function of temperature. The lower number represents the highest nitric acid concentration at which no third phase was observed. The higher number is the next highest nitric acid concentration tested where a third phase was observed. Third-phase material appeared at the organic-aqueous interface and was slightly yellow in color. At higher concentrations, where greater quantities of third phase formed and could be observed more easily, the third phase appeared more viscous and adhered more strongly to the wall of the glass container than either of the other two phases. Formation of the third phase also affected phase separation behavior. When no third phase formed, both phases separated quickly (<2 min) and were completely clear. Under conditions promoting third-phase formation, the bulk phases separated quickly but the organic phase remained cloudy much longer (sometimes >30 min). The lower limits of the ranges shown in Table 5.1 were, therefore, the upper limit of the acid concentrations where distribution ratios were measured free of third-phase effects.

Table 5.1. Nitric acid concentration range wherein a third phase forms

Temperature (°C)	Nitric acid concentration (*M*)
25.0	0.30–0.50
40.0	0.94–1.00
50.0	3.0–4.0

5.1.2 Stoichiometry by Slope Analysis

Experiments were performed at organic-phase CMPO concentrations of 0.05, 0.10, and 0.20 *M* to support slope-analysis estimation of the nitric acid extraction stoichiometry (sometimes called coordination number or solvation number). At a temperature of 25°C, a nominal aqueous acid concentration of 0.25 *M* was used to ensure measurable quantities of acid in the organic phase. At 40°C, the nominal aqueous acid concentration was 0.51 *M*. The results, along with the calculated distribution ratio (organic/aqueous concentration ratio), are summarized in Table 5.2.

Table 5.2. Slope-analysis data for the extraction of nitric acid

CMPO (*M*)	Aqueous phase (*M*)	Organic phase (*M*)	Distribution ratio, O/A	Data pair
At 25°C				
0.200	0.252	0.018	0.0714	D-4-13/14
0.200	0.254	0.017	0.0669	D-15-01/02
0.100	0.257	0.008	0.0311	D-15-03/04
0.100	0.257	0.0084	0.0327	D-15-05/06
0.050	0.256	0.004	0.0156	D-15-07/08
0.050	0.258	0.004	0.0155	D-15-09/10
At 40°C				
0.200	0.518	0.044	0.0849	D-3-09/10
0.200	0.508	0.042	0.0827	D-7-03/04
0.200	0.522	0.044	0.0843	D-16-01/02
0.100	0.519	0.021	0.0405	D-16-03/04
0.100	0.521	0.020	0.0384	D-16-05/06
0.050	0.518	0.010	0.0193	D-16-07/08
0.050	0.522	0.010	0.0192	D-16-09/10

These data are plotted in Figure 5.1 on log-log coordinates, as suggested by Eq. (2-59). Linear regression was used to calculate the slopes of the best straight lines through the data, which are also shown in the figure. At 25°C, the slope of the line is 1.076 ± 0.140 with a correlation coefficient of 0.9990. At 40°C, the slope is 1.065 ± 0.054 with a correlation coefficient of 0.9996.

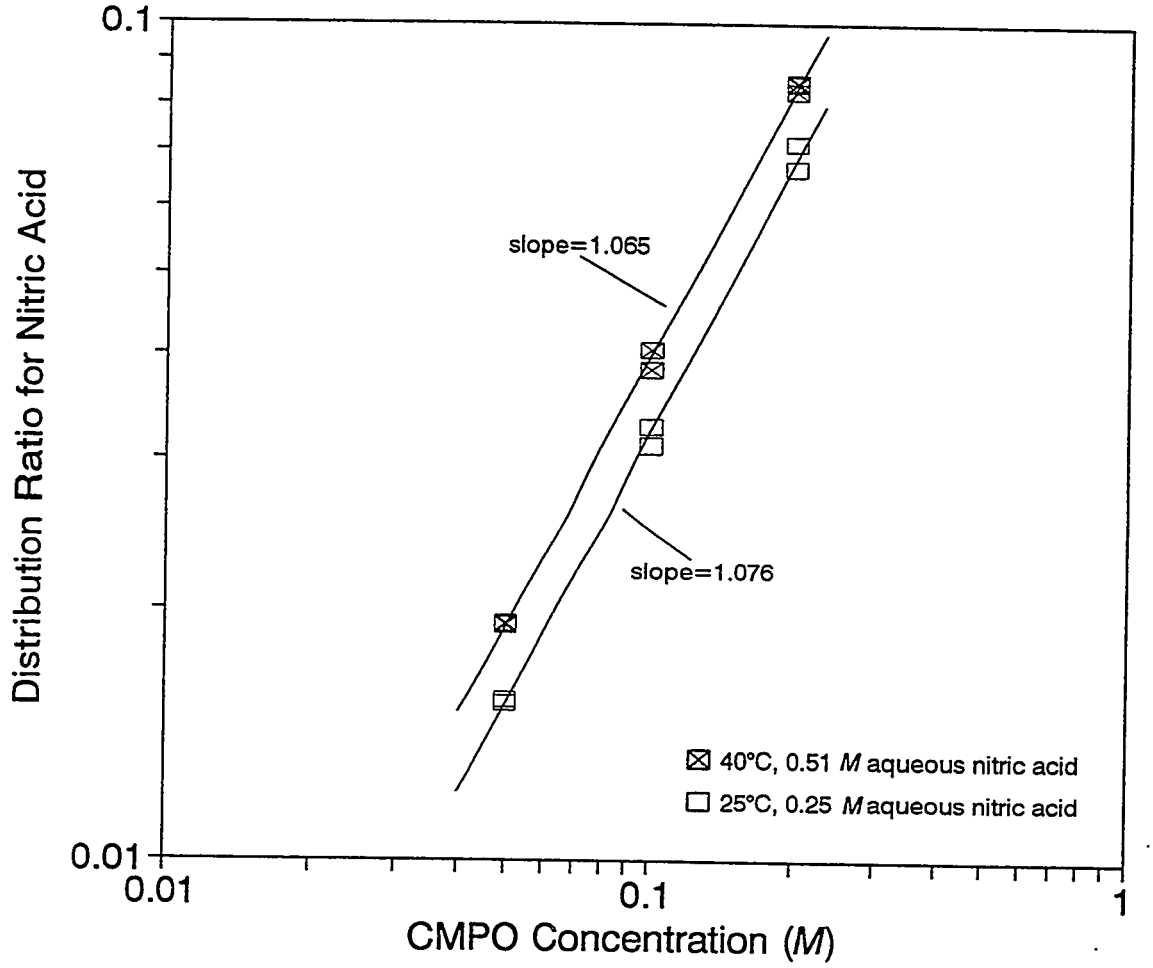

Figure 5.1. Extraction stoichiometry for nitric acid.

Before these results can be accepted, possible corrections to the slope-analysis method should be addressed. The variables that must be considered are shown in Eq. (4-6). In each of the two sets of experiments, the equilibrium constant, nitric acid concentration, and aqueous nitric acid activity coefficient are constant, either by definition or by experimental conditions and need not be considered further. The free CMPO concentration is reduced from its initial concentration by an amount proportional to both the amount of acid extracted and the solvation number. The correction is the largest when the solvation number is largest. Assuming that the solvation number is unity, corrections to the free CMPO concentration change the ln D-vs-ln[$CMPO$] slopes to 1.082 (correlation coefficient, 0.9988) and 1.081 (correlation coefficient, 0.9992) for data at 25 and 40°C, respectively. Thus, there is essentially no change. If the solvation number were 2, the slopes would become 1.089 (correlation coefficient, 0.9986) and 1.110 (correlation coefficient, 0.9985) at 25 and 40°C, respectively. Again, there is no appreciable change.

One last term in Eq. (4-6), the ratio of the activity coefficients of free CMPO and the nitric acid solvate, can affect the slope analysis. No data on activity coefficients are available for the CMPO–*n*-dodecane system. However, from the work of Diamond et al. (1986), it is known that the activity coefficients for CMPO in toluene are approximately the same for organic equilibrated with either pure water or with 0.5 M nitric acid; the activity coefficient is slightly less when the organic is equilibrated with acid. This suggests, for a solvation number of unity, that no correction is needed since the ratio of activity coefficients in Eq. (4-6) is about unity. On the other hand, at a solvation number of 2, the stated ratio varies directly with the CMPO concentration. The molar-scale activity coefficients read from the graph in the paper by Diamond et al. (1986) are approximately 0.98, 0.96, and 0.92 for CMPO concentrations of 0.05, 0.10, and 0.20 M, respectively. Correcting the distribution ratio by moving the activity coefficient ratio to the

left-hand side of Eq. (4-6) and reanalyzing the data gives slopes of 1.121 (correlation coefficient, 0.9989) and 1.110 (correlation coefficient 0.9998) for data at 25 and 40°C, respectively.

None of the corrections to the slope analysis significantly change the solvation numbers derived from the raw data. Since the slope is slightly larger than unity, it can be argued that a disolvate is also formed with a relatively small yield. These data show that nitric acid forms primarily a unisolvate with CMPO, [i.e., the 1:1 stoichiometry of Eq. (4-1) prevails].

5.1.3 Degree of Nonideal Behavior of Organic Phase

The solvent slope-analysis method derived in Sect. 4.4 is used to investigate the ratio, $\mathbb{R}$, of the activity coefficients of the free CMPO and the CMPO–nitric acid solvate. Because the slope-analysis method strongly suggests that the solvation number is 1:1, Eq. (4-106) may be written as

$$\ln d_{1:1} = \ln\left\{\frac{D'_{1:1}}{[NO_3^-][CMPO]}\right\} = \omega[CMPO] + \ln K_{1:1} \qquad (5\text{-}1)$$

for the extraction of nitric acid. The subscript 1:1 is a reminder of the assumed true extraction stoichiometry.

Values of the activity coefficient for nitric acid and the free CMPO concentrations, computed from the original data given in Table 5.2, are listed in Table 5.3. Transforming the appropriate values from the table into data pairs defined by Eq. (5-1), linear regression is used to compute the best values of the slope and intercept fitting Eq. (5-1) to the data. These values, along with a correlation coefficient, are recorded in Table 5.4. The transformed data and best straight-line fit to the data are illustrated in the semilog plot of Figure 5.2. The correlation coefficients indicate that the fit is moderately good. On the other hand, the model is not as good

Table 5.3. Activity coefficients of nitric acid and free CMPO concentrations for the nitric acid slope-analysis data

HNO_3 (M)	ρ_{aq} (g/mL)	$\gamma_{\pm, HNO_3}$	a_w	$[CMPO]_0$ (M)	$[CMPO]$ (M)	D	D'
At 25°C							
0.252	1.00531	0.75202	0.99142	0.200	0.182	0.07143	0.12630
0.254	1.00537	0.75175	0.99135	0.200	0.183	0.06693	0.11843
0.257	1.00547	0.75134	0.99125	0.100	0.092	0.03113	0.05514
0.257	1.00547	0.75134	0.99125	0.100	0.0916	0.03268	0.05790
0.256	1.00544	0.75148	0.99128	0.050	0.046	0.01563	0.02767
0.258	1.00551	0.75121	0.99121	0.050	0.046	0.01550	0.02747
At 40°C							
0.518	1.00886	0.73392	0.98196	0.200	0.156	0.08494	0.15770
0.508	1.00854	0.73393	0.98232	0.200	0.158	0.08268	0.15349
0.522	1.00899	0.73392	0.98181	0.200	0.156	0.08429	0.15649
0.519	1.00889	0.73392	0.98192	0.100	0.079	0.04046	0.07512
0.521	1.00896	0.73392	0.98185	0.100	0.080	0.03839	0.07127
0.518	1.00886	0.73392	0.98196	0.050	0.040	0.01931	0.03584
0.522	1.00899	0.73392	0.98181	0.050	0.040	0.01916	0.03557

Table 5.4. Solvent slope-analysis results for the extraction of nitric acid

Temperature (°C)	ω	$K_{1:1}$	Correlation Coefficient
25.0	0.9554	2.217	0.8830
40.0	1.016	1.642	0.9282

a fit as are the raw data to the usual slope-analysis method. This is an indicator that the activity coefficient ratio, $\mathbb{R}$, is poorly modeled by an exponential function (even over a narrow range) and that the estimations of the ratio may be in error. At CMPO concentrations of 0.20 M, the values of ω in Table 5.4 give values of $\mathbb{R}$ [see Eq. (4-103)] of 1.21 and 1.22 at 25 and 40°C, respectively. Ratios greater than unity imply that the activity coefficient of the CMPO–nitric acid

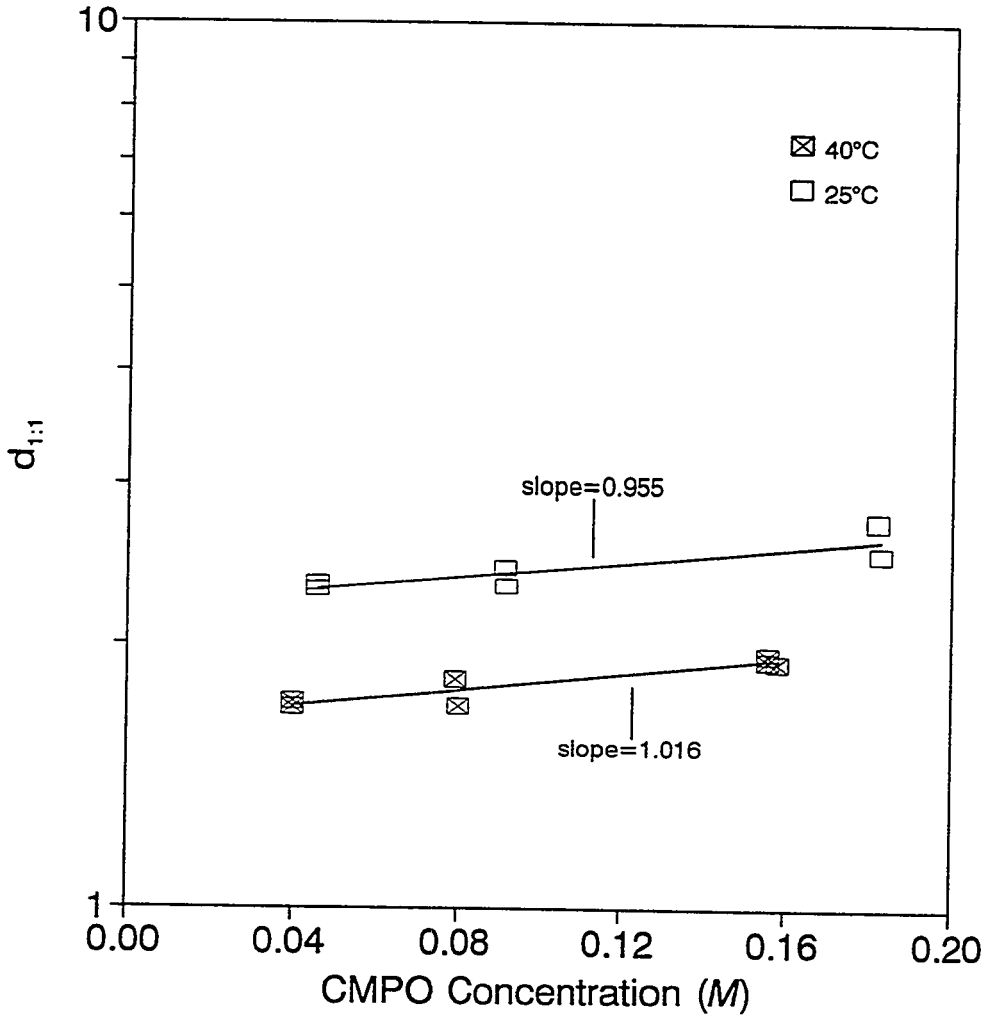

Figure 5.2. Solvent slope-analysis method for the extraction of nitric acid with CMPO–*n*-dodecane.

solvate is less than the activity coefficient of the free CMPO. This agrees with the measurements of Diamond et al. (1986).

Values of the equilibrium constants given in Table 5.4 are those associated with infinite dilution of the organic extractant. Equilibrium constants that include the effects of organic-phase nonideality, $K'_{1:1}$, may be evaluated by multiplying $K_{1:1}$ by $\mathbb{R}$. At CMPO concentrations of 0.20 M, values of $K'_{1:1}$ are 2.683 and 2.012 at 25 and 40°C, respectively. These values are compared with those calculated by other methods in Sect. 5.1.5.

5.1.4 Coextraction of Water

Organic samples were also analyzed for water content. The goal was to determine whether water is replaced as nitric acid is extracted or if hydrated nitric acid is extracted. These effects should manifest themselves as either a reduction or an increase, respectively, in organic-phase water content as organic-phase acid content is increased. The data are summarized in Table 5.5. Plots are shown in Figures 5.3 and 5.4 for data taken at 25 and 40°C, respectively.

Examination of the data obtained at 25°C indicate that the one point with a water concentration of 7.8 wt % is an obvious outlier, and it was discarded. Although the remaining data plotted in Figure 5.3 show extensive variation, they appear to indicate that the water concentration increases as the acid concentration increases. To determine whether a causal relationship exists, the water concentration is assumed to vary linearly with acid concentration. Linear regression analysis gives a positive slope, but a correlation coefficient of only 0.149 indicates a very poor correlation between water concentration and acid concentration. The data collected at 40°C, plotted in Figure 5.4, are even more scattered. Overall, they appear random and, therefore, do not permit definite conclusions to be drawn concerning the coextraction of water.

Table 5.5. Measured nitric acid and water contents of 0.20 *M* CMPO organic phase equilibrated with nitric acid solutions

HNO_3 (*M*)	H_2O (wt %)	Data pair
At 25°C		
<0.001	0.34	D-4-01/02
<0.001	0.47	D-4-03/04
<0.001	0.18	D-4-05/06
0.002	0.26	D-4-07/08
0.002	1.2	D-6-01/02
0.004	0.21	D-4-09/10
0.012	0.51	D-4-11/12
0.014	7.8	D-6-03/04
0.018	0.35	D-4-13/14
0.022	0.58	D-4-15/16
0.024	0.62	D-6-05/06
At 40°C		
0.001	0.21	D-3-01/02
0.001	0.15	D-3-03/04
0.003	<0.01	D-3-05/06
0.010	0.16	D-3-07/08
0.010	0.38	D-7-01/02
0.042	0.43	D-7-03/04
0.044	<0.01	D-3-09/10
0.062	0.43	D-7-05/06
0.081	0.02	D-3-13/14
0.086	0.05	D-3-15/16
0.091	0.02	D-3-11/12

Several phenomena could contribute to large errors in the water analysis. Entrainment of aqueous phase into the organic phase is considered unlikely; otherwise, the extraction data on the nitric acid (Sect. 5.1.5) would show the same degree of randomness. Most likely, the errors occurred in sample analysis. For example, as successive samples are injected into the Karl-Fischer analyzer, the integrity of the septum degrades and permits greater amounts of moisture-laden air to enter the titration chamber. Another possibility is the rate at which CMPO releases water as the

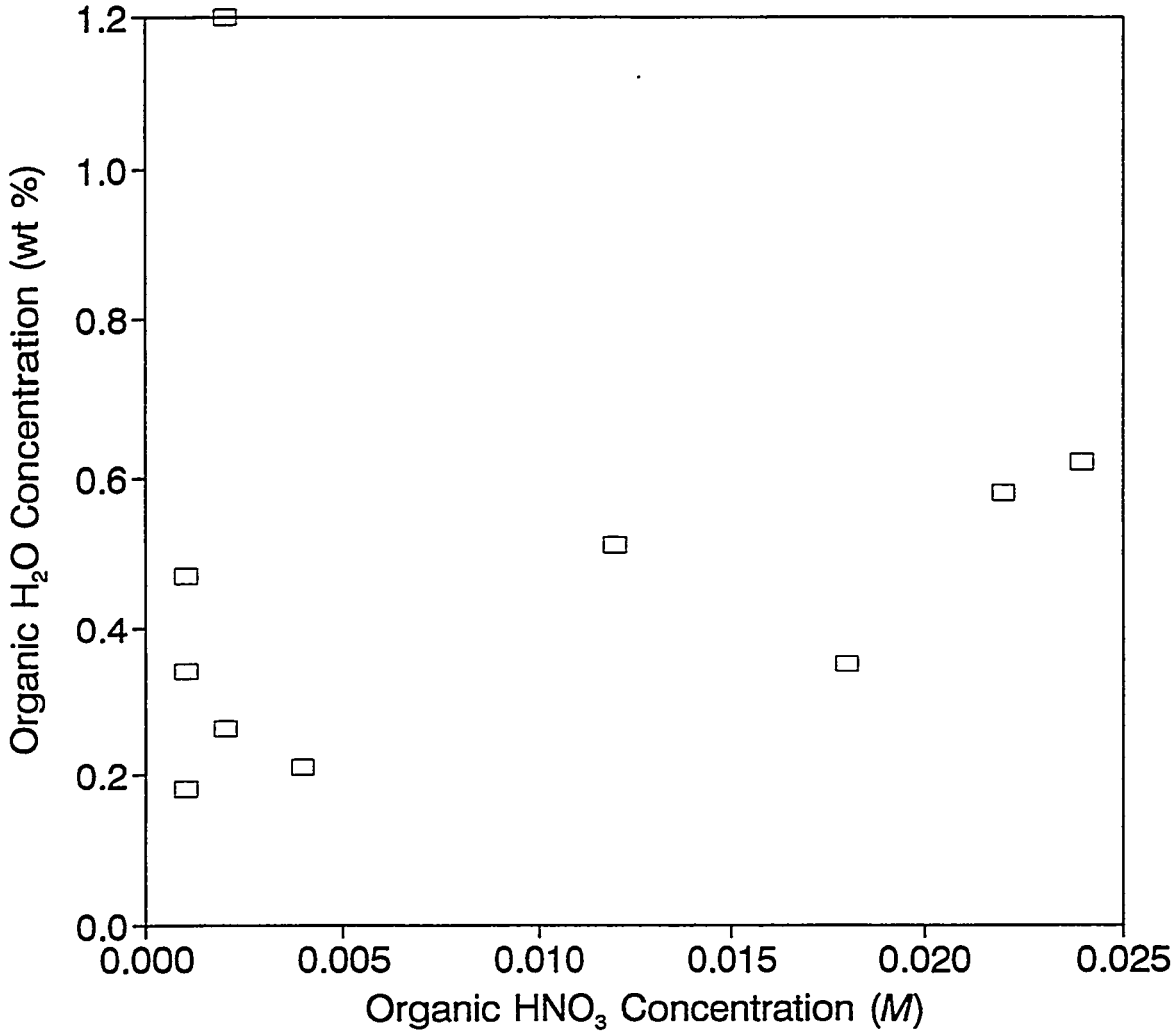

Figure 5.3. Lack of correlation between measured organic-phase water concentration and organic-phase nitric acid concentration at 25°C.

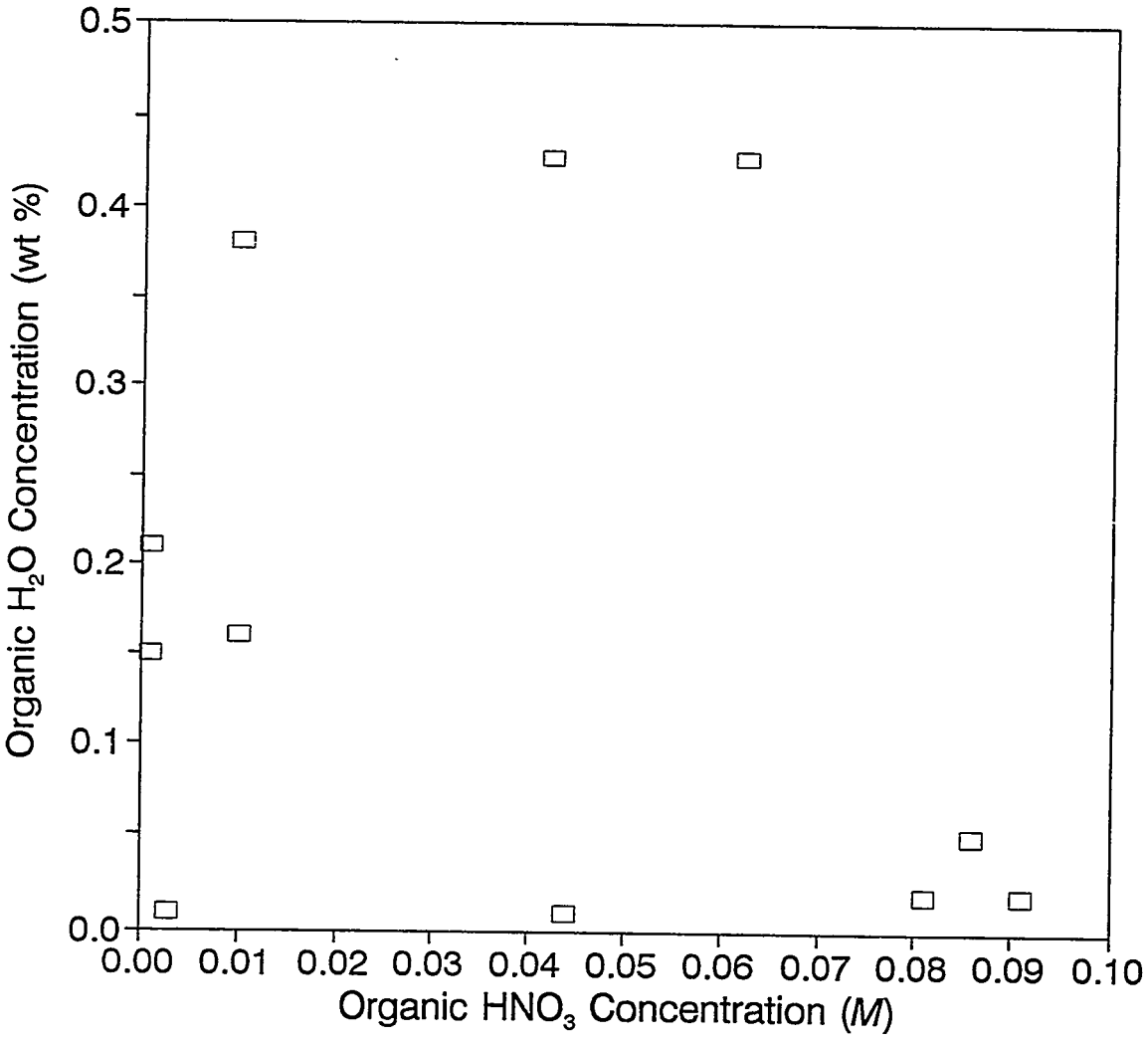

Figure 5.4. Lack of correlation between measured organic-phase water concentration and organic-phase nitric acid concentration at 40°C.

titration progresses. A titration may be prematurely considered complete due to a slow release of water. The possibilities of large errors in the water analysis, coupled with the small concentrations of extracted salts that may affect water extraction, resulted in a decision to abandon further analyses of organic-phase water concentrations.

5.1.5 Determination of Thermodynamic Equilibrium Constants

Equilibrium concentrations for nitric acid partitioned between an aqueous phase and a 0.2 *M* CMPO in *n*-dodecane organic phase were measured at three different temperatures: 25, 40, and 50°C. These data are given in Table 5.6. As shown, there are 9 data pairs at 25°C, 11 pairs at 40°C, and 3 pairs at 50°C. Data taken at 25 and 40°C contain some duplicate points from which the estimated standard deviation for measured organic nitric acid concentration is 0.00141 *M*. (More significant digits are given here than justified so that the effects of roundoff are reduced.) Few points were taken at 50°C because that test was done primarily to find the region of third-phase formation.

Nonlinear regression is used to fit the data obtained at 25 and 40°C to the mathematical models described in Sect. 4.1.2. The results obtained at 50°C are not treated this way because of the few number of data points and because one of those (1.00, 0.054) appears to be in error (organic nitric acid concentration is too low). The parameters of the regression are the equilibrium constants, K', on the molar concentration scale. Molar concentration units are used because the chemical analyses of the samples are on that basis and because there is a general lack of density data for the multicomponent organic phase with which to convert to other concentration units. The organic-phase densities of six samples were measured, as reported in Appendix C. Within measurement error, the density is not different from that of pure *n*-dodecane. Density changes are probably small because of the small amount of material transferred to the organic. Because

Table 5.6. Equilibrium concentrations of nitric acid with 0.20 *M* CMPO in *n*-dodecane from extraction experiments

Aqueous phase (*M*)	Organic phase (*M*)	Distribution coefficient, O/A	Data pair
At 25°C			
0.053	0.002	0.0377	D-4-07/08
0.102	0.002	0.0196	D-6-01/02
0.104	0.004	0.0385	D-4-09/10
0.202	0.014	0.0693	D-6-03/04
0.206	0.012	0.0583	D-4-11/12
0.252	0.018	0.0714	D-4-13/14
0.254	0.017	0.0669	D-15-01/02
0.296	0.024	0.0811	D-6-05/06
0.302	0.022	0.0728	D-4-15/16
At 40°C			
0.046	0.001	0.0217	D-3-03/04
0.116	0.003	0.0259	D-3-05/06
0.200	0.010	0.0500	D-7-01/02
0.236	0.010	0.0424	D-3-07/08
0.508	0.042	0.0827	D-7-03/04
0.518	0.044	0.0849	D-3-09/10
0.522	0.044	0.0843	D-16-01/02
0.756	0.062	0.0820	D-7-05/06
0.830	0.081	0.0864	D-3-13/14
0.910	0.086	0.0945	D-3-15/16
0.938	0.091	0.0970	D-3-11/12
At 50°C			
1.00	0.054	0.0540	D-12-01/02
1.85	0.146	0.0789	D-12-03/04
2.76	0.179	0.0649	D-12-05/06

Pitzer's correlation for aqueous electrolyte activity coefficients uses molal concentrations, it is necessary to calculate the density of the aqueous phase using the methods described in Sect. 2.3, calculate the equivalent molal concentration for each solute, calculate the molal scale activity coefficient for each component, and then convert the activity coefficient to the molar scale using Eq. (2-17).

Although the slope-analysis method indicates that the extraction stoichiometry is 1:1, the data were fit to every combination of the three stoichiometries shown in Eqs. (4-1) through (4-3). The results of the calculations are presented in Table 5.7. Each model is identified by the species

Table 5.7. Comparison of models describing the extraction of nitric acid: model statistics, model parameters, and standard deviations of model parameters

Temp. (°C)	χ^2	σ	K'	$\sigma_{K'}$	K'	$\sigma_{K'}$	K'	$\sigma_{K'}$
			$HNO_3 \cdot CMPO$					
25.0	6.561	0.00128	2.660	0.092				
40.0	61.78	0.00350	1.710	0.022				
			$HNO_3 \cdot 2CMPO$					
25.0	6.238	0.00124	14.21	0.51				
40.0	346.1	0.00830	6.425	0.029				
			$2HNO_3 \cdot CMPO$					
25.0	79.37	0.00444	28.47	0.98				
40.0	1882	0.01934	1.505	0.016				
			$HNO_3 \cdot CMPO$		$HNO_3 \cdot 2CMPO$			
25.0	5.881	0.00129	1.521	1.293	7.428	8.791		
40.0	42.85	0.00308	1.574	0.041	2.560	0.659		
			$2HNO_3 \cdot CMPO$		$HNO_3 \cdot 2CMPO$			
25.0	6.004	0.00131	4.070	3.250	15.68	2.202		
40.0	45.33	0.00316	1.076	0.033	15.79	0.741		
			$HNO_3 \cdot CMPO$		$2HNO_3 \cdot CMPO$			
25.0	5.820	0.00129	2.960	0.363	−3.462[a]	4.044		
40.0	48.02	0.00326	1.894	0.055	−0.197[a]	0.054		
			$HNO_3 \cdot CMPO$		$HNO_3 \cdot 2CMPO$		$2HNO_3 \cdot CMPO$	
25.0	5.793	0.00139	4.984	22.80	−10.31[a]	117.7	−6.345[a]	3.859
40.0	38.98	0.00311	0.7850	0.4440	8.384	3.582	0.7585	0.4323

[a]Negative values are not permitted and indicate "over-modeling" of the data.

formed. Values of the equilibrium constant for the species formed are listed directly under it, along with a value for the standard deviation in the equilibrium constant.

It should be noted that some equilibrium constants in the table are negative. These negative values resulted because no constraint that the parameters should be positive was imposed. Such values can be used as an indicator that a particular stoichiometry adversely affects the model. For each model, two figures of merit are given: the weighted residuals squared, χ^2; and the standard deviation, σ. The χ^2 is defined by

$$\chi^2 = \sum_{i=1}^{n} \left(\frac{[HNO_3]_{org,model} - [HNO_3]_{org,experimental}}{\sigma_{experimental}} \right)_i^2 , \qquad (5\text{-}2)$$

where n is the number of points and the standard deviation is defined by

$$\sigma = \sqrt{\frac{\sum_{i}^{n} \left([HNO_3]_{org,\ model} - [HNO_3]_{org,\ experimental} \right)_i^2}{n - p}} , \qquad (5\text{-}3)$$

where p is the number of model parameters. This definition of standard deviation describes the average deviation of measured points from those calculated by the model while accounting for the reduction in the degrees of freedom imposed by model parameters. Press et al. (1992) state that χ^2 for a "moderately" good fit to the data is equal to the degrees of freedom, $n - p$, with a standard deviation of $[2(n - p)]^{1/2}$.

Comparison of the results shown in Table 5.7 for one-parameter models indicates that 1:1 stoichiometry fits the 40°C data best. The model standard deviation is clearly smallest in this case. However, the data at 25°C are fit by either 1:1 or 2:1 stoichiometry equally well with standard deviations slightly less than the estimated deviations in the data (~0.00141). Given the definition of the standard deviations calculated by Eq. (5-3), Wadsworth et al. (1990) show that the F-test statistic can be computed by

$$F_{model\text{-}1,\ model\text{-}2} = \frac{\sigma^2_{model\text{-}1}}{\sigma^2_{model\text{-}2}} \quad . \tag{5-4}$$

With the data at 25°C listed in Table 5.7, $F_{1:1,2:1} = (0.00128/0.00124)^2 = 1.07$, which indicates that the one-parameter models are not statistically different. Equilibrium constants, $K_{1:1}'$, estimated by the solvent slope-analysis method (Sect. 5.1.3) are quite close to those in Table 5.7.

The best two-parameter model, as selected by the smallest model standard deviations, includes both 1:1 and 2:1 stoichiometries. However, the standard deviation in the second model parameter for the data at 25°C is larger than the parameter itself, implying that the parameter is not statistically different from zero. Additionally, the standard deviations of all the two-parameter models are essentially equal. For data at 40°C, the F-test statistic for the best one-parameter vs the best two-parameter model is $(0.00350/0.00308)^2 = 1.29$, which for eight and nine degrees of freedom, respectively, indicates the two models are not statistically different. The other two-parameter models and the three-parameter model are even less favorable.

Therefore, over the range of data provided here, a single stoichiometric representation for the extraction of nitric acid, the 1:1 stoichiometry, provides an adequate fit. The model is compared with the data at 25 and 40°C in Figures 5.5 and 5.6, respectively. As shown, the data are well modeled.

5.1.6 Enthalpy of Extraction

The van't Hoff equation, Eq. (2-6), shows that a plot of ln K vs $1/T$ (temperature on an absolute scale) may be used to estimate equilibrium constants at temperatures near that of the data. The slope of the line is used to obtain a value for the enthalpy of reaction. For the study of the extraction of nitric acid presented here, equilibrium constants are available from data collected at 25 and 40°C. Because there are only two points, direct substitution of the values into Eq. (2-6)

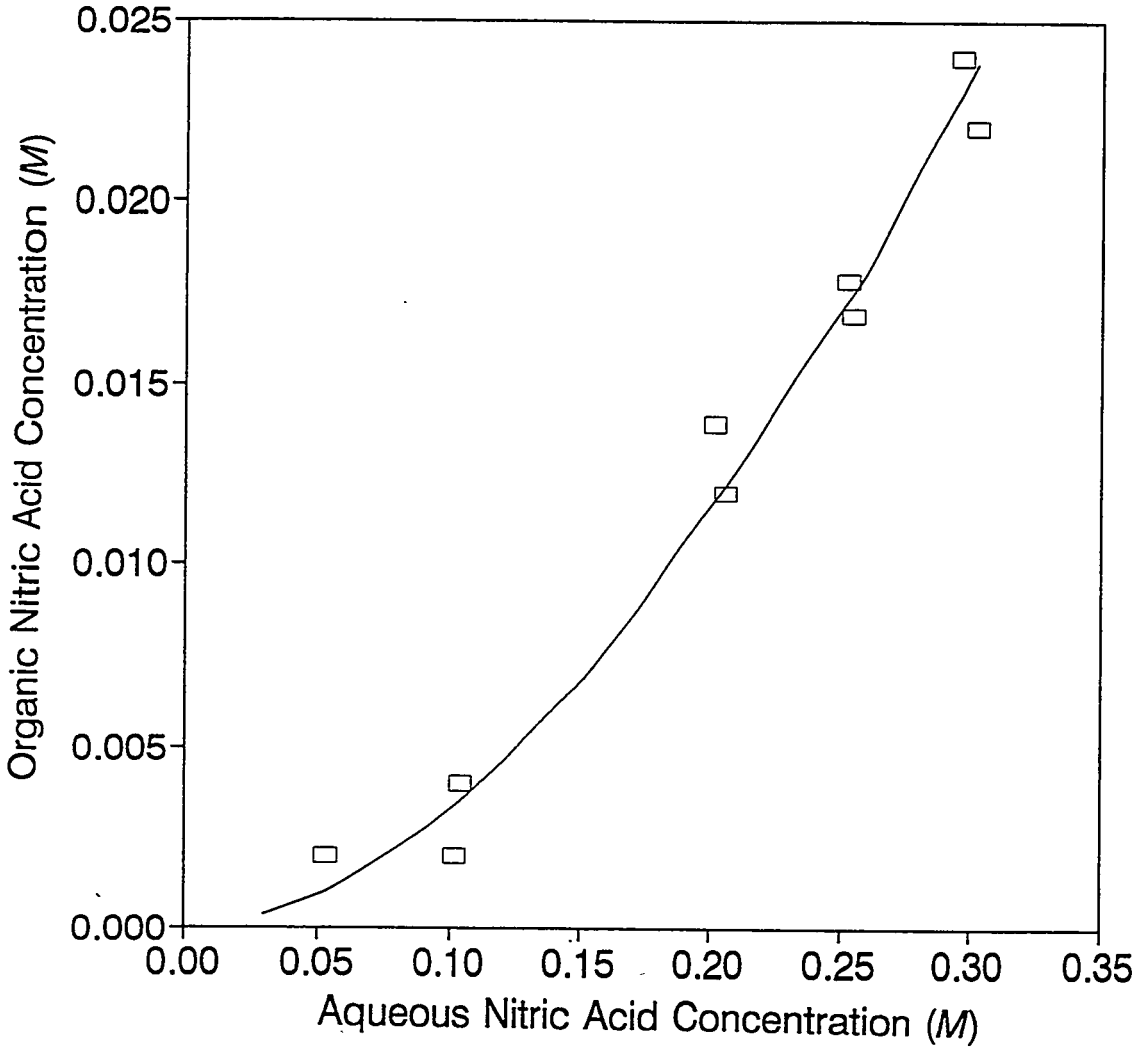

Figure 5.5. Comparison of the 1:1 stoichiometric-based model for extraction of nitric acid with the experimental data at 25°C.

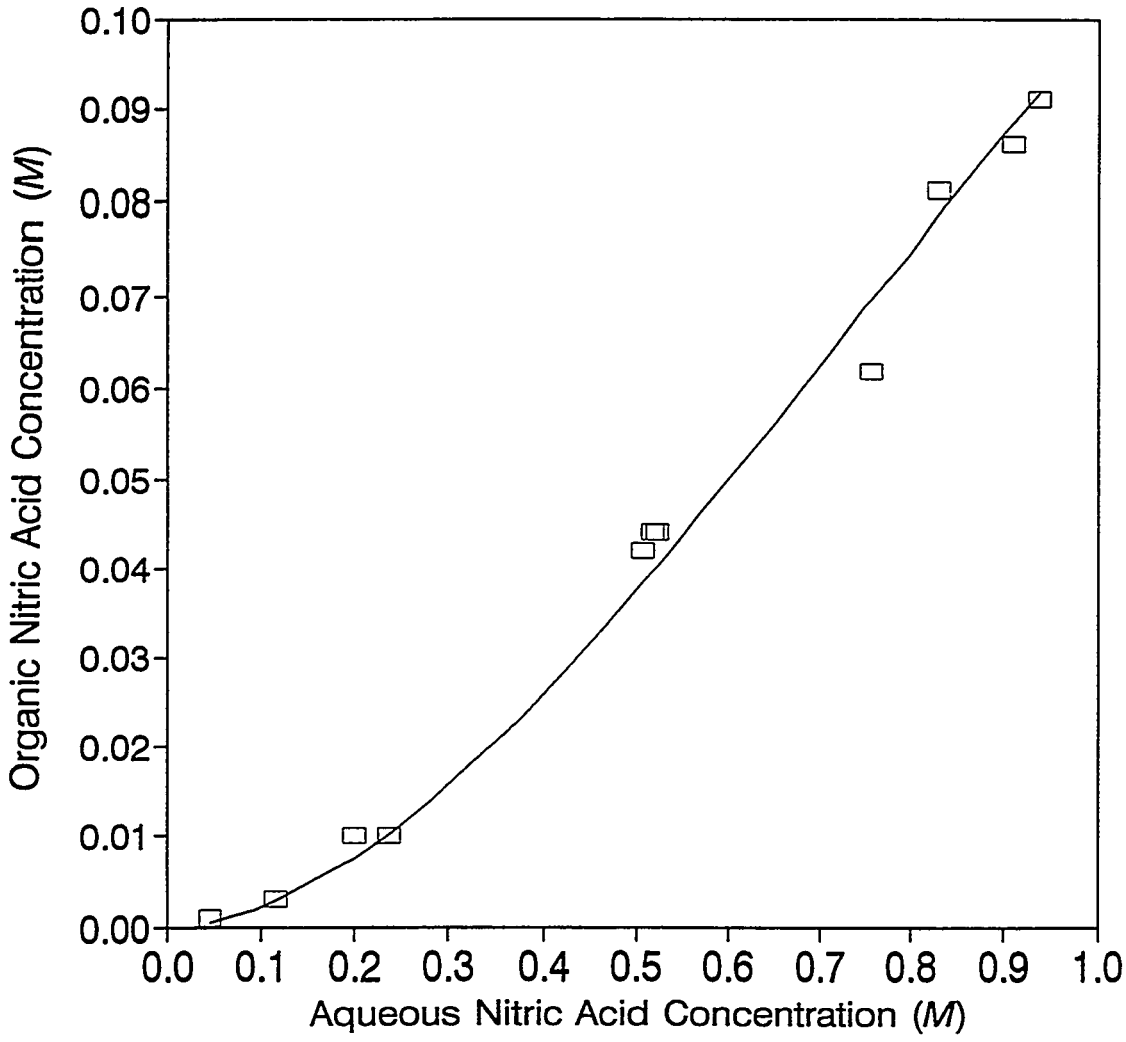

Figure 5.6. Comparison of the 1:1 stoichiometric-based model for extraction of nitric acid with the experimental data at 40°C.

gives the value of ΔH. According to Holman (1971), when a result is a known function of several independent variables,

$$y = y(x_1, x_2, x_3, \ldots, x_n) \quad , \tag{5-5}$$

the errors in the independent variables propagate to the result by

$$\sigma_y = \left[\left(\frac{\partial y}{\partial x_1} \sigma_1 \right)^2 + \left(\frac{\partial y}{\partial x_2} \sigma_2 \right)^2 + \ldots + \left(\frac{\partial y}{\partial x_n} \sigma_n \right)^2 \right]^{1/2} \quad . \tag{5-6}$$

Assuming that all the errors are in the K-values, the error in the left-hand side of Eq. (2-14) is given by

$$\sigma\left(\ln \frac{K_2}{K_1} \right) = \left[\left(\frac{1}{K_1} \sigma_{K_1} \right)^2 + \left(\frac{1}{K_2} \sigma_{K_2} \right)^2 \right]^{1/2} \quad . \tag{5-7}$$

The van't Hoff equation (illustrated in Figure 5.7), along with Eq. (5-7), gives $\Delta H = -5.46 \pm 0.46$ kcal/g-mol; thus, the reaction is slightly exothermic. At a temperature of 50°C, $K_{1:1}'$ is estimated to be 1.303. Figure 5.8 compares calculated and measured organic-phase nitric acid concentrations as a function of aqueous nitric acid concentration. The comparison is remarkably favorable, considering that the extrapolation is in the dimensions of both temperature and concentration. (The data point at 1.0 M aqueous nitric acid is a little low, as expected.) This is another indicator that the model is an adequate one.

5.2 Extraction of Uranyl Nitrate from Nitric Acid Media

Two classes of experiments were performed to obtain data to characterize the extraction of uranyl nitrate with CMPO. In one class of experiments, the nitric acid concentration and the

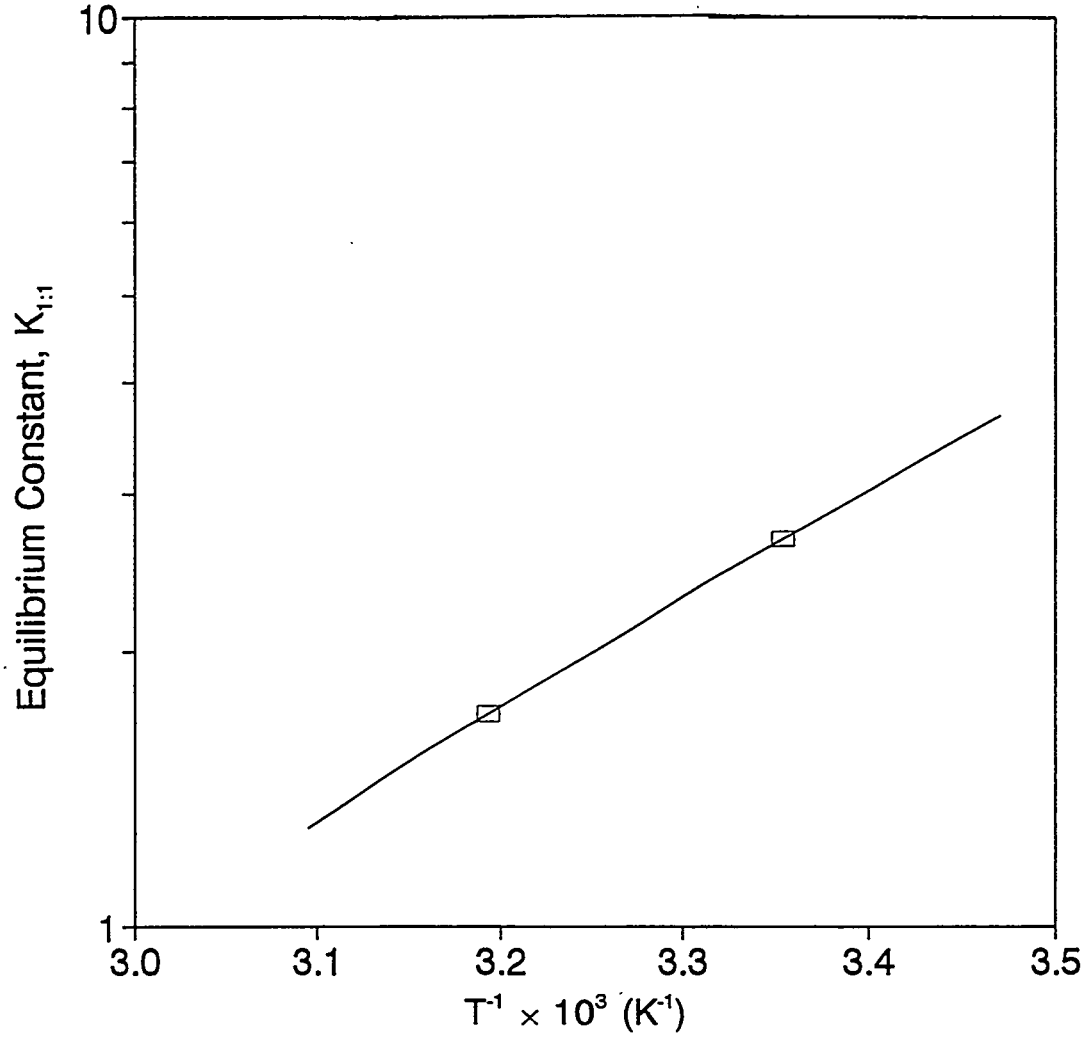

Figure 5.7. Extrapolation of measured equilibrium constants to 50°C.

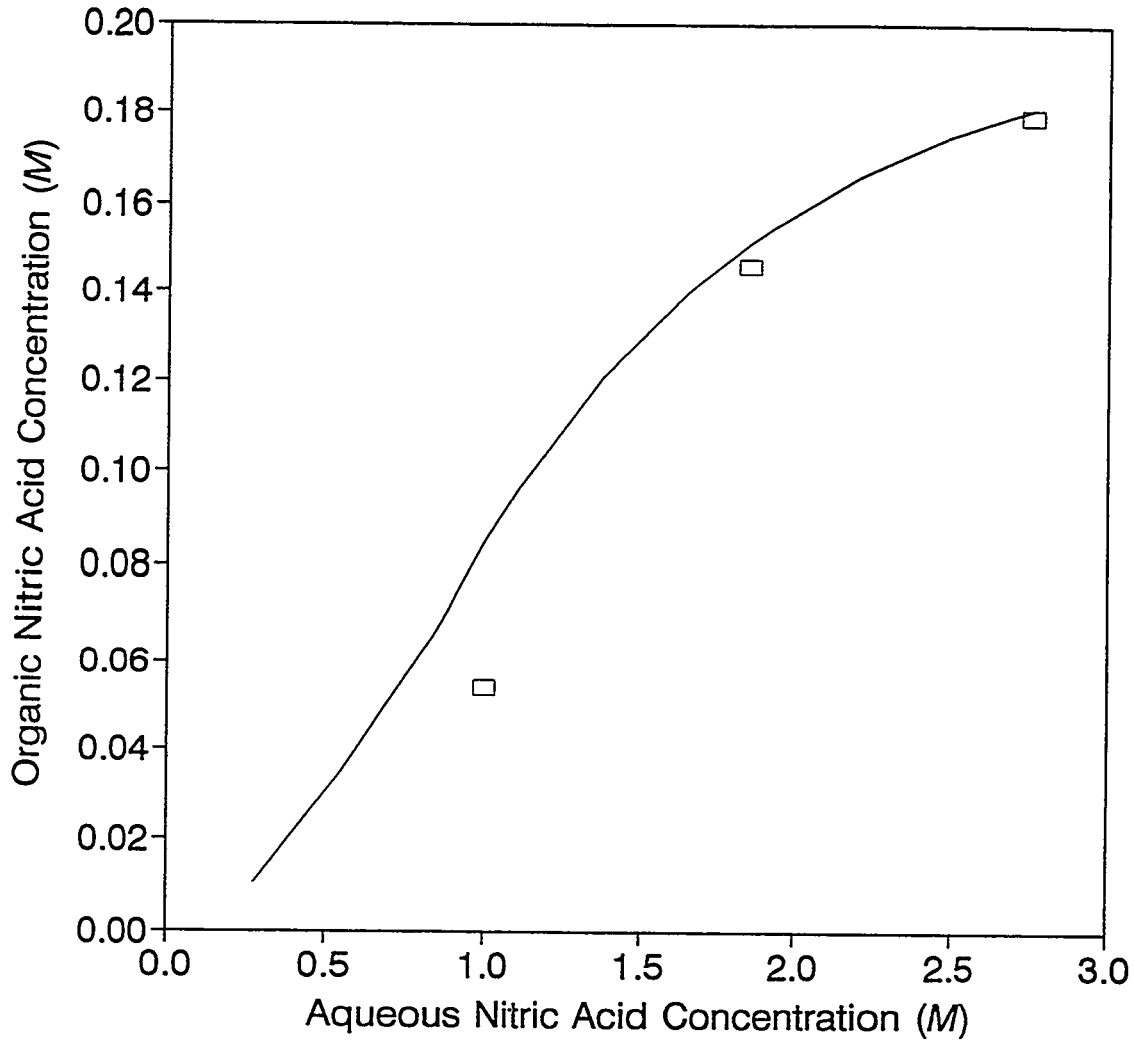

Figure 5.8. Comparison of the 1:1 stoichiometric-based model for extraction of nitric acid with the experimental data at 50°C, using the extrapolated equilibrium constant.

initial uranium concentration were made constant while the CMPO concentration was varied. These data support determination of the stoichiometry (or coordination number) of uranium extraction. In the second class of experiments, the CMPO concentration was constant while both the uranyl nitrate and the nitric acid concentrations were varied. Data from these experiments support determination of the equilibrium constant of the extraction as well as other necessary modeling parameters. Experiments in both classes were performed at temperatures of 25 and 40°C.

The original plan was to analyze all uranium samples using a liquid scintillation analyzer (essentially radiocounting). Interferences caused by the decay daughters of ^{233}U, as described in Sect. 3.4.4 and by Spencer (1994), resulted in the adoption of a back-extraction experimental method to reduce the interferences with radiocounting. To verify that the back-extraction method effectively eliminated the interferences, some samples were analyzed for ^{238}U concentration with an ICP-MS technique. Generally, both analytical methods gave the same results; however, the radiocounting method was more repeatable.

5.2.1 Approximate Regions of Third-Phase Formation

The phenomenon of third-phase formation for uranyl nitrate–CMPO complexes is very much the same as that of nitric acid, described in Sect. 5.1.1. Limited solubility of the CMPO-nitrate complex in *n*-dodecane results in a CMPO-rich phase. As discussed in Sect. 3, extraction experiments with metal nitrates were performed with organic that had been preequilibrated with pure nitric acid having the same concentration as the metal nitrate-bearing aqueous used in the final contact. Experimentally, solutions having constant nitric acid concentrations and increasing uranyl nitrate concentrations were prepared. The third-phase region was bracketed when one sample exhibited no third phase, and then the sample of next highest concentration did develop a third phase. The range of nitric acid and uranyl nitrate concentrations wherein a third phase

forms is listed in Table 5.8. The third phase, which was a deep yellow color, appeared at the interface of the bulk aqueous and organic phases. Even small quantities of the third phase were readily visible because of the color. Formation of a third phase was also signaled by long-lived cloudiness of the organic phase. At each condition of temperature and nitric acid concentration, the lower value of uranyl nitrate concentration listed in Table 5.8 is the highest concentration tested where a third phase did not form and, therefore, represents the upper limit of concentration used in the experimental program. To avoid third-phase difficulties, the uranyl nitrate concentrations were restricted to quite low values. If, for example, the distribution ratio is 100:1, only about 1% of the uranium remains in the aqueous phase. Equilibrium concentrations in the aqueous are, therefore, very small.

Table 5.8. Concentration ranges of uranyl nitrate in nitric acid resulting in third-phase formation

Temperature (°C)	Nitric acid concentration (*M*)	Initial uranyl nitrate concentration[a] (*M*)
25.0	0.020	0.005, *b*
25.0	0.100	0.002–0.005
25.0	0.200	0.001–0.002
40.0	0.020	0.005, *b*
40.0	0.100	0.005–0.010
40.0	0.200	0.002–0.005

[a]Uranyl nitrate concentration in aqueous phase before contact with an organic phase preequilibrated with pure nitric acid of the given concentration.

[b]No attempt was made to cause a third phase because it was likely that the uranium concentration need not be much higher than the listed value.

5.2.2 Stoichiometry by Slope Analysis

Distribution data derived from experiments with varying organic CMPO concentrations, a fixed aqueous nitric acid concentration, and a nearly fixed uranyl nitrate concentration are summarized in Tables 5.9 and 5.10. The raw data are included in Appendix D.

Table 5.9 lists the data obtained from radiocounting analyses. The initial uranyl nitrate concentration was 0.001 *M* in the forward-extraction. Because some uranium was left in the aqueous phase of the forward-extraction, the uranium carried in the organic phase to the back-extraction was slightly lower. The fraction carried to the back-extraction is simply the ratio of the measured count rate of the organic phase to the count rate of the aqueous feed. The equilibrium distribution ratio is obtained from the back-extraction experiments. It is simply the ratio of the count rates of the organic phase to those of the aqueous phase,

Table 5.9. Radiocounting measurements of equilibrium distribution ratios supporting slope analysis for the extraction of uranyl nitrate

CMPO (*M*)	HNO_3 (*M*)	U × 10^3 (*M*)[a]	*D*	σ_D[b]	Data pair
At 25°C					
0.200	0.100	0.970	79.06	10.48	D-29-13/14
0.200	0.100	0.958	71.93	0.975	D-31-13/14
0.200	0.100	0.958	75.25	0.781	D-31-15/16
0.100	0.100	0.937	29.32	0.552	D-31-17/18
0.100	0.100	0.934	27.76	0.433	D-31-19/20
0.050	0.100	0.877	9.107	0.082	D-31-21/22
0.050	0.100	0.876	9.219	0.052	D-31-23/24
At 40°C					
0.200	0.100	0.961	44.36	0.206	D-30-15/16
0.200	0.100	0.951	44.20	0.072	D-32-13/14
0.200	0.100	0.956	42.27	0.165	D-32-15/16
0.100	0.100	0.913	15.14	0.268	D-32-17/18
0.100	0.100	0.915	15.32	0.324	D-32-19/20
0.050	0.100	0.802	4.649	0.032	D-32-21/22
0.050	0.100	0.805	4.681	0.012	D-32-23/24

[a]Initial uranyl nitrate concentration before final phase contact.

[b]Standard deviation of distribution ratio based on radiocounting of two samples.

Table 5.10. ICP-MS measurements of equilibrium distribution ratios supporting slope analysis for the extraction of uranyl nitrate

CMPO (*M*)	HNO_3 (*M*)	U × 10^3 (*M*)[a]	*D*	Data pair
At 25°C				
0.200	0.100	1.000	43.3	D-17-01/02
0.200	0.100	1.000	54.1	D-17-03/04
0.100	0.100	1.000	28.1	D-17-05/06
0.100	0.100	1.000	29.0	D-17-07/08
0.050	0.100	1.000	10.6	D-17-09/10
0.050	0.100	1.000	10.0	D-17-11/12
At 40°C				
0.200	0.100	1.000	44.2	D-18-01/02
0.200	0.100	1.000	50.0	D-18-03/04
0.100	0.100	1.000	15.5	D-18-05/06
0.100	0.100	1.000	17.0	D-18-07/08
0.050	0.100	1.000	5.33	D-18-09/10
0.050	0.100	1.000	4.69	D-18-11/12

[a]Initial uranyl nitrate concentration before phase contact.

$$D = \frac{\mathbb{C}_{org}}{\mathbb{C}_{aq}}, \tag{5-8}$$

where $\mathbb{C}$ is the measured count rate, in disintegrations per minute per milliliter (dpm/mL). Because two samples of each phase were collected for scintillation analysis, an average count rate and associated standard deviation are reported as part of the raw data in Appendix D. The standard deviation in the computed distribution ratio is found by applying Eq. (5-6) to Eq. (5-8) and results in

$$\sigma_D = \left[\left(\frac{1}{\mathbb{C}_{aq}}\sigma_{org}\right)^2 + \left(\frac{\mathbb{C}_{org}}{\mathbb{C}_{aq}^2}\sigma_{aq}\right)^2\right]^{1/2}. \tag{5-9}$$

Values calculated by Eq. (5-9) are also listed in Table 5.9. These deviations represent only the error in withdrawing and analyzing the sample, not the total experimental error. However, the values can be used to determine those points that have large sampling errors.

Table 5.10 lists the data obtained from ICP-MS analysis of the forward-extraction samples. These data compare favorably with those listed in Table 5.9. When the distribution ratio is less than ~50, the values obtained by the different analytical methods are within ~10% of each other. At higher distribution ratios, the differences become much greater.

Tables 5.9 and 5.10 contain results from replicate experiments from which the total experimental error is estimated. Average distribution ratios and associated standard deviations calculated for the two sets of data are shown in Table 5.11. This table also includes the percentage relative standard deviation, which is calculated by dividing the standard deviation by the mean and expressing the result as a percentage. The distribution ratios derived from the samples analyzed by radiocounting have lower deviations than those derived from samples analyzed by ICP-MS. Additionally, as shown in Appendix D, the radiocounting data deviate only ~1% from a closed material balance, whereas the ICP-MS data balance to within ~10%. Because of the high distribution ratios, a fair balance can be obtained by ignoring the aqueous phase. This emphasizes that (1) poor balances may indicate large errors in the calculated distribution ratio and (2) good balances do not guarantee small errors. Because the data obtained from radioanalysis are less prone to errors, these data are used to model extraction behavior and to estimate values describing the chemical characteristics of interest.

The uncorrected distribution ratios and CMPO concentrations listed in Table 5.9 are plotted in Figure 5.9. Linear regression of the data at 25°C gives a slope of 1.513 ± 0.007 with a correlation coefficient of 0.9985. Similar treatment of the data at 40°C gives a slope of 1.607 ± 0.002 with a correlation coefficient of 0.9994. Because the standard deviations listed in

Table 5.11. Estimated errors in uranium distribution ratios based on replicate experiments; comparison of two analytical techniques

CMPO (*M*)	HNO_3 (*M*)	U × 10^3 (*M*)	Average *D*	σ_D	RSD (%)
		Radiocounting data			
At 25°C					
0.200	0.100	0.962	75.41	3.57	4.73
0.100	0.100	0.936	28.54	1.10	3.87
0.050	0.100	0.876	9.16	0.08	0.86
At 40°C					
0.200	0.100	0.956	43.61	1.16	2.67
0.100	0.100	0.914	15.23	0.13	0.84
0.050	0.100	0.804	4.665	0.022	0.48
		ICP-MS data			
At 25°C					
0.200	0.100	1.000	48.7	7.6	15.7
0.100	0.100	1.000	28.6	0.64	2.23
0.050	0.100	1.000	10.3	0.42	4.12
At 40°C					
0.200	0.100	1.000	47.1	4.10	8.71
0.100	0.100	1.000	16.3	1.06	6.53
0.050	0.100	1.000	5.01	0.45	9.03

Table 5.9 are used in the analysis, the standard deviations in the calculated slopes are small. The deviations inferred from replicate samples are about ten times larger (see Table 5.11), so the deviations in the values of the slope are about 0.07 and 0.02 for 25 and 40°C, respectively. In either case, the results suggest that uranyl nitrate is extracted with both 1:1 and 2:1 stoichiometries.

The distribution ratio can be corrected for aqueous-phase deviations from ideality as shown by Eq. (4-42). From the literature review, the expected coordination number is 2; thus, Eqs. (4-47) and (4-50) can be combined to calculate the free CMPO concentration,

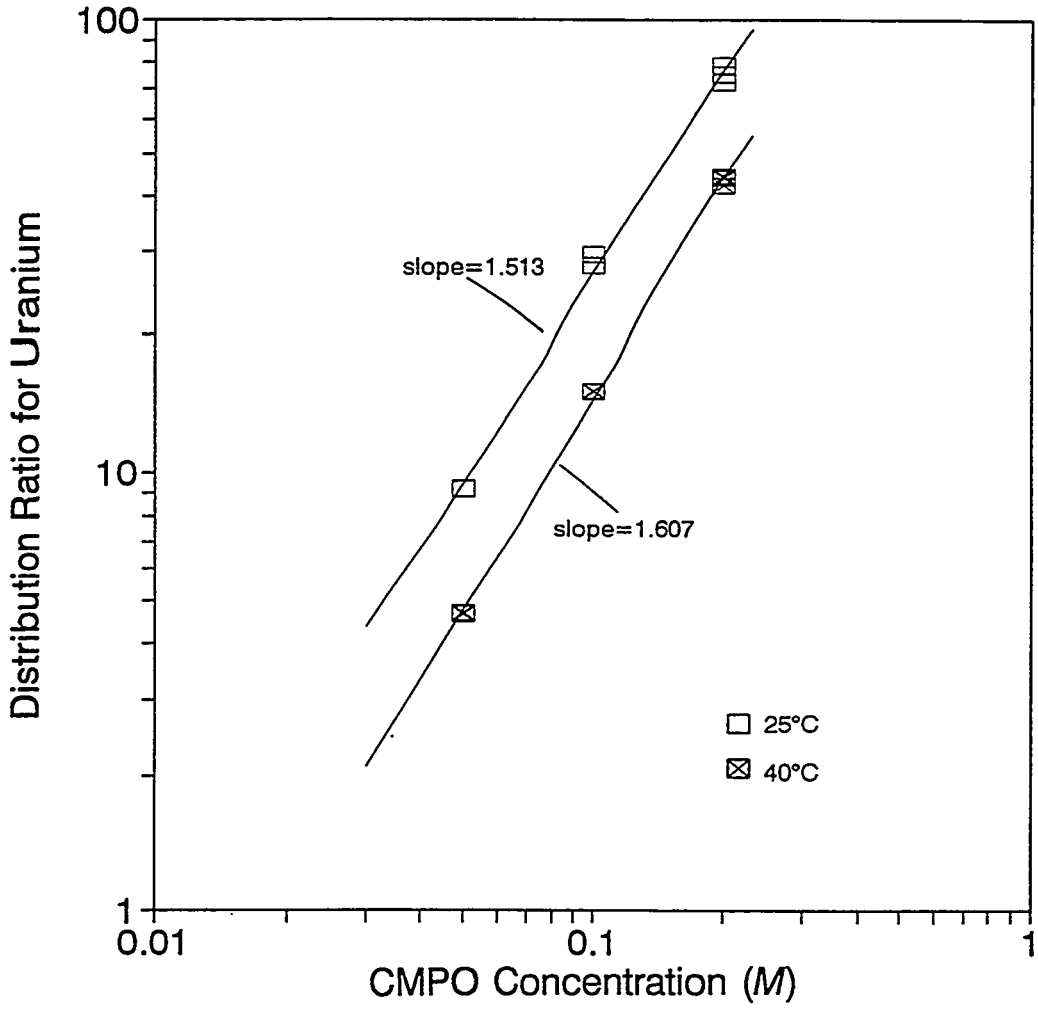

Figure 5.9. Slope-analysis determination of the extraction stoichiometry for uranyl nitrate.

$$[CMPO] = \frac{[CMPO]_0 - 2[U]_{org}}{1 + K'_{1:1}\left(\gamma^{(c)}_{\pm,HNO_3}\right)^2 [H^+][NO_3^-]} \quad , \tag{5-10}$$

which accounts for the CMPO consumed by both the uranyl nitrate and the nitric acid. When the equilibrated phases are of equal volume, the organic- and aqueous-phase uranyl nitrate concentrations are calculated from the initial uranyl nitrate concentration and the distribution ratio by

$$[U]_{aq} = \frac{[U]_{initial}}{D+1} \tag{5-11}$$

and

$$[U]_{org} = \frac{D[U]_{initial}}{D+1} = D[U]_{aq} \quad . \tag{5-12}$$

Table 5.12 lists the calculated values of the pertinent quantities. The aqueous uranyl nitrate concentration is very low, ranging from ~1.0×10^{-5} to ~1.5×10^{-4} *M*. The density of the aqueous phase approaches 1.0 in all cases. The activity coefficients of the nitric acid and the uranyl nitrate differ appreciably from unity, but are nearly constant over the range of the data. The activity of water in these solutions is close to unity and is also nearly constant. Consumption of the CMPO ranges up to only ~4%. Because no information is available on organic-phase activity coefficients, it is necessary to assume that activity coefficients of organic-phase species are unity. Now the slope-analysis method can be applied using D' and the free CMPO concentration in place of the uncorrected values. Linear regression analyses give slopes of 1.488 and 1.586 for data obtained at 25 and 40°C, respectively. Therefore, the corrections make no significant difference in the estimation of the coordination number by the slope-analysis method. It also means that any nonideal effects that impact the results, if they exist, lie with the organic phase.

Table 5.12. Uranium distribution ratios corrected for aqueous-phase nonidealities and free CMPO concentrations corrected for quantities consumed by uranyl nitrate and nitric acid

$U \times 10^5$ (M)	ρ_{aq} (g/mL)	$\gamma_{\pm, HNO_3}$	$\gamma_{\pm, UO_2(NO_3)_2}$	a_w	$[CMPO]_0$ (M)	$[CMPO]$ (M)	D_{U2}	D'_{U2}
At 25°C								
1.212	1.00041	0.79337	0.63276	0.99660	0.200	0.19482	79.06	305.74
1.314	1.00041	0.79336	0.63276	0.99660	0.200	0.19485	71.93	278.17
1.256	1.00041	0.79336	0.63276	0.99660	0.200	0.19485	75.25	291.01
3.090	1.00041	0.79334	0.63271	0.99659	0.100	0.09657	29.32	113.41
3.248	1.00042	0.79334	0.63271	0.99659	0.100	0.09658	27.76	107.38
8.677	1.00043	0.79326	0.63256	0.99659	0.050	0.04762	9.107	35.251
8.572	1.00043	0.79326	0.63257	0.99659	0.050	0.04762	9.219	35.684
At 40°C								
2.119	0.99553	0.78906	0.62304	0.99658	0.200	0.19603	44.36	179.69
2.104	0.99553	0.78906	0.62304	0.99658	0.200	0.19605	44.20	179.04
2.209	0.99553	0.78906	0.62303	0.99658	0.200	0.19604	42.27	171.23
5.657	0.99554	0.78901	0.62294	0.99658	0.100	0.09725	15.14	61.357
5.607	0.99554	0.78901	0.62294	0.99658	0.100	0.09725	15.32	62.086
14.20	0.99557	0.78888	0.62270	0.99658	0.050	0.04817	4.649	18.862
14.17	0.99557	0.78888	0.62270	0.99658	0.050	0.04816	4.681	18.991

5.2.3 Degree of Nonideal Behavior of Organic Phase

It is reported in the literature by several authors (see Sect. 2.4.4) that CMPO extracts uranyl nitrate with a 2:1 stoichiometry. Little detail on how this was deduced is given, except that Kolarik and Horwitz (1988) report using slope analysis. It is noteworthy that nearly all experimental work reported in the literature used CMPO dissolved in a mixture of TBP and an inert diluent such as *n*-dodecane. The TBP acts as a phase modifier to permit higher solvent loading without forming a third phase. TBP is known to extract uranium in a 2:1 stoichiometry, but its effect on the activity coefficient of CMPO is unknown.

Data describing the extraction of uranium with only CMPO in *n*-dodecane are reported in Sect. 5.2.2. In addition, the slope-analysis method gives a well correlated straight-line fit to the data with a slope of –1.5. If it is assumed that the true stoichiometry is 2:1, then the organic phase must be quite nonideal. These conditions fit the assumptions for the type of analysis developed in Sect. 4.4. For the extraction of uranyl nitrate from nitric acid by CMPO with a coordination number of 2, Eq. (4-106) may be written as

$$\ln d_{U2} \equiv \ln\left\{\frac{D'_{U2}}{\left[NO_3^-\right]^2\left[CMPO\right]^2}\right\} = \omega\left[CMPO\right] + \ln K_{U2} \quad , \tag{5-13}$$

where the subscript $U2$ is a reminder of the assumed true stoichiometry. Values for D'_{U2} and $[CMPO]$ are given in Table 5.12. The nitric acid concentration for the experiments under discussion is 0.10 *M*, and the uranyl nitrate concentration is so low that its contribution to the total nitrate concentration may be safely ignored.

Use of the solvent slope-analysis method is illustrated in Figure 5.10. Values for the slope and intercept of Eq. (5-13) are given by linear regression and are listed in Table 5.13.

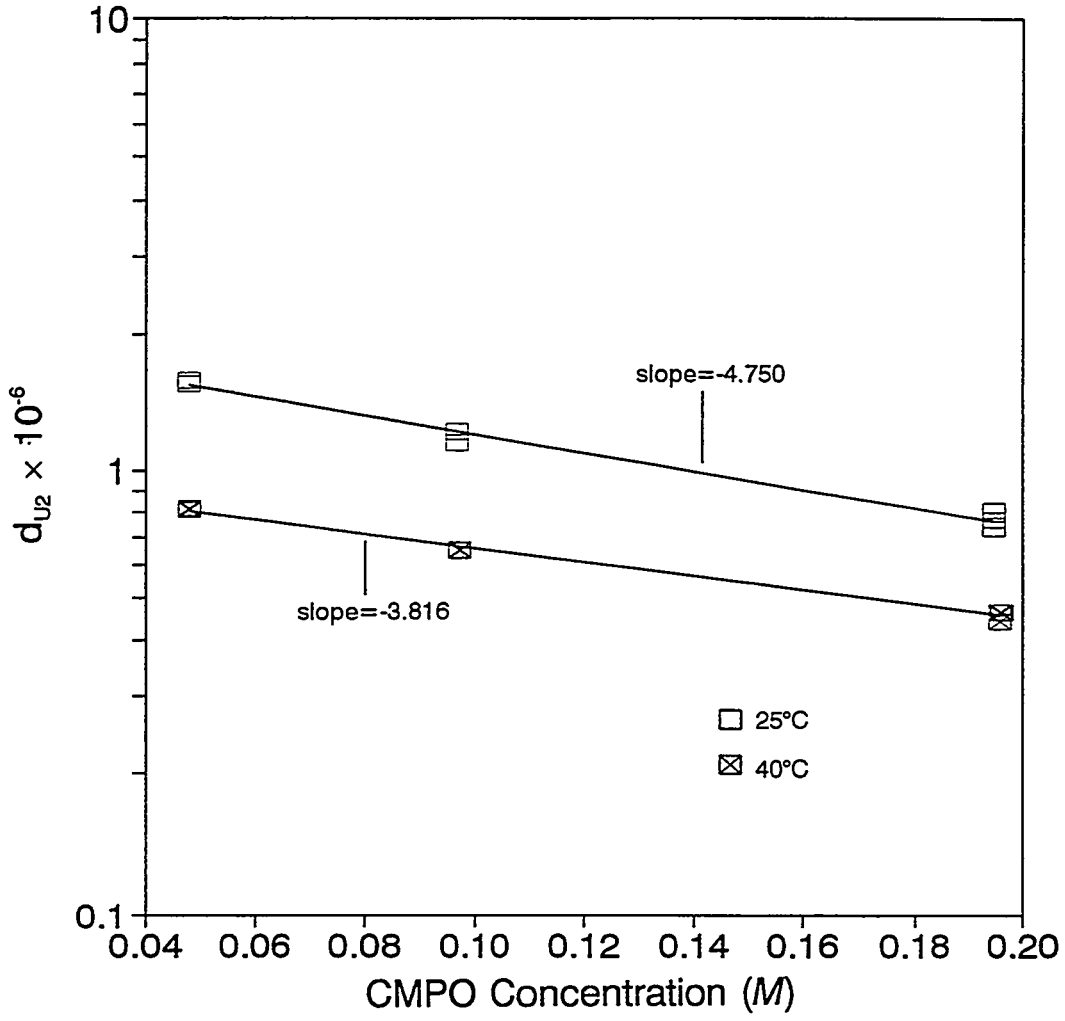

Figure 5.10. Solvent slope-analysis method for the extraction of uranyl nitrate with CMPO–*n*-dodecane.

Table 5.13. Solvent slope-analysis results for the extraction of uranyl nitrate

Temperature (°C)	ω	K_{U2}	Correlation coefficient
25.0	–4.750	1.925×10^6	–0.9935
40.0	–3.816	9.665×10^5	–0.9965

The correlation coefficient indicates that the data are highly correlated to a straight line with a negative slope. Values of the organic-phase activity coefficient ratio are given by combining Eqs. (4-94) and (4-103), which applied to the case at hand results in

$$\mathbb{R} = \frac{\left(\gamma^{(c)}_{CMPO}\right)^2}{\gamma^{(c)}_{UO_2(NO_3)_2 \cdot 2CMPO}} = e^{\omega[CMPO]} \quad . \tag{5-14}$$

When the CMPO concentration is 0.20 *M*, values of $\mathbb{R}$ are 0.3868 and 0.4661 at temperatures of 25 and 40°C, respectively. If the activity coefficient of free CMPO were the same as that reported by Diamond et al. (1986) for CMPO in toluene (i.e., ~0.92), then the activity coefficient of the disolvate would be ~2.2 at a temperature of 25°C.

The equilibrium constant for the extraction of uranium is given by the intercept of the solvent slope-analysis equation. The intercept corresponds with the traditional equilibrium quotient at infinite dilution of the extractant (in this case, CMPO). Computed values of the equilibrium constant shown in Table 5.13 are quite large. Values of the equilibrium constants that include effects of organic-phase nonideality, K'_{U2}, may be found by multiplying $\mathbb{R}$ by K_{U2}. At a free CMPO concentration of 0.20 *M*, the values of K'_{U2} are 7.445×10^5 and 4.506×10^5 at temperatures of 25 and 40°C, respectively. These values are compared with values calculated by other techniques in Sect. 5.2.4.

5.2.4 Determination of Thermodynamic Equilibrium Constants

Experiments were performed to measure the distribution ratio of uranium with varying aqueous-phase uranyl nitrate and nitric acid concentrations. To avoid third-phase difficulties, the concentrations were limited to low values, as already discussed. In these experiments, the organic-phase concentration of CMPO in *n*-dodecane was fixed at 0.20 *M*.

Data obtained through the use of radiocounting analysis are listed in Tables 5.14 and 5.15 for experiments performed at 25 and 40°C, respectively. As discussed in Sect. 5.2.2, the listed standard deviations only include the effects of sample withdrawal and counting errors. Total experimental error may be estimated from the data contained in the tables on replicate

Table 5.14. Distribution data derived from radiocounting analysis for the extraction of uranyl nitrate from nitric acid solutions with 0.20 *M* CMPO in *n*-dodecane at 25°C

HNO_3 (*M*)	U × 10^3 (*M*)[a]	*D*	σ_D[b]	Data pair
0.020	2.17	7.990	0.135	D-33-11/12
0.020	0.870	7.448	0.305	D-33-13/14
0.020	0.428	7.388	0.121	D-33-15/16
0.020	0.212	7.268	0.179	D-33-17/18
0.020	0.0856	7.321	0.299	D-33-19/20
0.020	1.73	7.517	0.097	D-33-23/24
0.100	1.193	78.12	4.66	D-29-11/12
0.100	0.970	79.06	10.48	D-29-13/14
0.100	0.390	76.19	7.04	D-29-15/16
0.100	0.195	78.33	4.29	D-29-17/18
0.100	0.0485	74.01	0.42	D-29-19/20
0.100	0.958	71.93	0.975	D-31-13/14
0.100	0.960	75.25	0.781	D-31-15/16
0.200	0.970	154.2	0.64	D-27-15/16
0.200	0.487	163.3	15.10	D-27-17/18
0.200	0.241	151.1	0.75	D-27-19/20
0.200	0.0967	143.0	8.23	D-27-21/22
0.200	0.0483	146.8	8.42	D-27-23/24
0.200	0.967	144.0	4.11	D-26-11/12
0.200	0.242	151.0	2.11	D-26-13/14
0.200	0.0484	151.5	4.39	D-26-15/16

[a]Initial uranyl nitrate concentration before phase contact.

[b]Standard deviation of distribution ratio based on radiocounting of two samples from each phase.

Table 5.15. Distribution data derived from radiocounting analysis for the extraction of uranyl nitrate from nitric acid solutions with 0.20 *M* CMPO in *n*-dodecane at 40°C

HNO_3 (*M*)	U × 10^3 (*M*)[a]	*D*	σ_D[b]	Data pair
0.020	3.97	4.433	0.032	D-34-13/14[c]
0.020	1.96	4.268	0.098	D-34-15/16[c]
0.020	0.779	3.762	0.143	D-34-17/18
0.020	0.381	3.673	0.014	D-34-19/20
0.020	0.191	3.479	0.018	D-34-21/22
0.020	0.0761	3.578	0.076	D-34-23/24
0.100	4.69	41.92	1.160	D-30-11/12
0.100	1.91	44.30	0.252	D-30-13/14
0.100	0.961	44.36	0.206	D-30-15/16
0.100	0.481	42.31	1.360	D-30-17/18
0.100	0.0957	42.11	0.388	D-30-19/20
0.100	0.951	44.20	0.072	D-32-13/14
0.100	0.956	42.27	0.165	D-32-15/16
0.200	1.92	101.2	5.51	D-28-13/14
0.200	0.957	103.1	0.78	D-28-15/16
0.200	0.481	99.38	0.453	D-28-17/18
0.200	0.240	98.69	3.127	D-28-19/20
0.200	0.0970	103.2	0.58	D-28-21/22
0.200	0.0481	88.57	7.768	D-28-23/24
0.200	1.92	103.2	6.13	D-25-01/02
0.200	0.964	109.3	7.02	D-25-03/04
0.200	0.483	110.8	10.80	D-25-05/06
0.200	0.242	107.6	6.22	D-25-07/08
0.200	0.0964	102.4	3.12	D-25-09/10
0.200	0.0483	107.5	1.76	D-25-11/12

[a]Initial uranyl nitrate concentration before phase contact.

[b]Standard deviation of distribution ratio based on radiocounting of two samples from each phase.

[c]Mildly cloudy aqueous phase; distribution ratio may contain large error. These points were not used in developing models.

experiments. Average distribution ratios and their standard deviations calculated from replicate experiments are summarized in Table 5.16. The percentage relative standard deviation is also listed in the table. Examination of the data in these tables reveals that (1) the distribution ratio varies strongly with acid concentration; (2) at a fixed acid concentration, the distribution ratio shows little, if any, variation with uranyl nitrate concentration (but this is a narrow range of

Table 5.16. Estimated errors in uranium distribution ratios derived from radiocounting analysis of replicate experiments

HNO_3 (M)	$U \times 10^3$ (M)	Average D	σ_D	RSD (%)
At 25°C				
0.100	0.963	75.41	3.57	4.73
0.200	0.0484	149.9	3.32	2.22
0.200	0.242	151.1	0.07	0.04
0.200	0.969	149.1	7.21	4.84
At 40°C				
0.100	0.956	43.61	1.16	2.66
0.200	0.0482	98.04	13.39	13.7
0.200	0.0967	102.8	0.57	0.55
0.200	0.241	103.2	6.30	6.11
0.200	0.482	105.1	8.07	7.68
0.200	0.961	106.2	4.38	4.12
0.200	1.92	102.2	1.41	1.38

concentration); and (3) the average error over the entire data set is ~5%. Additional distribution data for uranyl nitrate were obtained from experiments in which the samples were analyzed by ICP-MS. These data, which are shown in Table 5.17, verify the magnitude of distribution ratios developed from radiocounting analysis. However, the variability of the distribution ratios is much greater, especially when the distribution ratio is large. Again, these data are valuable as a verification tool but, because of the greater scatter, are not considered in the detailed modeling.

The data are fit to the models developed in Sect. 4.2.2 by nonlinear regression. To estimate the general effects of nitric acid concentration and temperature, the data are first subdivided into groups where the nitric acid concentration and temperature are constant. Then they are fit to one-parameter models representing formation of the disolvate and solvate [equilibria shown in Eqs. (4-36) and (4-53), respectively]. The equilibrium constant is the regression parameter. Quantities also calculated include the standard deviation of the model parameter,

Table 5.17. Distribution data derived from ICP-MS analysis for the extraction of uranyl nitrate from nitric acid solutions with 0.20 *M* CMPO in *n*-dodecane

HNO_3 (*M*)	U × 10^3 (*M*)[a]	*D*	Data pair
At 25°C			
0.020	2.00	8.60	D-19-03/04
0.020	0.500	7.36	D-19-07/08
0.020	0.200	7.29	D-19-09/10
0.020	0.100	7.20	D-19-11/12
0.100	2.00	88.9	D-21-01/02
0.100	0.500	78.2	D-21-05/06
0.100	0.200	67.3	D-21-07/08
0.100	0.100	38.9	D-21-09/10
0.100	0.050	40.5	D-21-11/12
0.200	1.00	133	D-23-03/04
0.200	0.500	84.0	D-23-05/06
0.200	0.100	66.7	D-23-09/10
At 40°C			
0.020	5.00	9.20	D-20-01/02
0.020	2.00	5.63	D-20-03/04
0.020	0.500	5.00	D-20-07/08
0.020	0.200	4.18	D-20-09/10
0.100	5.00	36.8	D-22-01/02
0.100	2.00	40.6	D-22-03/04
0.100	0.500	25.0	D-22-07/08
0.100	0.200	39.4	D-22-09/10
0.100	0.100	38.2	D-22-11/12
0.100	0.050	22.7	D-22-13/14
0.200	2.00	77.1	D-24-01/02
0.200	0.500	113	D-24-05/06
0.200	0.100	304	D-24-09/10

[a]Initial uranyl nitrate concentration before phase contact.

optimized values of the objective function (χ^2), the standard deviation between the data and the model, and the standard fractional deviation defined by

$$\sigma_f = \sqrt{\frac{\sum \left(\frac{experimental - model}{experimental} \right)^2}{n - p}} \quad . \tag{5-15}$$

The results are shown in Table 5.18. Values of χ^2 are much larger than the number of degrees of freedom, not because of a lack of fit but because the standard deviations in the sample analysis results do not include all experimental errors (as already discussed). The standard deviation of the model is larger when the distribution ratio is large. The standard fractional deviation, on the other hand, indicates a nearly constant deviation of the model of ~5%. The 1:1 stoichiometric model fits the data slightly better than the 2:1 stoichiometric model.

The most interesting aspect of the results shown in Table 5.18 concerns the equilibrium constants for the two extraction stoichiometries. First, the equilibrium constant, K'_{U2}, at 0.10 *M*

Table 5.18. One-parameter models of uranium extraction used for fixed nitric acid concentrations

Temp. (°C)	HNO_3 (*M*)	χ^2	σ	σ_f	Parameter	Deviation
					K'_{U2}	$\sigma_{K'U2}$
25.0	0.020	15.84	0.268	0.0349	1.041×10^6	8.39×10^3
25.0	0.100	12.67	4.052	0.0519	7.449×10^5	3.48×10^3
25.0	0.200	37.49	7.276	0.0487	5.262×10^5	1.63×10^3
40.0	0.020	65.47	0.110	0.0302	5.069×10^5	1.54×10^3
40.0	0.100	180.8	1.612	0.0380	4.626×10^5	6.46×10^2
40.0	0.200	50.58	6.477	0.0656	3.539×10^5	1.10×10^3
					K'_{U1}	$\sigma_{K'U1}$
25.0	0.020	9.463	0.195	0.0251	2.048×10^5	1.62×10^3
25.0	0.100	9.420	3.557	0.0456	1.458×10^5	6.77×10^2
25.0	0.200	21.52	6.895	0.0460	9.824×10^4	3.01×10^2
40.0	0.020	59.97	0.100	0.0275	1.010×10^5	3.06×10^2
40.0	0.100	152.0	1.387	0.0328	9.023×10^4	1.24×10^2
40.0	0.200	51.70	6.181	0.0625	6.769×10^4	2.10×10^2

HNO_3 and 25°C is 7.449×10^5 as compared with 7.445×10^5 estimated in Sect. 5.2.3 by the solvent slope-analysis method. At 40°C, the value in Table 5.18 is 4.626×10^5 as compared with 4.506×10^5 estimated by the solvent slope-analysis method. Remarkably, the values obtained by the different methods are within 4% of each other. Second, for both models given in Table 5.18, the equilibrium constant decreases with increasing nitric acid concentration and decreases with increasing temperature. The effect of nitric acid could be to increase the concentration of an inextractable nitrate complex. The decrease of K' with increasing temperature indicates an exothermic reaction.

The data are now divided into two groups according to the temperature at which the experiments were performed. Basically, this means that both the uranyl nitrate and the nitric acid concentrations vary in each group. The two groups of data are fit to various one-parameter and two-parameter models. Results are summarized in Table 5.19. As expected, the one-parameter model does not fit the entire data set well. The two-parameter model, which includes both 1:1 and 2:1 stoichiometries, does not fit the data well; and, in the unconstrained minimization, the equilibrium constant for 1:1 solvation assumes negative values that have no physical meaning. Because the initial CMPO concentration is not varied (except for the few points obtained for slope analysis) and because high solvent loadings are prohibited by third-phase formation, the free CMPO concentration at equilibrium conditions does not vary much. The effect on the regression of the data is to cause grouped parameters in mixed stoichiometric models [e.g., $K'_{U2}[CMPO]^2 + K'_{U1}[CMPO]$ in Eq. (4-61)] to behave as a single parameter. Models that include coextraction [equilibria shown by Eq. (4-37)] did not converge and, therefore, are not considered further.

Addition of a nitrate complexation equilibrium [Eq. (4-38)] to either a 1:1 or a 2:1 solvation model greatly improves the fit of that model to the data. The model for 2:1 solvation with nitrate complexation appears to be slightly better but cannot be distinguished statistically.

Table 5.19. Comparison of models describing the extraction of uranyl nitrate: model statistics, model parameters, and standard deviations of parameters

Temp. (°C)	χ^2	σ	σ_f	Parameter[a]	Standard deviation	Parameter[a]	Standard deviation
				K'_{U2}	$\sigma_{K'U2}$		
25.0	6,485	16.70	0.291	5.806×10^5	1.45×10^3		
40.0	9,410	17.89	0.195	4.434×10^5	5.24×10^2		
				K'_{U1}	$\sigma_{K'U1}$		
25.0	7,768	17.70	0.314	1.089×10^5	2.72×10^2		
40.0	11,410	19.72	0.209	8.620×10^4	1.01×10^2		
				K'_{U2}	$\sigma_{K'U2}$	K'_{U1}	$\sigma_{K'U1}$
25.0	3,162	16.39	0.219	3.215×10^6	4.25×10^4	-4.889×10^5	7.78×10^3
40.0	6,309	15.65	0.180	1.823×10^6	2.66×10^4	-2.647×10^5	5.05×10^3
				K'_{U1}	$\sigma_{K'U1}$	β_U	$\sigma_{\beta U}$
25.0	156.1	5.838	0.062	2.503×10^5	2.31×10^3	9.928	0.171
40.0	1,537	6.096	0.071	1.135×10^5	3.65×10^2	3.715	0.050
				K'_{U2}	$\sigma_{K'U2}$	β_U	$\sigma_{\beta U}$
25.0[b]	101.3	5.586	0.056	1.228×10^6	1.12×10^4	8.619	0.157
40.0[b]	1,513	5.992	0.071	5.655×10^5	1.80×10^3	3.249	0.048

[a]Negative equilibrium constants are not permitted since they may indicate "over-modeling" of data.

[b]Selected model.

Model deviations are reduced to the estimated error in the data, so additional parameters are not warranted. Because the slope-analysis results indicate a solvation number greater than 1 and because the 2:1 solvation is reported in the literature, the model including disolvate formation is selected.

The error estimates in the model parameters shown in Table 5.19 are low because the standard deviations in the experimental data do not include all aspects of experimental error, as discussed previously. This does not invalidate the results because all tested models are compared on an equal basis. The total experimental error is about 5.6 and 7.1% at 25 and 40°C, respectively, based on the values of standard fractional deviation listed in Table 5.19. Errors in the measured

distribution ratios are scaled to these percentages, and the regression is repeated for the selected model. The results are listed in Table 5.20. Values of the standard fractional deviations are about the same as those in Table 5.19. The χ^2 minimization parameter is close to the number of degrees of freedom, as it should be. The model parameters have changed slightly but are within their estimated standard deviations. Values of the standard deviations of model parameters are larger than those in Table 5.19 and are more reflective of the quality of the data.

The model is compared with the experimental data in Figures 5.11 through 5.14. In Figures 5.11 and 5.12, the organic-phase uranyl nitrate concentrations computed with the model are compared with experimental values at temperatures of 25 and 40°C, respectively. The data are reproduced quite well by the model. Figures 5.13 and 5.14 illustrate the variation of the distribution ratio with the aqueous uranyl nitrate concentration. The distribution ratio decreases slightly as the aqueous uranyl nitrate concentration increases.

In fitting the distribution data to the model, values of the nitrate complexation constant, β_U, for the uranyl ion are estimated. With these values, the aqueous-phase speciation of the uranyl nitrate can be estimated. For given nitric acid and uranyl nitrate concentrations, the total nitrate concentration is found from rearrangement of Eq. (4-68). The result is, then, back-substituted into Eq. (4-65) to obtain the concentration of $UO_2(H_2O)_6^{2+}$. The fraction of the aqueous uranyl nitrate in the $UO_2(H_2O)_6^{2+}$ form can be found by dividing both sides of Eq. (4-65) by the total aqueous

Table 5.20. Calculation of extraction model parameters, using more realistic error estimates

Temp. (°C)	$n-p^a$	χ^2	σ	σ_f	K'_{U2}	$\sigma_{K'U2}$	β_U	$\sigma_{\beta U}$
25.0	19	18.94	5.684	0.056	1.213×10^6	3.56×10^4	8.412	0.579
40.0	23	15.09	4.726	0.060	5.577×10^5	2.12×10^4	3.537	0.476

[a]The number of data points minus the number of parameters, $n-p$, is the number of degrees of freedom.

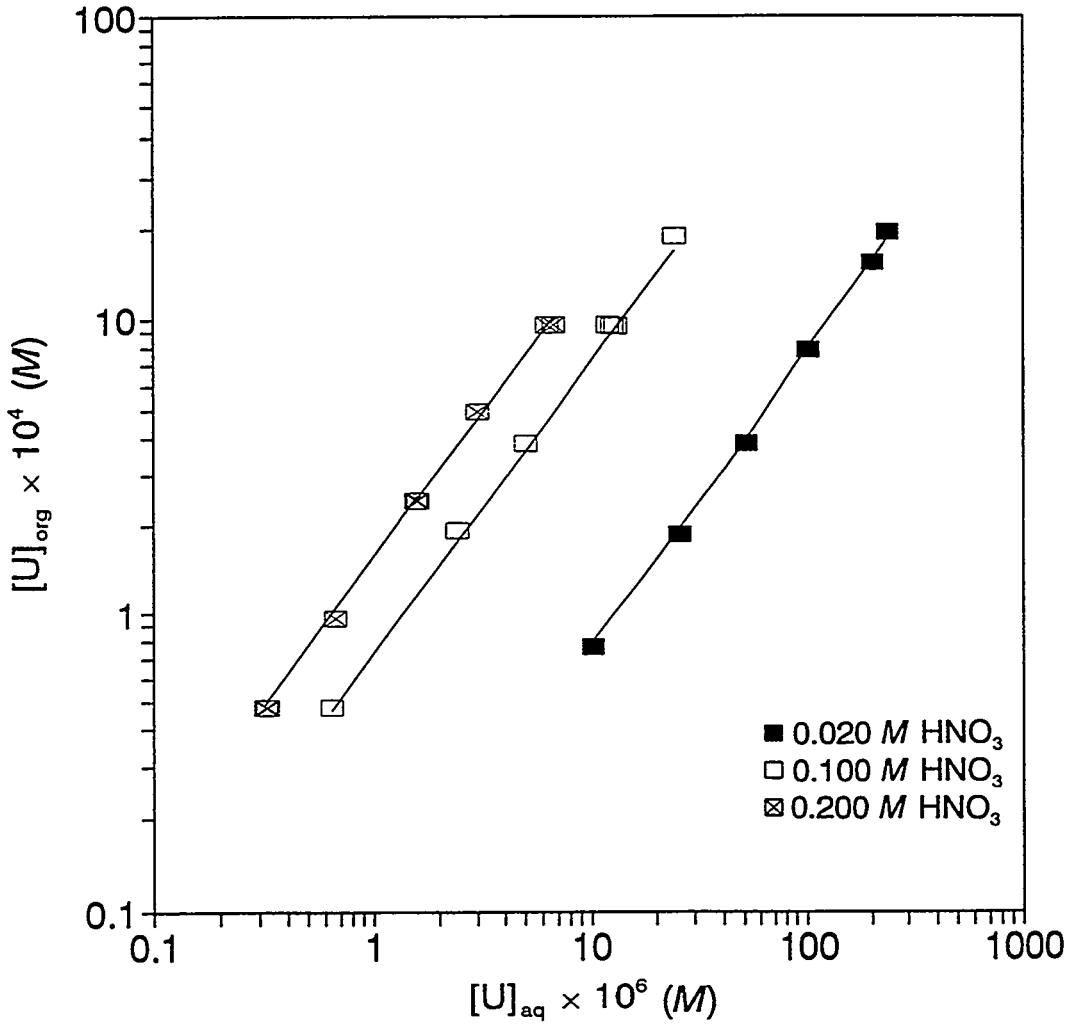

Figure 5.11. Variation of the organic-phase uranyl nitrate concentration with the aqueous-phase uranyl nitrate concentration at 25°C; comparison of experimental data with model.

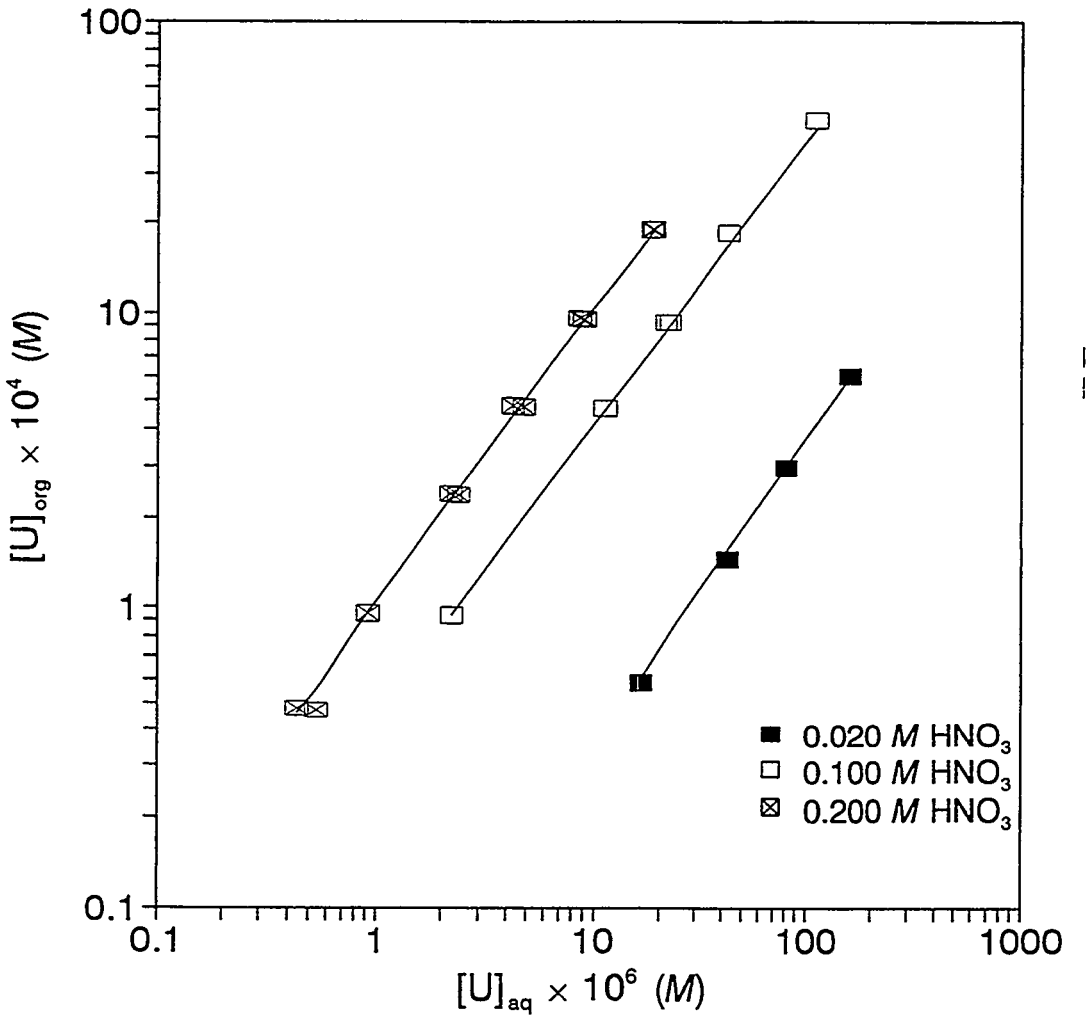

Figure 5.12. Variation of the organic-phase uranyl nitrate concentration with the aqueous-phase uranyl nitrate concentration at 40°C; comparison of experimental data with model.

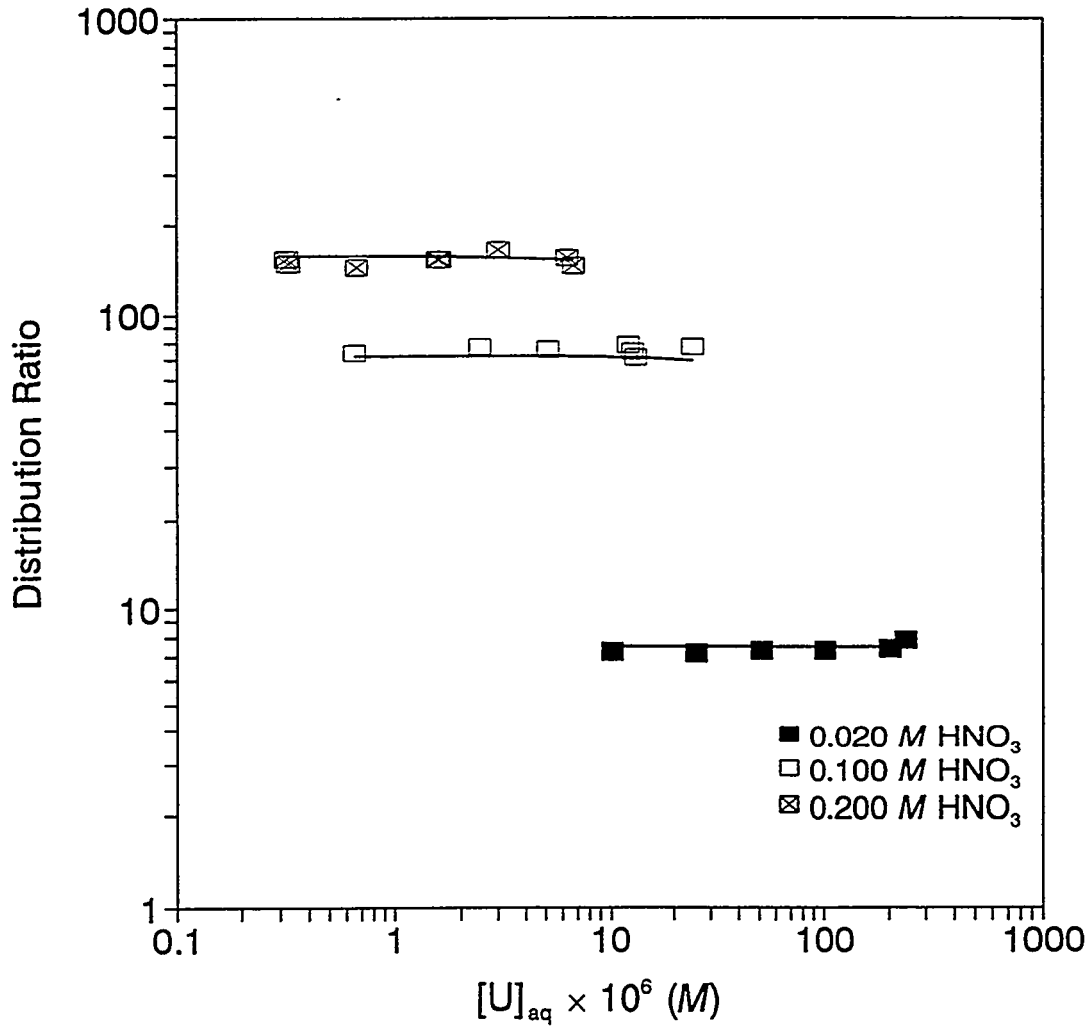

Figure 5.13. Variation of the distribution ratio of uranyl nitrate with the aqueous-phase uranyl nitrate concentration at 25°C; comparison of experimental data with model.

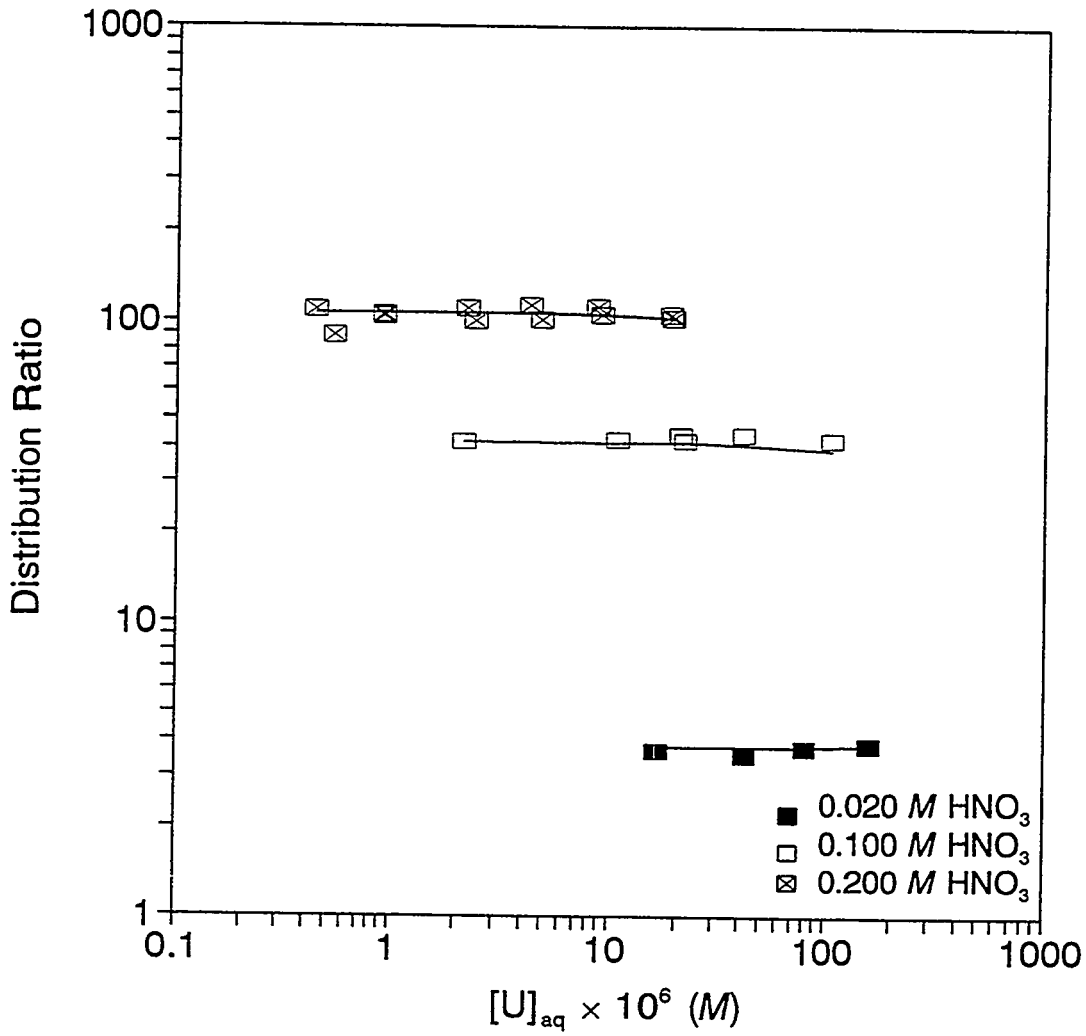

Figure 5.14. Variation of the distribution ratio of uranyl nitrate with the aqueous-phase uranyl nitrate concentration at 40°C; comparison of experimental data with model.

uranyl nitrate concentration. Results of calculations with a uranyl nitrate concentration of 10^{-4} *M* and nitric acid concentrations ranging from 0 to 1.0 *M* are plotted in Figure 5.15. As shown in the figure, the concentration of the uncomplexed uranyl ion decreases rapidly with increasing nitric acid concentration. Therefore, by difference, the inextractable nitrate complex increases in concentration. Increasing the temperature increases the uncomplexed uranyl ion concentration. Changes in nitric acid concentration and temperature have the expected effect on the ionization of uranyl nitrate in aqueous solution.

5.2.5 Enthalpy of Extraction

Equilibrium constants of the two equilibria describing the extraction of uranyl nitrate decrease with increasing temperature, indicating that the reactions are exothermic. With only two points, Eq. (2-6) is used directly to calculate the enthalpy of reaction and Eq. (5-7) is used to estimate the error in the result. For the extraction equilibrium shown in Eq. (4-36) and the nitrate complexation equilibrium shown in Eq. (4-38), $\Delta H = -9.610 \pm 0.594$ kcal/mol and $\Delta H = -10.72 \pm 1.87$ kcal/mol, respectively.

5.3 Extraction of Bismuth Nitrate from Nitric Acid Media

Two classes of experiments were performed to characterize the extraction of bismuth nitrate with CMPO in a manner parallel to the experiments performed with uranyl nitrate. In one class of experiments, the concentration of CMPO in the organic phase was varied while the aqueous-phase nitric acid and initial bismuth nitrate concentrations were fixed. These experiments support slope analysis to determine extraction stoichiometry. In the second class of experiments, the organic-phase CMPO concentration was fixed, while both the bismuth nitrate and nitric acid

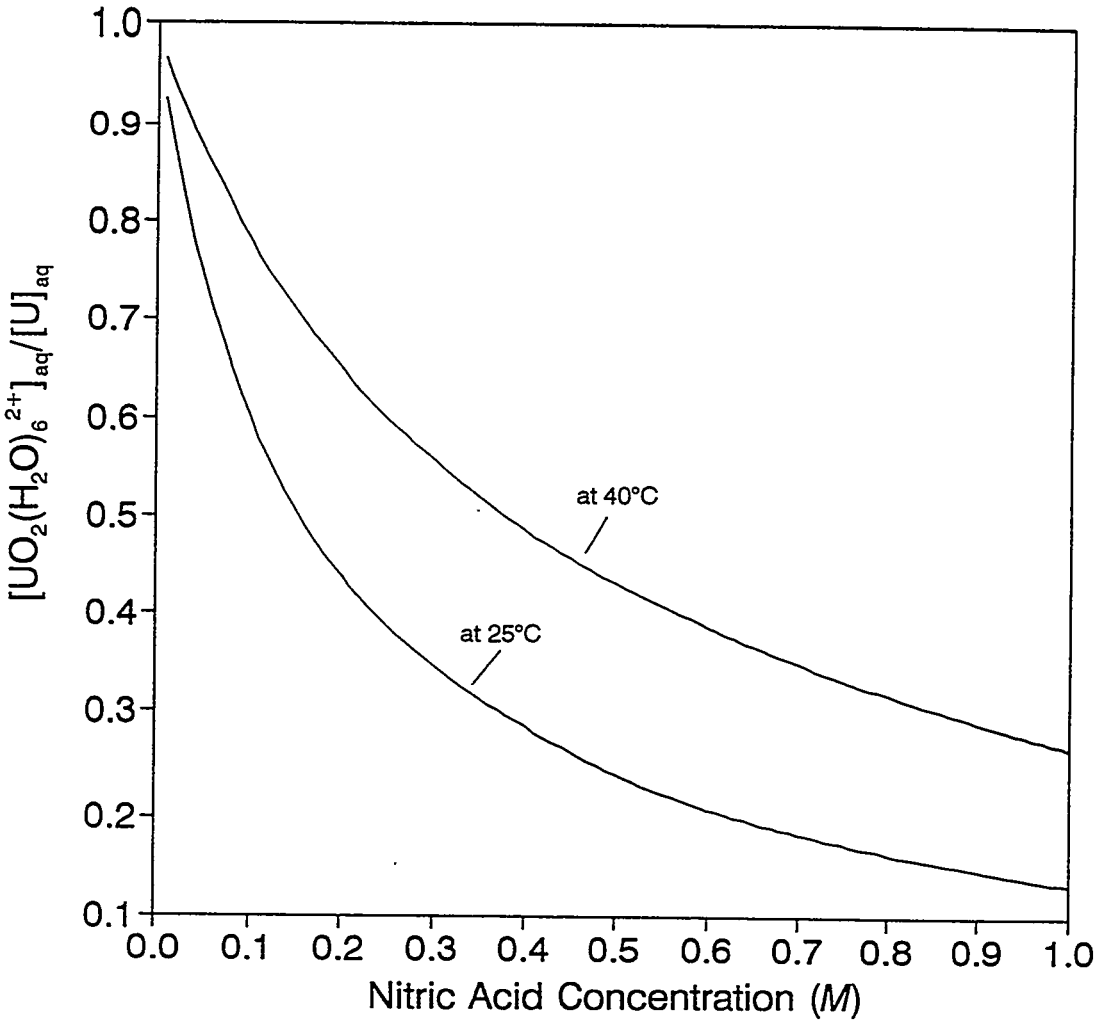

Figure 5.15. Effects of nitric acid concentration and temperature on the fraction of uncomplexed uranyl ion in aqueous solution.

concentrations were varied. These data support determination of the equilibrium constant. Both classes of experiments were performed at temperatures of 25 and 40°C.

Because there was no readily available supply of a radioactive isotope of bismuth, ICP-MS was used for all bismuth analyses. The raw data are tabulated in Appendix E.

5.3.1 Experimental Limits of Bismuth Nitrate Concentration

As previously discussed, the limited solubility of metal nitrate–CMPO complexes in the organic diluent leads to the formation of a third phase. Experiments were performed at 25°C with solutions having nitric acid concentrations of 0.20 *M* and various bismuth nitrate concentrations. When the initial bismuth nitrate concentration was 0.002 *M*, no third phase formed; but, at 0.005 *M* bismuth nitrate, a third phase was observed at the liquid-liquid interface. At a temperature of 40°C, an initial bismuth nitrate concentration of 0.005 *M* in 0.20 *M* nitric acid did not cause formation of a third phase. Decreasing the nitric acid concentration to 0.10 *M* eliminated the formation of third-phase material at 0.005 *M* bismuth nitrate and 25°C. However, at nitric acid concentrations of ~0.05 *M* or less, the bismuth nitrate precipitated from the aqueous solution. Of course, decreasing the bismuth nitrate concentration when decreasing the nitric acid concentration alleviated the latter problem. Essentially the two phenomena, third-phase formation and precipitation, bracketed the range of experimental conditions to narrow limits of concentration. Extraction experiments were performed at only two different nitric acid concentrations with maximum bismuth nitrate concentrations shown in Table 5.21. The experiments were conducted at 25 and 40°C.

When the third phase formed, it appeared at the liquid-liquid interface as a viscous, white, translucent film. To examine the third-phase formation further, one experiment was carried out with an initial bismuth concentration of 0.020 *M*. The results showed that a large quantity of third

Table 5.21. Maximum bismuth nitrate concentrations at each nitric acid concentration utilized for extraction tests

Temperature (°C)	Nitric acid concentration (*M*)	Initial bismuth nitrate concentration[a] (*M*)
25.0	0.100	0.005
25.0	0.200	0.002
40.0	0.100	0.005
40.0	0.200	0.005

[a]Bismuth nitrate concentration in aqueous phase before contact with an organic phase preequilibrated with pure nitric acid of the given concentration.

phase formed, as expected, but some of the material settled beneath the aqueous phase, while the remainder stayed at the liquid-liquid interface. Conditions favoring formation of the third phase were avoided during the extraction tests.

5.3.2 Stoichiometry by Slope Analysis

Measured distribution ratios for bismuth nitrate in systems with different CMPO concentrations are summarized in Table 5.22. The usual slope-analysis method of plotting the distribution ratio as a function of extractant concentration on log-log coordinates is illustrated in Figure 5.16. The data appear to be on a straight line. Values of the slopes of the lines are calculated by linear regression to be 1.560 ± 0.044 (correlation coefficient, 0.9986) at 25°C and 1.785 ± 0.022 (correlation coefficient, 0.9919) at 40°C. No data are available in the literature on the extraction stoichiometry of bismuth nitrate with CMPO with which to compare these results. The raw data may be corrected for CMPO usage and aqueous-phase nonidealities. Trivalent americium nitrate is reported to extract with a 3:1 stoichiometry; and, if valence state is the

Table 5.22. Measured distribution ratios for the extraction of bismuth nitrate at different CMPO concentrations

CMPO (*M*)	HNO_3 (*M*)	Bi × 10^3 (*M*)[a]	*D*	σ_D	Data pair
At 25°C					
0.200	0.100	1.00	146.9	6.4[b]	D-10-05/06
0.100	0.100	1.00	52.62	1.37	D-13-01/02
0.100	0.100	1.00	54.56	1.37	D-13-03/04
0.050	0.100	1.00	16.47	1.05	D-13-05/06
0.050	0.100	1.00	17.96	1.05	D-13-07/08
At 40°C					
0.200	0.100	1.00	44.57	1.24	D-11-01/02
0.200	0.100	1.00	42.82	1.24	D-11-03/04
0.100	0.100	1.00	16.94	0.44	D-14-01/02
0.100	0.100	1.00	16.32	0.44	D-14-03/04
0.050	0.100	1.00	3.765	0.121	D-14-05/06
0.050	0.100	1.00	3.594	0.121	D-14-07/08

[a]Initial bismuth nitrate concentration before final phase contact.
[b]Estimated; see Appendix E.

primary variable, then a 3:1 stoichiometry may be expected for bismuth nitrate. Assuming a 3:1 extraction stoichiometry and accounting for extraction of nitric acid, the free CMPO concentration can be found by combining Eqs. (4-50) and (4-83); thus,

$$[CMPO] = \frac{[CMPO]_0 - 3[Bi]_{org}}{1 + K'_{1:1}\left(\gamma^{(c)}_{\pm,HNO_3}\right)^2[H^+][NO_3^-]} \quad . \tag{5-16}$$

If the stoichiometry were 2:1, the free CMPO concentration could be obtained from

$$[CMPO] = \frac{[CMPO]_0 - 2[Bi]_{org}}{1 + K'_{1:1}\left(\gamma^{(c)}_{\pm,HNO_3}\right)^2[H^+][NO_3^-]} \quad . \tag{5-17}$$

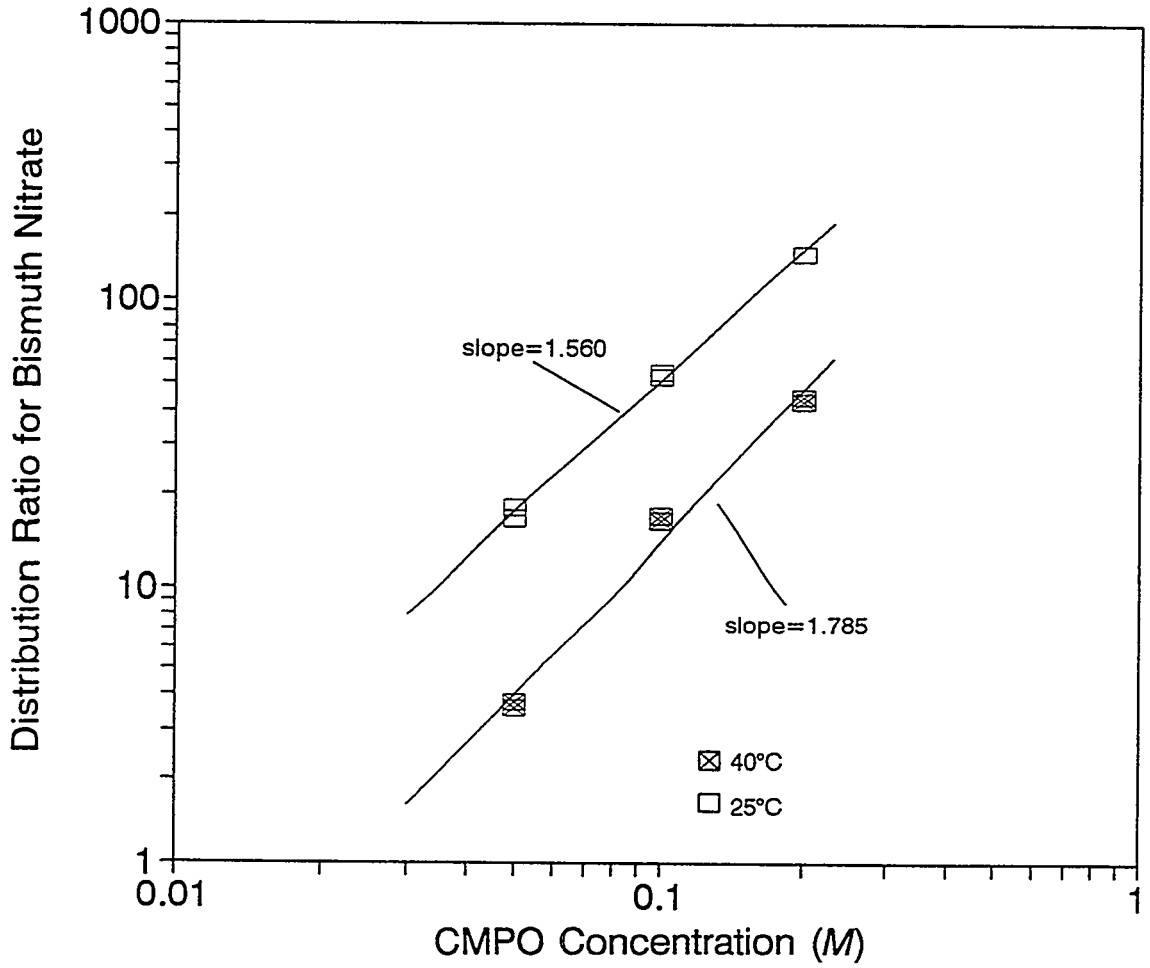

Figure 5.16. Slope-analysis determination of the extraction stoichiometry for bismuth nitrate.

The total nitrate concentration is given by Eq. (4-82), and the organic-phase bismuth concentration is computed from the initial bismuth feed concentration and the distribution ratio with equations analogous to Eq. (5-12).

Nonidealities in the aqueous phase are included by modifying the distribution ratio as shown by Eq. (4-78). Results of the calculations with intermediate quantities, including the mean stoichiometric activity coefficient of nitric acid, mean stoichiometric activity coefficient of bismuth nitrate, and the activity of water, are given in Table 5.23. These data show that the aqueous-phase activity coefficients are essentially constant, so the usual assumptions of the slope-analysis method are supported. With an assumed 3:1 stoichiometry, regression analysis on the data pairs D'_B and $[CMPO]_{B3}$ gives values of the slope of 1.509 (correlation coefficient, 0.9988) at 25°C and 1.735 (correlation coefficient, 0.9923) at 40°C. With an assumed 2:1 stoichiometry, regression on D'_B and $[CMPO]_{B2}$ gives values of the slope of 1.526 (correlation coefficient, 0.9988) and 1.749 (correlation coefficient, 0.9922) at 25 and 40°C, respectively. Therefore, accounting for aqueous-phase nonidealities and consumption of the CMPO does not significantly change the results. Slope analysis indicates that the solvation number of bismuth nitrate is about 1.6:1, suggesting a combination of two different stoichiometries (e.g., 1:1 and 2:1, or 1:1 and 3:1). The result is closer to a 2:1 stoichiometry than that found for uranyl nitrate by identical means. If the organic phase is very nonideal, these results may be considerably affected.

5.3.3 Degree of Nonideal Behavior of Organic Phase

It has been reported in the literature that trivalent americium is extracted by CMPO with a 3:1 stoichiometry. Assuming that valence is the primary variable, bismuth nitrate should extract with 3:1 stoichiometry; however, slope analysis indicates a coordination number of less than 2. If the organic phase were highly nonideal, the slope-analysis method could give erroneous results.

Table 5.23. Bismuth distribution ratios corrected for aqueous-phase nonidealities and free CMPO concentrations corrected for quantities consumed by bismuth nitrate and nitric acid

$Bi \times 10^6$ (M)	ρ_{aq} (g/mL)	$\gamma_{\pm, HNO_3}$	$\gamma_{\pm, Bi(NO_3)_3}$	a_w	$[CMPO]_0$ (M)	$[CMPO]_{B3}$ (M)	$[CMPO]_{B2}$ (M)	D_B	D'_B
At 25°C									
6.761	1.00041	0.79336	0.51437	0.99660	0.200	0.19378	0.19475	146.9	2063.1
18.65	1.00041	0.79333	0.51428	0.99660	0.100	0.09546	0.09642	52.62	739.51
18.00	1.00041	0.79333	0.51429	0.99660	0.100	0.09546	0.09642	54.56	766.75
57.24	1.00042	0.79322	0.51399	0.99659	0.050	0.04639	0.04732	16.47	231.99
52.74	1.00042	0.79324	0.51402	0.99659	0.050	0.04638	0.04731	17.96	252.91
At 40°C									
21.94	0.99553	0.78903	0.50697	0.99658	0.200	0.19499	0.19596	44.57	663.26
22.82	0.99553	0.78903	0.50696	0.99658	0.200	0.19499	0.19596	42.82	637.25
55.74	0.99554	0.78894	0.50671	0.99658	0.100	0.09614	0.09708	16.94	252.60
57.74	0.99554	0.78893	0.50670	0.99658	0.100	0.09615	0.09708	16.32	243.38
209.9	0.99559	0.78851	0.50556	0.99657	0.050	0.04713	0.04791	3.765	56.654
217.7	0.99560	0.78849	0.50550	0.99657	0.050	0.04715	0.04792	3.594	54.105

The solvent slope-analysis method (Sect. 4.4) provides a means of evaluating this possibility. For the extraction of bismuth nitrate from nitric acid by CMPO with a stoichiometry of 3:1, Eq. (4-106) may be written as

$$\ln d_{B3} \equiv \ln\left\{\frac{D_B'}{\left[NO_3^-\right]^3\left[CMPO\right]^3}\right\} = \omega\left[CMPO\right] + \ln K_{B3} \,, \tag{5-18}$$

where the subscript $B3$ is a reminder of the assumed true stoichiometry. Slope analysis indicates that the stoichiometry is closer to 2:1; and, if this is the true stoichiometry, Eq. (4-106) may be written as

$$\ln d_{B2} \equiv \ln\left\{\frac{D_B'}{\left[NO_3^-\right]^3\left[CMPO\right]^2}\right\} = \omega\left[CMPO\right] + \ln K_{B2} \,. \tag{5-19}$$

Values for D'_B and the free CMPO concentration for both stoichiometries are given in Table 5.23. The nitric acid concentration at each point is 0.10 *M*. At the concentrations given in the table, the bismuth nitrate contributes insignificantly to the total nitrate concentration and may be ignored. Values of the slope and intercept of Eq. (5-19) are calculated by linear regression and are listed in Table 5.24, along with values of the correlation coefficient. The ratio of the organic-phase activity coefficients is given by either

$$\mathbb{R} = \frac{\left(\gamma_{CMPO}^{(c)}\right)^3}{\gamma_{Bi(NO_3)_3\cdot 3CMPO}^{(c)}} = e^{\omega[CMPO]} \tag{5-20}$$

for 3:1 stoichiometry or by

Table 5.24. Solvent slope-analysis results for the extraction of bismuth nitrate

Temperature (°C)	ω	Equilibrium constant	Correlation coefficient
		K_{B3}	
25.0	−14.57	4.203×10^9	−0.9804
40.0	−12.09	9.170×10^8	−0.9992
		K_{B2}	
25.0	−4.664	1.317×10^8	−0.9863
40.0	−2.688	2.995×10^7	−0.8629

$$\mathbb{R} = \frac{\left(\gamma^{(c)}_{CMPO}\right)^2}{\gamma^{(c)}_{Bi(NO_3)_3 \cdot 2CMPO}} = e^{\omega[CMPO]} \qquad (5\text{-}21)$$

for 2:1 stoichiometry. The very low activity coefficients suggested when the assumed stoichiometry is 3:1 are not realistic; values of $\mathbb{R}$ are 0.054 and 0.089 at 25 and 40°C, respectively. Those for 2:1 stoichiometry are more reasonable and are chosen for further discussion. The solvent slope-analysis method for a 2:1 stoichiometry is illustrated in Figure 5.17.

When the CMPO concentration is 0.20 *M*, values of $\mathbb{R}$ are 0.394 and 0.584 at temperatures of 25 and 40°C, respectively. If the activity coefficient of free CMPO was the same as that reported by Diamond et al. (1986) for CMPO in toluene (i.e., ~0.92), then the activity coefficient for the bismuth nitrate disolvate would be −2.15 at a temperature of 25°C. The equilibrium constant is given by the intercept of the solvent slope-analysis line, and values at each temperature are also listed in Table 5.24. Values of the equilibrium constants that include the effects of organic-phase nonideality, K'_{B2}, are computed by multiplying K_{B2} by $\mathbb{R}$. At a free CMPO concentration of 0.20 *M*, the values of K'_{B2} are 5.18×10^7 and 1.75×10^7 at temperatures of 25 and 40°C, respectively.

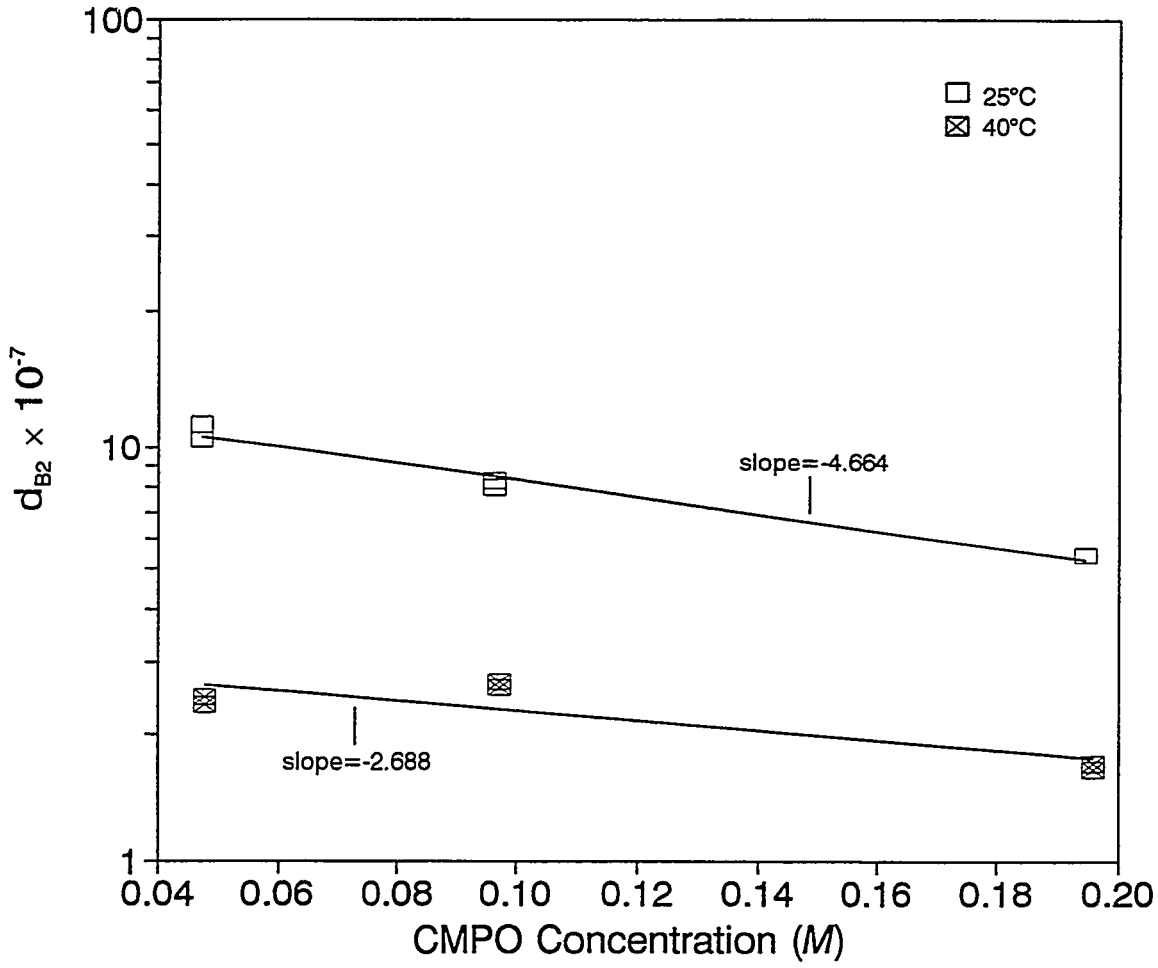

Figure 5.17. Solvent slope-analysis method for the extraction of bismuth nitrate with CMPO–*n*-dodecane with an assumed true stoichiometry of 2:1.

5.3.4 Determination of Thermodynamic Equilibrium Constants

Experiments were performed to measure the distribution ratio of bismuth nitrate with varying aqueous-phase bismuth nitrate and nitric acid concentrations. As previously discussed, the range of concentrations was limited to avoid third-phase formation. The organic-phase concentration of CMPO in *n*-dodecane was fixed at 0.20 *M*.

The measured distribution ratios are given in Table 5.25. Standard deviations in the measured ratios are estimated from replicate experiments and are quite large. As shown in the table, the distribution ratio increases greatly with increasing nitric acid concentration but decreases with increasing temperature. As the distribution ratio increases, the percentage error in the data increases, presumably because of the difficulty in accurately measuring the low bismuth concentrations remaining in the aqueous phase.

The data are fit to the models developed in Sect. 4.3.2 by nonlinear regression methods. Model parameters are the equilibrium constants of the equilibria on which the models are based. To determine the effects of nitric acid concentration and temperature in a more quantitative manner, the data are subdivided into groups where the nitric acid concentration and temperature are constant. The data are then fit to one-parameter models, describing the formation of disolvate and trisolvate. Calculated values include the equilibrium constant (K'), the standard deviation of the equilibrium constant (σ_K), the optimized value of the objective function (χ^2), and the standard deviation (σ) and the standard fractional deviation (σ_f) of the model as compared with the data. The results are given in Table 5.26. Neither model clearly fits the data best, but the standard fractional deviations illustrate the large errors in the data at 0.20 *M* nitric acid where the distribution ratios are large. In each model, the equilibrium constant decreases with increasing nitric acid concentration and with increasing temperature. The effect of increasing nitric acid concentration is similar to that found for uranyl nitrate, which indicates that a nitrate complexation

Table 5.25. Distribution data for the extraction of bismuth nitrate from nitric acid solutions with 0.20 *M* CMPO in *n*-dodecane

HNO_3 (*M*)	Bi × 10^3 (*M*)[a]	*D*	σ_D	Data pair
At 25°C				
0.102	0.500	152.0	4.45	D-10-01/02
0.102	0.500	158.3	4.45	D-10-03/04
0.100	1.00	146.9	6.4[b]	D-10-05/06
0.102	2.00	142.2	1.70	D-10-07/08
0.102	2.00	144.6	1.70	D-10-09/10
0.2	0.050	152.0	100.[b]	D-5-11/12
0.201	0.100	440.8	100.[b]	D-5-09/10
0.2	0.200	315.7	33.52	D-5-07/08
0.202	0.200	363.1	33.52	D-8-01/02
0.200	0.500	438.5	41.37	D-5-03/04
0.202	0.500	380.0	41.37	D-5-05/06
0.202	1.00	453.1	107.5	D-5-01/02
0.202	1.00	301.1	107.5	D-8-03/04
At 40°C				
0.102	1.00	44.57	1.24	D-11-01/02
0.102	1.00	42.82	1.24	D-11-03/04
0.102	2.00	48.23	4.2[b]	D-11-05/06
0.104	5.00	39.29	1.16	D-11-07/08
0.104	5.00	37.65	1.16	D-11-09/10
0.201	0.100	150.6	29.3[b]	D-9-01/02
0.198	0.200	147.7	29.3[b]	D-9-03/04
0.200	0.500	141.9	17.11	D-9-05/06
0.200	0.500	166.1	17.11	D-9-07/08
0.200	1.00	166.7	29.3[b]	D-9-09/10
0.200	5.00	185.4	29.34	D-9-11/12
0.200	5.00	226.9	29.34	D-9-13/14

[a]Initial bismuth nitrate concentration before phase contact.
[b]Standard deviation estimated: see Appendix E.

equilibrium should be included in the model. The effect of temperature indicates an exothermic extraction.

The data are now divided into only two groups according to conditions of temperature. Within each group; both the nitric acid concentration and the bismuth nitrate concentration are

Table 5.26. One-parameter models of bismuth nitrate extraction at fixed nitric acid concentrations

Temp. (°C)	HNO_3 (*M*)	χ^2	σ	σ_f	Parameter	Deviation
					K'_{B3}	$\sigma_{K'B3}$
25.0	0.100	2.218	2.857	0.0186	2.777×10^8	2.29×10^6
25.0	0.200	11.76	100.1	0.5447	1.495×10^8	7.25×10^6
40.0	0.100	3.542	2.952	0.0620	8.433×10^7	1.36×10^6
40.0	0.200	12.38	40.10	0.1992	6.872×10^7	3.94×10^6
					K'_{B2}	$\sigma_{K'B2}$
25.0	0.100	7.389	5.746	0.0373	5.221×10^7	4.13×10^5
25.0	0.200	11.54	99.59	0.5409	2.793×10^7	1.34×10^6
40.0	0.100	13.61	3.937	0.0859	1.553×10^7	2.37×10^5
40.0	0.200	9.522	34.63	0.1725	1.303×10^7	7.26×10^5

variable. The data are fit to the one-parameter and two-parameter models developed in Sect. 4.3.2 by nonlinear regression methods. The results of the calculations are listed in Table 5.27. As might be expected, the one-parameter models based only on distribution equilibria do not fit this larger range of data well.

The two-parameter models include distribution and nitrate complexation equilibria. Each model fits the data within the estimated errors in the data. The ratio of the standard deviations of the two-parameter models is near unity, so the models are indistinguishable on that basis. The model based on the formation of the trisolvate is associated with values of χ^2 nearly equivalent to the number of degrees of freedom, but the model based on formation of the disolvate is associated with the lowest values of the standard fractional deviation. Additionally, disolvate formation is supported by slope analysis to a greater extent, so the model selected as best includes disolvate formation and aqueous nitrate complexation equilibria. The model is compared with the experimental data in Figures 5.18 through 5.21. The organic-phase bismuth nitrate concentration is plotted as a function of aqueous-phase bismuth nitrate concentration at temperatures of 25 and

Table 5.27. Comparison of models describing the extraction of bismuth nitrate: model statistics, model parameters, and standard deviations of parameters[a]

Temp. (°C)	χ^2	σ	σ_f	Parameter	Standard deviation	Parameter	Standard deviation
				K'_{B3}	$\sigma_{K'B3}$		
25.0	293.7	241.7	1.089	2.665×10^8	2.17×10^6		
40.0	29.96	35.17	0.2221	8.268×10^7	1.29×10^6		
				K'_{B2}	$\sigma_{K'B2}$		
25.0	315.2	250.0	1.108	5.015×10^7	3.94×10^5		
40.0	33.87	30.41	0.1979	1.529×10^7	2.25×10^5		
				K'_{B3}	$\sigma_{K'B3}$	β_B	$\sigma_{\beta B}$
25.0	13.92	80.45	0.4388	4.144×10^8	2.25×10^7	74.83	11.88
40.0	15.99	31.13	0.1593	9.271×10^7	3.67×10^6	15.03	5.322
				K'_{B2}	$\sigma_{K'B2}$	β_B	$\sigma_{\beta B}$
25.0	18.58	80.05	0.4357	7.847×10^7	4.27×10^6	76.47	12.03
40.0	22.46	27.13	0.1439	1.690×10^7	6.33×10^5	13.17	4.984

[a]Negative equilibrium constants are not permitted; may indicate "over-modeling" of data.

40°C in Figures 5.18 and 5.19, respectively. Nitric acid concentration is a fixed parameter for each curve. Results from the model agree with the experimental data. The distribution ratio for bismuth nitrate is plotted as a function of the aqueous bismuth nitrate concentration at 25 and 40°C in Figures 5.20 and 5.21, respectively, with nitric acid concentration as a parameter. The scatter in the distribution ratios is more apparent in these graphs. The data are, however, described adequately by the model. The distribution ratio tends to decrease with increasing aqueous concentrations of bismuth nitrate.

Values of the nitrate complexation constant are determined as part of the data-fitting process. With these values, the behavior of the aqueous-phase speciation of bismuth nitrate can be estimated. A total nitrate balance, together with Eqs. (4-91) and (4-92), gives the aqueous nitrate concentration; thus,

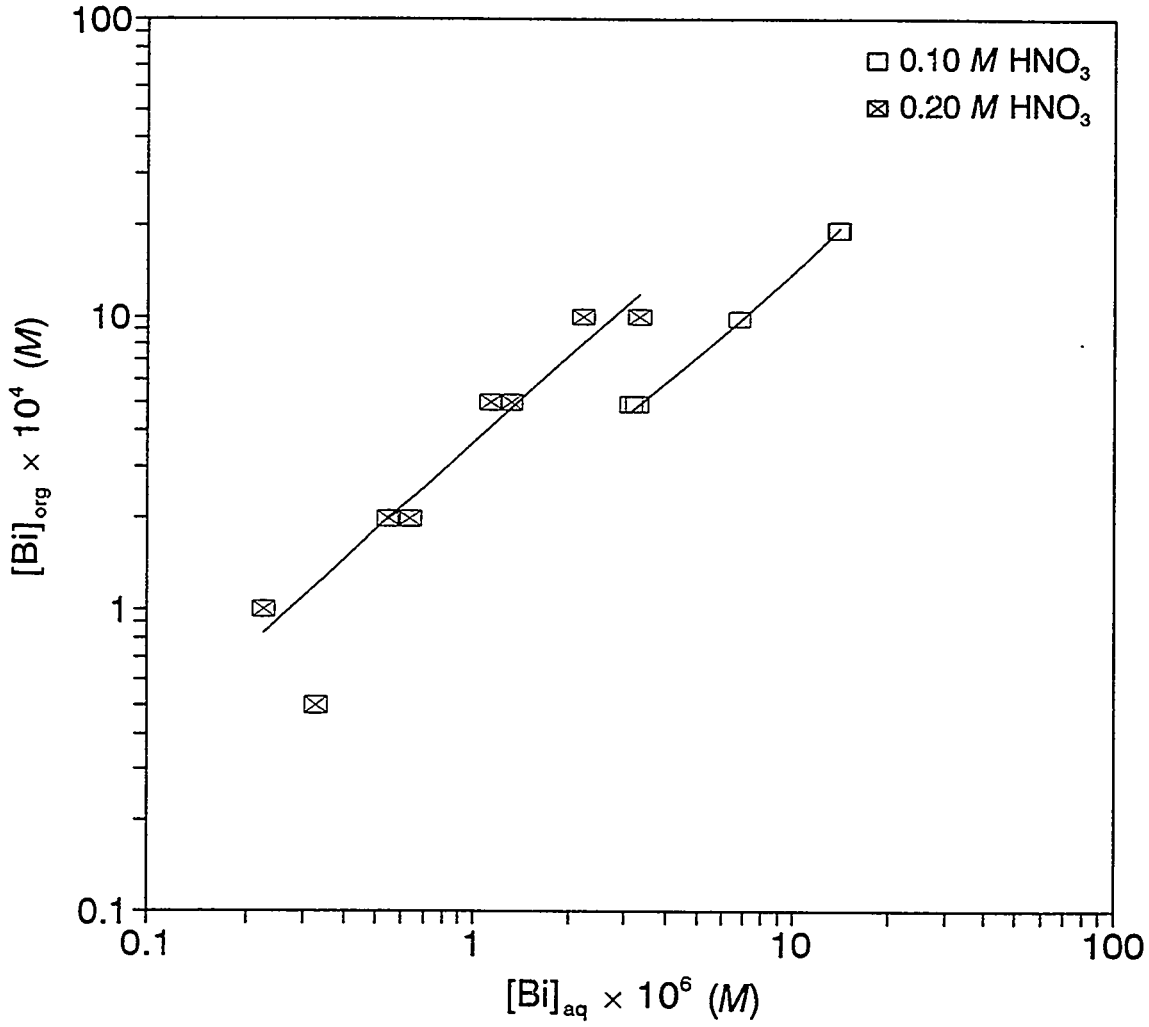

Figure 5.18. Variation of organic-phase bismuth nitrate concentration with aqueous-phase bismuth nitrate concentration at 25°C; comparison of experimental data with model.

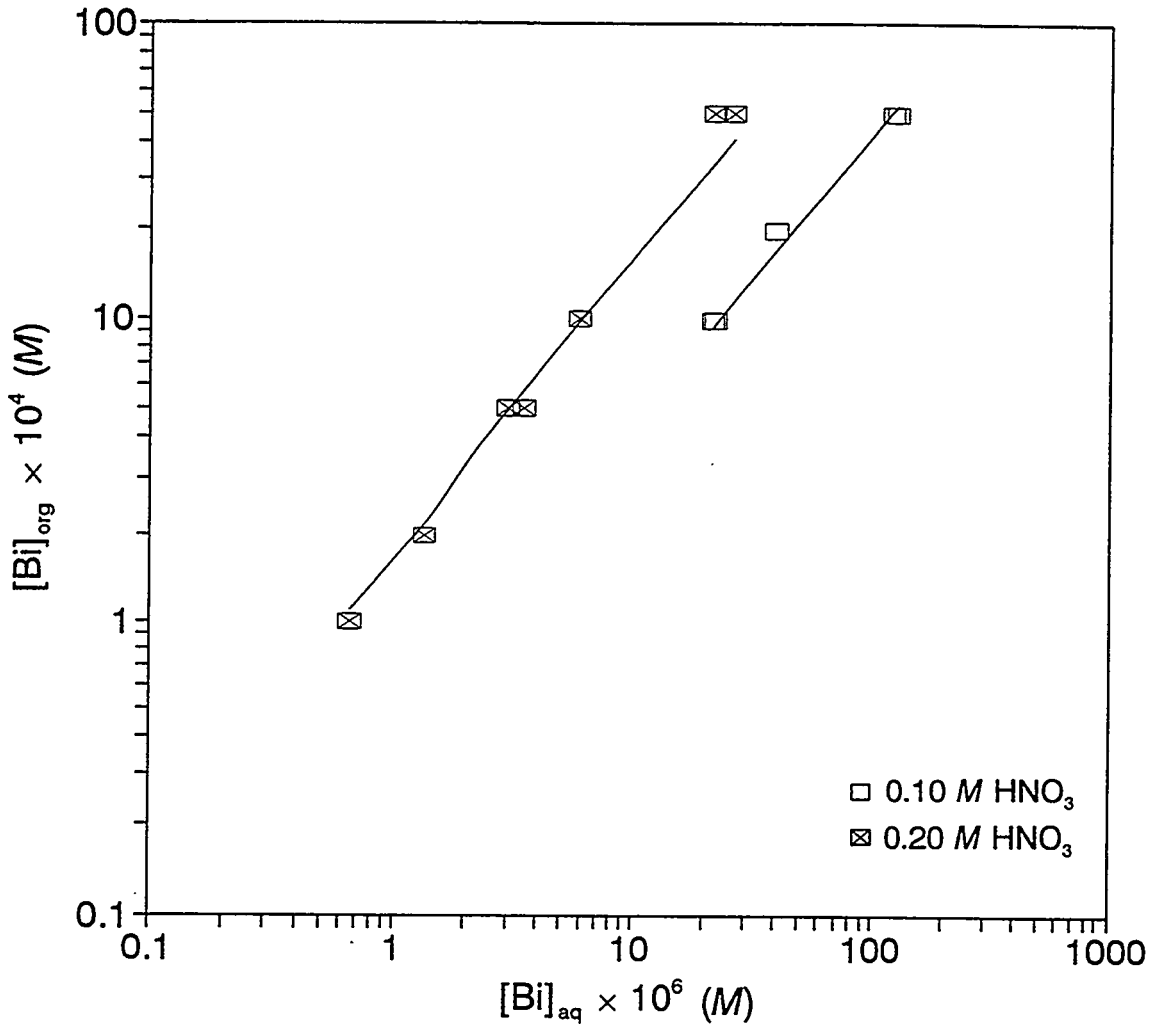

Figure 5.19. Variation of organic-phase bismuth nitrate concentration with aqueous-phase bismuth nitrate concentration at 40°C; comparison of experimental data with model.

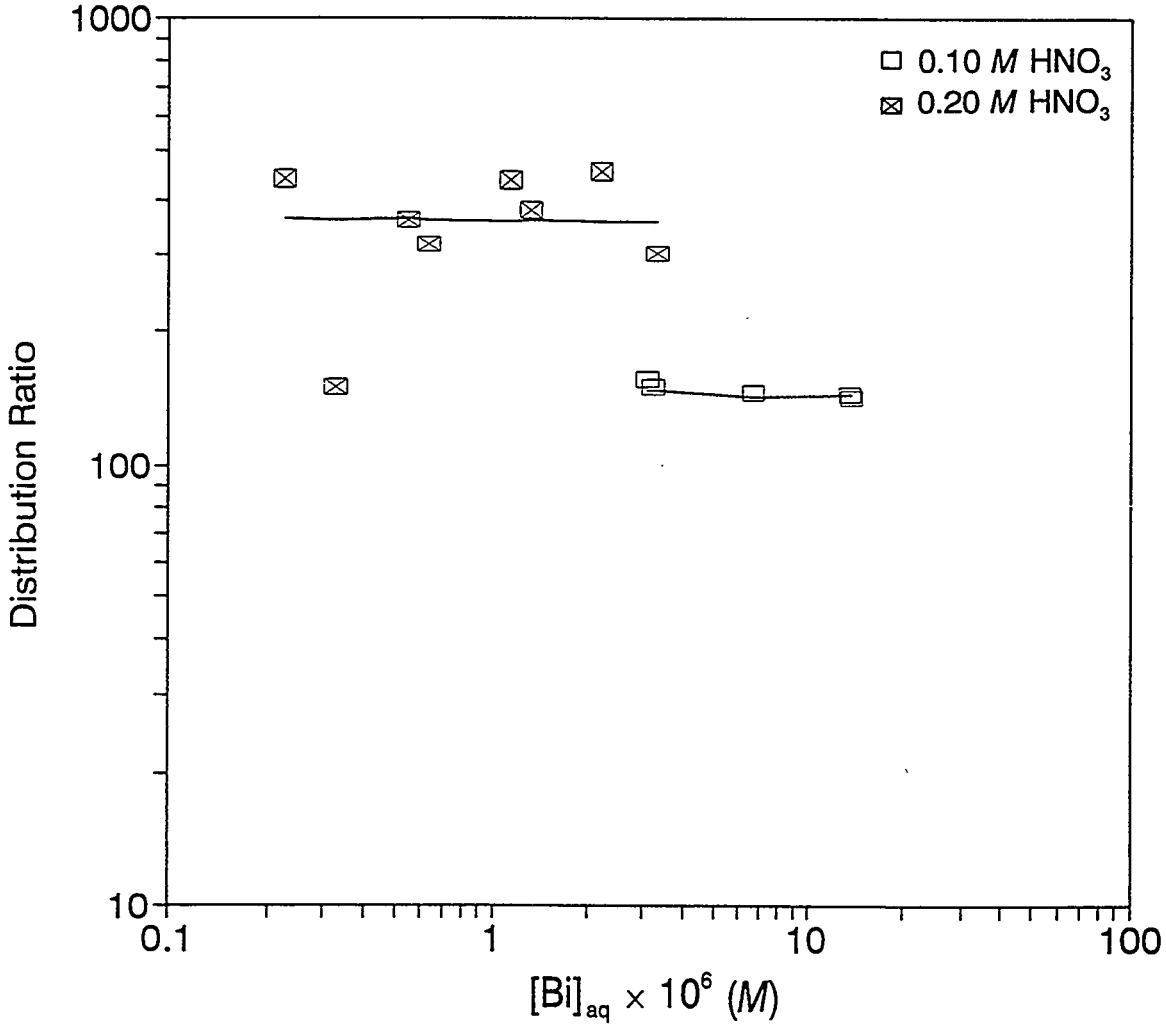

Figure 5.20. Variation of the distribution ratio of bismuth nitrate with aqueous-phase bismuth nitrate concentration at 25°C; comparison of experimental data with model.

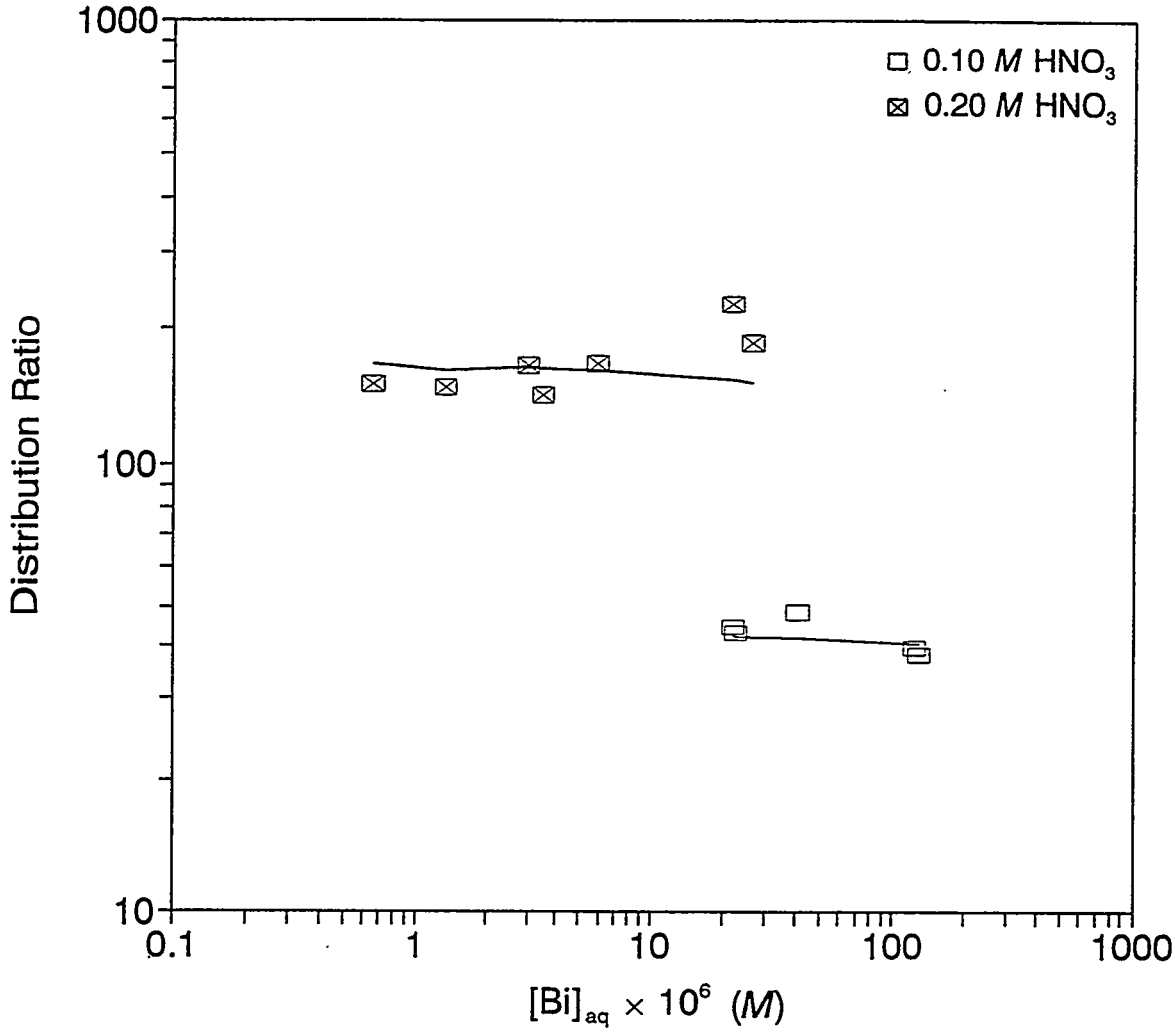

Figure 5.21. Variation of the distribution ratio of bismuth nitrate with aqueous-phase bismuth nitrate concentration at 40°C; comparison of experimental data with model.

$$\left[NO_3^-\right]_{aq} = \left[HNO_3\right]_{aq} + \frac{3a_w^2 + \beta_B\left[NO_3^-\right]^2\left(\gamma_{NO_3^-}^{(c)}\right)^2}{a_w^2 + \beta_B\left[NO_3^-\right]^2\left(\gamma_{NO_3^-}^{(c)}\right)^2}\left[Bi\right]_{aq} \quad . \tag{5-22}$$

This cubic equation gives the nitrate concentration in an implicit form but can be solved numerically. Substitution of the values into Eq. (4-92) gives the concentration of the uncomplexed bismuth ion. Dividing both sides of Eq. (4-92) by the total aqueous-phase bismuth nitrate concentration gives the fraction of aqueous bismuth nitrate in the $Bi(H_2O)_5^{3+}$ form. Results of calculations with a bismuth nitrate concentration of 10^{-4} *M* and nitric acid concentrations ranging from 0 to 1.0 *M* are shown graphically in Figure 5.22. As shown in the figure, the concentration of the uncomplexed bismuth ion decreases rapidly with increasing nitric acid concentration. Increasing the temperature increases the dissociation of bismuth nitrate, thereby increasing the fraction present as the uncomplexed ion. These trends are expected of ionizing salts.

5.3.5 Enthalpy of Extraction

Equilibrium constants of the two equilibria describing the extraction of bismuth nitrate decrease with increasing temperature, indicating that the reactions are exothermic. With values of the equilibrium constants at the two conditions of temperature studied, Eq. (2-6) is used to calculate the enthalpy of the reaction and Eq. (5-7) is used to estimate the error in the result. For the equilibrium involving the bismuth disolvate, Eq. (4-86), and the equilibrium involving nitrate complexation, Eq. (4-89), $\Delta H = -18.99 \pm 0.82$ kcal/mol and $\Delta H = -21.75 \pm 5.07$ kcal/mol, respectively.

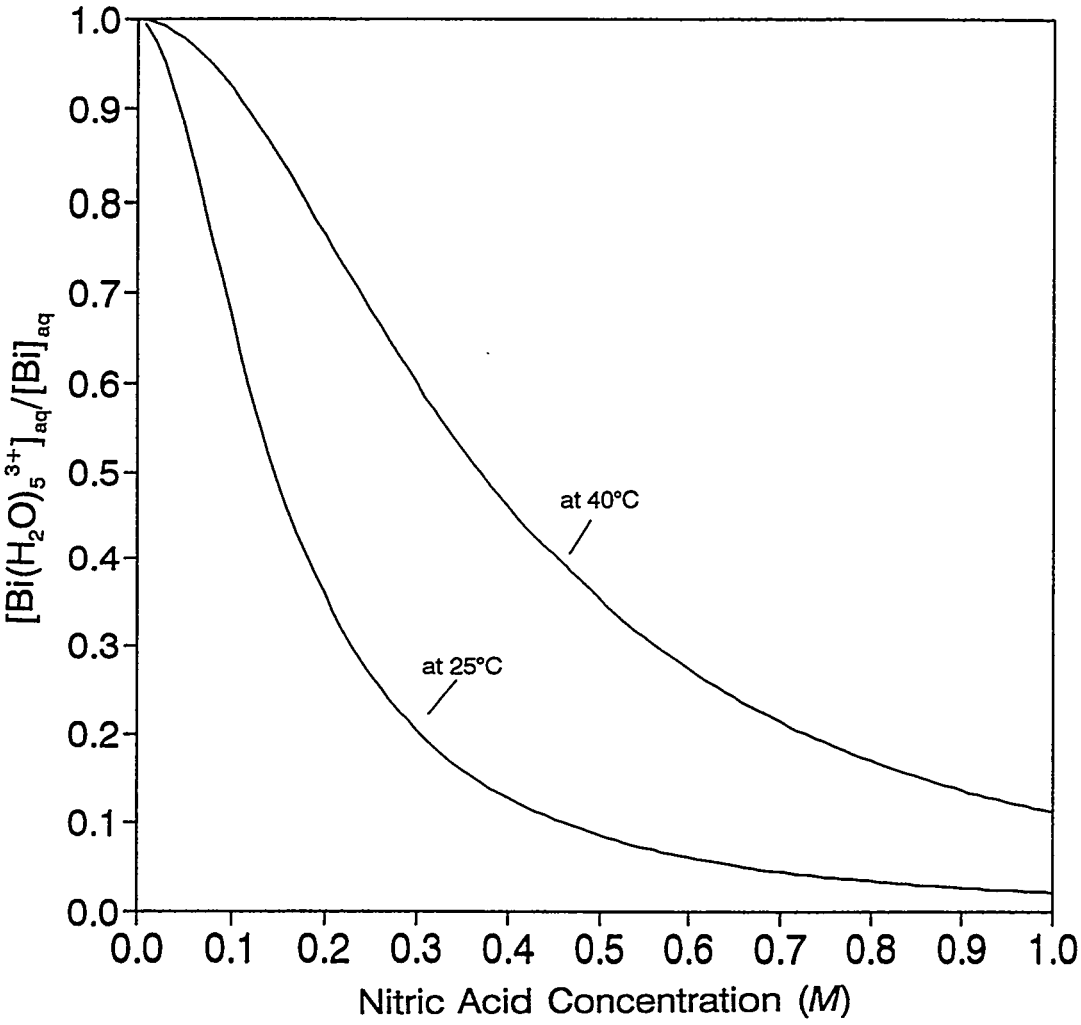

Figure 5.22. Effects of nitric acid concentration and temperature on the fraction of uncomplexed bismuth ion in aqueous solution.

6. CONCLUSIONS

The extraction characteristics of nitric acid, uranyl nitrate, and bismuth nitrate with CMPO were studied in an experimental program where CMPO was dissolved in *n*-dodecane to produce the organic extracting medium. Three different aqueous systems were used in the experiments: (1) nitric acid, (2) uranyl nitrate in nitric acid, and (3) bismuth nitrate in nitric acid. In each case, the aqueous solution was equilibrated with the organic extractant and then the concentration of the solute was measured in each phase to obtain distribution data. The objectives of the project were to estimate extraction stoichiometry and equilibrium constants for the extraction of nitric acid, uranyl nitrate, and bismuth nitrate with the CMPO extractant.

Two types of experiments were performed. In the first type, the organic-phase CMPO concentration was varied while the aqueous-phase concentration was fixed to support the slope-analysis method of estimating the extraction stoichiometry. In the second type of experiment, the aqueous-phase nitric acid concentration and the concentration of the extractable salt (if one was used) were varied to support estimation of the thermodynamic equilibrium constant. The constants are inferred by fitting models based on various equilibria to the data and then selecting those models that fit the data best. Both types of experiments were performed at 25 and 40°C for each of the three different aqueous systems. A few experiments were also conducted at 50°C for the aqueous system containing only nitric acid. Formation of a third phase (second organic phase) occurred when the solubility of the extract complex was exceeded and limited the range of concentrations for both phases.

This study provides fundamental information on the important parameters of extraction equilibria for nitric acid, uranyl nitrate, and bismuth nitrate. Such information includes the extraction stoichiometry, estimated values of the equilibrium constants on the molar scale at temperatures of 25 and 40°C, and estimated values of the enthalpy of each extraction reaction.

Nitrate complexation constants for uranyl and bismuth ions were estimated at 25 and 40°C. Enthalpies of the nitrate complexation equilibria were also estimated. In addition, a method was devised to approximate the ratio of the activity coefficients of the free CMPO to the complexed CMPO in the organic phase.

6.1 Nitric Acid

Equilibrium concentrations of nitric acid distributed between the aqueous and organic phases were measured at aqueous nitric acid concentrations ranging from 0 to ~0.30 *M* at 25°C, 0 to ~1.0 *M* at 40°C, and 0 to ~3.0 *M* at 50°C.

Traditional slope analysis indicated a coordination number of 1.065 at 25°C and 1.076 at 40°C; therefore, a 1:1 extraction stoichiometry is strongly indicated. Various models based on a range of stoichiometries are fit to the data by regression methods. The model fitting the data best is based on the equilibrium

$$H^{+}_{(aq)} + NO^{-}_{3(aq)} + CMPO_{(org)} \rightleftharpoons HNO_3 \cdot CMPO_{(org)} \quad , \tag{6-1}$$

which is a 1:1 stoichiometry. Since the fit is within the estimated errors in the data, the addition of more parameters to the model is not justified statistically.

The equilibrium constant for Eq. (6-1) that includes the activity coefficients of the organic phase was estimated. At 25°C the value of the equilibrium constant was found to be 2.660 ± 0.092; at 40°C, it was 1.710 ± 0.022. The enthalpy of the extraction was estimated to be −5.46 ± 0.46 kcal/mol, which suggests an exothermic reaction.

As indicated above, the traditional slope-analysis method gives a coordination number slightly different from unity. Using a newly developed solvent slope-analysis technique, the

deviation is ascribed to the ratio of the organic-phase activity coefficients that can be represented by

$$\frac{\gamma^{(c)}_{CMPO}}{\gamma^{(c)}_{HNO_3 \cdot CMPO}} = e^{\omega[CMPO]}, \qquad (6\text{-}2)$$

where $\omega = 0.9554$ at 25°C and $\omega = 1.016$ at 40°C. Resolution into the separate activity coefficients by this method alone is not possible. Use of the solvent slope-analysis method to estimate values of the equilibrium constant for Eq. (6-1) gave values of 2.683 at 25°C and 2.012 at 40°C. This is a point of verification, but these values are not considered as accurate as those quoted above.

6.2 Uranyl Nitrate

Equilibrium concentrations of uranyl nitrate distributed between aqueous nitric acid media and the organic phase were measured at tracer levels of uranyl nitrate. Nitric acid concentrations ranged from 0.02 to 0.20 *M*, and measurements were made at both 25 and 40°C. Over this narrow range of conditions, the distribution ratios ranged from 3.5 to 165, indicating how strongly uranium is extracted by CMPO.

Using traditional slope-analysis techniques, the coordination numbers for the extraction of uranyl nitrate were estimated to be 1.513 at 25°C and 1.607 at 40°C. These values seemed to indicate a mixed equilibria of 1:1 and 2:1 stoichiometries occurring in nearly equal proportion. Fitting the data to models based on various equilibria resulted in values of equilibrium constants that varied strongly with nitric acid concentration, suggesting the need to add a nitrate complexation equilibrium to the model. The data were fit within the experimental error by a model based on only two equilibria: a 2:1 extraction equilibrium,

$$UO_2(H_2O)^{2+}_{6(aq)} + 2NO^-_{3(aq)} + 2CMPO_{(org)} \rightleftarrows UO_2(NO_3)_2 \cdot 2CMPO_{(org)} + 6H_2O_{(aq)} \quad , \tag{6-3}$$

and a nitrate complexation of the uranyl ion,

$$UO_2(H_2O)^{2+}_{6(aq)} + NO^-_{3(aq)} \rightleftarrows UO_2NO_3(H_2O)^+_{5(aq)} + H_2O_{(aq)} \quad . \tag{6-4}$$

This model fits the data much better than one based on both 1:1 and 2:1 stoichiometries. A coordination number of 2 was indicated by this approach.

The equilibrium constants for Eq. (6-3) inferred from fitting the data to the model were $1.213 \times 10^6 \pm 3.56 \times 10^4$ at 25°C and $5.77 \times 10^5 \pm 2.12 \times 10^4$ at 40°C. The enthalpy of the reaction was estimated to be -9.610 ± 0.594 kcal/mol, indicating an exothermic reaction. The nitrate complexation constants for Eq. (6-4) were 8.412 ± 0.579 at 25°C and 3.537 ± 0.476 at 40°C. The enthalpy of the complexation was estimated to be -10.72 ± 1.87 kcal/mol, which is also exothermic.

Investigation of the degree of nonideality of the organic phase was accomplished by use of the solvent slope-analysis method. Ratios of the organic-phase activity coefficients are represented by

$$\frac{\left(\gamma^{(c)}_{CMPO}\right)^2}{\gamma^{(c)}_{UO_2(NO_3)_2 \cdot 2CMPO}} = e^{\omega[CMPO]} \quad , \tag{6-5}$$

where $\omega = -4.750$ at 25°C and $\omega = -3.816$ at 40°C. Equilibrium constants inferred by the solvent slope-analysis method only verified those estimated at the same conditions of nitric acid concentration and with models involving only the extraction equilibria.

6.3 Bismuth Nitrate

Equilibrium concentrations of bismuth nitrate distributed between aqueous nitric acid media and the organic phase were measured at tracer levels of bismuth nitrate. Nitric acid

concentrations were either 0.10 or 0.20 *M*, and measurements were made at both 25 and 40°C. Over this narrow range of conditions the distribution ratio varied from ~3.5 to 450.0, but the data were rather scattered. These data suggest that bismuth was more strongly extracted than uranium.

Traditional slope-analysis techniques indicated that the coordination numbers were 1.560 at 25°C and 1.785 at 40°C. A mixed equilibria of, perhaps, 1:1 and 2:1 stoichiometries were suggested. Again, various models were fit to the data by regression methods. Models fitting the data best included an extraction equilibrium and a nitrate complexation. There was no statistical difference between 3:1 and 2:1 extraction equilibria with respect to the data fit, but the 2:1 equilibrium was chosen because it was closer to the coordination number inferred using slope analysis. The selected model was based on the following two equilibria:

$$Bi(H_2O)^{3+}_{5(aq)} + 3NO^{-}_{3(aq)} + 2CMPO_{(org)} \rightleftharpoons Bi(NO_3)_3 \cdot 2CMPO_{(org)} + 5H_2O_{(aq)} \qquad (6\text{-}6)$$

and

$$Bi(H_2O)^{3+}_{5(aq)} + 2NO^{-}_{3(aq)} \rightleftharpoons Bi(NO_3)_2(H_2O)^{+}_{3(aq)} + 2H_2O_{(aq)} \quad . \qquad (6\text{-}7)$$

The equilibrium constant for the extraction equilibrium, Eq. (6-6), was estimated to be $7.847 \times 10^7 \pm 4.27 \times 10^6$ at 25°C and $1.690 \times 10^7 \pm 6.33 \times 10^5$ at 40°C. The enthalpy of the extraction was estimated to be -18.99 ± 0.82 kcal/mol, indicating an exothermic reaction. The nitrate complexation constants for Eq. (6-7) were estimated to be 76.47 ± 12.03 at 25°C and 13.17 ± 4.984 at 40°C. The complexation was exothermic, and the enthalpy of the complexation was estimated at -21.75 ± 5.07 kcal/mol.

Assuming that the true coordination number of bismuth nitrate extraction is 2, the solvent slope-analysis method indicated that the ratio of the organic-phase activity coefficients was approximately

$$\frac{\left(\gamma^{(c)}_{CMPO}\right)^2}{\gamma^{(c)}_{Bi(NO_3)_3 \cdot 2CMPO}} = e^{\omega[CMPO]}, \qquad (6\text{-}8)$$

where $\omega = -4.664$ at 25°C and $\omega = -2.688$ at 40°C.

7. RECOMMENDATIONS

The work reported here provides a better understanding of the extraction properties of CMPO. Most work reported in the literature is based on experiments with mixed CMPO-TBP extractants, making analysis of the individual extraction equilibria unreliable. Reliable equilibria data are important in the development of useful models to design extraction processes. The equilibria constants and enthalpy of reaction data provided here on the extraction of nitric acid, uranyl nitrate, and bismuth nitrate should be used in these models. These chemical properties will be particularly valuable for modeling processes that operate at low nitric acid concentrations, such as the stripping stages of a solvent extraction system. Calculations may be made with confidence for processes operating between 25 and 40°C, and extrapolations near this temperature range are likely to be fairly accurate.

Data already available on the mixed CMPO-TBP extractant should be reexamined to ascertain the existence and magnitude of any synergism between CMPO and TBP with respect to the extraction behavior of nitric acid, uranyl nitrate, and bismuth nitrate. Such a study will ultimately result in improved models of processes using the mixed extractant.

Data on the activity coefficients of organic-phase CMPO species are needed. Results reported in the literature show that the activity coefficients of the nitric acid–CMPO complex in toluene are lower than those of the uncomplexed CMPO. Based on the present study, the nitric acid and CMPO form a 1:1 complex. An experimental program should be conducted to measure the activity coefficients of these species in a *n*-dodecane matrix. More importantly, the activity coefficients of a metal nitrate disolvate (preferably containing uranium) should be measured. Based on the present study, it is likely that such a high-molecular-weight complex will exhibit large deviations from ideality.

8. LIST OF REFERENCES

Alcock, K., et al. 1958. "Tri-*n*-Butyl Phosphate as an Extracting Solvent for Inorganic Nitrates—V: Further Results for the Tetra- and Hexavalent Actinide Nitrates," *J. Inorg. Nucl. Chem.* **6**, 328–33.

Baes, C. F., and Moyer, B. A. 1988. "Estimating Activity and Osmotic Coefficients in $UO_2(NO_3)_2$–HNO_3–$NaNO_3$ Mixtures," *Solvent Extr. Ion Exch.* **6**(4), 675–97.

Blanco, R. E., et al. May 1961. *Chemical Technology Division: Quarterly Progress Report for Chemical Development Section B*, ORNL/TM-177, Union Carbide Nuclear Company, Oak Ridge National Laboratory.

Bradley, D. J., and Pitzer, K. S. 1979. "Thermodynamics of Electrolytes. 12. Dielectric Properties of Water and Debye-Hückel Parameters to 350°C and 1 kbar," *J. Phys. Chem.* **83**(12), 1599–1603.

Bradley, D. J., and Pitzer, K. S. 1983. "Thermodynamics of Electrolytes. 12. Dielectric Properties of Water and Debye-Hückel Parameters to 350°C and 1 kbar" (Corrections), *J. Phys. Chem.* **87**(19), 3798.

Chaiko, D. J., and Vandegrift, G. F. 1988. "A Thermodynamic Model of Nitric Acid Extraction by Tri-*n*-Butyl Phosphate," *Nucl. Technol.* **82**(1), 52–59.

Chaiko, D. J., et al. 1988a. "Modeling of Aqueous and Organic Phase Speciation for Solvent Extraction Systems," *J. Metals* **40**(11), 107.

Chaiko, D. J., et al. 1988b. "Thermodynamic Modeling of Chemical Equilibria in Metal Extraction," *Sep. Sci. Technol.* **23**(12&13), 1435–51.

Chaiko, D. J., et al. February 1989. "Modeling of Aqueous and Organic Phase Speciation for Solvent Extraction Systems," paper presented at the Fall Meeting of the Metallurgical Society, Las Vegas, Nev.

Clegg, S. L., and Brimblecombe, P. 1986. "The Dissociation Constant and Henry's Law Constant of HCl in Aqueous Solution," *Atmos. Environ.* **20**(12), 2483–85.

Clegg, S. L., and Brimblecombe, P. 1990. "Equilibrium Partial Pressures and Mean Activity and Osmotic Coefficients of 0-100% Nitric Acid as a Function of Temperature," *J. Phys. Chem.* **94**(13), 5369–80.

Davis, W., Jr. 1962a. "Thermodynamics of Extraction of Nitric Acid by Tri-*n*-Butyl Phosphate–Hydrocarbon Diluent Solutions: I. Distribution Studies with TBP in Amsco 125-82 at Intermediate and Low Acidities," *Nucl. Sci. Eng.* **14**, 159–68.

Davis, W., Jr. 1962b. "Thermodynamics of Extraction of Nitric Acid by Tri-*n*-Butyl Phosphate–Hydrocarbon Diluent Solutions: II. Densities, Molar Volumes, and Water Solubilities of TBP–Amsco 125-82–HNO_3–H_2O Solutions," *Nucl. Sci. Eng.* **14**, 169–73.

Davis, W., Jr., 1962c. "Thermodynamics of Extraction of Nitric Acid by Tri-*n*-Butyl Phosphate–Hydrocarbon Diluent Solutions: III. Comparison of Literature Data," *Nucl. Sci. Eng.* **14**, 174–78.

Dean, J. A., ed. 1973. *Lange's Handbook of Chemistry*, 11th ed., Handbook Publishers, Inc., Sandusky, Ohio.

DeMuth, S. F. 1989. "The Transport Dynamics of Zirconium Liquid-Liquid Extraction Based on the PUREX Process Used for Reprocessing Spent Nuclear Reactor Fuel," Ph.D. Dissertation, The University of Tennessee, Knoxville.

Denbigh, K. 1971. *Principles of Chemical Equilibrium*, 3rd ed., Cambridge University Press, Cambridge.

Diamond, H., et al. 1986. "Activity Coefficients of Carbamoylmethylphosphoryl Extractants in Toluene," *Solvent Extr. Ion Exch.* **4**(5), 1009–27.

Gatrone, R. C., et al. 1987. "The Synthesis and Purification of the Carbamoylmethylphosphine Oxides," *Solvent Extr. Ion Exch.* **5**(6), 1075–1116.

Goldberg, R. N. 1979. "Evaluated Activity and Osmotic Coefficients for Aqueous Solutions: Bi-Univalent Compounds of Lead, Copper, Manganese, and Uranium," *J. Phys. Chem. Ref. Data* **8**(4), 1005–50.

Guggenheim, E. A. 1935. "The Specific Thermodynamic Properties of Aqueous Solutions of Strong Electrolytes," *Phil. Mag. Ser. 7* **19**(127), 588–643.

Hamer, W. J. 1968. *Theoretical Mean Activity Coefficients of Strong Electrolytes in Aqueous Solutions from 0 to 100°C*, National Standard Reference Data Series—National Bureau of Standards, Washington, D.C.

Hamer, W. J., and Wu, Y. C. 1972. "Osmotic Coefficients and Mean Activity Coefficients of Uni-univalent Electrolytes in Water at 25°C," *J. Phys. Chem. Ref. Data* **1**(4), 1047–99.

Harned, H. S., and Owen, B. B. 1943. *The Physical Chemistry of Electrolyte Solutions*, Reinhold, New York.

Hesford, E., and McKay, H. A. C. 1958. "The Extraction of Nitrates by Tri-*n*-Butyl Phosphate, Part 3. Extraction at Trace Concentrations," *Trans. Faraday Soc.* **54**, 573–86.

Hesford, E., et al. 1959. "Tri-*n*-Butyl Phosphate as an Extracting Agent for Inorganic Nitrates. VI. Further Results for the Rare Earth Nitrates," *J. Inorg. Nucl. Chem.* **9**, 279–89.

Holman, J. P. 1971. *Experimental Methods for Engineers*, 2nd ed., McGraw-Hill, New York.

Horwitz, E. P., and Schulz, W. W. May 1990. "The TRUEX Process: A Vital Tool for Disposal of U.S. Defense Nuclear Wastes," paper presented at the Conference on New Separation Chemistry for Radioactive Waste and Other Specific Applications, Rome, Italy.

Horwitz, E. P., et al. 1982. "Selected Alkyl(phenyl)-N,N-dialkylcarbamoylmethylphosphine Oxides as Extractants for Am(III) from Nitric Acid Media," *Sep. Sci. Technol.* **17**(10), 1261–79.

Horwitz, E. P., et al. 1985. "The TRUEX Process—A Process for the Extraction of the Transuranic Elements from Nitric Acid Wastes Utilizing Modified PUREX Solvent," *Solvent Extr. Ion Exch.* **3**(1&2), 75–109.

Horwitz, E. P., et al. 1987a. "Extraction of Americium(III) from Chloride Media by Octyl(Phenyl)-N,N-Diisobutylcarbamoylmethylphosphine Oxide," *Solvent Extr. Ion Exch.* **5**(3), 419–46.

Horwitz, E. P., et al. 1987b. "The Extraction of Selected Actinides in the (III), (IV), and (VI) Oxidation States from Hydrochloric Acid by OϕD(iB)CMPO: The TRUEX-Chloride Process," *Solvent Extr. Ion Exch.* **5**(3), 447–70.

Kim, H. T., and Frederick, W. J. 1988a. "Evaluation of Pitzer Ion Interaction Parameters of Aqueous Electrolytes at 25°C. I. Single Salt Parameters," *J. Chem. Eng. Data* **33**(2), 177–84.

Kim, H. T., and Frederick, W. J. 1988b. "Evaluation of Pitzer Ion Interaction Parameters of Aqueous Mixed Electrolyte Solutions at 25°C. II. Ternary Mixing Parameters," *J. Chem. Eng. Data* **33**(3), 278–83.

Kolarik, Z., and Horwitz, E. P. 1988. "Extraction of Metal Nitrates with Octyl(Phenyl)-N,N-Diisobutyl-Carbamoylmethyl Phosphine Oxides in Alkane Diluents at High Solvent Loadings," *Solvent Extr. Ion Exch.* **6**(1), 61–91.

Koma, Y., et al. February 28–March 4, 1993. "Application of Modified TRUEX Flowsheet to Monitor Actinide Separation from High Level Liquid Waste," *Proceedings of International Symposium on Waste Management, Tucson, Ariz.*

Leonard, R. A., et al. September 1985. *The Extraction and Recovery of Plutonium and Americium from Nitric Acid Waste Solutions by the TRUEX Process—Continuing Development Studies*, ANL-85-45, The University of Chicago, Argonne National Laboratory.

Leonard, R. A., et al. March 1987. *The TRUEX Process for Recovery of Plutonium and Americium from Nitric Acid Waste Solutions—Continuing Development Studies, FY 1986*, ANL-87-3, The University of Chicago, Argonne National Laboratory.

Lietzke, M. H., et al. 1963. "A Mathematical Model for the Solvent Extraction of Uranyl Nitrate and Nitric Acid," *Nucl. Sci. Eng.* **16**(1), 25–30.

Lumetta, G. J., et al. June 1993. *Underground Storage Tank Integrated Demonstration: Evaluation of Pretreatment Options for Hanford Tank Wastes*, PNL-8537, Pacific Northwest Laboratory, Richland, Wash.

Mailen, J. C., et al. 1980. "Solvent Extraction Chemistry and Kinetics of Zirconium," *Sep. Sci. Technol.* **15**(4), 959–73.

Marcus, Y. 1989. "Diluent Effects in Solvent Extraction," *Solvent Extr. Ion Exch.* **7**(4), 567–75.

Marsh, S. F., and Yarbro, S. L. 1988. *Comparative Evaluation of DHDECMP and CMPO as Extractants for Recovering Actinides from Nitric Acid*, LA-11191, Los Alamos National Laboratory, Los Alamos, N.M.

Masson, D. O. 1929. "Solute Molecular Volumes in Relation to Solvation and Ionization," *Phil. Mag.* **7**(8), 218–35.

Mathur, J. N., et al. 1993. "Partitioning of Actinides from High-Level Waste Streams of PUREX Process Using Mixtures of CMPO and TBP in Dodecane," *Waste Manage.* **13**, 317–25.

McGinnis, C. P. December 1992. Technical Task Plan, "Comprehensive Sludge/Supernate DT&E," Oak Ridge National Laboratory

Meisenhelder, J. H., and Siczek, A. A. 1980. "An Infrared Study of Zirconium Retention in 30% Tributyl Phosphate," *Radiochim. Acta* **27**, 223–27.

Mikhailov, V. A., and Torgov, V. G. 1964. "Determination of the Activity Coefficient of Uranyl Nitrate in Dilute Aqueous Solutions by an Extraction Method," *Russ. J. Phys. Chem.* **38**(2), 151–54.

Millero, F. J. 1971. "The Molal Volumes of Electrolytes," *Chem. Rev.* **71**(2), 147–76.

Mincher, B. J. 1989. "The Separation of Neptunium and Plutonium from Nitric Acid Using *n*-Octyl(Phenyl)-N,N-Diisobutylcarbamoylmethyl Phosphine Oxide Extraction and Selective Stripping," *Solvent Extr. Ion Exch.* **7**(4), 645–54.

Moghissi, A. A., et al. 1986. *Radioactive Waste Technology*, The American Society of Mechanical Engineers, New York.

Moyer, B. A., et al. 1991. "Liquid-Liquid Equilibrium Analysis in Perspective. Part 1. Slope Analysis of the Extraction of Uranyl Nitrate from Nitric Acid by Di-2-ethylhexylsulfoxide," *Solvent Extr. Ion Exch.* **9**(5), 833–64.

Navratil, J. D. 1985. *Plutonium and Americium Extraction Studies with Bifunctional Organophosphorus Extractants*, RFP-3977, Rocky Flats Plant, Rockwell International, Golden, Colo.

Olander, D. R., and Benedict, M. 1963. "The Mechanism of Extraction by Tributyl Phosphate–*n*-Hexane Solvents: Part II. Nitric Acid Extraction," *Nucl. Sci. Eng.* **15**, 354–65.

Ozawa, M., et al. 1992. "Partitioning of Actinides and Fission Products in Highly-Active Raffinate from PUREX Process by Mixer-Settlers," *Solvent Extr. Ion Exch.* **10**(5), 829–46.

Perry, R. H., ed. 1973. *Chemical Engineer's Handbook*, 5th ed., McGraw-Hill, New York.

Phutela, R. C., and Pitzer, K. S. 1986. "Thermodynamics of Electrolyte Mixtures. Enthalpy and the Effect of Temperature on the Activity Coefficient," *J. Solution Chem.* **15**(8), 649–62.

Pitzer, K. S. 1973. "Thermodynamics of Electrolytes. I. Theoretical Basis and General Equations," *J. Phys. Chem.* **77**(2), 268–77.

Pitzer, K. S. 1975. "Thermodynamics of Electrolytes. V. Effects of Higher-Order Electrostatic Terms," *J. Solution Chem.* **4**(3), 249–65.

Pitzer, K. S. 1991. *Activity Coefficients in Electrolyte Solutions*, 2nd ed., CRC Press, Inc., Boca Raton, Fla.

Pitzer, K. S., and Kim, J. J. 1974. "Thermodynamics of Electrolytes. IV. Activity and Osmotic Coefficients for Mixed Electrolytes," *J. Am. Chem. Soc.* **96**(15), 5701–7.

Pitzer, K. S., and Mayorga, G. 1973. "Thermodynamics of Electrolytes. II. Activity and Osmotic Coefficients for Strong Electrolytes with One or Both Ions Univalent," *J. Phys. Chem.* **77**(19), 2300–2308.

Pitzer, K. S., and Mayorga, G. 1974. "Thermodynamics of Electrolytes. III. Activity and Osmotic Coefficients for 2-2 Electrolytes," *J. Solution Chem.* **3**(7), 539–46.

Pitzer, K. S., and Silvester, L. F. 1976. "Thermodynamics of Electrolytes. VI. Weak Electrolytes Including H_3PO_4," *J. Solution Chem.* **5**(4), 269–78.

Pitzer, K. S., et al. 1977. "Thermodynamics of Electrolytes. VII. Sulfuric Acid," *J. Am. Chem. Soc.* **99**(15), 4930–36.

Pitzer, K. S., et al. 1978. "Thermodynamics of Electrolytes. IX. Rare Earth Chlorides, Nitrates, and Perchlorates," *J. Solution Chem.* **7**(1), 45–56.

Press, W. H., et al. 1992. *Numerical Recipes in FORTRAN: The Art of Scientific Computing*, 2nd ed., Cambridge University Press, Cambridge.

Rard, J. A., et al. 1977. "Isopiestic Determination of the Activity Coefficients of Some Aqueous Rare Earth Electrolyte Solutions at 25°C. 3. The Rare Earth Nitrates," *J. Chem. Eng. Data* **22**(3), 337–47.

Robinson, F. V., and Topp, N. E. 1964. "The Extraction of Rare Earth Nitrates with Tri-*n*-Butyl Phosphate," *J. Inorg. Nucl. Chem.* **26**(3), 473–77.

Root, W. C. 1933. "An Equation Relating Density and Concentration," *J. Am. Chem. Soc.* **55**, 850–51.

Roux, A., et al. 1978. "Apparent Molal Heat Capacities and Volumes of Aqueous Electrolytes at 25°C: $NaClO_3$, $NaClO_4$, $NaNO_3$, $NaBrO_3$, $KClO_3$, $KBrO_3$, KIO_3, NH_4NO_3, NH_4Cl, and NH_4ClO_4," *Can. J. Chem.* **56**, 24–28.

Sato, T. 1958. "The Extraction of Uranyl Nitrate from Nitric Acid Solutions by Tributyl Phosphate," *J. Inorg. Nucl. Chem.* **6**, 334–37.

Schulz, W. W., and Horwitz, E. P. 1988. "The TRUEX Process and the Management of Liquid TRU Waste," *Sep. Sci. Technol.* **23**(12&13), 1191–1210.

Schulz, W. W., and Navratil, J. D. March 1984a. *Bifunctional Organophosphorus Liquid-Liquid Extraction Reagents: Development and Applications*, RFP-3685, Rocky Flats Plant, Rockwell International, Golden, Colo. (Also in *Proc. Am. Chem. Soc.*, St. Louis, April 1984.)

Schulz, W. W., and Navratil, J. D., eds. 1984b. *CRC Science and Technology of Tributyl Phosphate, Vol. I*, CRC Press, Inc., Boca Raton, Fla.

Sears, F. W., and Zemansky, M. W. 1964. *University Physics*, 3rd ed., Addison-Wesley Publishing Co., Inc., Reading, Mass.

Sears, M. B., et al. September 1990. *Sampling and Analysis of Radioactive Liquid Wastes and Sludges in the Melton Valley and Evaporator Facility Storage Tanks at ORNL*, ORNL/TM-11652, Martin Marietta Energy Systems, Inc., Oak Ridge National Laboratory.

Sears, M. B., et al. September 1991. *Exploratory Tests of Washing Radioactive Sludge Samples from the Melton Valley and Evaporator Facility Storage Tanks at ORNL*, ORNL/M-1528, Martin Marietta Energy Systems, Inc., Oak Ridge National Laboratory.

Siczek, A. A., and Meisenhelder, J. H. 1980. "Zirconium Retention in 30% Tributyl Phosphate/*n*-dodecane," *Radiochim. Acta* **27**, 217–21.

Silvester, L. F., and Pitzer, K. S. 1977. "Thermodynamics of Electrolytes. VIII. High-Temperature Properties, Including Enthalpy and Heat Capacity, with Application to Sodium Chloride," *J. Phys. Chem.* **81**(19), 1822–28.

Silvester, L. F., and Pitzer, K. S. 1978. "Thermodynamics of Electrolytes. X. Enthalpy and the Effect of Temperature on the Activity Coefficients," *J. Solution Chem.* **7**(5), 327–37.

Smith, J. M., and Van Ness, H. C. 1975. *Introduction to Chemical Engineering Thermodynamics*, 3rd ed., McGraw-Hill Book Company, New York.

Söhnel, O., and Novotny, P. 1985. *Densities of Aqueous Solutions of Inorganic Substances*, Elsevier Science Publishing Co., Inc., New York.

Spencer, B. B. September 29–October 4, 1991. "Simultaneous Determination of Nitric Acid and Uranium Concentrations in Aqueous Solution from Measurements of Electrical Conductivity, Density and Temperature," paper presented at the Fourth International Conference on Facility Operations—Safeguards Interface, sponsored by the American Nuclear Society.

Spencer, B. B. December 1994."Thermodynamics of the Extraction of Uranium from Strong Aqueous Electrolyte Solutions," Ph.D. Dissertation, The University of Tennessee, Knoxville.

Tedder, D. W., and Davis, W., Jr. 1983. "Alternative Models for Predicting the Extraction of Water and Uranyl Nitrate in the Two-Phase System: Water–Uranyl Nitrate–Tributyl Phosphate–AMSCO 125-82," *Solvent Extr. Ion Exch.* **1**(1), 43–75.

Tse, P. K., and Vandegrift, G. F. August 1989. *Development of Supercritical Fluid Chromatography for Analysis of TRUEX Process Solvents*, ANL-89/21, The University of Chicago, Argonne National Laboratory.

Vandegrift, G. F. Apr. 15, 1993. Argonne National Laboratory, personal communication to B. B. Spencer, Oak Ridge National Laboratory.

Vandegrift, G. F., et al. July 1984. *Transuranic Decontamination of Nitric Acid Solutions by the TRUEX Solvent Extraction Process—Preliminary Development Studies*, ANL-84-45, The University of Chicago, Argonne National Laboratory.

Wadsworth, H. M., Jr., ed., 1990. *Handbook of Statistical Methods for Engineers and Scientists*, McGraw-Hill, New York.

Weast, R. C., ed. 1972. *CRC Handbook of Chemistry and Physics*, 53rd ed., CRC Press, Inc., Boca Raton, Fla.

Weast, R. C., ed., 1989. *CRC Handbook of Chemistry and Physics*, 70th ed., CRC Press, Inc., Boca Raton, Fla.

Yukhin, Y. M., et al. 1988. "Solvent Extraction of Bismuth from Nitric Acid Solutions," *J. Appl. Chem. USSR*, **61**(9), 1796–99.

9. NOMENCLATURE

Roman

A = Debye-Hückel constant
A_γ = Debye-Hückel constant for activity coefficient, 0.511 $kg^{½}$ $mol^{-½}$ at 25°C
A_ϕ = Debye-Hückel constant for osmotic pressure
a = activity of a species
or an anion
B = an arbitrary adjustable parameter
or a function in Pitzer's model defined by Eq. (2-30)
b = a constant (found to be ~1.2 in Pitzer's model)
C = an arbitrary adjustable constant
or a function in Pitzer's model defined by Eq. (2-32)
c = molar concentration, mol/L,
or a cation
$\mathbb{C}$ = radioactivity count rate, dpm/mL
D = dielectric constant
or a distribution ratio
d = modified distribution ratio for solvent slope-analysis method, defined by Eq. (4-106)
E = symbol for an arbitrary extractant
F = function in Pitzer's model defined by Eq. (2-28)
or the F-statistic
f = empirical equation to account for hard-core effects in Debye-Hückel theory, Eq. (2-29)
G = Gibbs free energy, cal/mol
or total Gibbs free energy in Pitzer's model
or partial molar free energy if a subscript is used
g = function in Pitzer's correlation defined in Eq. (2-36)
g' = function in Pitzer's correlation defined in Eq. (2-40)
H = enthalpy, cal/mol
or partial molar enthalpy if a subscript is used
h = number of waters of hydration
I = molal ionic strength, mol/kg
K = thermodynamic equilibrium constant (a function of temperature and pressure)
k = Boltzmann's constant, 1.38045×10^{-16} erg/K
M = molecular weight
M = a cation
m = molal concentration, mol/kg of solvent
N_A = Avagadro's number, 6.0232×10^{23} mol^{-1}
n = number of moles
or number of data points
or the nth power
or the solvation number
P = pressure, atm (or bars, as indicated in the text)
p = number of parameters in a model
R = universal ideal gas law constant, 1.9872 cal/(mol·K)

r = a reactant
$\mathbb{R}$ = ratio of activity coefficients of free CMPO and CMPO-nitrate complex
T = absolute temperature, K (or °C as noted)
u = coefficients describing temperature variation in Pitzer parameters
or arbitrary adjustable coefficients
V = volume, L
or partial molar volume when a subscript is used
X = an anion
x = mole fraction
or a general independent variable
y = a general dependent variable
Z = ionic strength function defined by Eq. (2-33) (used in Pitzer's method)
z = the charge number of an ion
or a specific stoichiometric coefficient
[ ] = molar concentration of the chemical enclosed within the brackets

Greek

α = a parameter in Pitzer's model
β = a parameter in Pitzer's method
or the nitrate complexation constant
γ = the activity coefficient
Δ = a change in the given value
ε = electronic charge, 1.60206×10^{-19} coulomb or 4.8029×10^{-10} e.s.u.
λ = second virial coefficients in Pitzer's model (dependent on ionic strength)
μ = chemical potential or partial molar Gibbs free energy, cal/mol
or third virial coefficients in Pitzer's model (independent of ionic strength)
ν = stoichiometric coefficient
or number of ions produced from a dissolved salt
π = ratio of circumference of a circle to its diameter , ~3.1415927
ρ = density of a material, g/mL or g/cm^3
σ = standard deviation defined by Eq. (5-3)
Φ = difference parameter in Pitzer's model
ϕ = the osmotic coefficient
or apparent molal quantity
χ^2 = scaled sum of errors squared, defined by Eq. (5-2)
ψ = difference parameter in Pitzer's model
Ω = function defined by Eq. (4-18)
ω = coefficient in solvent slope-analysis equation

Superscripts

$'$ = derivative
or indicates parameter modified to include nonideal effects
or a marker to indicate molar quantity
0 = evaluated at a standard or reference state
(0) = identifier for coefficient in Pitzer's model
(1) = identifier for coefficient in Pitzer's model

(2)	=	identifier for coefficient in Pitzer's model
(*c*)	=	concentration, or molar-based
ex	=	excess
(*x*)	=	mole fraction-based
γ	=	activity-based Pitzer parameter
ϕ	=	osmotic-based Pitzer parameter

Subscripts

−	=	refers to anions
+	=	refers to cations
±	=	mean ionic or mean stoichiometric
0	=	of, or related to, the solvent
a	=	an anion
a´	=	an anion differentiated from *a*
aq	=	of, or related to, aqueous phase
B	=	bismuth, or related to bismuth
c	=	a cation
c´	=	a cation differentiated from *c*
D	=	related to distribution coefficient
f	=	fractional
H	=	nitric acid
i	=	counter or identifier for reactants or solutes
j	=	counter or identifier for solutes
M	=	cation of a salt
n	=	a constant quantity (moles) of material or an identifier for neutral solutes
n´	=	neutral solute differentiated from *n*
n:m	=	stoichiometric ratio
org	=	of, or related to, organic phase
P	=	with respect to pressure or at constant pressure
ref	=	reference
s	=	value given by slope analysis
T	=	with respect to temperature or at constant pressure
U	=	uranium, or related to uranium
V	=	volume
vac	=	vacuum
X	=	anion of a salt
w	=	of, or related to, water

APPENDIXES

A. Estimation of Pitzer Parameters for Bismuth Nitrate

No pure-component Pitzer parameters are available for bismuth nitrate [$Bi(NO_3)_3$], presumably because bismuth nitrate precipitates as basic bismuth nitrate [$BiONO_3$] in pure water and, thus, prevents measurements on the pure salt system. According to Weast (1972), bismuth salts, in general, precipitate as the basic salt in water. However, bismuth nitrate dissolves readily as the trinitrate form in aqueous nitric acid. Since bismuth nitrate exists in the aqueous nitric acid waste solutions and it is desired that the extraction of bismuth nitrate by CMPO be measured and modeled, estimates of the activity coefficients for bismuth nitrate in solutions containing it are necessary. When the Pitzer model is used to compute such properties in multicomponent systems, the need for Pitzer parameters is implied.

Rard et al. (1977) determined activity coefficients for aqueous rare-earth nitrates using the isopiestic method. They observed that the activity coefficients at constant molal concentrations (e.g., 1.0 *m*) formed an S-shaped curve when plotted vs the ionic radii of the cations. Shortly after the appearance of this paper, Pitzer et al. (1978) reported Pitzer parameters for these trinitrates and showed that the primary parameter, $\beta^{(0)}$, formed an S-shaped curve when plotted against the ionic radii of the cation. In an earlier paper, Pitzer and Mayorga (1973) found that the $\beta^{(1)}$ parameter varied linearly with $\beta^{(0)}$ for 3-1 electrolytes. These observations indicate that the Pitzer parameters for a homologous series vary regularly with the cationic radius, providing a means to estimate the parameters for bismuth nitrate.

Pure-electrolyte Pitzer parameters and their first temperature derivatives as given by Pitzer and coworkers (1978 and 1991) for the rare-earth nitrates are summarized in Table A.1. The ionic radius of the fully ionized cation (charge, 3+) is also given in the table. As shown, the $\beta^{(1)}$ parameter is constant, implying that the slope of the linear relationship to $\beta^{(0)}$ is zero. Different values of the Pitzer parameters for the rare-earth nitrates covering a greater concentration range

Table A.1. Pitzer parameters for selected trinitrate salts

Salt	$3\beta^{(0)}/2^a$	$3\beta^{(1)}/2^a$	$3^{1.5}C^{\phi}/2^a$	Maximum[a] conc. (m)	Ionic radii (Å[b])	$\partial(3\beta^{(0)}/2)/\partial T^c \times 10^3$	$\partial(3\beta^{(1)}/2)/\partial T^c \times 10^2$	$\partial(3^{1.5}C^{\phi}/2)\partial T^c \times 10^3$
$Y(NO_3)_3$	0.9158	7.70	−0.1898	2.0	0.893			
$La(NO_3)_3$	0.7374	7.70	−0.1989	1.5	1.061	2.592	1.643	−1.172
$Pr(NO_3)_3$	0.7245	7.70	−0.1734	1.5	1.013	2.439	1.854	−1.121
$Nd(NO_3)_3$	0.7023	7.70	−0.1427	2.0	0.995	2.364	2.068	−1.114
$Sm(NO_3)_3$	0.701	7.70	−0.131	1.5	0.964	2.152	2.533	−1.003
$Eu(NO_3)_3$	0.7133	7.70	−0.1257	2.0	0.950			
$Gd(NO_3)_3$	0.776	7.70	−0.170	1.4	0.938	2.181	2.002	−1.053
$Tb(NO_3)_3$	0.838	7.70	−0.202	1.4	0.923	1.807	1.585	−1.012
$Dy(NO_3)_3$	0.8484	7.70	−0.1809	2.0	0.908	1.988	1.639	−1.049
$Ho(NO_3)_3$	0.8769	7.70	−0.1852	2.0	0.894	1.681	1.631	−1.010
$Er(NO_3)_3$	0.938	7.70	−0.226	1.5	0.881	1.724	1.650	−1.105
$Tm(NO_3)_3$	0.952	7.70	−0.222	1.5	0.870	1.836	1.669	1.208
$Yb(NO_3)_3$	0.948	7.70	−0.208	1.5	0.858	1.898	1.685	−1.233
$Lu(NO_3)_3$	0.9264	7.70	−0.1749	2.0	0.850	1.927	1.709	−1.209
$Bi(NO_3)_3$[d]	0.704	7.70	−0.129	1.5	0.960	2.19	2.58	−1.01

[a]K. S. Pitzer, *Activity Coefficients in Electrolyte Solutions*, 2nd ed., CRC Press, Boca Raton, Fla., 1991, p. 107.

[b]R. C. Weast, Ed., *CRC Handbook of Chemistry and Physics*, 70th ed., CRC Press, Inc., Boca Raton, Fla., 1989, p. F-187.

[c]K. S. Pitzer et al., "Thermodynamics of Electrolytes. IX. Rare Earth Chlorides, Nitrates, and Perchlorates," *J. Solution Chem.* **7**(1), 45–56 (1978).

[d]Estimates based on variation with ionic radii.

are given by Kim and Frederick (1988). In their parameter set, $\beta^{(1)}$ is not constant. As is the usual case, the deviations from the data are greater when the range is larger; and since the ranges shown in Table A.1 are adequate for the present study, those parameters will be used.

Since the value for $3\beta^{(1)}/2$ is the same for all the trinitrates shown in Table A.1, that value was assigned for bismuth nitrate and entered into the last row of the table. Values of $3\beta^{(0)}/2$ are plotted vs cationic radius in Figure A.1, and the expected S-shaped pattern may be observed. A smooth curve was drawn through the data points. A value of $3\beta^{(0)}/2$ was read from the curve at an ordinate position of 0.960 Å and assigned to bismuth nitrate (see the last row of Table A.1). Although there was no precedent for doing so, a similar graphical construction, shown in Figure A.2, was used to obtain a value of C^{ϕ} for bismuth nitrate.

Because it was expected that the parameters $\beta^{(0)}$ and $\beta^{(1)}$ would vary regularly with cationic radius, it was anticipated that the temperature derivatives would also demonstrate similar regular behavior. Figures A.3 and A.4 show the resulting plots, from which parameter values for bismuth nitrate were selected. Again, for lack of another procedure, the temperature derivative of C^{ϕ} vs the cationic radius was plotted in Figure A.5 as a means of estimating a value for bismuth nitrate. Parameter values assigned to bismuth nitrate are shown in the last row of Table A.1.

It is likely that the above methods have produced only approximate values of the Pitzer parameters for bismuth nitrate. There may be additional factors other than cationic radius, such as electron shell configuration, that may influence these parameters. Errors in the primary parameters are of greatest concern except at low concentrations where the model collapses to the Debye-Hückel limiting law. When the temperature range of interest is narrow, the first temperature derivatives of the Pitzer parameters will have little influence on the performance of the model. For the rare-earth trinitrates shown in Table A.1, Pitzer et al. (1978) note that a temperature change

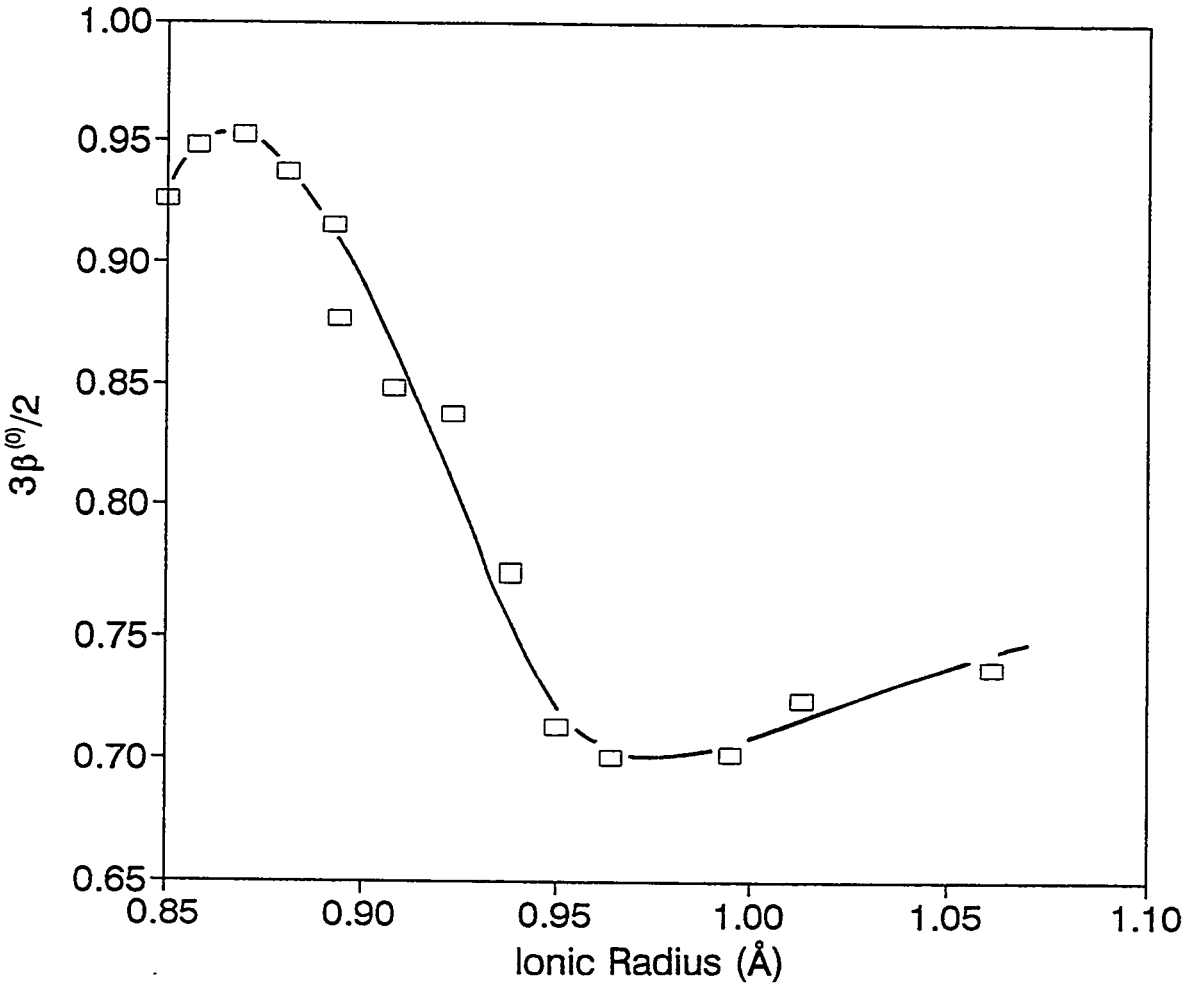

Figure A.1. Variation of $\beta^{(0)}$ with ionic radius for rare-earth nitrates.

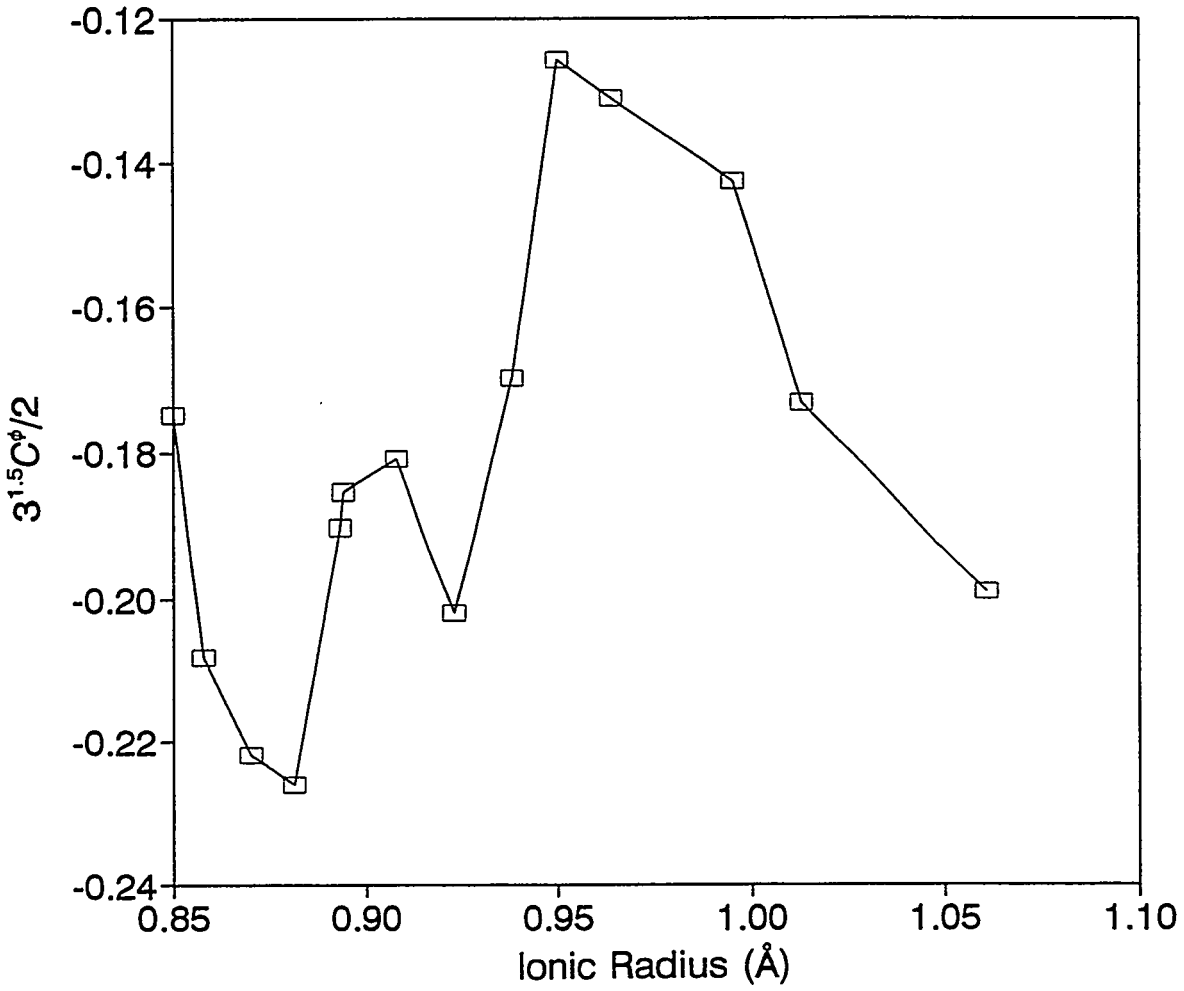

Figure A.2. Variation of C^{ϕ} with ionic radius for rare-earth nitrates.

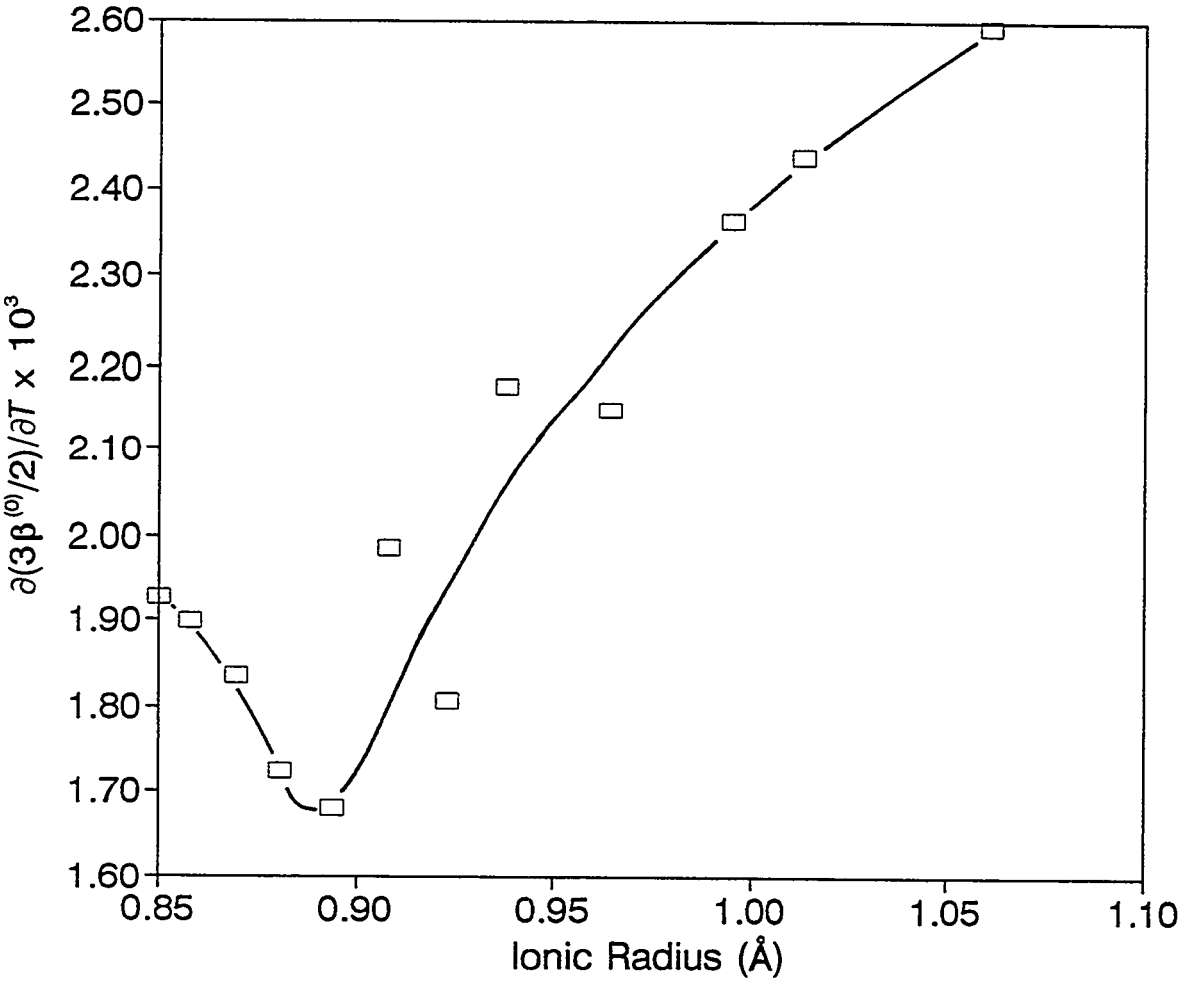

Figure A.3. Variation of the temperature derivative of $\beta^{(0)}$ with ionic radius for rare-earth nitrates.

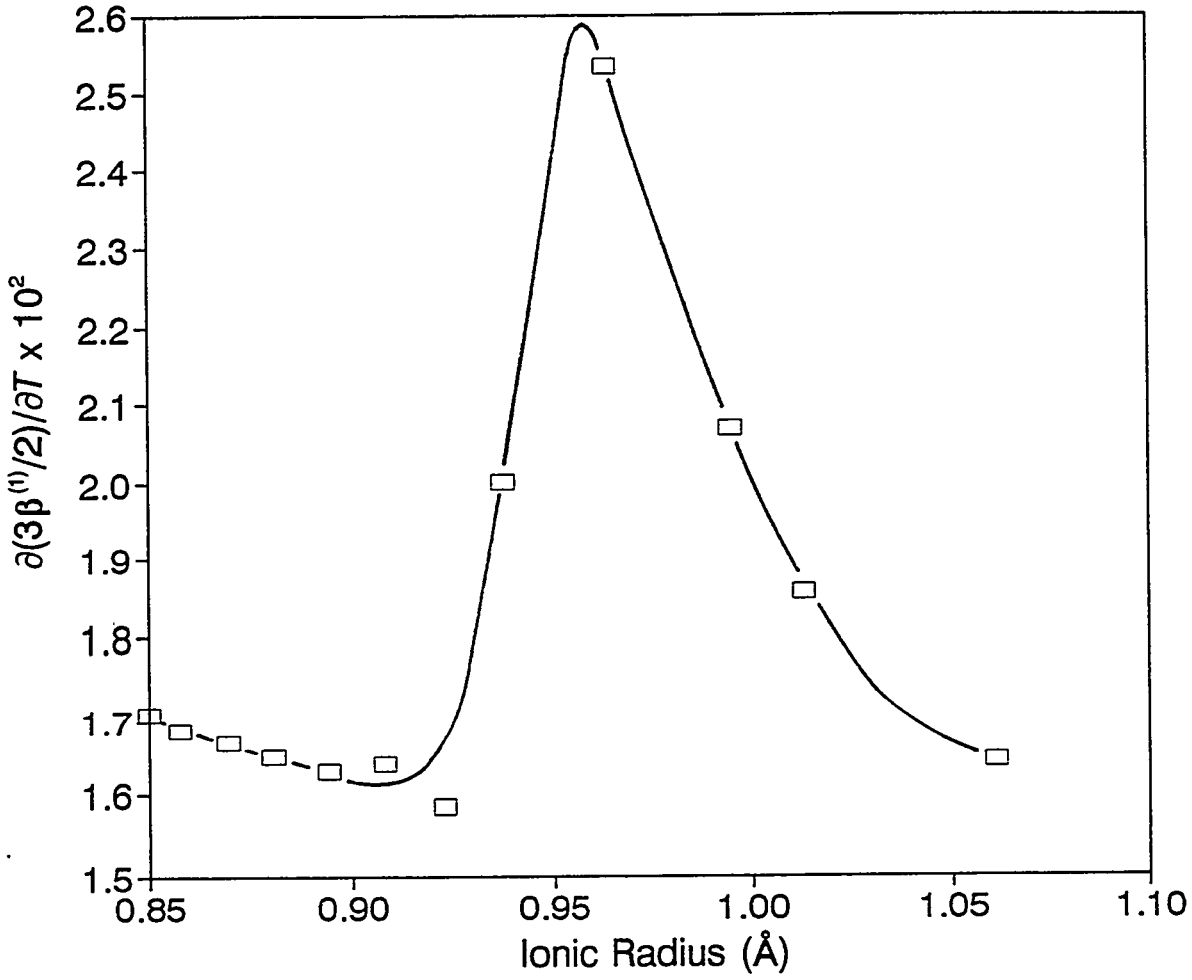

Figure A.4. Variation of the temperature derivative of $\beta^{(1)}$ with ionic radius for rare-earth nitrates.

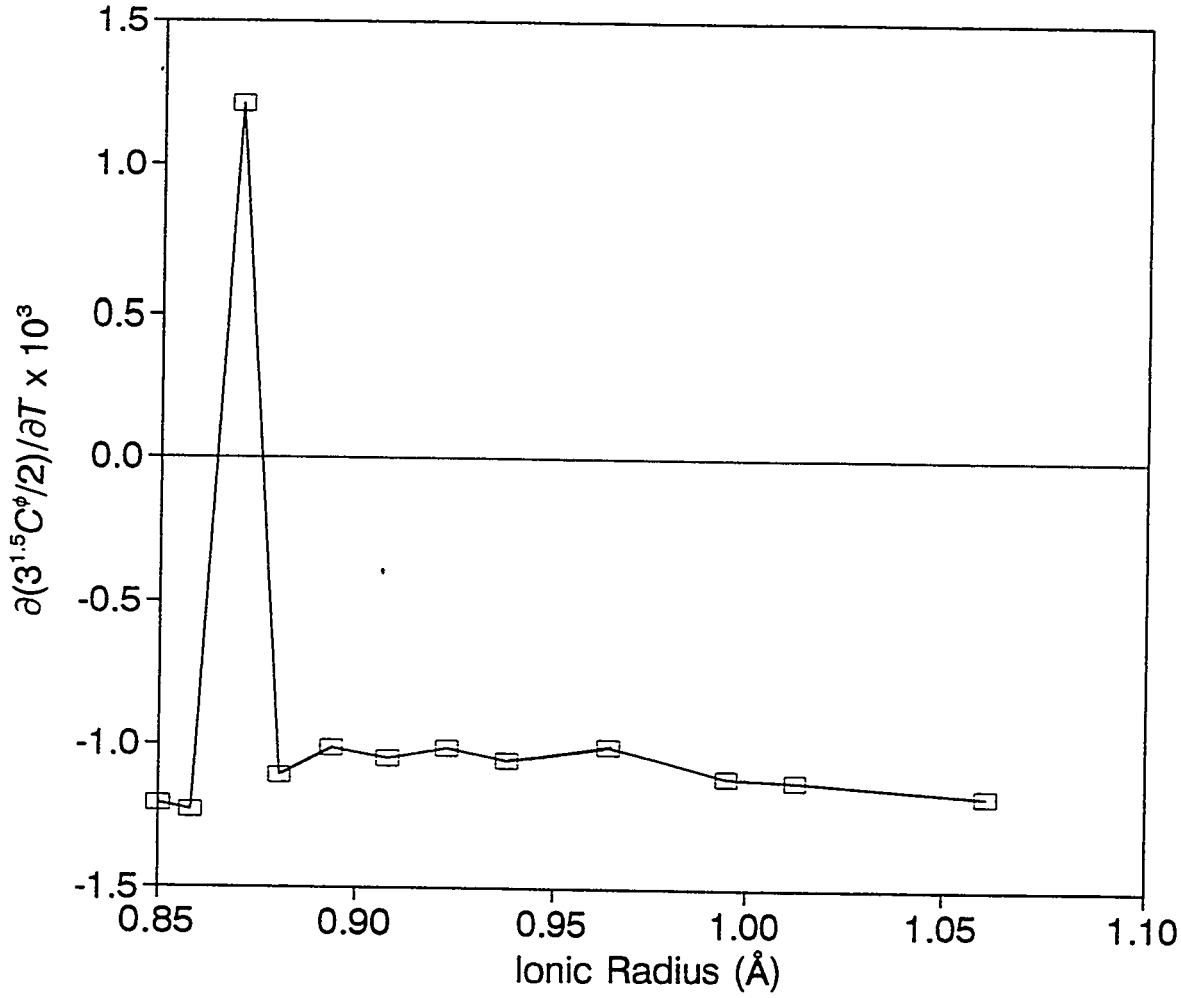

Figure A.5. Variation of the temperature derivative of C^{Φ} with ionic radius for rare-earth nitrates.

of 25°C "causes less than a 1% change in $\beta^{(0)}$ or a 2% change in $\gamma_{\pm}$ at 1 molal." Errors in the temperature derivative of the parameters are likely to be insignificant.

Using the pure-component Pitzer parameters for bismuth nitrate, estimated as described in the preceding discussion, activity and osmotic coefficients can be calculated as though the material remains as the nitrate form in solution. No data on bismuth nitrate are available for comparison, but the calculated values are shown in Figures A.6 and A.7. Also shown in Figure A.6 is the Debye-Hückel limiting law for a 3-1 electrolyte, which may be written as

$$\ln \gamma_{\pm} = -A6\sqrt{3}\sqrt{m} \quad , \tag{A-1}$$

where $A = 1.1745$ mol^{½}/kg^{½}, and

m = concentration of the electrolyte, molal.

Values for the limiting law computed from Eq. (A-1) were verified with the tabulated values of Hamer (1968). Calculated activity coefficients for bismuth nitrate are different from the limiting law by 10% or more when the concentration exceeds 0.0005 molal (i.e., an ionic strength of 0.006 m).

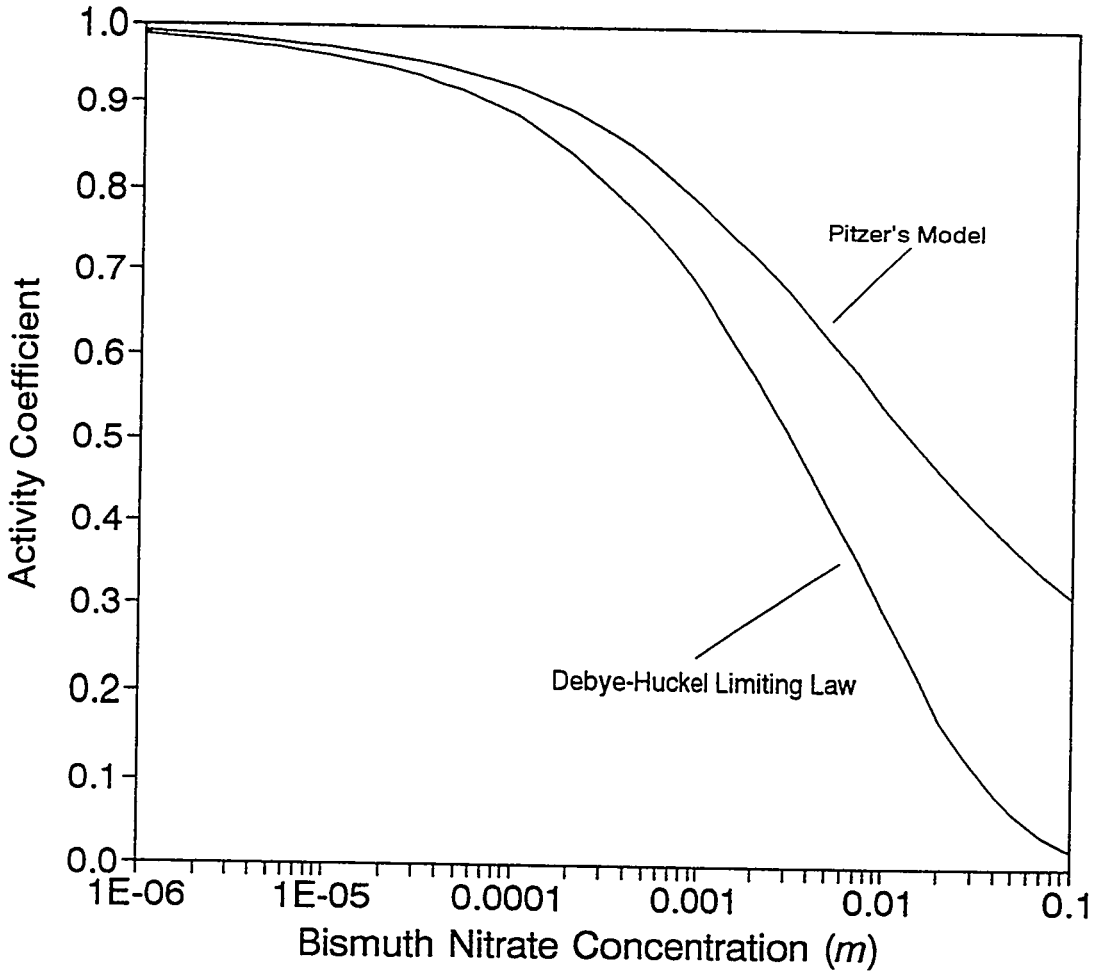

Figure A.6. Estimated activity coefficient of aqueous bismuth(III) nitrate at 25°C, using hypothetical pure-component Pitzer parameters.

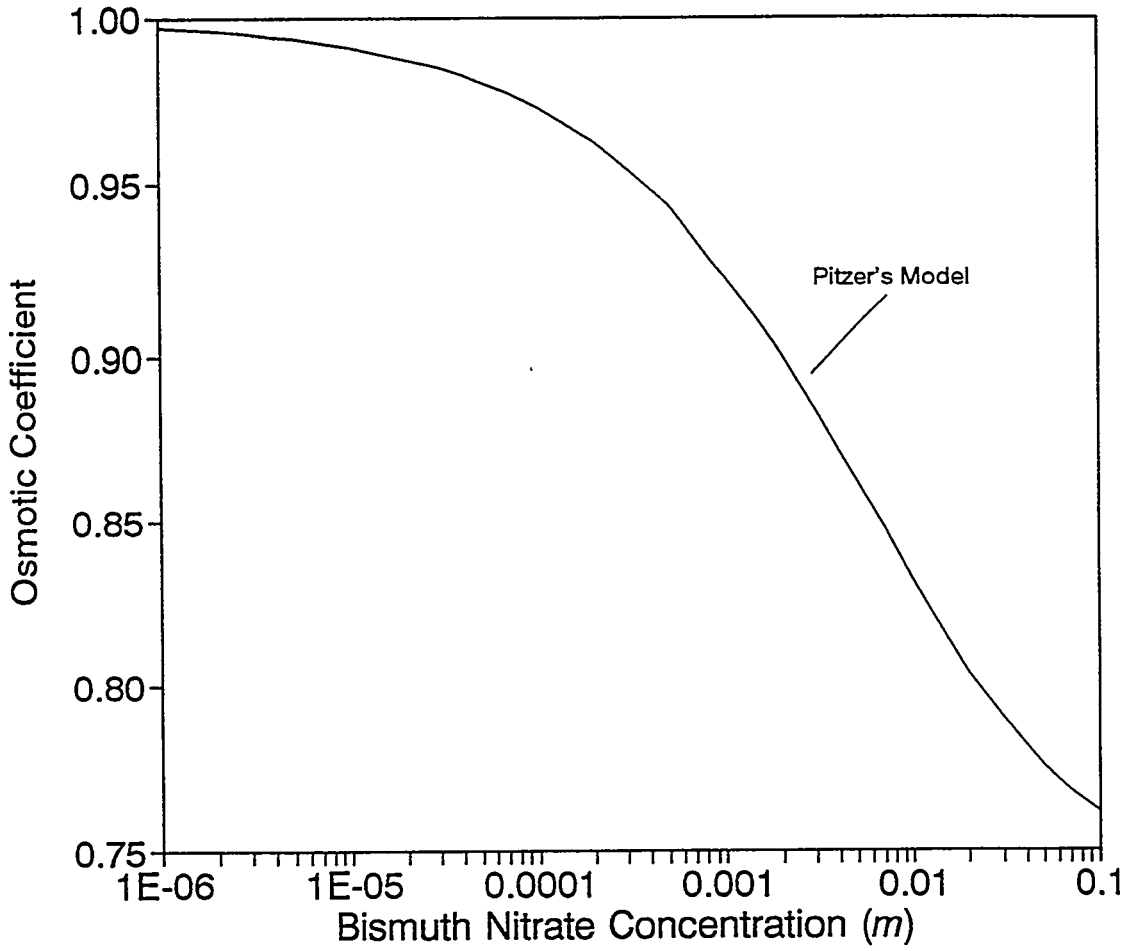

Figure A.7. Estimated osmotic coefficient of aqueous bismuth(III) nitrate solution at 25°C, using hypothetical pure-component Pitzer parameters.

B. Estimation of the Apparent Molal Volume of the Bismuth Ion

The apparent molal volume (AMV) of bismuth(III) ion is not available in the literature, but data have been reported for several other trivalent metals (see Table B.1). It was thought that the AMV might vary regularly with either the ionic radius of the ion or the density of the pure metal.

Examination of the data in Table B.1 shows that bismuth is more dense than all the other elements listed there, implying an extrapolation to estimate the AMV of bismuth. In addition, the AMV of the ion does not vary regularly with the density of the element. However, if the AMVs of the rare earths are plotted as a function of ionic radius, as in Figure B.1, a regular pattern

Table B.1. Apparent molal volumes, ionic radii, and densities of some metal ions at 25°C

Trivalent ion	Apparent molal volume[a] (cm^3/mol)	Crystal ionic radius[b] (Å)	Density[c] (g/cm^3)
Al	–42.2	0.51	2.702
Fe	–43.7	0.64	7.86
Cr	–39.5	0.63	7.194
Yb	–44.22	0.858	6.977
Er	–42.86	0.881	9.164
Ho	–41.76	0.894	8.803
Dy	–40.83	0.908	8.556
Tb	–40.24	0.923	8.272
Gd	–40.41	0.938	7.948
Sm	–42.33	0.964	7.536
Nd	–43.31	0.995	7.004
Pr	–42.53	1.013	6.782
La	–39.10	1.061	6.194
Bi	–42.03[d]	0.960	9.80

[a]F. J. Millero, "The Molal Volumes of Electrolytes," *Chem. Rev.* **71**(2), 147–76 (1971).

[b]R. C. Weast, ed., *CRC Handbook of Chemistry and Physics*, 70th ed., CRC Press, Inc., Boca Raton, Fla., 1989, p. F-187.

[c]R. C. Weast, ed., *CRC Handbook of Chemistry and Physics*, 53rd ed., CRC Press, Inc., Boca Raton, Fla., 1972, pp. B-62–B-156.

[d]Estimate based on variation with ionic radius.

emerges. (The pattern is disrupted if aluminum, iron, and chromium, the other trivalent ions listed in Table B.1, are included.) Straight lines were drawn between the data points, for convenience, and a value of the AMV of bismuth was read from the graph corresponding to the ordinate value of bismuth's ionic radius. This result is included in the last row of Table B.1.

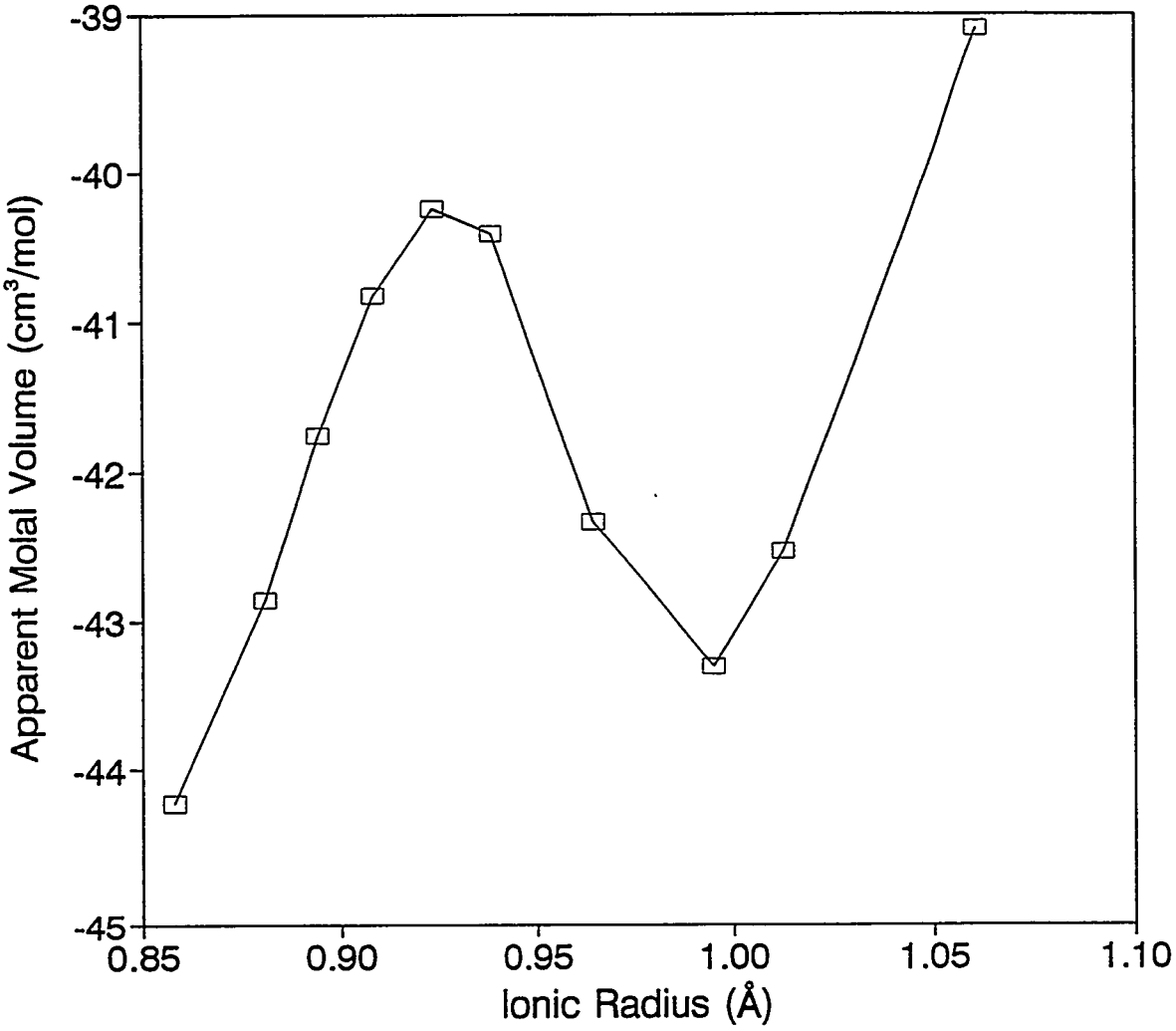

Figure B.1. Variation of the apparent molal volume with ionic radius for trivalent rare-earth ions.

C. Raw Data from Nitric Acid Extraction Experiments

The experimental data obtained on the extraction of nitric acid with CMPO is recorded here. The analytical measurements include molar concentrations of nitric acid in each phase, some values of the water concentration in the organic phase, and five measurements on the density of the organic phase. Because the analytical method gives the concentrations in molar units, rather than weight percent, for example, density measurements are not required for conversion of the measured concentration to other units. The density of a solution of 0.20 *M* CMPO in *n*-dodecane is, within the error of the measurement, the same as the density of pure *n*-dodecane, (i.e., ~0.750).

Data on the distribution of nitric acid between the aqueous-phase and organic solutions of varying CMPO concentrations are given in Tables C.1 and C.2 for temperatures of 25 and 40°C, respectively. Distribution data on systems comprised of 0.20 *M* CMPO in *n*-dodecane and aqueous solutions of varying nitric acid concentrations are listed in Tables C.3 through C.5. The operating temperature is given as part of the table title.

Table C.1. Data from nitric acid extraction tests at 25°C and 0.25 *M* HNO_3

	Analytical results			
	Aqueous phase		Organic phase	
CMPO (*M*)	Sample	HNO_3 (*M*)	Sample	HNO_3 (*M*)
0.200	D-15-01	0.254	D-15-02	0.017
0.100	D-15-03	0.257	D-15-04	0.008
0.100	D-15-05	0.257	D-15-06	0.0084
0.050	D-15-07	0.256	D-15-08	0.004
0.050	D-15-09	0.258	D-15-10	0.004

Table C.2. Data from nitric acid extraction tests at 40°C and 0.50 *M* HNO_3

	Analytical results			
	Aqueous phase		Organic phase	
CMPO (*M*)	Sample	HNO_3 (*M*)	Sample	HNO_3 (*M*)
0.200	D-16-01	0.522	D-16-02	0.044
0.100	D-16-03	0.519	D-16-04	0.021
0.100	D-16-05	0.521	D-16-06	0.020
0.050	D-16-07	0.518	D-16-08	0.010
0.050	D-16-09	0.522	D-16-10	0.010

Table C.3. Data from nitric acid extraction tests at 25°C and 0.20 *M* CMPO

	Analytical results					
	Aqueous phase		Organic phase			
HNO_3 (*M*)	Sample	HNO_3 (*M*)	Sample	HNO_3 (*M*)	H_2O (wt %)	Density (g/mL)
0.0		0	D-0-01	0.0	<0.01	0.743[a]
0.0		0	D-0-02	0.0	<0.01	0.753[b]
0.0	D-1-01		D-1-02		<0.01	0.765
0.0	D-4-01	0.002	D-4-02[c]	<0.001	0.34	
0.010	D-4-03	0.011	D-4-04[c]	<0.001	0.47	
0.020	D-4-05	0.021	D-4-06[c]	<0.001	0.18	
0.050	D-4-07	0.053	D-4-08	0.002	0.26	
0.100	D-4-09	0.104	D-4-10	0.004	0.21	
0.200	D-4-11	0.206	D-4-12	0.012	0.51	
0.250	D-4-13	0.252	D-4-14[c]	0.018	0.35	
0.300	D-4-15	0.302	D-4-16	0.022	0.58	0.7544
0.100	D-6-01	0.102	D-6-02	0.002	1.2	
0.200	D-6-03	0.202	D-6-04	0.014	7.8	
0.300	D-6-05	0.296	D-6-06	0.024	0.62	

[a]Pure *n*-dodecane; true density, 0.750 g/mL.
[b]Pure *n*-dodecane contacted with water.
[c]Overnight separation.

Table C.4. Data from nitric acid extraction tests at 40°C and 0.20 *M* CMPO

	Analytical results					
	Aqueous phase		Organic phase			
HNO_3 (*M*)	Sample	HNO_3 (*M*)	Sample	HNO_3 (*M*)	H_2O (wt %)	Density (g/mL)
0.0	D-3-01	0.010	D-3-02	0.001	0.21	0.757
0.020	D-3-03	0.046	D-3-04	0.001	0.15	
0.100	D-3-05	0.116	D-3-06	0.003	<0.01	
0.200	D-3-07	0.236	D-3-08	0.010	0.16	
0.500	D-3-09	0.518	D-3-10	0.044	<0.01	
1.0[a]	D-3-11	0.938	D-3-12	0.091	0.02	
2.0[a]	D-3-13	0.830	D-3-14	0.081	0.02	
3.0[a]	D-3-15	0.910	D-3-16	0.086	0.05	0.763
0.200	D-7-01	0.200	D-7-02	0.010	0.38	
0.500	D-7-03	0.508	D-7-04	0.042	0.43	
0.762	D-7-05	0.756	D-7-06	0.062	0.43	

[a]This concentration caused formation of a third phase, which occurred on the first preequilibration. Water was added in 10-mL increments to cause back-extraction and break the third phase. Measured concentrations in the aqueous phase were expected to be lower than the initial concentration.

Table C.5. Data from nitric acid extraction tests at 50°C and 0.20 *M* CMPO

	Analytical results					
	Aqueous phase		Organic phase			
HNO_3 (*M*)	Sample	HNO_3 (*M*)	Sample	HNO_3 (*M*)	H_2O[a] (wt %)	Density[a] (g/mL)
1.0[b]	D-12-01	1.00	D-12-02	0.054		
2.0[b]	D-12-03	1.85	D-12-04	0.146		
3.0[b,c]	D-12-05	2.76	D-12-06	0.179		
4.0[b,d]	D-12-07		D-12-08			

[a]Not measured at this temperature.

[b]Single contact; no preequilibration. Measured aqueous concentrations were expected to be lower than the initial concentration.

[c]Visual indication that a very small quantity of third phase may have been present.

[d]A slightly yellow third phase formed; sample was not analyzed.

D. Raw Data from Uranyl Nitrate Extraction Experiments

Samples prepared to obtain equilibrium data for the distribution of uranyl nitrate between an aqueous nitric acid phase and an organic CMPO–*n*-dodecane phase were analyzed by two different techniques, radiocounting and ICP-MS. The radiocounting data are listed in Tables D.1 through D.10, and the ICP-MS data are summarized in Tables D.11 through D.13. The use of these data to calculate distribution ratios and perform material balances is straightforward because equal volumes of each phase were equilibrated in each test.

Radiocounting Data. The radiocounting data are recorded in Tables D.1 through D.10. The tables list (1) the measured count rate of the uranium-bearing solution prior to phase contact, (2) the count rates of both the aqueous and organic phases following equilibration, (3) standard deviations in the measured count rates, (4) a uranium material balance, and (5) the value of the distribution ratio. The measured disintegration rate in the radiocounting data is directly proportional to the concentration of the uranium in the sample. At least two samples were withdrawn from each phase of an equilibrated pair and used to compute an average count rate and standard deviation in the count rate. The distribution ratio is calculated from the raw data by the ratio of the organic-phase count rate to the aqueous-phase count rate. Because all the uranium in the equilibrated pair was initially in one of the phases, a material balance may be represented by

$$mat\ bal = \frac{aqueous\ counts + organic\ counts}{initial\ counts} \qquad \text{(D-1)}$$

and has a value of unity for a perfect balance. Deviations from unity, multiplied by 100, represent the percentage error in closing the material balance.

ICP-MS Data. The ICP-MS data are recorded in Tables D.11 through D.13. Analysis by this method is specific for ^{238}U; however, the concentration of uranium measured in these particular samples is only proportional to the true molar concentration of uranium. This

Table D.1. Data from uranyl nitrate extraction tests at different CMPO concentrations, 0.100 *M* HNO_3, and 25°C[a]

		Analytical results							
		Aqueous phase			Organic phase				
CMPO (*M*)[b]	U × 10^3 (*M*)[b]	Sample	$UO_2(NO_3)_2$ (dpm/mL)	σ[c] (dpm/mL)	Sample	$UO_2(NO_3)_2$ (dpm/mL)	σ[c] (dpm/mL)	Material balance[d]	Distribution ratio
0.200	1.00	D-31-01	1597.06	50.06	D-31-02	47,938.3	456.7	0.990	30.02
0.200	1.00	D-31-03	1581.76	4.384	D-31-04	47,994.4	70.72	0.991	30.34
0.100	1.00	D-31-05	2561.96	0.7077	D-31-06	46,873.4	413.0	0.988	18.30
0.100	1.00	D-31-07	2599.76	14.57	D-31-08	46,730.1	111.3	0.986	17.98
0.050	1.00	D-31-09	5812.56	28.43	D-31-10	43,908.5	50.77	0.993	7.554
0.050	1.00	D-31-11	5823.46	110.3	D-31-12	43,842.9	34.37	0.992	7.529
0.200	0.958	D-31-13	657.24	8.910	D-31-14	47,273.6	8.371	1.000	71.93
0.200	0.959	D-31-15	629.54	6.505	D-31-16	47,372.2	47.82	1.000	75.25
0.100	0.937	D-31-17	1547.54	28.00	D-31-18	45,371.2	236.7	1.001	29.32
0.100	0.933	D-31-19	1631.74	25.46	D-31-20	45,303.5	15.08	1.004	27.76
0.050	0.877	D-31-21	4353.24	38.89	D-31-22	39,644.6	52.89	1.002	9.107
0.050	0.876	D-31-23	4299.41	24.01	D-31-24	39,635.2	43.28	1.002	9.219

[a]The table is organized such that the forward-extraction data are listed, followed by a blank line and then the back-extraction data.

[b]Each experiment was performed using 0.100 *M* HNO_3 and an initial $UO_2(NO_3)_2$ concentration of 0.001 *M*. The measured count rate for the initial aqueous solution was (50,048.6 ± 147.6) dpm/mL.

[c]Two samples were taken from each phase following equilibration, and each sample was counted. The standard deviation is, therefore, based on these two measurements.

[d]Calculated by (aqueous counts + organic counts)/(initial counts); unity is a perfect balance.

Table D.2. Data from uranyl nitrate extraction tests at different CMPO concentrations, 0.100 *M* HNO_3, and 40°C[a]

		Analytical results							
		Aqueous phase			Organic phase				
CMPO (*M*)[b]	U × 10^3 (*M*)[b]	Sample	$UO_2(NO_3)_2$ (dpm/mL)	σ[c] (dpm/mL)	Sample	$UO_2(NO_3)_2$ (dpm/mL)	σ[c] (dpm/mL)	Material balance[d]	Distribution ratio
0.200	1.00	D-32-01	1981.44	7.778	D-32-02	48,176.2	239.3	0.990	24.31
0.200	1.00	D-32-03	2025.44	14.28	D-32-04	48,450.2	194.6	0.996	23.92
0.100	1.00	D-32-05	4052.14	53.17	D-32-06	46,262.9	205.2	0.993	11.42
0.100	1.00	D-32-07	3943.94	1.980	D-32-08	46,360.2	97.02	0.992	11.75
0.050	1.00	D-32-09	9583.54	101.8	D-32-10	40,647.4	290.5	0.991	4.241
0.050	1.00	D-32-11	9659.94	43.27	D-32-12	40,801.4	383.3	0.996	4.224
0.200	0.951	D-32-13	1073.54	0.5657	D-32-14	47,452.1	73.40	1.007	44.20
0.200	0.956	D-32-15	1118.84	4.101	D-32-16	47,298.2	64.20	0.999	42.27
0.100	0.913	D-32-17	2887.44	51.05	D-32-18	43,704.2	48.08	1.007	15.14
0.100	0.915	D-32-19	2839.64	56.43	D-32-20	43,507.6	317.3	1.000	15.32
0.050	0.802	D-32-21	7230.24	34.93	D-32-22	33,610.0	159.8	1.005	4.649
0.050	0.805	D-32-23	7248.24	18.24	D-32-24	33,931.6	11.30	1.009	4.681

[a]The table is organized such that the forward-extraction data are listed, followed by a blank line and then the back-extraction data.

[b]Each experiment was performed using 0.100 *M* HNO_3 and an initial $UO_2(NO_3)_2$ concentration of 0.001 *M*. The measured count rate for the initial aqueous solution was (50,684.5 ± 16.60) dpm/mL.

[c]Two samples were taken from each phase following equilibration, and each sample was counted. The standard deviation is, therefore, based on these two measurements.

[d]Calculated by (aqueous counts + organic counts)/(initial counts); unity is a perfect balance.

Table D.3. Data from uranyl nitrate extraction tests at 25°C, 0.20 *M* CMPO, and 0.200 *M* HNO_3[a]

				Analytical results							
				Aqueous phase			Organic phase				
HNO_3 (*M*)	U × 10^3 (*M*)[b]	Count rate (dpm/mL)	σ[c] (dpm/mL)	Sample	U (dpm/mL)	σ[c] (dpm/mL)	Sample	U (dpm/mL)	0.σ[c] (dpm/mL)	Material balance[d]	Distribution ratio
0.200	2.00	195,714	267.8								
0.200	1.00	97,856.5	*e*	D-26-01	2431.2	72.69	D-26-02	94,644.0	39.60	0.992	38.93
0.200	0.500	195,373	54.94	D-26-03	5013.80	48.37	D-26-04	188,408.	367.7	0.990	37.58
0.200	0.250	97,686.5	*e*	D-26-05	2574.00	2.263	D-26-06	94,474.0	327.5	0.993	36.69
0.200	0.100	194,855	122.3	D-26-07	5059.00	6.223	D-26-08	187,902	3012	0.990	37.14
0.200	0.050	97,427.5	*e*	D-26-09	2588.00	24.61	D-26-10	94,295.5	266.9	0.994	36.44
0.200	0.967	94,644.0	39.60	D-26-11	651.76	18.53	D-26-12	93,842.1	212.3	0.998	144.0
0.200	0.242	94,474.0	327.5	D-26-13	620.26	8.485	D-26-14	93,684.5	274.2	0.998	151.0
0.200	0.0484	94,295.5	266.9	D-26-15	619.56	17.68	D-26-16	93,874.4	461.9	1.002	151.5

[a]The table is organized such that the forward-extraction data are listed, followed by a blank line and then the back-extraction data.

[b]Initial $UO_2(NO_2)_3$ concentration before phase contact.

[c]Two samples were taken from each phase following equilibration, and each sample was counted. The standard deviation is, therefore, based on these two measurements.

[d]Calculated by (aqueous counts + organic counts)/(initial counts); unity is a perfect balance.

[e]No standard deviation is given because counting was not done. The solution was prepared by simple dilution of the last listed solution for which a standard deviation is given.

Table D.4. Data from uranyl nitrate extraction tests at 25°C, 0.20 *M* CMPO, and 0.200 *M* HNO_3; replicate experiment[a]

				Analytical results							
				Aqueous phase			Organic phase				
HNO_3 (*M*)	U x 10^3 (*M*)[b]	Count rate (dpm/mL)	σ[c] (dpm/mL)	Sample	U (dpm/mL)	σ[c] (dpm/mL)	Sample	U (dpm/mL)	σ[c] (dpm/mL)	Material balance[d]	Distribution ratio
0.200	2.00	195,713	189.4								
0.200	1.00	97,856.5	*e*	D-27-03	3011.54	75.24	D-27-04	94,961.7	450.1	1.001	31.53
0.200	0.500	195,373	38.85	D-27-05	6140.04	50.77	D-27-06	190,313	976.4	1.006	31.00
0.200	0.250	97,686.5	*e*	D-27-07	2988.04	9.192	D-27-08	94,255.7	343.5	0.995	31.54
0.200	0.100	194,855	86.50	D-27-09	6193.04	14.57	D-27-10	188,399	117.5	0.999	30.42
0.200	0.050	97,427.5	*e*	D-27-11	3095.94	29.13	D-27-12	94,050.9	119.8	0.997	30.38
0.200	0.970	94,961.7	450.1	D-27-15	609.60	2.546	D-27-16	93,971.2	0.396	0.996	154.2
0.200	0.487	190,313	976.4	D-27-17	1149.30	105.9	D-27-18	87,722.	1433.	0.992	163.3
0.200	0.241	94,255.7	343.5	D-27-19	622.30	2.687	D-27-20	94,053.7	229.5	1.004	151.1
0.200	0.0967	188,399	117.5	D-27-21	1307.00	75.24	D-27-22	186,841.7	250.2	0.999	143.0
0.200	0.0483	94,050.9	119.8	D-27-23	638.90	36.63	D-27-24	93,811.2	149.1	1.004	146.8

[a]The table is organized such that forward-extraction data are listed, followed by a blank line and then the back-extraction data.

[b]Initial $UO_2(NO_2)_3$ concentration before phase contact.

[c]Two samples were taken from each phase following equilibration, and each sample was counted. The standard deviation is, therefore, based on these two measurements.

[d]Calculated by (aqueous counts + organic counts)/(initial counts); unity is a perfect balance.

[e]No standard deviation is given because counting was not done. The solution was prepared by simple dilution of the last listed solution for which a standard deviation is given.

Table D.5. Data from uranyl nitrate extraction tests at 25°C, 0.20 *M* CMPO, and 0.100 *M* HNO_3[a]

				Analytical results							
				Aqueous phase			Organic phase				
HNO_3 (*M*)	U × 10^3 (*M*)[b]	Count (dpm/mL)	σ[c] (dpm/mL)	Sample	U (dpm/mL)	σ[c] (dpm/mL)	Sample	U (dpm/mL)	σ[c] (dpm/mL)	Material balance[d]	Distribution ratio
0.100	5.00	175,603.5	380.3								
0.100	2.00	70,241	e	D-29-01	2062.74	56.29	D-29-02	67,743.5	306.2	0.994	32.84
0.100	1.00	49,546.2	22.63	D-29-03	1456.94	41.86	D-29-04	48,038.3	84.15	0.999	32.97
0.100	0.400	19,818	e	D-29-05	578.24	4.384	D-29-06	19,320.1	58.83	1.004	33.41
0.100	0.500	173,763.3	153.7								
0.100	0.200	69,505	e	D-29-07	2035.24	29.84	D-29-08	67,665.3	284.7	1.003	33.25
0.100	0.100	174,118.2	406.4								
0.100	0.050	87,059	e	D-29-09	2497.24	33.23	D-29-10	84,497.0	428.5	0.999	33.84
0.100	1.93	67,743.5	306.2	D-29-11	858.44	51.05	D-29-12	67,058.3	261.8	1.003	78.12
0.100	0.970	48,038.3	84.15	D-29-13	602.34	79.76	D-29-14	47,618.2	272.7	1.004	79.06
0.100	0.390	19,320.1	58.83	D-29-15	250.94	23.19	D-29-16	19,119.5	32.53	1.003	76.19
0.100	0.195	67,665.3	284.7	D-29-17	853.74	46.67	D-29-18	66,874.4	229.1	1.001	78.33
0.100	0.0485	84,497.0	428.5	D-29-19	1124.94	5.091	D-29-20	83,256.3	286.7	0.999	74.01

[a]The table is organized such that forward-extraction data are listed, followed by a blank line and then the back-extraction data.

[b]Initial $UO_2(NO_2)_3$ concentration before phase contact.

[c]Two samples were taken from each phase following equilibration, and each sample was counted. The standard deviation is, therefore, based on these two measurements.

[d]Calculated by (aqueous counts + organic counts)/(initial counts); unity is a perfect balance.

[e]No standard deviation is given because counting was not done. The solution was prepared by simple dilution of the last listed solution for which a standard deviation is given.

Table D.6. Data from uranyl nitrate extraction tests at 25°C, 0.20 *M* CMPO, and 0.020 *M* HNO_3[a]

				Analytical results							
				Aqueous phase			Organic phase				
HNO_3 (*M*)	U × 10^3 (*M*)[b]	Count rate (dpm/mL)	σ[c] (dpm/mL)	Sample	U (dpm/mL)	σ[c] (dpm/mL)	Sample	U (dpm/mL)	σ[c] (dpm/mL)	Material balance[d]	Distribution ratio
0.020	5.00	20,011.97	34.83								
0.020	2.50	10,006	*e*	D-33-01	1278.84	6.364	D-33-02	8,696.64	5.516	0.997	6.800
0.020	1.00	4,002	*e*	D-33-03	501.74	14.14	D-33-04	3,482.24	12.59	0.996	6.940
0.020	0.500	19,840.24	96.59	D-33-05	2813.44	0.9904	D-33-06	16,979.44	3.817	0.998	6.035
0.020	0.250	9,920	*e*	D-33-07	1407.94	10.47	D-33-08	8,428.44	68.31	0.992	5.986
0.020	0.100	3,968	*e*	D-33-09	565.34	14.71	D-33-10	3,396.84	47.66	0.999	6.008
0.020	2.00	8,005.	*e*	D-33-21	1031.34	1.414	D-33-22	6,930.94	69.01	0.995	6.720
0.020	2.17	8,696.64	5.516	D-33-11	970.10	16.26	D-33-12	7,751.04	17.96	1.003	7.990
0.020	0.870	3,482.24	12.59	D-33-13	413.30	16.55	D-33-14	3,078.34	25.46	1.003	7.448
0.020	0.428	16,979.44	3.817	D-33-15	2023.90	33.23	D-33-16	14,953.44	10.90	1.000	7.388
0.020	0.212	8,428.44	68.31	D-33-17	1026.40	24.61	D-33-18	7,459.44	42.57	1.007	7.268
0.020	0.0856	3,396.84	47.66	D-33-19	406.70	16.11	D-33-20	2,977.34	28.85	0.996	7.321
0.020	1.73	6,930.94	69.01	D-33-23	814.70	10.32	D-33-24	6,124.24	13.43	1.001	7.517

[a]The table is organized such that forward-extraction data are listed, followed by a blank line and then the back-extraction data.

[b]Initial $UO_2(NO_2)_3$ concentration before phase contact.

[c]Two samples were taken from each phase following equilibration, and each sample was counted. The standard deviation is, therefore, based on these two measurements.

[d]Calculated by (aqueous counts + organic counts)/(initial counts); unity is a perfect balance.

[e]No standard deviation is given because counting was not done. The solution was prepared by simple dilution of the last listed solution for which a standard deviation is given.

Table D.7. Data from uranyl nitrate extraction tests at 40°C, 0.20 *M* CMPO, and 0.200 *M* HNO_3[a]

				Analytical results							
				Aqueous phase			Organic phase				
HNO_3 (*M*)	U × 10^3 (*M*)[b]	Count rate (dpm/mL)	σ[c] (dpm/mL)	Sample	U (dpm/mL)	σ[c] (dpm/mL)	Sample	U (dpm/mL)	σ[c] (dpm/mL)	Material balance[d]	Distribution ratio
0.200	2.00	198,897.1	227.0	D-24-01	4287.44	285.2	D-24-02	191,332.2	400.5	0.984	44.26
0.200	1.00	99,448.6	*e*	D-24-03	1991.74	78.35	D-24-04	95,836.5	3.937	0.984	48.12
0.200	0.500	199,969.2	459.3	D-24-05	4191.04	52.75	D-24-06	193,101.5	1882	0.987	46.08
0.200	0.250	99,984.6	*e*	D-24-07	2045.84	0.990	D-24-08	96,634.0	716.2	0.987	47.23
0.200	0.100	199,367.4	182.7	D-24-09	3997.44	9.475	D-24-10	192,095.9	281.9	0.984	48.05
0.200	0.050	99,683.7	*e*	D-24-11	1960.24	25.03	D-24-12	96,374.1	989.5	0.986	49.16
0.200	1.92	191,332.2	400.5	D-25-01	1832.20	108.33	D-25-02	189,067.9	1080.9	0.998	103.2
0.200	0.964	95,836.5	3.937	D-25-03	861.30	55.30	D-25-04	94,177.6	10.18	0.992	109.3
0.200	0.483	193,101.5	1882	D-25-05	1726.30	168.2	D-25-06	191,300.6	444.3	1.000	110.8
0.200	0.242	96,634.0	716.2	D-25-07	889.20	50.91	D-25-08	95,694.4	758.0	0.999	107.6
0.200	0.0964	192,095.9	281.9	D-25-09	1858.80	56.29	D-25-10	190,326.5	554.5	1.000	102.4
0.200	0.0483	96,374.1	989.5	D-25-11	888.50	14.57	D-25-12	95,518.6	46.67	1.000	107.5

[a]The table is organized such that forward-extraction data are listed, followed by a blank line and then the back-extraction data. This is the only table where the forward-extraction sample numbers have a series number different from that of the back-extraction samples.

[b]Initial $UO_2(NO_2)_3$ concentration before phase contact.

[c]Two samples were taken from each phase following equilibration, and each sample was counted. The standard deviation is, therefore, based on these two measurements.

[d]Calculated by (aqueous counts + organic counts)/(initial counts); unity is a perfect balance.

[e]No standard deviation is given because counting was not done. The solution was prepared by simple dilution of the last listed solution for which a standard deviation is given.

Table D.8. Data from uranyl nitrate extraction tests at 40°C, 0.20 *M* CMPO, and 0.200 *M* HNO_3; replicate experiment[a]

				Analytical results							
				Aqueous phase			Organic phase				
HNO_3 (*M*)	U × 10^3 (*M*)[b]	Count rate (dpm/mL)	σ[c] (dpm/mL)	Sample	U (dpm/mL)	σ[c] (dpm/mL)	Sample	U (dpm/mL)	σ[c] (dpm/mL)	Material balance[d]	Distribution ratio
0.200	2.00	195,713	189.4	D-28-01	6754.06	103.2	D-28-02	187,413	1021.	0.992	27.75
0.200	1.00	97,856.5	*e*	D-28-03	3516.76	38.89	D-28-04	93,688.0	578.1	0.993	26.64
0.200	0.500	195,373	38.85	D-28-05	6893.86	36.49	D-28-06	188,054	197.0	0.998	27.28
0.200	0.250	97,686.5	*e*	D-28-07	3461.36	38.61	D-28-08	93,936.0	77.50	0.997	27.14
0.200	0.100	194,855	86.50	D-28-09	7207.16	206.6	D-28-10	189,061	140.6	1.007	26.23
0.200	0.050	97,427.5	*e*	D-28-11	3475.26	93.06	D-28-12	93,759.9	152.9	0.998	26.98
0.200	1.92	187,413	1021	D-28-13	1847.7	100.6	D-28-14	187,022	55.86	1.008	101.2
0.200	0.957	93,688.0	578.1	D-28-15	909.6	3.111	D-28-16	93,756.7	628.6	1.010	103.1
0.200	0.481	188,054	197.0	D-28-17	1886.1	1.556	D-28-18	187,432	841.0	1.007	99.38
0.200	0.240	93,936.0	77.50	D-28-19	948.1	30.04	D-28-20	93,566.3	25.88	1.006	98.69
0.200	0.0970	189,061	140.6	D-28-21	1807.3	0.9899	D-28-22	186,544.	1035	0.996	103.2
0.200	0.0481	93,759.9	152.9	D-28-23	1049.9	91.78	D-28-24	92,987.0	666.7	1.003	88.57

[a]The table is organized such that forward-extraction data are listed, followed by a blank line and then the back-extraction data.

[b]Initial $UO_2(NO_2)_3$ concentration before phase contact.

[c]Two samples were taken from each phase following equilibration, and each sample was counted. The standard deviation is, therefore, based on these two measurements.

[d]Calculated by (aqueous counts + organic counts)/(initial counts); unity is a perfect balance.

[e]No standard deviation is given because counting was not done. The solution was prepared by simple dilution of the last listed solution for which a standard deviation is given.

Table D.9. Data from uranyl nitrate extraction tests at 40°C, 0.20 *M* CMPO, and 0.100 *M* HNO_3[a]

				Analytical results							
				Aqueous phase			Organic phase				
HNO_3 (*M*)	U × 10^3 (*M*)[b]	Count rate (dpm/mL)	σ[c] (dpm/mL)	Sample	U (dpm/mL)	σ[c] (dpm/mL)	Sample	U (dpm/mL)	σ[c] (dpm/mL)	Material balance[d]	Distribution ratio
0.100	5.00	175,603.5	380.3	D-30-01	6819.66	8.485	D-30-02	164,628.9	450.7	0.976	24.14
0.100	2.00	70,241	*e*	D-30-03	2650.46	59.68	D-30-04	67,096.5	402.6	0.993	25.32
0.100	1.00	49,546.2	22.63	D-30-05	1869.96	14.00	D-30-06	47,597.9	76.51	0.998	25.45
0.100	0.500	173,763.3	153.7	D-30-07	6644.66	202.5	D-30-08	167,213.1	149.2	1.001	25.17
0.100	0.100	174,118.2	406.4	D-30-09	6823.06	53.17	D-30-10	166,682.6	115.7	0.996	24.43
0.100	4.69	164,628.9	450.7	D-30-11	3847.3	106.5	D-30-12	161,261.0	28.57	1.003	41.92
0.100	1.91	67,096.5	402.6	D-30-13	1489.2	8.485	D-30-14	65,965.5	6.647	1.005	44.30
0.100	0.961	47,597.9	76.51	D-30-15	1052.2	0.2828	D-30-16	46,678.4	216.7	1.003	44.36
0.100	0.481	167,213.1	149.2	D-30-17	3862.1	122.6	D-30-18	163,388.1	831.1	1.000	42.31
0.100	0.0957	166,682.6	115.7	D-30-19	3870.3	8.627	D-30-20	162,989.2	1456	1.001	42.11

[a]The table is organized such that forward-extraction data are listed, followed by a blank line and then the back-extraction data.

[b]Initial $UO_2(NO_2)_3$ concentration before phase contact.

[c]Two samples were taken from each phase following equilibration, and each sample was counted. The standard deviation is, therefore, based on these two measurements.

[d]Calculated by (aqueous counts + organic counts)/(initial counts); unity is a perfect balance.

[e]No standard deviation is given because counting was not done. The solution was prepared by simple dilution of the last listed solution for which a standard deviation is given.

Table D.10. Data from uranyl nitrate extraction tests at 40°C, 0.20 *M* CMPO, and 0.020 *M* HNO_3[a]

				Analytical results							
				Aqueous phase			Organic phase				
HNO_3 (*M*)	U × 10^3 (*M*)[b]	Count rate (dpm/mL)	σ[c] (dpm/mL)	Sample	U (dpm/mL)	σ[c] (dpm/mL)	Sample	U (dpm/mL)	σ[c] (dpm/mL)	Material balance[d]	Distribution ratio
0.020	5.00	20,011.97	34.83	D-34-01	3976.00	9.475	D-34-02	15,889.10	37.48	0.993	3.996
0.020	2.50	10,006	*e*	D-34-03	2011.80	10.18	D-34-04	7,827.20	43.56	0.983	3.891
0.020	1.00	4,002	*e*	D-34-05	844.10	40.59	D-34-06	3,118.60	36.49	0.990	3.695
0.020	0.500	1,9840.24	96.59	D-34-07	4516.00	37.34	D-34-08	15,111.80	28.85	0.989	3.346
0.020	0.250	9,920	*e*	D-34-09	2282.00	3.394	D-34-10	7,564.60	26.30	0.993	3.315
0.020	0.100	3,968	*e*	D-34-11	932.30	3.536	D-34-12	3,021.30	30.69	0.996	3.241
0.020	3.97	15,889.10	37.48	D-34-13[f]	2912.30	16.55	D-34-14	12,909.90	57.84	0.996	4.433
0.020	1.96	7,827.20	43.56	D-34-15[f]	1490.00	34.22	D-34-16	6,358.70	0.7071	1.003	4.268
0.020	0.779	3,118.60	36.49	D-34-17	661.60	25.17	D-34-18	2,488.90	0.4243	1.010	3.762
0.020	0.381	15,111.80	28.85	D-34-19	3252.20	11.03	D-34-20	11,946.70	22.77	1.006	3.673
0.020	0.191	7,564.60	26.30	D-34-21	1686.90	6.930	D-34-22	5,869.20	19.52	0.999	3.479
0.020	0.0761	3,021.30	30.69	D-34-23	655.73	9.273	D-34-24	2,346.10	36.91	0.994	3.578

[a]The table is organized such that forward-extraction data are listed, followed by a blank line and then the back-extraction data.

[b]Initial $UO_2(NO_2)_3$ concentration before phase contact.

[c]Two samples were taken from each phase following equilibration, and each sample was counted. The standard deviation is, therefore, based on these two measurements.

[d]Calculated by (aqueous counts + organic counts)/(initial counts); unity is a perfect balance.

[e]No standard deviation is given because counting was not done. The solution was prepared by simple dilution of the last listed solution for which a standard deviation is given.

[f]Mildly cloudy aqueous.

Table D.11. Data from uranyl nitrate extraction tests at different CMPO concentrations, 0.100 *M* HNO_3, and 0.001 *M* U[a]

CMPO (*M*)	Temp. (°C)	Analytical results: Aqueous phase Sample	Aqueous phase U (mg/L)	Organic phase Sample	Organic phase U (mg/L)	Material balance	Distribution ratio
0.200	25.0	D-17-01	0.30	D-17-02	13	0.620	43.3
0.200	25.0	D-17-03	0.37	D-17-04	20	0.949	54.1
0.100	25.0	D-17-05	0.64	D-17-06	18	0.869	28.1
0.100	25.0	D-17-07	0.62	D-17-08	18	0.868	29.0
0.050	25.0	D-17-09	1.7	D-17-10	18	0.918	10.6
0.050	25.0	D-17-11	1.7	D-17-12	17	0.872	10.0
0.200	40.0	D-18-01	0.43	D-18-02	19	0.906	44.2
0.200	40.0	D-18-03	0.36	D-18-04	18	0.856	50.0
0.100	40.0	D-18-05	1.1	D-18-06	17	0.844	15.5
0.100	40.0	D-18-07	1.0	D-18-08	17	0.839	17.0
0.050	40.0	D-18-09	3.0	D-18-10	16	0.886	5.33
0.050	40.0	D-18-11	3.2	D-18-12	15	0.848	4.69

[a]Samples were analyzed by ICP-MS.

Table D.12. Data from uranyl nitrate extraction tests at 25°C and 0.20 *M* CMPO[a]

		Analytical results					
		Aqueous phase		Organic phase			
HNO_3 (*M*)	U × 10^3 (*M*)	Sample	U (mg/L)	Sample	U (mg/L)	Material balance	Distribution ratio
0.020	2.00	D-19-03	4.3	D-19-04	37	0.954	8.60
0.020	0.500	D-19-07	1.1	D-19-08	8.1	0.858	7.36
0.020	0.200	D-19-09	0.48	D-19-10	3.5	0.928	7.29
0.020	0.100	D-19-11	0.25	D-19-12	1.8	0.956	7.20
0.100	2.00	D-21-01	0.45	D-21-02	40	0.943	88.9
0.100	0.500	D-21-05	0.11	D-21-06	8.6	0.871	78.2
0.100	0.200	D-21-07	0.052	D-21-08	3.5	0.888	67.3
0.100	0.100	D-21-09	0.036	D-21-10	1.4	1.032	38.9
0.100	0.050	D-21-11	0.020	D-21-12	0.81	1.193	40.5
0.200	1.00	D-23-03	0.12	D-23-04	16	0.761	133
0.200	0.500	D-23-05	0.10	D-23-06	8.4	0.858	84.0
0.200	0.100	D-23-09	0.021	D-23-10	1.4	1.109	66.7

[a]Samples were analyzed by ICP-MS.

Table D.13. Data from uranyl nitrate extraction tests at 40°C and 0.20 *M* CMPO[a]

		Analytical results					
		Aqueous phase		Organic phase			
HNO_3 (*M*)	$U \times 10^3$ (*M*)	Sample	U (mg/L)	Sample	U (mg/L)	Material balance	Distribution ratio
0.020	5.00	D-20-01	8.8	D-20-02	81	0.830	9.20
0.020	2.00	D-20-03	6.4	D-20-04	36	0.980	5.63
0.020	0.500	D-20-07	1.8	D-20-08	9.0	1.007	5.00
0.020	0.200	D-20-09	0.79	D-20-10	3.3	0.953	4.18
0.100	5.00	D-22-01	2.5	D-22-02	92	0.881	36.8
0.100	2.00	D-22-03	0.96	D-22-04	39	0.931	40.6
0.100	0.500	D-22-07	0.34	D-22-08	8.5	0.884	25.0
0.100	0.200	D-22-09	0.094	D-22-10	3.7	0.949	39.4
0.100	0.100	D-22-11	0.034	D-22-12	1.3	0.959	38.2
0.100	0.050	D-22-13	0.033	D-22-14	0.75	1.126	22.7
0.200	2.00	D-24-01	0.48	D-24-02	37	0.885	77.1
0.200	0.500	D-24-05	0.078	D-24-06	8.8	0.896	113.
0.200	0.100	D-24-09	0.0046	D-24-10	1.4	1.096	304.

[a]Samples were analyzed by ICP-MS.

phenomenon occurs for two reasons: (1) a portion of the uranium in the samples was ^{233}U, which was not detected; and (2) the samples had been prepared for radiocounting analysis by placing a 0.5-mL aliquot of equilibrated solution (either aqueous or organic) in 5.0 mL of liquid scintillation fluid, thereby changing the concentration. Without corrections, the ratio of the measured organic-phase uranium concentration to the measured aqueous-phase uranium concentration provides a good estimate of the distribution ratio. In addition, any proportional bias in the measured concentrations is eliminated when the ratio is calculated. The material balances shown in the tables have been corrected for both the dilution factor and the fraction of uranium present as ^{238}U.

E. Raw Data from Bismuth Nitrate Extraction Experiments

Laboratory data on the extraction of bismuth nitrate from nitric acid media by CMPO–*n*-dodecane are listed in Tables E.1 through E.3. The data in Table E.1 were obtained from experiments wherein the CMPO concentration is either 0.05 or 0.10 *M* and the nitric acid and initial bismuth nitrate concentrations are fixed. Tables E.2 and E.3 contain data on extraction by 0.20 *M* CMPO where the nitric acid and bismuth nitrate concentrations are varied. All experiments were performed with equal volumes of each phase.

Concentration data in the tables are reported in units of mg/L for the aqueous phase and μg/g for the organic phase. Both of these are concentrations of atomic bismuth. The few density measurements made of the organic phase show that its density is close to that of *n*-dodecane. Conversion of the organic bismuth concentrations to a volume basis (e.g., mg/L) only requires multiplication by the density. For this purpose, the density of the organic phase was taken as 0.760 g/mL at 25°C and 0.753 g/mL at 40°C. Distribution ratios were then calculated as the ratio of the organic-phase bismuth concentration to the aqueous-phase bismuth concentration. A material balance was calculated by adding the concentrations in each phase and dividing the result by the initial bismuth concentration. Values of unity represent a perfect balance.

Replicate measurements in the tables permit estimation of the standard deviation of the distribution ratio. For those points for which there is no replicate, the standard deviation may be estimated somewhat crudely. The estimate is based on the average relative standard deviation of those points within the same series (e.g., D-10, which were all analyzed at the same time) for which there are replicates. It is assumed that the relative standard deviation for a given series is constant and that the standard deviation for a single point is estimated by multiplying the distribution ratio by the average relative standard deviation of the series.

Table E.1. Data from bismuth nitrate extraction tests[a] at different CMPO concentrations and 0.10 *M* HNO_3

		Analytical results								
		Aqueous phase			Organic phase					
CMPO (*M*)	Temp. (°C)	Sample	HNO_3 (*M*)	Bi (mg/L)	Sample	HNO_3 (*M*)	Bi (μg/g)	Density (g/mL)	Material balance	Distribution ratio
0.100	25.0	D-13-01	0.092	3.90	D-13-02	0.004	270		1.001	52.62
0.100	25.0	D-13-03	0.092	3.90	D-13-04	0.005	280		1.037	54.56
0.050	25.0	D-13-05	0.092	12.0	D-13-06		260		1.003	16.47
0.050	25.0	D-13-07[b]	0.088	11.0	D-13-08		260	0.743	0.998	17.96
0.100	40.0	D-14-01	0.096	12.0	D-14-02	0.004	270		1.030	16.94
0.100	40.0	D-14-03	0.096	12.0	D-14-04	0.004	260		0.994	16.32
0.050	40.0	D-14-05	0.092	42.0	D-14-06		210		0.958	3.765
0.050	40.0	D-14-07[c]	0.096	44.0	D-14-08		210	0.778	0.967	3.594

[a]Each experiment was performed using 0.10 *M* HNO_3 and an initial $Bi(NO_3)_3$ concentration of 0.001 *M*.
[b]Density of aqueous was 0.985 g/mL.
[c]Density of aqueous was 0.998 g/mL.

Table E.2. Data from bismuth nitrate extraction tests at 25°C

		Analytical results								
		Aqueous phase			Organic phase					
HNO_3 (*M*)	$Bi(NO_3)_3$ (*M*)	Sample	HNO_3 (*M*)	Bi (mg/L)	Sample	HNO_3 (*M*)	Bi (μg/g)	Density (g/mL)	Material balance	Distribution ratio
0.200	0.001	D-5-01	0.202	0.52	D-5-02		310		1.130	453.1
0.200	0.0005	D-5-03	0.200	0.26	D-5-04		150		1.094	438.5
0.200	0.0005	D-5-05	0.202	0.30	D-5-06		150		1.094	380.0
0.200	0.0002	D-5-07	0.174	0.13	D-5-08		54		0.985	315.7
0.200	0.0001	D-5-09	0.201	0.05	D-5-10		29		1.057	440.8
0.200	0.00005	D-5-11	0.178	0.08	D-5-12		16		1.171	152.0
0.200	0.0002	D-8-01	0.202	0.090	D-8-02	0.012	43		0.784	363.1
0.200	0.001	D-8-03	0.202	0.530	D-8-04	0.015	210		0.766	301.1
0.100	0.0005	D-10-01	0.102	0.750	D-10-02	0.006	150		1.098	152.0
0.100	0.0005	D-10-03	0.102	0.720	D-10-04	0.004	150		1.098	158.3
0.100	0.001	D-10-05	0.100	1.50	D-10-06	0.006	290		1.062	146.9
0.100	0.002	D-10-07	0.102	3.10	D-10-08	0.008	580		1.062	142.2
0.100	0.002	D-10-09[a]	0.102	3.10	D-10-10	0.010	590	0.760	1.080	144.6

[a]Density of aqueous was 0.999 g/mL.

Table E.3. Data from bismuth nitrate extraction tests at 40°C

		Analytical results								
		Aqueous phase			Organic phase					
HNO_3 (*M*)	$Bi(NO_3)_3$ (*M*)	Sample	HNO_3 (*M*)	Bi (mg/L)	Sample	HNO_3 (*M*)	Bi (μg/g)	Density (g/mL)	Material balance	Distribution ratio
0.200	0.0001	D-9-01	0.201	0.130	D-9-02	0.010	26		0.943	150.6
0.200	0.0002	D-9-03	0.198	0.260	D-9-04	0.010	51		0.925	147.7
0.200	0.0005	D-9-05	0.200	0.690	D-9-06	0.012	130		0.943	141.9
0.200	0.0005	D-9-07	0.200	0.680	D-9-08	0.012	150		1.087	166.1
0.200	0.001	D-9-09	0.200	1.40	D-9-10	0.012	310		1.124	166.7
0.200	0.005	D-9-11	0.200	6.50	D-9-12	0.020	1600		1.159	185.4
0.200	0.005	D-9-13	0.200	7.30	D-9-14	0.020	2200		1.592	226.9
0.100	0.001	D-11-01	0.102	4.90	D-11-02	0.006	290		1.068	44.57
0.100	0.001	D-11-03	0.102	5.10	D-11-04	0.006	290		1.069	42.82
0.100	0.002	D-11-05	0.102	8.90	D-11-06	0.008	570		1.048	48.23
0.100	0.005[a]	D-11-07	0.104	23.00	D-11-08	0.012	1200		0.887	39.29
0.100	0.005	D-11-09[b]	0.104	22.00	D-11-10	0.013	1100	0.752[c]	0.814	37.65

[a]Initial bismuth nitrate concentration was probably somewhat lower than this value.
[b]Density of aqueous was 1.01 g/mL.
[c]Replicate result was 0.753.

INTERNAL DISTRIBUTION

1. E. C. Beahm
2. J. F. Birdwell
3. E. D. Collins
4. J. L. Collins
5. A. G. Croff
6. D. J. Davidson
7. B. Z. Egan
8. D. D. Ensor
9. L. K. Felker
10. J. N. Herndon
11–15. R. T. Jubin
16. L. N. Klatt
17. L. M. Kyker
18. D. D. Lee
19. B. E. Lewis
20. A. P. Malinauskas
21. C. P. McGinnis
22. L. E. McNeese
23. G. W. Parker
24–26. K. E. Plummer
27. J. D. Randolph
28. J. C. Rudolph
29–33. B. B. Spencer
34. M. G. Stewart
35. J. S. Watson
36. Central Research Library
37. Y-12 Technical Library
Document Reference Center
38. ORNL Patent Section
39–40. ORNL Laboratory Records
41. ORNL Laboratory Records, RC

EXTERNAL DISTRIBUTION

42. L. A. Bray, Pacific Northwest Laboratory, M&CS Center—Chem PMC Systems Section, Battelle Boulevard, P.O. Box 999, Richland, WA 99352
43. N. G. Colton, Pacific Northwest Laboratory, Battelle Boulevard, P.O. Box 999, MS P8-30, Richland, WA 99352
44. T. A. Freyberger, Trevion II Building, 12800 Middlebrook Road, Germantown, MD 20874
45. S. M. Gibson, Trevion II Building, 12800 Middlebrook Road, Germantown, MD 20874
46. R. D. Korynta, Department of Energy, Oak Ridge Operations, P.O. Box 2001, Oak Ridge, TN 37831-8620
47. W. L. Kuhn, Pacific Northwest Laboratory, Battelle Boulevard, P.O. Box 999, Richland, WA 99352
48. G. J. Lumetta, Pacific Northwest Laboratory, Battelle Boulevard, P.O. Box 999, MS P7-25, Richland, WA 99352
49. J. O. Moore, Oak Ridge Technical Program Officer, Department of Energy, Oak Ridge Operations, P.O. Box 2001, Oak Ridge, TN 37831-8620
50. J. J. Swanson, Pacific Northwest Laboratory, Battelle Boulevard, P.O. Box 999, MS P7-25, Richland, WA 99352
51. P. S. Szerszen, SAIC, 555 Quince Orchard Road, Suite 500, Gaithersburg, MD 20878
52. I. Tasker, Waste Policy Institute, 555 Quince Orchard Road, Suite 600, Gaithersburg, MD 20878-1437
53. T. Todd, Idaho National Engineering Laboratory, P.O. Box 4000, Idaho Falls, ID 83415
54. G. F. Vandegrift, Chemical Technology Division, Argonne National Laboratory, Argonne, IL 90439
55. Office of Assistant Manager, Energy Research and Development, DOE-ORO, P.O. Box 2008, Oak Ridge, TN 37831-6269
56–57. Office of Scientific and Technical Information, P.O. Box 62, Oak Ridge, TN 37831